DISSERTATION

Characterization of intestinal antibacterial factors of *Triatoma infestans* (Reduviidae, Insecta) and their interaction with *Trypanosoma cruzi* (Trypanosomatidae, Kinetoplastida)

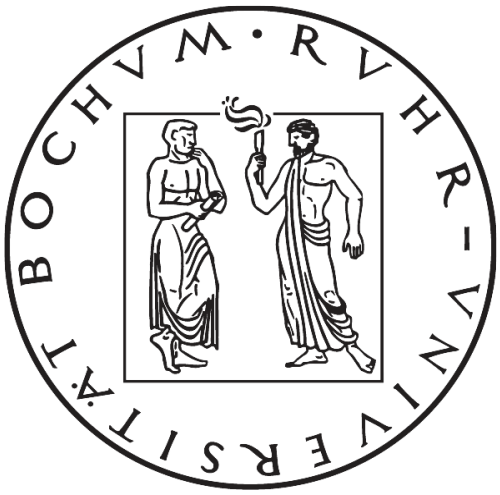

JENNIFER KATHARINA PAUSCH

Research Group Zoology/Parasitology

Ruhr-Universität Bochum

Characterization of intestinal antibacterial factors of *Triatoma infestans* (Reduviidae, Insecta) and their interaction with *Trypanosoma cruzi* (Trypanosomatidae, Kinetoplastida)

DISSERTATION

to obtain the degree

Doctor Rerum Naturalium (Dr. rer. nat.)

at the Faculty of Biology and Biotechnology

Ruhr-University Bochum

International Graduate School of Biosciences

Ruhr-University Bochum

Research Group Zoology/Parasitology

submitted by

JENNIFER KATHARINA PAUSCH

from Bottrop, Germany

Bochum, February 2012

Charakterisierung intestinaler antibakterieller Faktoren von *Triatoma infestans* (Reduviidae, Insecta) und ihre Interaktion mit *Trypanosoma cruzi* (Trypanosomatidae, Kinetoplastida)

DISSERTATION

zur Erlangung des Grades eines Doktors der Naturwissenschaften

der Fakultät für Biologie und Biotechnologie

Internationale Graduiertenschule Biowissenschaften

der Ruhr-Universität Bochum

angefertigt in der

Arbeitsgruppe Zoologie/Parasitologie

vorgelegt von

JENNIFER KATHARINA PAUSCH

aus

Bottrop

Bochum, Februar 2012

This work has been performed between May 2008 and February 2012 by Jennifer Katharina Pausch under the supervision of Prof. Dr. Günter A. Schaub in the Research Group Zoology/Parasitology, Faculty of Biology and Biotechnology of the Ruhr-University Bochum.

Author Jennifer Katharina Pausch

Title Characterization of intestinal antibacterial factors of *Triatoma infestans* (Reduviidae, Insecta) and their interaction with *Trypanosoma cruzi* (Trypanosomatidae, Kinetoplastida)

1st referee Prof. Dr. Günter A. Schaub

2nd referee Prof. Dr. Klemens Störtkuhl

Dedicated to my parents

Peter & Roswitha Pausch

“Nature prefers that neither host nor parasite should be too hard on the other.”

(BURNET & WHITE 1972)

CHAPTER 1

CHAPTER 3

CHAPTER 4

CHAPTER 8

CHAPTER 9

CHAPTER 1

CHAPTER 3

CHAPTER 4

CHAPTER 8

BLAST	**B**asic **L**ocal **A**lignment **S**earch **T**ool
bp	**B**ase **p**air
cDNA	**C**omplementary **DNA**
C. bombi	***C**rithidia bombi*
C. fasciculata	***C**rithidia fasciculata*
Da	**Da**lton
daf	**D**ays **a**fter **f**eeding
D. maris	***D**ietzia maris*
DNA	**D**esoxyribo**n**ucleic **a**cid
e.g.	exempli gratia
E. coli	***E**scherichia coli*
et al.	**E**t aliae
Fig.	**F**igure
g	**G**ramm
g	**G**ravitation
G. rubropertinctus	***G**ordonia rubropertinctus*
h	**H**our
i.p.	**i**ntra**p**eritoneal
k	**K**ilo
l	**L**itre
M	**M**olar
m	**M**illi
N1-N5	Nymphal instar stages 1-5
A	**A**mpere
min	**M**inutes
mRNA	**M**essenger **r**ibo**n**ucleic **a**cid
NCBI	**N**ational **C**enter of **B**iotechnology **I**nformation
n	Nano

OD	**O**ptical **d**ensity
PAGE	**P**oly**a**crylamide **g**el **e**lectrophoresis
PAHO	**P**an **A**merican **H**ealth **O**rganisation
PCR	**P**olymerase-**c**hain-**r**eaction
pH	**P**ondus **h**ydrogenii
pI	**I**soelectric **p**oint
p.i.	**p**ost **i**nfection
P. megistsus	***P****anstrongylus megistus*
qRT-PCR	**q**uantitative **r**everse **t**ranscriptase **PCR**
R. prolixus	***R****hodnius prolixus*
R. triatomae	***R****hodococcus triatomae*
RNA	**R**ibo**n**ucleic **a**cid
RT	**R**oom **t**emperature
SDS	**S**odium **d**odecyl **s**ulfate
s	**s**econd
s.c.	**s**ub**c**utan
Tab.	**T**able
T. brasiliensis	***T****riatoma brasiliensis*
T. cruzi	***T****rypanosoma cruzi*
T. infestans	***T****riatoma infestans*
T. klugi	***T****riatoma klugi*
T. protracta	***T****riatoma protracta*
T. rangeli	***T****rypanosoma rangeli*
T. sordida	***T****riatoma sordida*
T. vitticeps	***T****riatoma vitticeps*
Tris	**Tris**(hydroxymethyl)aminomethane
U	**U**nit
V	**V**olt

v/v	**V**olume per **v**olume
WHO	**W**orld **H**ealth **O**rganisation
w/v	**W**eight per **v**olume
°C	degrees Celsius
µ	micro
Gene	capitals, italic, e.g. *LYS1*
Protein	capitals, e.g. LYS1

Scientifical genus names and names of species are written in italic (e.g. *Trypanosoma*, *Triatoma infestans*). Authors and first describers are written in small caps (e.g. CHAGAS).
The three letter code is used for denotation of amino acids according to the nomenclature of IUPAC; the following number indicates the position of the amino acid in the mature protein.

Ala (A)	Alanine	Ile (I)	Isoleucine	Arg (R)	Arginine
Cys (C)	Cysteine	Lys (K)	Lysine	Ser (S)	Serine
Asp (D)	Aspartic Acid	Leu (L)	Leucine	Thr (T)	Threonine
Glu (E)	Glutamic Acid	Met (M)	Methionine	Val (V)	Valine
Phe (F)	Phenylalanine	Asn (N)	Asparagine	Trp (W)	Tryptophan
Gly (G)	Glycine	Pro (P)	Proline	Tyr (Y)	Tyrosine
His (H)	Histidine	Gln (Q)	Glutamine		

First I would like to thank my doctoral adviser Prof. Dr. G. A. Schaub for giving me the opportunity to work on this exciting project in his Research Group. I'm grateful for his constant interest and confidence in the progress of my studies. I furthermore appreciate his continuous support and invaluable suggestions as well as his critical comments on the thesis.

I would like to thank Prof. Dr. K. Störtkuhl for the acceptance to work as a second reviewer of this thesis.

My appreciation also goes to Prof. Dr. H. E. Meyer and Dr. K. Kuhlmann, Medizinisches Proteom Center (Ruhr-Universität Bochum), for the opportunity to analyze my samples by mass spectrometry. In detail, I would like to thank S. Loroch for his critical support and his personal encouragement in these investigations.

Further, I would like to thank Prof. Dr. P. Azambuja, Prof. Dr. E. S. Garcia and Dr. F. Genta for the opportunity to work in their laboratory at the Fundaçao Oswaldo Cruz, Rio de Janeiro. The financial support of the Deutscher Akademischer Austausch Dienst is gratefully acknowledged.

Especially, I would like to thank Dr. C. Balczun and Dr. C. Meiser for never ending patience, many inspirations, continuous advisory help and many constructive discussions.

Very special thanks go to the present and former members of the Research Group Zoology/Parasitology. The familiar atmosphere of this group encouraged me to finalize my investigations.

I would also like to thank Dr. L. Weiss for many encouraging conversations.

I am very grateful for the everlasting support of my parents Peter and Roswitha Pausch. They always encouraged me to remain defiant to achieve higher goals in life. They believed in me and supported me the best they could. Their continuous motivation helped me to achieve my aims and accomplish this work.

I thank my sisters Linda and Laura for many wonderful memories, for laughing and crying together, many heart-to-heart talks and for termless trusting each other.

Last but not least, I wish to give my thanks to Stefan, who supported me in the last years of these investigations, for his loving help and understanding.

CHAPTER 1

GENERAL INTRODUCTION

PARTS OF THIS CHAPTER ARE BASED ON **PAUSCH JK**, BALCZUN C AND SCHAUB GA (IN PRESS): INTERACTIONS OF *TRYPANOSOMA CRUZI*, THE ETIOLOGIC AGENT OF CHAGAS DISEASE, AND TRIATOMINES (REDUVIIDAE). *MITTEILUNGEN DER DEUTSCHEN GESELLSCHAFT FÜR ALLGEMEINE UND ANGEWANDTE ENTOMOLOGIE* BAND 18

1. General introduction

1.1 Chagas disease (American Trypanosomiasis)

1.1.1 History, geographical distribution and epidemiology of Chagas disease

In the early 20th century, Dr. Carlos J. R. Chagas (*1879 †1934) described the protozoan hemoflagellate *Trypanosoma cruzi* as the etiological agent of a so far unknown disease (thus later named in his honor) (CHAGAS 1909; SCHOFIELD & DIAS 1999). During a malaria expedition in Minas Gerais, a Federal State of southeast Brazil, Dr. Carlos Chagas first found the parasite in the posterior intestine of the blood sucking bug *Panstrongylus megistus* (CHAGAS 1909). Later, he detected the flagellate in the blood of a young girl and her cat (CHAGAS 1909, 1922). Thus Dr. Carlos Chagas original report is acknowledged unique in medicine history with regard to his detailed work, describing the transmission cycle (vector, host and a novel infectious organism). Furthermore, he was the first to describe the course of disease in a human case. Since 4,000 to 9,000 years old mummies from South America contained DNA from the disease's etiological agent, Chagas disease has been a scourge to humans since antiquity. Chagas disease continued to be a relevant social and economic problem in most Latin American countries and is classified by the World Health Organisation (WHO) as one of the world's 13 most neglected tropical diseases (GUHL *et al.* 1999; AUFDERHEIDE *et al.* 2004; HOTEZ *et al.* 2007; MATHERS *et al.* 2007; MONCAYO & SILVEIRA 2009).

Originally, Chagas disease was restricted to poor, rural areas of South and Central America, in which vector-borne transmission to man occurs (RASSI *et al.* 2010). During the last 20 years, improved vector control programmes such as the Southern Cone Initiative to Control/Eliminate Chagas Disease, the Andean Pact Initiative to Control/Eliminate Chagas Disease and the Central America Initiative to Control/Eliminate Chagas Disease as well as compulsory blood-bank screening have substantially reduced new infection cases and decreased the burden of Chagas disease in the endemic regions (MONCAYO 2003). In the 1980s, 100 million people (25 % of all habitants of Latin America) were estimated to be at risk of infection, while 17.4 million people were infected in 18 endemic countries (WHO 2002) (Table 1.1). In 2005, according to estimations of the Pan American Health Organization, 20 % of the Latin American population were at the risk of infection (109 million people) and about 7.7 million people were infected (PAHO 2006) (Table 1.1). Most recent reports contain estimations of about 10 million infected people for 2010 (WHO 2011). The highest infection rates in Latin America were documented in Colombia, Bolivia, Paraguay and Argentina with

rates ranging from 21 %-30 % (WHO 2002). Since then the prevalence of *T. cruzi* infections decreased to values ranging from 1 %-6.8 % in 2005. However, 19 %-58 % are currently at risk of infection (RASSI *et al.* 2010) (Table 1.1). Chagas disease can result in significant morbidity. In 25-30 % of all infections it may become chronic and approximately 14,000 death were reported each year (MATTOCK & PINK 2005). Due to growing population movements, Chagas disease is becoming an emerging health problem in non endemic areas such as the USA, Canada and many parts of Europe and the western Pacific. Here an increasing number of infected immigrants has already been identified (SCHMUNIS 2007; GUERRI-GUTTENBERG *et al.* 2008; BERN & MONTGOMERY 2009; GASCON *et al.* 2010; RASSI *et al.* 2010) (Figure 1.1).

Table 1.1: Prevalence of *Trypanosoma cruzi* infection in Latin American countries in 1980-1985 (WHO 2002) and 2005 (PAHO 2006), and effect of initiatives to control or eliminate Chagas disease (RASSI *et al.* 2010, modified).*

	1980-1985		2005	
	Infected individuals [number (%)]	Individuals at risk of infection (%)	Infected individuals [number (%)]	Individuals at risk of infection (%)
Southern Cone Initiative (launched in 1991)				
Argentina	2,640,000 (10.0)	23	1,600,000 (4.1)	19
Bolivia	1,300,000 (32.0)	32	620,000 (6.8)	35
Brazil	6,180,000 (4.2)	32	1,900,000 (1.0)	12
Chile	1,460,000 (16.9)	63	160,200 (1.0)	5
Paraguay	397,000 (21.4)	31	150,000 (2.5)	58
Uruguay	37,000 (3.4)	33	21,700 (0.7)	19
Andean Pact Initiative (launched in 1997)				
Colombia	900,000 (30.0)	11	436,000 (1.0)	11
Ecuador	30,000 (10.7)$^{\Delta}$	41	230,000 (1.7)	47
Peru	621,000 (9.8)	39	192,000 (0.7)	12
Venezuela	1,200,000 (3.0)	72	310,000 (1.2)	18
Central America Initiative (launched in 1997)				
Belize	-	-	2,000 (0.7)	50
Costa Rica	130,000 (11.7)	45	23,000 (0.5)	23
El Salvador	900,000 (20.0)	45	232,000 (3.4)	39
Guatemala	1,100,000 (16.6)	54	250,000 (2.0)	17
Honduras	300,000 (15.2)	47	220,000 (3.1)	49
Nicaragua	-	-	58,600 (1.1)	25
Panama	200,000 (17.7)	47	21,000 (0.01)	31
Mexico	-	-	1,100,000 (1.0)	28
Total	17,395,000 (4.3)	25	7,694,500 (1.4)†	20

*(- =Data not available. $^{\Delta}$Prevalence of infected individuals was underestimated (AGUILAR *et al.* 1999). †Includes about 150,000 infected individuals living in USA and 18,000 in the Guianas, but data for these regions are not shown in the table.)

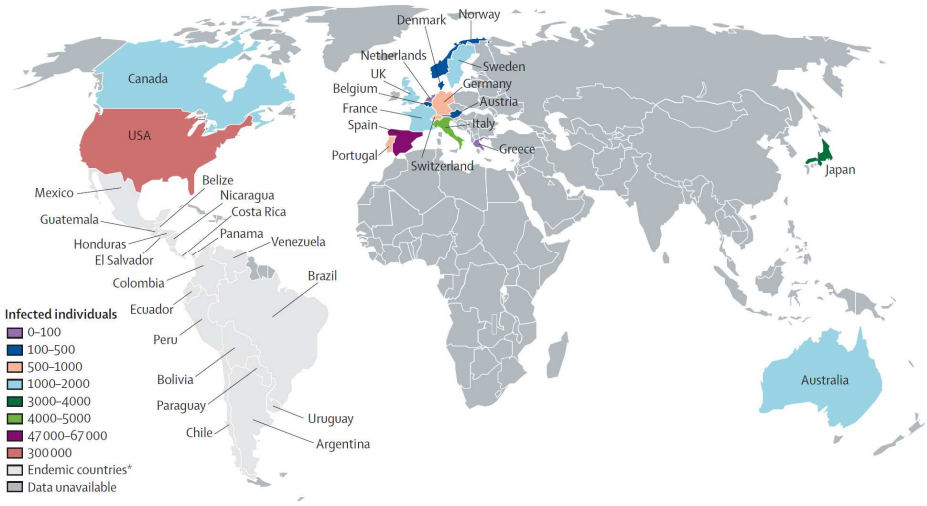

Figure 1.1: Estimated number of immigrants with *T. cruzi* infection living in non-endemic countries (RASSI *et al.* 2010).
Data are supplied for Canada, Australia and Japan in 2006; the USA in 2005; Spain in 2008 and other European countries in 2004-2006 (SCHMUNIS 2007; GUERRI-GUTTENBERG *et al.* 2008; BERN & MONTGOMERY 2009; GASCON *et al.* 2010).

1.1.2 The etiological agent *Trypanosoma cruzi*

T. cruzi, a protozoan flagellate, belongs to the family Trypanosomatidae, within the order Kinetoplastida. Recently, six lineages of *T. cruzi* strains (TcI-TcVI) have been classified (ZINGALES *et al.* 2009). TcI is the principal agent of Chagas disease north of the Amazon. TcII, TcV and TcVI are the main agents in the Southern Cone region. TcIII and TcIV are only sporadically infectious to humans. TcIV has divergent genotypes in South and North America (Figure 1.2) (LLEWELLYN & MILES 2010). During the parasite's developmental cycle, *T. cruzi* changes between a mammalian and an insect host. It passes through different developmental stages, which are a-, trypo-, epi- and spheromastigotes in line with the respective intermediary stages (BRACK 1968; SCHAUB & WUNDERLICH 1985; SCHAUB 1988c; SCHAUB & LÖSCH 1988; SCHAUB 1989; TANOWITZ *et al.* 1992; SCHAUB & POSPISCHIL 1995; TYLER & ENGMAN 2001).

The transmission of *T. cruzi* differs from that of other major insect-borne diseases in which the parasites invade the salivary glands of the insect host and are injected into the vertebrate host during a blood meal. In contrast, *T. cruzi* resides in the intestine, especially in the rectum of the triatomines. Here the metacyclic trypomastigotes develop. Sometimes during but always after engorgement, triatomines defecate, and droplets containing the parasites are deposited on the host's skin. The parasite may enter its host by passing through the bite site or the mucosal membranes (SCHUSTER & SCHAUB 2000).

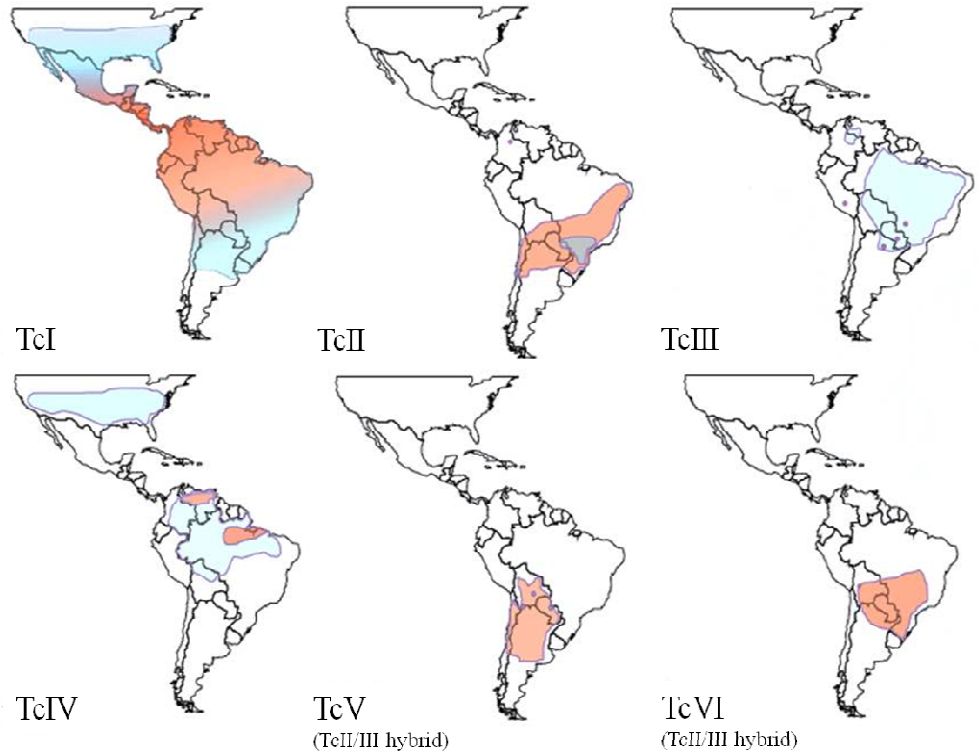

Figure 1.2: Approximate distributions of *T. cruzi* lineages.
Red labeled regions imply domestic populations (transmission cycles within domestic dwellings), blue labeled regions imply sylvatic populations (natural transmission cycles outside domestic dwellings) (LLEWELLYN & MILES 2010, modified).

Inside the vertebrate host, the parasite infects primarily cells in the surrounding of the entrance area, generally macrophages. In the phagosome of a macrophage, the parasite transforms into the amastigote form. After secretion of pore-forming proteins, it evades into the cytosol before the phagosome and the lysosomes fuse (BURLEIGH & ANDREWS 1995; CONTRERAS *et al.* 2002). The amastigotes divide repeatedly within the cytosol of the host cell and cystic nests, also known as pseudocysts, are formed in the tissue (SACKS & SHER 2002). Once the host cell's resources are depleted, the amastigote stages develop via pro- and epimastigote forms to trypomastigotes. These are released upon the bursting of the host cell. Blood trypomastigotes can only be detected within a short period of time in the blood. They are protected against the host's immune system by a surface coat of glycoproteins (HALL & JOINER 1991). Taking advantage of the circulating bloodstream, these trypomastigotes infect other organs. The flagellate changes again to the amastigote form and multiplies. If these blood trypomastigotes are ingested by a triatomine bug, they develop within the stomach, the main region of the anterior midgut, to epi- and spheromastigote forms. These developmental stages attach to the perimicrovillar membranes of the small intestine, the posterior midgut,

and multiply. Once the flagellates are passed to the rectum of the bug, they multiply and transform into the non-replicative metacyclic trypomastigote. This will be excreted with the feces of the bug.

Besides vectorial transmission, transmission by contaminated blood transfusion is another important transmission pathway. In contrast, transmission caused by contaminated food, organ transplants or perinatal transmissions from mother to child during pregnancy or birth is only of marginal importance (WHO 2008).

1.1.3 The disease

Chagas disease in humans is subdivided into two phases. The initial, acute phase of *T. cruzi* infection lasts for 4-8 weeks and is usually asymptomatic (DIAS *et al.* 1956; DIAS 1984; WHO 2002). In some cases, a focal oedema develops at the site of inoculation due to the parasites entering the host cells. An unilateral orbital oedema is named Romaña sign (CAROD-ARTAL & GASCON 2010). Clinical acute Chagas disease can involve febrile syndrome, headache, myalgia, facial oedema, abdominal pain, exanthema, lymphadenopathy and hepatosplenomegaly (PINTO *et al.* 2008). Severe myocarditis and acute encephalitis can also occur (MEDEIROS *et al.* 2008). Due to severe myocarditis or meningoencephalitis, <5-10 % of symptomatic cases die in the acute phase (RASSI *et al.* 2010). Most patients (60-70 %) seem to recover a healthy state and enter into the chronic phase. This phase is sometimes regarded to comprise two phases which are referred to as the intermediate and the determinate form. Both forms persist for the whole lifespan (DIAS *et al.* 1956; DIAS 1984; WHO 2002). In the intermediate phase, infected individuals develop no clinically apparent symptoms (RASSI *et al.* 2010). While the patients are positive for antibodies against *T. cruzi* in serum, they are asymptomatic, and no organ damage can be detected (normal electrocardiogram, normal in radiological examination of the chest, oesophagus and colon) (DIAS 1989; RASSI *et al.* 2010). The determinate chronic form of Chagas disease develops in 30-40 % of the cases (RASSI *et al.* 2010). Usually 10-30 years after initial infection, it can manifest as cardiac (extension of the heart), digestive (megaoesophagus and megacolon) or cardiodigestive (DIAS 1995; ARMAGANIJAN & MORILLO 2010; RASSI *et al.* 2010). A direct progression from the initial, acute phase to a clinical form of Chagas disease is reported in 5-10 % of cases (RASSI *et al.* 2010). Cardiomyopathy and its complications have been associated with death in 52 % of the cases (ARMAGANIJAN & MORILLO 2010). Autopsies of chagasic patiens with cardiomyopathy indicate cerebral damages in 17.5 % of the cases (ARMAGANIJAN & MORILLO 2010).

Human Chagas disease infections are treated by chemotherapy with two antiparasitic drugs, Nifurtimox® and Benznidazole®. Both are primarily disposed in the acute phase to treat the blood stages of *T. cruzi*. These therapeutic agents do not have a significant impact on parasites in the tissues. Patients treated in the acute phase are cured in 50-80 % of all cases (RASSI *et al.* 2010). Apart from this nonsatisfying therapeutic success, these therapeutics have strong side effects (SCHAUB & WUNDERLICH 1985; DOCAMPO 2007).

1.2 Triatominae

1.2.1 Systematic classification and distribution of Triatominae

The order Hemiptera is a very diverse order characterized by piercing sucking mouth parts. The majority of these species feed on plant juices or predates other insects. In the suborder Heteroptera, which is characterized by basal hardened forewings (hemielytra), all species of the families Cimicidae (bedbugs) and Polyctenidae (bat bugs) are bloodsuckers, whereas in the family Reduviidae (assassin bugs) only species of the subfamily Triatominae are obligate haematophagous. Only 0.18 % of the approximately 80,000 hemipteran species are triatomines, i.e. 140 species classified into six tribes (Alberproseniini, Cavernicolini, Bolboderini, Linshcosteusinii, Rhodniini and Triatomini) and 18 genera (SCHOFIELD & GALVAO 2009). The tribes Alberproseniini and Cavernicolini both contain only 1 genus, each with 2 species. The tribe Bolboderini consists of 4 genera with 14 species, while Linshcosteusinii possesses 1 genus with 6 species. The species-richest tribes are the Rhodniini with the genera *Rhodnius* and *Psammolestes* (in total 19 species) and the Triatomini with 9 genera and nearly 100 species; the genus *Triatoma* itself consists of 67 species (GALVÃO *et al.* 2003; SCHOFIELD & GALVAO 2009).

Triatomines are mainly occurring on the American continent from latitude 42° N to 46° S, a region between the Great Lakes of North America and Argentina (LENT & WYGODZINSKY 1979; SCHOFIELD 1994; GORLA *et al.* 1997). Species of the genus *Linshcosteus* are confined to the Indian subcontinent (SCHAUB 2009). *Triatoma rubrofasciata*, originating from the New World, has been distributed to many ports in tropical and subtropical regions by sailing ships (HARIDASS & ANANTHAKRISHNAN 1980; GORLA *et al.* 1997). Latin American triatomines mainly settle in sylvatic habitats, usually closely associated with their specific hosts, e.g. burrows of rodents, caves of bats and nests of birds (SCHAUB 2009). Nests are often colonized by species of Rhodniini, which prefer palm trees. Species of the genus *Panstrongylus* prefer tree cavities and burrows. *Triatoma* species often colonize rocky

habitats and rodent burrows (GAUNT & MILES 2000; SCHOFIELD & GALVAO 2009). In the course of colonization of forests and use of forest material to build human dwellings, individual species successfully adapted to peridomestic habitats, mainly using farm animals near the houses as host, and domestic habitats sucking blood of humans and animals inside the house (SCHAUB 2009). All triatomine species are potential vectors of *T. cruzi*, but *Triatoma infestans*, *P. megistus* and *Rhodnius prolixus* are representing the most important vectors in South America. Presumably due to the high adaption to human dwellings but also the wide distribution, *T. infestans* is the most important domestic species, most likely originating from sylvatic populations in the Andean valleys of Bolivia (NOIREAU *et al.* 2005). Although the appearance of *T. infestans* was seriously minimized by insecticide spraying campaigns, this species is still of big relevance in many regions of Latin America.

1.2.2 Developmental cycle of triatomines

Triatomines are temporary ectoparasites with a maximal size of 4.5 cm. They pass through a hemimetabolous development with 5 nymphal stages (first to fifth instar) to the adult stage within 3 to 24 months. The duration of nymphal developmental stages depends on species and environmental conditions like temperature and food supply (LENT & WYGODZINSKY 1979; SCHAUB 2008). About 20 to 30 days after copulation, the adult female starts to lay up to 600 eggs, mainly on the ground. Species inhabiting trees or nests glue the eggs to the leaves or feathers of birds (LENT & WYGODZINSKY 1979; SCHAUB 2008). The 3-12 months life span of adults depends on species, abiotic factors and availability of blood. First instars hatch 10 to 40 days after egg deposition, depending on species and environmental temperature (SCHOFIELD 1994). Already 3 days later, they are disposed for ingesting the first blood. If a food source is lacking, nymphal stages of triatomines can starve several weeks (SCHAUB & LÖSCH 1988). The starvation resistance of *T. infestans* after feeding in the second nymphal stage averages up to 275 days, in the third up to 432 days and in the fourth up to 322 days (SCHAUB & LÖSCH 1989). To reach the next nymphal stage, a full bloodmeal is essential. The abdominal extension activates stretching receptors. These induce moulting hormone secretion via the nervous system (BECKEL & FRIEND 1964). Secondary, ecdysone initiates the development of the new cuticle (WIGGLESWORTH 1940; ANWYL 1972; CHIANG & DAVEY 1988). This process may take 1.5 to 4 weeks. Under optimal conditions, *T. infestans* and *R. prolixus* require for the first, second, third, fourth and fifth nymphal stage 10, 10, 12, 17

and 28 and 9, 9, 10, 13 and 14 days between the first feeding and the moulting to the next nymphal stage, respectively (SCHAUB 1988b).

1.2.3 Host finding and feeding

Predominantly, triatomines are nocturnally active insects (ZELEDÓN & RABINOVICH 1981; LORENZO *et al.* 1991; LAZZARI 1992). They are classified as obligate bloodsuckers, although some species like *Triatoma klugi* ingest haemolymph of other insects (CARVALHO-PINTO *et al.* 2000). In contrast to mosquitos' males, male triatomines exclusively feed on blood. Triatomine bugs are vessel feeders, obtaining their blood meals directly from venules or arterioles of their vertebrate hosts (WENK & RENZ 2003; PEREIRA *et al.* 2006). The localization of a putative host is driven by different factors like carbon dioxide as part of the hosts' respiration, body heat and sweat components (NÚÑEZ 1982; LAZZARI & NÚÑEZ 1989; FLORES & LAZZARI 1996). These factors are recognized by different receptors in the antennae and mouthparts of the reduviid bug (SCHOFIELD 1994). Furthermore, ammonia derived from fresh conspecifics' feces is attracting (SCHAUB & POSPISCHIL 1995; GUERENSTEIN & GUERIN 2001; VITTA *et al.* 2002).

The insect's mouthparts consist of labrum, labium, mandibles and maxillae. In triatomines, the labrum and labium are forming the visible part of the biting apparatus, the proboscis, which is folded under the body at rest and protects the internal mandibles and maxillae. The maxillae are modified as needle-like stylets and joined to a maxillary bundle, which is placed between the mandibles. The left and right maxilla are moveable against each other in the longitudinal axis. Between them, the dorsally located food tube (38.6 µm diameter) and the ventral salivary tube (4.8 µm diameter) are formed (WIRTZ 1987; GULLAN & CRANSTON 1994).

After the bug has pierced the host skin, a blood vessel is searched by rapid whip-like intradermal movements of the maxillae (LAVOIPIERRE *et al.* 1959). A direct movement induced by the slightly higher temperature of the vessel also occurs (FERREIRA *et al.* 2007). If a vessel is found the right maxilla penetrates into the vessel while the left maxilla attaches on the vessel wall (LAVOIPIERRE *et al.* 1959; WIRTZ 1987). Then the bugs inject saliva and probe whether or not the vessel is suitable. The duration of this probing phase differs between a few seconds and several minutes (LAVOIPIERRE *et al.* 1959; SANT'ANNA *et al.* 2001). If no suitable vessel is found or the bug is disturbed, ingestion is interrupted, and the bug starts new attempts elsewhere (LAVOIPIERRE *et al.* 1959; SANT'ANNA *et al.* 2001). The blood is ingested

by the action of the pharyngeal and cibarial pump. The pumping is achieved by a complex of strong muscles occupying most of the insects head (BENNETT-CLARK 1963).

Triatomines ingest large amounts of blood, compared to other blood-sucking ectoparasites. The volumes vary – depending on species and nymphal stage – for nymphs between 3 and 23 times and for adults 1 and 3 times of their own body weight (summarized by MEISER 2009). *Dipetalogaster maxima* females ingest a volume of up to 3.8 ml of blood in only a single meal (SCHAUB & POSPISCHIL 1995). During the whole blood meal, which takes 20-50 minutes, saliva is released into the capillary of the host (LENT & WYGODZINSKY 1979; SCHAUB & POSPISCHIL 1995; SOARES *et al.* 2000).

The salivary glands of triatomines are located beside the pharynx in the anterior part of the thorax. The number of salivary glands differs between Rhodniini and Triatomini. Rhodniini possess two paired salivary glands, the larger reddish main gland, which shows a weak division into an anterior and a posterior lobe, and the uncolored smaller gland with supplemental function (BAPTIST 1941; MEIRELLES *et al.* 2003). Triatomini possess 3 paired salivary glands, a circular main gland (D1), a kidney-shaped supplemental gland (D2) and a reservoir gland (D3), which is the biggest one. While salivary gland D1 is slightly yellow, D2 is milky-white and D3 is transparent. All glands possess a single epithelial layer, covered by muscles and tracheae. The luminal contents of the three salivary glands are mixed during the release of saliva (BARTH 1954; LACOMBE 1999).

According to the proteome and transcriptome of salivary glands of different triatomines, the saliva contains a multitude of components. These facilitate the different steps of the feeding-process (SANTOS *et al.* 2007; ASSUMPCAO *et al.* 2008). Several salivary substances inhibit host pain enabling the bugs to feed without interruption by the host. A so far unspecified molecule from *T. infestans* inhibits sodium channel activity in nerves (DAN *et al.* 1999). Nitric oxide has a vasodilatatory effect, and in *R. prolixus* it is carried along with the saliva into the host skin by nitrophorines (NUSSENZVEIG *et al.* 1995). Coagulation of the hosts' blood is inhibited by a multitude of factors acting against different steps of hemostasis. Apyrase activity inhibits platelet aggregation and is reported for the saliva of more than 25 species of triatomines (RIBEIRO *et al.* 1998). Serine protease inhibitors of the Kazal-type inhibit thrombin, the most important factor of the blood coagulation cascade in vertebrates.

Components of the saliva of triatomines which are ingested during blood meal have to be considered for affecting *T. cruzi*, especially the pore-forming molecule trialysin, originating from the saliva of *T. infestans* (summarized by PAUSCH *et al.* in press).

1.2.4 Digestion

The digestive tract of triatomines is a simple tube without any diverticula (Figure 1.3). Ingested blood passes through the foregut to the midgut, which can be divided into the anterior region, subdivided into cardia and the anterior midgut (stomach), and the posterior region, the small intestine. The hindgut mainly consists of the rectum (KOLLIEN & SCHAUB 2000). The cardia is short and can hardly be separated from the adjacent, strongly distensible stomach (SCHAUB 2009). Morphologically, the small intestine can be divided into three parts of similar length: a thick anterior section, followed by a significantly narrowed middle section and a dilated posterior part (Figure 1.3). The hindgut begins with a very short pylorus region, in which the Malpighian tubules end, followed by the rectal sac (Figure 1.3) (SCHAUB 2009).

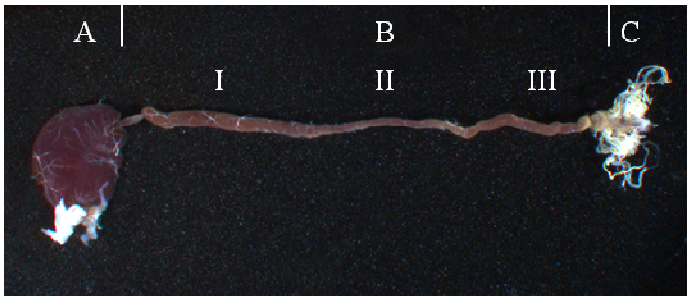

Figure 1.3: Digestive tract of fifth instar nymphs of *T. infestans* at 5 days after feeding.
A: cardia and stomach; B: small intestine with anterior (I), middle (II) and posterior region (III); C: Malpighian tubules and rectum.

After a blood meal, the ultrastructure of stomach and small intestine changes. The basal membranes in the epithelial cells of the stomach are unfolded to increase the surface area. This enables a rapid transport of aqueous compounds into the haemolymph (BILLINGSLEY & DOWNE 1989). The perimicrovillar membranes (syn. extracellular membrane layers; ecml) are formed in the midgut 12-24 h after blood ingestion. Microvilli of epithelial cells are covered by a staple of these apical membranes, which compartmentize the small intestine and thereby spatially separate primary and secondary digestion processes (BILLINGSLEY & DOWNE 1985, 1986; FERREIRA *et al.* 1988).

The ingested blood is stored mainly undigested in the stomach. Here the erythrocytes are lysed (AZAMBUJA *et al.* 1983). The ions are pumped through the stomach wall into the haemolymph. This drives water out of the stomach into the haemolymph and consequently, into the Malpighian tubules. Small portions of the blood meal are passed into the small intestine, where the blood is digested by cathepsin B and L-like cysteine proteases (TERRA *et al.*

1988; LOPEZ-ORDOÑEZ *et al.* 2001; KOLLIEN *et al.* 2004). Activities of cathepsin B and L-like proteases seem to be controlled on a transcriptional level while those of the aminopeptidase translationally or posttranslationally (HOUSEMAN & DOWNE 1983a). In the small intestine an additional cathepsin D-like aspartic protease is active (HOUSEMAN & DOWNE 1982, 1983a; TERRA *et al.* 1988; BORGES *et al.* 2006; BALCZUN *et al.* 2012). Blood contains many proteins, lipids and carbohydrates. Peptides are degraded by carboxy- and aminopeptidases (GARCIA & GUIMARAES 1979; HOUSEMAN & DOWNE 1981, 1983a; WANIEK *et al.* 2005). This aminopeptidase activity is associated with the outer perimicrovillar membranes (BILLINGSLEY & DOWNE 1985; FERREIRA *et al.* 1988).

The proteolytic activity is positively correlated to the degree of saturation (HOUSEMAN & DOWNE 1983b). The increase is proportional to the amount of ingested blood and the corresponding protein concentration in the small intestine (GARCIA & GARCIA 1977; HOUSEMAN *et al.* 1985). For enzyme production or secretion, mechanical factors, such as the distension of the stomach due to the ingestion of blood, were excluded as inducers (GARCIA & GARCIA 1977). The secretion of proteolytic enzymes into the lumen of the small intestine is managed by "membranous" lysosomes, while digestive activity in the rectum was excluded (GARCIA 1987; BILLINGSLEY & DOWNE 1988). Residuals of blood meal are stored in the rectum for further absorption processes, like the reabsorption of water or possibly amino acids by the rectal pads, before they are defecated (SCHAUB 2009).

1.2.5 Microorganisms in the digestive tract of triatomines

Communities of naturally occurring microorganisms in the digestive tract of insects are a widespread phenomenon in many taxa. Besides symbiotic bacteria, a wide variety of non-symbiotic microorganisms occurs in the digestive tract of triatomines (Table 1.2). During coprophagy, symbionts and these air-borne microorganisms get access to the intestinal tract. The contact of the mouthparts with the host's skin before penetration also bears a potential contamination risk (SCHAUB 2009). Furthermore, like all terrestrial insects triatomines swallow air before moulting (KOLLIEN *et al.* 2003). The digestive tract of *R. prolixus* hosts few bacterial species, the intestines of *P. megistus* and *T. infestans* possess up to 13 and 16 different bacteria, respectively (FISCHER 1989; REINTJES 1993). In addition to bacteria, also other microorganisms, e.g. fungi, flagellates and viruses, were found. From *P. megistus*, 37 fungi from 13 genera were isolated, among others *Penicillium corylophilum*, *Aspergillus fumigates* and *A. awamori* (MORAES *et al.* 2001). *Triatoma sordida* possessed also a slime mold of the

genus *Dictyostelium*. On agar plates of homogenates of the intestine of this nymph no bacteria developed (EICHLER 1998).

Another interaction is known for the hemolytic bacterium *Serratia marcescens*. This bacterium was isolated from the stomach of *R. prolixus* and seems to be apathogenic for this triatomine, but is pathogenic for other insects (FLYG *et al.* 1980; O'CALLAGHAN *et al.* 1996; AZAMBUJA *et al.* 2004). Prodigiosin producing *S. marcescens* (variant SM365) strains kill promastigotes of *Leishmania* and epimastigotes of the *T. cruzi* Y strain, but not those of the clone Dm28c (AZAMBUJA *et al.* 2004). However, after inhibition of the production of prodigiosin *Leishmania* are also killed (CASTRO *et al.* 2007b). D-mannose, an inhibitor of specific lectins, protects the flagellates against lysis (CASTRO *et al.* 2007a). However, this carbohydrate is not able to interfere with hemolysis. Probably, mannose receptors are involved in the attachment of bacteria and also in killing the flagellates (summarized by PAUSCH *et al.* in press).

Intestine homogenates of field-derived bugs also contained $Gram^+$ actinomycetes, on which the development of triatomines depends, since the food source blood is not sufficient for a suitable growth and reproduction of the triatomines (WIGGLESWORTH 1929; ASCHNER 1931) (Table 1.3). An absence of symbionts (aposymbiosis) induces various pathological effects in the bug. Typical aposymbiosis symptoms include disorders of digestion, excretion and moulting in line with a weakly melanised cuticle. Additionally, disturbance of nymphal development (>L3) results in a higher nymphal mortality rate (BRECHER & WIGGLESWORTH 1944; GEIGY *et al.* 1953; BEWIG & SCHWARTZ 1954; HARINGTON 1960; GUMPERT 1962; GUMPERT & SCHWARTZ 1962; BEN-YAKIR 1987).

Classification of symbiotic microorganisms always requires the proof of a noticeable positive host effect. All thus far identified symbionts of triatomines are actinomycetes, filamentous bacteria with a GC-rich genome, which develop in contrast to other bacteria not only as solitary cells but rather as filamentary mycels (WAKSMAN 1940). Each triatomine species possesses its own typical symbiont, but some bacteria are semi-symbiotic, i.e. they slightly support the development of triatomines. For *T. infestans, Rhodococcus triatomae* is totally symbiotic (Table 1.3) (summarized by PAUSCH *et al.* in press). Up to now the function of these symbionts remains elusive. A symbiotic involvement in digestive process was ruled out. Vitamin B supply through actinomycetes, known from other haematophagous insects, was furthermore excluded as auxotrophic mutant symbionts allow normal bug development (BRECHER & WIGGLESWORTH 1944; BEWIG & SCHWARTZ 1954; HILL *et al.* 1976).

Table 1.2: Genera of microorganisms isolated from the intestine of triatomine bugs in different investigations.[#]

bacterial genus/triatomine species	*R. prolixus*	*P. megistus*	*T. protracta*	*T. vitticeps*	*T. brasiliensis*	*T. sordida*	*T. infestans*	*T. klugi*
Acetinobacter								15
Achromobacter		13						
Actinobacter				18				
Actinomyces		13						
Alcaligenes								15
Athrobacter		13			15			
Aureobacterium		13						
Aurococcus								15
Bacillus		13		18	15		13, 17	
Bacterium							4	
Bordetella					15			15
Brevibacterium		15					13	
Candida						17	16	
Cellulomonas							16	
Citrobacter					15			
Corynebacterium	8, 10	13	4		15		4, 8, 10	
*Dietzia**								15
Enterococcus	3, 8, 10	8, 14		8, 18	8		1	
Escherichia	10							
Flavimonas								15
*Gordonia**				18	15	17		
Micrococcus				18			4, 10, 16	15
Micromonospora				18				
Moraxella							16	
Mycobacterium	10			18		17	8	
*Nocardia**	10						10, 16,17	
Paenibacillus				18				
Pasteurella					15			15
Pseudomonas	9	8, 13, 14		8, 18			2, 8	15
Psychrobacter		15						15
*Rhodococcus**	1, 4, 5, 6, 7, 8, 9, 11, 12	8			8	17	1, 4, 8, 16	
Saccaropolyspora				18				
Serratia	19							
Sporosarcina		15						
Staphylococcus	10	13, 15	4	18	15		8, 10	15
Streptococcus	8	14		18			3	
Streptomyces							4,16	
Symbiotes	8						8	
Weeksella/ Emptobacter		15			15			

[#]summarized from HOFFMANN (1992) and EICHLER (1998); actinomycetes are marked by an asterisk*; numbers refer to the following respective investigation: 1: BRECHER & WIGGLESWORTH (1944); 2: WEURMAN (1946); 3: BEWIG & SCHWARTZ (1954); 4: GOODCHILD (1955); 5: BAINES (1956); 6: MÜHLPFORDT (1959); 7: HARINGTON (1960); 8: GUMPERT & SCHWARTZ (1962); 9: LAKE & FRIEND (1967); 10: CAVANAGH & MARSDEN (1969); 11: HILL *et al.* (1976); 12: BEN-YAKIR (1987); 13: FISCHER (1989); 14: FIGUEIREDO *et al.* (1990); 15: HOFFMANN (1992); 16: REINTJES (1993); 17: EICHLER (1998); 18: ROGL (2001); 19: AZAMBUJA *et al.* (2004)

Table 1.3: Interaction of actinomycetes and the reduviid bug *T. infestans*.*
(JUNG 1995, modified)

Actinomycete	Establish-ment	Develop-ment	Repro-duction	Hatching rate [%]	Classification
Nocardia asteroides	+	-	-	-	non-symbiotic
Nocardia farcinica	+	±	±	59	partially symbiotic
Rhodococcus equi	+	+	±	67	partially symbiotic
Rhodococcus rhodnii	-	+	±	17	non-symbiotic
Dietzia maris	+	+	+	61	partially symbiotic
Rhodococcus triatomae	+	+	+	80	totally symbiotic

*Establishment: Actinomycete is able (+)/not able (-) to establish within the intestine of *T. infestans*; Development: Actinomycete has positive (+) or no influence (-) on the development of *T. infestans*; Reproduction: Actinomycete has positive (+) or no influence (-) on the reproduction of *T. infestans*; Hatching rate: Percentage of eggs, of which nymphs hatched

Symbionts develop extracellularly in the lumen of the intestinal tract of triatomines and not – like in other insects – in special organs (mycetomes), which are protecting the symbionts against immune defense mechanisms of the host (BRECHER & WIGGLESWORTH 1944; BROOKS 1963; HINDE 1971; DOUGLAS 1989). Within a bug population symbionts are transmitted via coprophagy immediately after feeding (SCHAUB 1988c; SCHAUB 1989). First nymphal stages can also obtain their symbionts via feces contaminations on eggshells (BRECHER & WIGGLESWORTH 1944; BAINES 1956). Transovarial transfer via the cytoplasm of the oocytes does not occur in triatomines. After ingestion of a mixture of complement-inactivated blood and *Rhodococcus rhodnii* or *R. triatomae*, the respective symbionts of *R. prolixus* and *T. infestans*, only *R. triatomae* establishes in the intestine of *T. infestans*, indicating refractory mechanisms (EICHLER 1998). Feeding *T. infestans* a mixture of *Candida* sp., *Dietzia maris*, *Escherichia coli* or *Gordonia rubropertinctus*, *Candida* sp. is killed immediately after ingestion. Numbers of *D. maris*, *E. coli* and *G. rubropertinctus* are substantially reduced within the first week in *T. infestans*. However, in *R. prolixus* only *Candida* sp. and *E. coli* are killed likewise, whereas the actinomycetes *D. maris* and *G. rubropertinctus* establish in the stomach and small intestine (EICHLER 1998).

In the stomach of fifth instars of *R. prolixus*, the number of symbiotic and non-symbiotic bacteria increases approximately 10,000-fold in the first two days after blood ingestion. This number is stable for 5 days after feeding. The number decreases with starvation but increases again after the next feeding (AZAMBUJA *et al.* 2004). In *R. prolixus* as well as *T. infestans*, the population of the respective symbiont *R. triatomae* (Table 1.3) is strongly di-

luted by the ingested blood and increases only in the stomach within the first week. The small intestine of both species show a 99 % reduced number of symbionts, compared to the stomach of the unfed nymphs (EICHLER & SCHAUB 2002).

1.3 Interactions of *Trypanosoma cruzi* and triatomines

1.3.1 Subpathogenicity of *Trypanosoma cruzi* in triatomines

In a comparison of the development and mortality of uninfected and *T. cruzi*-infected regularly fed nymphs, there are no effects evident (summarized by SCHAUB 2009). Under optimal conditions, the amount of ingested blood seems to be adequate to compensate the loss of metabolites due to the parasite's presence. However, in *T. cruzi*-infected bugs starvation capacity is reduced. Established infections of third, fourth and fifth instar nymphs that are fed and thereby molt into the next instar, reduce the starvation capacity by 3 %, 14 % and 32 %, respectively (SCHAUB & LÖSCH 1989). Since many parasites die in starved bugs, an accumulation of *T. cruzi* derived toxins seems to be unlikely (KOLLIEN & SCHAUB 1998a). Since the intestine of dead bugs contains remnants of digested blood, it is not the competition for the nutrients but rather essential metabolites which determines the starvation capacity.

An effect on the intestinal immune homeostasis is evident in long-term infected *T. infestans* (summarized by SCHAUB *et al.* 2011). A supplementation of blood with fungi and bacteria and the experimental infection of nymphs results in a development of these microorganisms, whereas in uninfected bugs the development is inhibited. The number of symbionts is similar in both bug groups (see 1.2.5 and 1.4.2).

1.3.2 Interactions with digestive enzymes, hemolysins and agglutinins of the vector

The parasite is capable of establishing in the bug's gut. Here, a diversity of digestive enzymes is constantly present. Different compositions of digestive factors have been reported to characterize the different gut regions (summarized by SCHAUB 2009). *T. cruzi* population size in the rectum is significantly higher compared to the population size of the small intestine, where the proteolysis takes place via cathepsins. Thus, the function of digestive enzymes as possible population controlling factors seems possible. Therefore, the question arose, whether these enzymes act as a barrier to infection or affect the development. Nevertheless, the rectal cuticle offers better attachment facilities for the flagellates in contrast to the small intestine, where the perimicrovillar membranes develop after blood ingestion. Feeding experiments using blood supplemented with pepstatin, a SH-proteinase acting as a cathepsin D in-

hibitor, show no effect on the population density of *T. cruzi* in the vector *R. prolixus* (GARCIA & Gilliam 1980). In the small intestine, levels of cathepsin B encoding mRNA are similar in *T. cruzi*-infected and uninfected insects (URSIC-BEDOYA & LOWENBERGER 2007). However, cathepsin D activity in the small intestine is increased at one and three days after ingestion of *T. cruzi* infectious blood (BORGES *et al.* 2006).

Hemolytic factors are responsible for the lysis of erythrocytes in the stomach of triatomines. After the release of the hemoglobin, proteolytic enzymes can digest this protein in the small intestine. In the stomach of *R. prolixus*, hemolytic factors lyse epimastigotes of *T. cruzi* strain Y, which are not agglutinated. Epimastigotes of *T. cruzi* clone Dm28c and strain Cl are agglutinated and not lysed (AZAMBUJA *et al.* 1989). A possible explanation is the different genotype of the strains, since strain Y belongs to lineage TcII, while clone Dm28c is classified into TcI and the strain Cl into TcIV (ZINGALES *et al.* 2009).

1.3.3 Interactions with the mammalian complement system in the vector

Relating to the complement system of the mammalian hosts, only metacyclic trypomastigotes possess the capacity to survive in mammals. Epimastigotes are lysed by the complement system (VICKERMAN 1985). After complete genome sequencing a variety of surface encoding genes is known. These numerous genes probably allow the evasion of the vertebrate host immune response (EL-SAYED *et al.* 2005). Differentiation of trypomastigotes into epimastigotes is initiated shortly after ingestion. Genes encoding for surface molecules, such as the members of the mucin and mucin-associated surface proteins are concurrently expressed in the epimastigote phase of *T. cruzi* (EL-SAYED *et al.* 2005). The corresponding gene products may prevent lysis of the intermediate stages by factors present in the intestine of the vector, e.g. the vertebrate complement system. In *R. prolixus*, the complement system is not inhibited immediately, but within two hours after blood ingestion a significantly reduced activity can be detected, which persists up to two days afterwards (Garcia, unpublished). In addition, the saliva and the stomach of triatomines contain inhibitors, which are able to inhibit the complement system (BARROS *et al.* 2009). The sensitivity of *T. cruzi* is demonstrated by the fate of the population in the stomach. In established *T. cruzi* infections, epimastigotes in the stomach are killed after ingestion of blood from chickens or rats. Mouse blood possesses only a weak complement system. Thus, the epimastigotes survive after blood ingestion (summarized by SCHAUB 2009). If the complement system of ingested blood kills the trypanosomes, the stomach is not re-colonized by trypanosomes from the small intestine

before all blood has passed to the small intestine. The reflux is also indicated by a brownish colorization of the stomach contents.

1.4 The immune system of insects

Not only mammals but also insects possess innate immunity. Herein, activation cascades are quite similar. In insects, the hemolymph acts as an open circulation system in which both cellular and humoral reactions occur. Cellular immune response involves e.g. haemocytes. In contrast, the intestinal immune system is suggested to possess only humoral components (summarized by MÜLLER *et al.* 2008).

1.4.1 Cellular immune response

The cellular immune response is controlled and activated by circulating haemocytes in the abdominal cavity (MATOVA & ANDERSON 2006). The classification of haemocytes varies according to species and authors (MÜLLER *et al.* 2008). Therein often five types of haemocytes have been classified in insects: the prohaemocytes, plasmatocytes, granular cells, oenocytoides and spherulocytes (ARAUJO *et al.* 2008). The defense mechanism against pathogens and therefore the interaction of haemocytes is adapted to the cruelty of the infection. A slight infection with only few bacteria induces phagocytosis (BRIGGS & ROCKSTEIN 1964; LACKIE 1988a). After phagocytosis, haemocytes use lysosomal acidic enzymes such as phosphatases, peroxidases and esterases to kill and digest the ingested bacteria. Higher numbers of bacteria and bigger particles induce cellular encapsulations (GÖTZ 1988; LACKIE 1988b). Mostly, encapsulation is accompanied by the formation of melanin. Therefore, the proteolytically activated phenoloxidase oxidizes mono- and diphenols, such as tyrosine, and the resulting quinines polymerize to melanin (TRENCZEK 1992). In cellular encapsulations, plasmatocytes change to a fibroblast-like shape and attach to the foreign surface. After attachment, the granular cells are releasing components of the humoral immune response and mediators that attract other haemocytes. Nodule formation is a combination of the described mechanisms. Therein, masses of bacteria are not only phagocytised, but haemocytes aggregate to prevent the spread of pathogens in the haemocoel (SALT 1970; TRENCZEK 1992).

1.4.2 Humoral immune response

Different soluble proteins of the haemolymph, e.g. lectins, which agglutinate foreign cells, are involved in the humoral immune response of insects. Although insects do not pos-

sess an immune response controlled by specific antibodies, the activation of genes for the production of the humoral components is comparable with vertebrates' immune response (MÜLLER *et al.* 2008). In some dipteran larvae, such an encapsulation and melanisation occurs without an involvement of haemocytes, which is so-called humoral encapsulation (GÖTZ & VEY 1974).

Other components of the humoral immune response are mainly antibacterial peptides or proteins, which can be classified into five groups, corresponding to their biochemical properties (Table 1.4). Due to the lack of cysteine residues, α-helical peptides are linear. Cecropins, belonging to this group, were the first inducible antimicrobial peptides isolated from insects (HULTMARK *et al.* 1982). Acting against $Gram^-$ as well as $Gram^+$ bacteria and fungi, cecropins are small peptides of 31-39 amino acid residues (Table 1.4). So far, 21 cecropins were isolated from the haemolymph and the digestive tracts of insects (MORISHIMA *et al.* 1995; BREY & HULTMARK 1998; EKENGREN & HULTMARK 1999; SAITO *et al.* 2005; WANG *et al.* 2007). Produced by transformed symbionts in the gut of the reduviid bug *R. prolixus*, cecropin kills all *T. cruzi* stages. In contrast, bugs containing non-modified symbionts remain infected (BEARD *et al.* 2002). Other antimicrobial peptides are acting against *T. cruzi* only *in vitro* (summarized by PAUSCH *et al.* in press).

Defensins belong to the cysteine-rich peptides, characterized by a high number of cysteine residues. Based on the arrangement of the disulfide bridge-forming cysteine residues four types of defensins can be classified: classical defensins, β-defensins, cyclic defensins and insect defensins (Table 1.4) (GANZ & LEHRER 1995). Insect defensins possess six cysteine residues, forming three disulfide bridges. They are classified as pore-forming peptides with activity against $Gram^+$ bacteria and fungi as well as some $Gram^-$ bacteria (Table 1.4). Defensins are synthesized by Diptera, Coleoptera, Hymenoptera and Heteroptera (BULET *et al.* 1993; ARAUJO *et al.* 2006).

Proline-rich peptides are characterized by a Pro-Arg-Pro sequence as well as by O-glycosylated substitutions (COCIANCICH *et al.* 1994). Within this group, there is no consistent classification related to the area of action. Abaecin and apidaecin are known from honey bees. While abaecin is active against $Gram^+$ and $Gram^-$ bacteria, apidaecin is only slightly effective against $Gram^-$ bacteria (Table 1.4) (CASTEELS *et al.* 1989; 1990).

Glycine-rich peptides are representing the most variable group of the antibacterial peptides and proteins and are characterized by a high content of glycine residues in their amino acid sequence (Table 1.4). Attacins are the best studied members in this group with a molecular mass of 20-23 kDa. They were first isolated from the haemolymph of the silk moth

Hyalophora cecropia (ENGSTRÖM *et al.* 1984a). In this insect, different isoforms of attacins occur, characterized by different isoelectric points (HULTMARK *et al.* 1983; ENGSTRÖM *et al.* 1984b). Recently, sequences of antimicrobial peptides from triatomines, related to the diptericin/attacin family were included in the database (GenBank accessions ACC68686.1, ACB06753.1 and ACG50017.1). However, the interaction with flagellates and bacteria remains to be investigated (summarized by PAUSCH *et al.* in press).

Lysozymes are ubiquitous in all multicellular animals and plants and are classified into four groups, corresponding to the position of the active centre: chicken (c)-type, goose (g)-type, the invertebrate (i)-type and the T4-type from bacteriophages (HULTMARK 1996; GRUNCLOVÀ *et al.* 2003). C-type lysozymes were so far found in birds, mammals, fishes, reptiles and invertebrates (JOLLÈS *et al.* 1979; GRINDE *et al.* 1988). They are characterized by their ability to hydrolyze the β-(1,4)-glycosidic linkages between the C1 of N-acetylmuramic acid and the C4 of N-acetylglucosamine in the peptidoglycan layer of bacterial cell walls. Insect lysozymes mostly belong to c-type lysozymes (DAFFRE *et al.* 1994; LEE & BREY 1995; HULTMARK 1996; DIMARCQ *et al.* 1998). Some, like a lysozyme from *Anopheles gambiae*, are members of the group of i-type lysozymes (PASKEWITZ *et al.* 2008). Despite their different origin, the biochemical characteristics of the different lysozymes are comparable. The preferential basic proteins with a molecular mass between 13 and 16 kDa are heat stable in acidic milieus whereas they are instable in basic milieus (ABRAHAM 1939; KINOSHITA & INOUE 1977). Mostly, the pH-optimum is between pH 6 and pH 7, in the case of the rainbow trout *Salmo gairdneri* and the scallop *Chlamys islandica* at pH 5.5 or rather pH 4 (GRINDE *et al.* 1988; NILSEN *et al.* 1999).

At the beginning of the 20th century, bacteriolytic activity in the gut of triatomines was first described (DUNCAN 1926). The expression of genes encoding for lysozymes were detected in the digestive tract and the fat body of *R. prolixus*, *T. infestans* and *T. brasiliensis* (KOLLIEN *et al.* 2003; ARAUJO *et al.* 2006; BALCZUN *et al.* 2008; URSIC-BEDOYA *et al.* 2008). In contrast to other antimicrobial peptides, genes encoding lysozymes are often expressed constitutively, e.g. in the fatbody of *Bombyx mori* (MORISHIMA *et al.* 1995). Subsequent to the synthesis in the fatbody, lysozyme is transported to the haemolymph. There, it acts as part of the unspecific immune defense (ANDERSON & COOK 1979). Defensin encoding genes were expressed in the digestive tract and fat body of *R. prolixus*, the salivary glands and the fat body of *T. brasiliensis* (LOPEZ *et al.* 2003; ARAUJO *et al.* 2006; WANIEK *et al.* 2009a).

In addition to their antibacterial activity, some non-triatomine peptides like mellitin, magainin, dermaseptin and tachyplesin also possess the ability to kill trypanosomes *in vitro*

(GARCIA *et al.* 2010). However, this occurs using higher than the naturally occurring concentrations. More relevant for an understanding of the interaction of *T. cruzi* and antibacterial compounds are investigations considering nitric oxide (WHITTEN *et al.* 2007). The gene encoding for nitric oxide synthase is up-regulated in the stomach after infection. In the small intestine and rectum, more nitrite can be detected, in the rectum even before the parasite is present. The expression of a lysozyme encoding gene in *R. prolixus* is induced after infection with *T. cruzi*, a different one is only expressed in the hemolymph (URSIC-BEDOYA *et al.* 2008).

Table 1.4: Groups and representatives of antibacterial peptides and proteins in insects.

	Insect group	Mass [kDa]	Spectrum	References*
α-helical peptides				
Cecropins	Lepidoptera, Diptera	4-7	$Gram^+$, $Gram^-$, fungi, viruses	4, 11, 12, 13, 22
Cysteine-rich peptides				
Defensins	Diptera, Hemiptera	4-5	$Gram^+$, fungi, protozoa	8, 10, 14, 15, 16
Drosomycin	Diptera	5	fungi	17
Proline-rich peptides				
Thanatin	Hemiptera	2.4	$Gram^+$, $Gram^-$, fungi	18
Drosocin	Diptera	2.5	$Gram^-$	15, 20
Abaecin	Hymenoptera	4	$Gram^+$, $Gram^-$	9, 15
Apidaecin	Hymenoptera	2	$Gram^-$	15, 20
Metalnikowins	Hemiptera	3	$Gram^-$	20
Pyrrhocoricin	Hemiptera	4	$Gram^+$, $Gram^-$	20, 21
Glycine-rich peptides				
Attacins	Lepidoptera, Diptera	20-23	$Gram^-$	5, 6, 7, 15
Sarcotoxins II	Diptera	24-30	$Gram^-$	15, 20
Diptericin	Diptera	9	$Gram^-$	20
Coleoptaecin	Coleoptera	8	$Gram^-$	17
Hymenoptaecin	Hymenoptera	10	$Gram^-$	15, 20
Drosomycin	Diptera	5	$Gram^-$, fungi	17
Hemiptericin	Hemiptera	15	$Gram^-$	15, 20
Lysozymes	ubiquitary	13-17	$Gram^+$	1, 2, 3, 19

*The references corresponding to the respective number are the following:
1: MALKE (1965); 2: MOHRIG & MESSNER (1968); 3: JOLLÈS *et al.* (1979); 4: HULTMARK *et al.* (1982); 5: HULTMARK *et al.* (1983); 6: ENGSTRÖM *et al.* (1984a); 7: ENGSTRÖM *et al.* (1984b); 8: MATSUYAMA & NATORI (1988); 9: CASTEELS *et al.* (1989); 10: LAMBERT *et al.* (1989); 11: KYLSTEN *et al.* (1990); 12: MORISHIMA *et al.* (1990); 13: TANIAI *et al.* (1992); 14: CHALK *et al.* (1994); 15: COCIANCICH *et al.* (1994); 16: DIMARCQ *et al.* (1994); 17: FEHLBAUM *et al.* (1994); 18: FEHLBAUM *et al.* (1996); 19: REES *et al.* (1997); 20: BULET *et al.* (1999); 21: SCHNEIDER & DORN (2001); 22: LAVINE & STRAND (2002)

1.5 Objectives

The development of *T. cruzi* in the invertebrate host has been intensively investigated throughout the past decades (CHAGAS 1909; BRACK 1968; ZELEDÓN *et al*. 1984; SCHAUB 1988c; ALVARENGA & BRONFEN 1997; KOLLIEN & SCHAUB 2000; SCHOFIELD 2000). Previous studies focused on the population density and the developmental stages of *T. cruzi* in the digestive tract and the effect of the bug's nutritional stage, i.e. of feeding and starvation (summarized by KOLLIEN & SCHAUB 2000; SCHAUB 2009). However, in the interactions between *T. infestans* and *T. cruzi*, a parasite induced intestinal immune response has rarely been considered (summarized by GARCIA *et al*. 2010). Pathogen detection and identification precede the development of an immune response and are crucial for an organism's survival (MÜLLER *et al.* 2008). Therefore, new investigations need to focus on the physiological reactions following parasite identification.

The present thesis aimed to investigate the parasite induced immune response to *T. cruzi*-infection in *T. infestans* applying molecular and protein biochemical tools. Elucidation of the intestinal immune responsive bacteriolytic active compounds will provide a more detailed understanding of host parasite interactions. The thesis is divided into 2 chapters addressing the parasite induced humoral immune response in *T. infestans* and characterizing bacteriolytically active compounds. Lysozymes were biochemically characterized as antimicrobial compounds of the insects' humoral immune system using an *in vivo* approach. Taking advantage of their charge, lysozymes were separated by high-performance liquid chromatography. Bacteriolytic activity of separated fractions was determined, including determinations of the optimal pH-conditions of this activity. Subsequently, peptidergic components were identified through mass spectrometry. The bacteriolytic activities in the posterior digestive tract were examined using a qualitative approach and correlated to the concentration of soluble proteins in the digestive tract. The major part focused on investigations of the intestinal bacteriolytic activity of non-infected and long- and short-term *T. cruzi*-infected *T. infestans*. Factors inducing the intestinal immune response were elucidated by the feeding of mixtures of blood with blood trypomastigotes, surface coat of blood trypomastigotes, blood trypomastigotes without surface coat and epimastigotes. At different days after feeding, the level of bacteriolytic compounds was determined photometrically at different pH-values and the composition of these compounds in zymograms. This was correlated to genes encoding different lysozymes, of which the expression level was determined in quantitative reverse transcriptase PCR (qRT-PCR).

CHAPTER 2

GENERAL MATERIALS AND METHODS

THIS CHAPTER DESCRIBES MATERIAL AND METHODS, WHICH ARE USED IN CHAPTERS 3 AND 4.

2. General Materials and Methods

In the following, the material and methods used in chapters 3 and 4 are described in detail.

2.1 Materials: Insect source and maintenance

Triatoma infestans strain "Chile" originates from Cachiyuyo, Chile. Non-infected bugs were fed on chickens every 3-4 weeks and reared at 27 ± 1 °C, 70-80 % relative humidity and a 16h/8h light/dark rhythm (KOLLIEN & SCHAUB 1998a). The bugs were maintained in groups of about 150 specimens in two-liter beakers (SCHAUB 1989). An *in vitro* culture of the *T. infestans* symbiont *Rhodococcus triatomae* (YASSIN 2005, YASSIN & SCHAAL 2005) was cultured in Standard I medium (Merck, Darmstadt, Germany), harvested in the exponential growth phase and added to the triatomines after each feeding (EICHLER & SCHAUB 2002).

2.2 Methods

2.2.1 Measurement of protein concentrations and antibacterial activity

The concentration of soluble protein was determined in a commercial Bradford assay (BRADFORD 1976) modified according to ZOR & SELINGER (1996). For each measurement, 15 µl high-purity water were mixed with 5 µl sample and 80 µl reagent (Roti®-Nanoquant, Roth). Duplicates of 40 µl were aliquoted. The readings of the 96-well plates were done in a Model 680 ELISA-reader (Biorad, München, Germany). Different concentrations of BSA ranging from 10 µg/ml up to 175 µg/ml were used as protein standards. Protein concentration of individual samples was calculated by determining the slope of a standard optical density curve.

Bacteriolytic activity of small intestine contents and homogenates and rectum homogenates against *Micrococcus lysodeikticus* was measured as change in optical density of a mixture of 30 µl Britton-Robinson-Buffer (0.15 % (w/v) boric acid, 0.15 % (v/v) acetic acid, 0.19 % (v/v) phosphoric acid) (BRITTON & ROBINSON 1931) with the respective pH (pH 3.0 to pH 8.0), 50 µl substrate (final concentration 0.015 % (w/v) lyophilized *M. lysodeikticus*), 12 µl high-purity water and 5 µl of the respective sample. A similar mixture was used to determine the bacteriolytic activity after chromatographic separation. Here, a Britton-Robinson buffer pH 6.0 and no water was used, but 20 µl of the respective sample. Blanks were per-

formed without sample but high-purity water. The optical density was measured at 415 nm for 30 min in a Model 680 ELISA-reader (Biorad, München, Germany). The resulting differences of optical density (ΔOD) were used to calculate the activity/µg protein. Three independent biological samples were used in duplicate measurements. All statistics were done using *t*-tests in pairwise comparisons (DATEN-CONSULT 2011).

2.2.2 SDS-polyacrylamide gel electrophoresis and zymography

Protein separation was performed using SDS-polyacrylamide gel electrophoresis according to LAEMMLI (1970) under non-reducing conditions using 13 % T separating gels. Gels of 75 x 80 x 0.5 mm were run in a Hoefer SE 260 (GE Healthcare, Freiburg, Germany) with a maximum voltage of 300 V. After electrophoresis, proteins were stained for 15 min in Coomassie solution (0.002 % (w/v) Coomassie Brilliant Blue G250, 47.5 % (v/v) methanol, 10 % (v/v) acetic acid) and destained in 10 % (v/v) acetic acid until the background was clear (MEISER 2009).

Zymography was performed using 0.3 % *M. lysodeikticus* in separating gels (CYTRYNSKA *et al.* 2001; HARDT *et al.* 2003). After electrophoresis, proteins were renaturated twice in Britton-Robinson buffer (pH 6.0) (BRITTON & ROBINSON 1931) supplemented with 0.1 % (v/v) Triton X-100 (Sigma, Steinheim, Germany). After pH verification, buffer was changed and zymograms were incubated at 37 °C over night. Staining was performed for 1-2 min in freshly prepared 0.1 % (w/v) methylene blue in 0.001 % (w/v) NaOH. Zymograms were destained in water until the stacking gel was clear. Gels and zymograms were analyzed and molecular masses were calculated in reference to a standard protein mix (Fermentas, St. Leon-Roth, Germany) using ImageMaster™ 1D Version 4.0 (GE Healthcare, München, Germany).

2.2.3 Enzymatic digestion of proteins for mass spectrometry

Supernatants of small intestine contents from non-infected and *T. cruzi*-infected *T. infestans* (see 3.2.4) and protein samples of small intestine homogenates separated via anion exchange chromatography (see 4.2.2) were used. Proteins were separated by SDS-PAGE (see 2.2.2) to determine the bacteriolytically active compounds of small intestine contents and proteins of about 13 and 25 kDa were considered. In order to distinguish patterns of bacteriolytic compounds from small intestine homogenates after anion exchange chromatography, flow-through and fractions of bacteriolytic activity were concentrated at 4 °C and

13,000 *g* in ultra filtration tubes with a 4 kDa exclusion limit (Interstep, Witten, Germany) and mixed with reducing sample buffer (30 % (v/v) glycerol, 150 mM Tris-HCl, pH 7, 12 % (w/v) SDS, 60 mM DTT supplemented with bromphenol blue) and loaded on a 4-12 % Anamed^{Pro} gel (Anamed, Groß-Bieberau, Germany). Electrophoresis was carried out in running buffer (25 mM Tris, 192 mM glycine, 35 mM SDS) for 15 min in a XCell surelock apparatus (Invitrogen, Karlsruhe, Germany) using 50 V and 3,000 W as limits. After fixation in 50 % (v/v) methanol and 2 % (v/v) phosphoric acid, gels were washed three times for 10 min in high-purity water, then equilibrated in 34 % (v/v) methanol, 2 % (v/v) phosphoric acid and 17 % (w/v) ammonium sulfate for 30 min and stained over night in equilibration solution supplemented with 0.01 % (w/v) Coomassie G250.

Subsequently, protein bands obtained from homogenates and small intestine contents were excised and destained by alternating incubations in 10 mM ammonium bicarbonate and 5 mM ammonium bicarbonate in 50 % (v/v) acetonitrile for 10 min, respectively, until the bands were transparent. In-gel digestion and sample preparation for LC/MS analysis was performed according to MEISER (2010).

2.2.4 Nano-HPLC and Electrospray ionization tandem mass spectrometry

Online reversed-phase nano HPLC separations were performed using the Dionex U3000nano HPLC system (Dionex, Idstein, Germany) with a C18 precolumn and a C18 separation column. Peptides were loaded on-line and preconcentrated with 0.1 % (v/v) trifluoroacetic acid with a flow rate of 7 µl/min for 10 min on the precolumn (0.075 mm I.D. x 20 mm length, 3 µm particle size, 100 Å pore size, 60 °C column temperature, Acclaim PepMap100, Dionex) using the loading pump. Separation was performed using a separation column (75 µm I.D. x 250 mm length, 2 µm particle size, 100 Å pore size, 60 °C column temperature, Acclaim PepMap100, Dionex) and a nanopump with a flow rate of 400 nl/min. Solvent A (0.1 % (v/v) formic acid) was used for equilibration, while solvent B (0.1 % (v/v) formic acid, 84 % (v/v) acetonitrile) was used to generate a gradient of 5 % to 30 % in 95 min. Solvent B was increased to 95 % within a 2 min time frame. Both columns were washed with 95 % solvent B for 7 min. The columns were reequilibrated with 5 % solvent B for at least 20 min.

Electrospray ionization tandem mass spectrometry (ESI-MS/MS) was performed on a LTQ Velos Orbitrap equipped with a nanoelectrospray ion source (Thermo Scientific, Bremen, Germany). The mass spectrometer was externally calibrated with standard com-

pounds. General parameters for mass spectrometry were as follows: spray voltage: 1.4-1.5 kV; capillary temperature: 275 °C; minimum signal threshold: 1,500 counts; maximum fill-time: 100 ms. For MS/MS peptide analysis the 20 most intense ions with an assigned charge of $z \geq 2+$ were chosen for fragmentation by low energy collision-induced dissociation (low energy CID). Dynamic exclusion was automatically placed on previously selected m/z for 30 s. MS-Scan was performed in the Orbitrap-mass analyser with a resolution of 30,000 at m/z=400 and fragment ions have been scanned in the linear ion trap with a resolution of ~1,000.

2.2.5 Mass spectrometric data analysis

MS/MS spectra have been processed using the software Proteome Discoverer v1.2 (Thermo Scientific, Bremen). For peptide and protein identification, fragment spectra were searched with Mascot v2.3.2 (www.matrixscience.com) on an in house installed server (PERKINS *et al.* 1999) against TrEMBL protein entries for *T. infestans* (257 protein entries) and Swiss-Prot protein entries for *Gallus gallus* and *Rattus rattus*. Mascot searching parameters were set to a tolerance of 10 ppm for protein precursor ions and 0.4 Da for fragment ions. Oxidation of methionine and propionamidation of cysteine was considered as variable modification and a maximum of four missed cleavage sites were allowed in case of incomplete trypsin digestion. For positive protein identification, at least two unique peptides and a minimum protein score of 40 were required.

CHAPTER 3

INFLUENCE OF TRYPANOSOMA CRUZI ON TRIATOMA INFESTANS: INTESTINAL BACTERIOLYTIC ACTIVITY AND EXPRESSION PATTERN OF LYSOZYMES

3. Influence of *Trypanosoma cruzi* on *Triatoma infestans*: intestinal bacteriolytic activity and expression pattern of lysozymes

3.1 Introduction

Chagas disease is caused by the protozoan parasite *Trypanosoma cruzi*, first found in the digestive tract of the triatomine *Panstrongylus megistus* (CHAGAS 1909). Principally, *T. cruzi* is transmitted to humans by the infectious feces of haematophagous triatomine species such as *Triatoma infestans*. A successful insecticide spraying campaign, organized by the Southern Cone Initiative in the 1990th, eliminated the domestic populations of *T. infestans* in many of the affected countries (SCHOFIELD & DIAS 1999). Although the incidence of *T. infestans* was seriously minimized by the efforts of the Southern Cone Initiative, *T. infestans* is still relevant in many regions of Latin America (see 1.1).

Triatomines possess an intestinal innate immune system acting against air-borne microbes or pathogens and presumably regulating the development of symbionts. The bacteriolytic activity in the gut of *Rhodnius prolixus* and *T. infestans* is feeding dependent (RIBEIRO & PEREIRA 1984; MEISER 2009). This inducible antimicrobial activity is most probably based on multiple factors and some of them are suggested to affect parasite development in the vector (summarized by URSIC-BEDOYA *et al.* 2008; GARCIA *et al*. 2010). Also digestive enzymes like cathepsins were described as putative factors that interact with *T. cruzi* in the small intestine (see 1.3.2 and 1.4.2). Focusing on antimicrobial peptides, the only doubtless effect is stated for the lepidopteran cecropin. If it is produced by genetically modified symbionts of triatomines, *T. cruzi* is killed in the vector.

Several triatomine-produced antimicrobial compounds are induced by an infection with *T. cruzi*. Nitric oxide (NO) is known as widespread immune effector and signaling molecule in many organisms. In studies that assessed NO synthase (*NOS*) gene expression as well as NO production in *Rhodnius prolixus*, the tissues of the digestive tract react pathogen specifically to infections with *T. cruzi* and *Trypanosoma rangeli*, but the levels of mRNA encoding NO synthase does not always reflect the concentration of NO in the gut (WHITTEN *et al.* 2007). The gene of prolixicin, an attacin-like peptide is expressed after an infection, but the peptide does not affect the parasite *in vitro* (URSIC-BEDOYA *et al*. 2011). According to molecular biological data in different triatomine species, genes encoding the antimicrobial peptide defensin are expressed together with genes encoding for lysozymes in the digestive tract (LOPEZ *et al.* 2003; ARAUJO *et al.* 2006; WANIEK *et al.* 2009a). In contrast to lysozymes, defensins are small, presumably pore-forming peptides of about 4 kDa (BULET *et al.* 1999).

After feeding of *T. infestans* and *Triatoma brasiliensis*, the levels of mRNA encoding for lysozyme and defensin are higher in the stomach than in the small intestine (KOLLIEN *et al.* 2003; ARAUJO *et al.* 2006; WANIEK *et al.* 2009a). After *T. cruzi* infection in *R. prolixus*, the transcript level of *RpLys-A* is increased, while *RpLys-B* remains to be unaffected (URSIC-BEDOYA *et al*. 2008).

Considering the molecular basis of these interactions has become a major field of research within the last years (URSIC-BEDOYA *et al.* 2008; WANIEK *et al*. 2011). However, the organization and physiological role of these interactions are not clearly understood. Therein, understanding lysozyme expression pattern together with the respective bacteriolytic activity after *T. cruzi*-infection poses an initial step. The present study focuses on the time course of the bacteriolytic activity in small intestine and rectum samples of non-infected and *T. cruzi*-infected *T. infestans* fifth instar nymphs after blood ingestion as well as the corresponding expression pattern of the lysozyme genes. The intestinal bacteriolytic activity of triatomines was analyzed using a liquid assay and the zymogram technique to indicate the presence and changes of concentration of bacteriolytic compounds. The relative expression of two lysozyme genes was determined using qRT-PCR. A better understanding of such complex molecular interactions between the insects and parasites could help to develop new strategies to fight the transmission of Chagas disease.

3.2 Methods

3.2.1 Mammal maintenance, parasites and exposure to *Trypanosoma cruzi*

Nude mice and rats (RNU/rnu$^-$ and Ztm/NZNU) of both genders were obtained from the Zentralinstitut für Versuchstierzucht, Hannover, Germany. They were maintained in filter cap cages and were supplied with sterile water and food *ad libitum* (HÖLSCHER *et al*. 2000). All procedures with rats were conducted under deep anesthesia including carefully monitoring during recovery. *T. cruzi* strain "Chile 5" belongs to the zymodeme 1 (EBERT & SCHAUB 1983). Isolated from *T. infestans* from the same village, it is cyclically maintained between this vector and mice or stored as aliquots at -80 °C (SCHAUB 1988b). For passaging of trypanosomes, female immunocompetent Balb/c mice were intraperitoneally (i.p.) infected with trypanosomes and the resulting parasitemia was controlled daily according to BRENER (1973). About three weeks post infection (p.i.), at the peak of parasitemia in the Balb/c mice, nude mice were infected with 100 µl sterile heart blood, containing about 0.8 million trypanosomes/ml blood for a subsequent passage. After 18 days at high parasitemia in the

nude mice four male nude rats (RNU/rnu$^-$) were infected i.p. with 150 µl sterile heart blood of the nude mice, containing about 0.12 million trypomastigotes. After 21 days the nude rats were used to infect fifth instar nymphs of *T. infestans*. In addition, blood trypomastigotes were isolated at the peak of parasitemia.

For the isolation of surface coats from blood trypomastigotes, the blood was obtained by cardiac puncture in 0.1% (w/v) heparin-sodium salt (Hoffmann-La Roche, Grenzach Wyhlen, Germany) using about 1 ml/rat. After differential centrifugation (10 min, 350 *g*, 4 °C), resuspension in rat serum and a second differential centrifugation, the parasite-containing supernatants were pooled and centrifuged for 10 min at 900 *g* and 4 °C according to HÖLSCHER *et al*. (2003) with the following slight modifications. The trypanosomes were resuspended in 2 ml phosphate buffered saline solution supplemented with 5 % (w/v) glucose (SCHAUB 1991). After centrifugation (20 min, 400 *g*, 4 °C), supernatant was additionally centrifuged for 10 min at 10,000 *g* and 4 °C. An induction of surface coat shedding was achieved by resuspending all pelleted blood trypomastigotes in protein-free buffer followed by a strong centrifugation for 5 min at 10,000 *g* and 4 °C (HÖLSCHER *et al*. 2003). Resulting supernatant and pellet were mixed using an injection needle (0.50 x 25 mm, BD, Heidelberg, Germany) to increase the shedding of the surface coats and centrifuged for 5 min at 10,000 *g* and 4 °C. This procedure was repeated. After additional centrifugation (10 min, 10.000 *g*, 4 °C), the supernatant contained shed surface coats and the pellet the trypomastigotes with less surface coat, termed “naked” trypomastigotes. For artificial feeding, heparinized rat blood was centrifuged (10 min, 350 *g*, 4 °C) and the complement system inactivated by incubating the serum for 30 min at 50 °C. Subsequently, the serum was mixed with the cellular blood components and either surface coats or naked trypomastigotes.

3.2.2 *In vitro* cultivation of *Trypanosoma cruzi* epimastigotes

For cultivation of *T. cruzi* epimastigotes, a cryopreserved stabilate of *T. cruzi* “Chile 5” was thawed rapidly and inoculated into 2 ml LIT medium (CAMARGO 1964) supplemented with fetal bovine serum (final concentration 5 % (v/v)). Epimastigotes were cultivated at 28 °C and passaged four times in intervals of two days. Thereby, the cultures contained only epimastigotes. These were harvested by centrifugation for 10 min at 400 *g* and room temperature and washed twice in LIT medium. Epimastigotes were resuspended in 5 ml LIT medium, counted (BRENER 1973) and mixed with complement-inactivated rat blood for artificial feeding (Table 3.1).

3.2.3 Establishment of experimental groups

First (N1) and fifth (N5) instar nymphs were used in two approaches (Table 3.1). For the long-trypo group and the corresponding long-control group, first instar nymphs were fed 2 weeks after hatching on uninfected Balb/c mice or on *T. cruzi* infected Balb/c mice at the peak of parasitaemia with about 0.16 million trypomastigotes/ml blood (Table 3.1). Subsequently, both groups were fed on chicken in the second, third and fourth instar about four weeks after the previous feeding. 40 days after feeding (daf) of the fourth instar nymphs, the resultant fifth instars were dissected either without previous feeding as unfed or fed on chicken. The high number of fifth instar nymphs did not enable a feeding on rats. Only fully engorged fed nymphs were considered and dissected at 2, 3, 5, 10 and 15 daf.

In the short-term groups, the feeding schedule of the first to fourth instars and the feeding and dissection schedule of fifth instars until 5 daf were identical with those of the long-control group. The fifth instars of the short-control group were fed on uninfected anesthesized rats, the short-trypo group on infected anesthesized nude rats at the peak of parasitaemia with about 0.8 million trypomastigotes/ml blood (Table 3.1). The other fifth instar nymphs were fed through silicone membranes (SCHAUB 1990) with a mixture of complement-inactivated blood of uninfected rats and either shed surface coats (short-surface group), derived from the corresponding number of parasites (0.9 million trypomastigotes/ml blood) or these trypomastigotes without surface coats (short-naked-trypo group). The short-epi group received complement-inactivated rat blood containing about 0.9 million epimastigotes/ml blood (Table 3.1), and the nymphs were dissected at 2 and 5 daf.

Table 3.1: Characteristics of experimental groups.

name	established as	feeding on (instar)	approach
long-control	N1	uninfected mice (L1); chicken (L2-L5)	1
long-trypo	N1	infected mice (L1) (blood trypomastigotes); chicken (L2-L5)	1
short-control	N5	uninfected mice (L1); chicken (L2-L4); uninfected rats (L5)	1, 2
short-trypo	N5	uninfected mice (L1); chicken (L2-L4); infected rats (L5) (blood trypomastigotes)	1, 2
short-surface	N5	uninfected mice (L1); chicken (L2-L4); rat blood containing shed surface coats (L5) (membrane feeding)	1, 2
short-naked-trypo	N5	uninfected mice (L1); chicken (L2-L4); rat blood containing trypanosomes without surface coats (L5) (membrane feeding)	2
short-epi	N5	uninfected mice (L1); chicken (L2-L4); rat blood containing *in vitro* cultured epimastigotes (L5) (membrane feeding)	2

3.2.4 Sample preparation

For measurements of the bacteriolytic activity, always nine *T. infestans* were dissected in physiological saline (0.9 % (w/v) NaCl) to obtain 3 independent biological samples of 3 bugs each at each time point. Small intestines were submerged with forceps in 210 µl ice cold 0.9 % (w/v) NaCl and slightly agitated to support the outflow of the contents. Recta were pestled 210 µl 0.9 % (w/v) NaCl. At 2, 3 and 5 daf, trypanosomes in small intestine contents and rectum homogenates of short-trypo group and short-naked-trypo group were counted (BRENER 1973). Contents of small intestine as well as homogenates of recta were centrifuged for 20 min at 400 *g* and room temperature to remove trypanosomes. These low centrifugation forces were used to strongly reduce the shedding of the surface coat of trypanosomes (HÖLSCHER *et al.* 2003). Supernatants were then centrifuged at 16,000 *g* for 45 min at 4 °C. The resulting supernatants were used for activity measurements, SDS-PAGE, zymography and subsequent mass spectrometry (see 2.2.1-2.2.5). For SDS-PAGE and zymography, 15 µl of each sample were used. Since we focused on the bacteriolytic activity, identical volumes of the independent samples rather than identical amounts of proteins were used, because protein content is strongly affected by the feeding status.

For quantitative expression analysis, small intestines were immediately transferred into liquid nitrogen. Always two small intestines were pooled to obtain four independent biological samples for each time point and stored at -80 °C. Total RNA was isolated using the RNeasy Kit (Qiagen, Hilden, Germany) following manufacturer's instructions. Quality of RNA was controlled and the concentration determined by capillary electrophoresis using the Experion system (Biorad, München, Germany). RNA samples were not heat denatured before electrophoresis because of the endogenous "hidden break" occurring in the 28S rRNA of most insects (WINNEBECK *et al.* 2010), resulting in a misinterpretation of the RNA profile. Since degradation pattern recognition of an RNA sample by the Experion system software is automatically generated using saved pherograms of human liver RNA of different quality as degradation standards (DENISOV *et al.* 2008), the slightly divergent pattern of insect RNA often leads to an inaccurate low RNA quality index value (RQI). Therefore, pherograms of all RNA samples were additionally analyzed by eye. In general, samples with an RQI value of ≥6.8 were used for quantitative PCR except for three and one sample at 3 and 5 daf, respectively, of the non-infected control group and one sample at 2 and 3 daf of the short-trypo group (Tables S8.1.17-S8.1.19, Suppl.). These RNA samples were also used in qPCR because the respective pherograms indicated a better quality than specified by the RQI value. To remove

traces of genomic DNA, RNA samples were incubated for one hour at 37 °C with two units DNase I (Fermentas, St. Leon-Roth, Germany) according to the manufacturer's recommendations. Finally, RNA concentrations of 2.5 ng/µl were adjusted using RNase free water.

3.2.5 qRT-PCR and data analysis

Expression analysis was performed using the iScript RT-PCR Kit (Biorad) according to the manufacturer's recommendations in an Opticon2 cycler (MJ Research, Quebec, Canada) with oligonucleotides 268 (5'-GGGGTGGACCAAACCATGATG-3') and 269 (5'-CCAACCTTGACGACTCTTGATTAG-3') for *TiLys1*, 267 (5'-TAACTGGATCAGACTTTGATGGCGT-3') and 468 (5'-ACCATGAATTCCAGCCTTGTTGAT-3') for *TiLys2* or 469 (5'-GTATGTAGCGATCCAAGCTGTTCT-3') and 470 (5'-CATAACCTTCATAGATGGGGACTG-3') for ß-actin. Real time PCR experiments were carried out with three independent samples for each time point and in triplicates according to BALCZUN *et al.* (2012). As a control for successful DNase I treatment, each reverse transcription was carried out twice, with or without reverse transcriptase. Samples in which the control without reverse transcriptase yielded a PCR product were treated again, controlled and then used. Presence of PCR inhibitors was ruled out by determining threshold cycle (Ct) values of different dilutions of three representative RNAs as template for real time PCR reaction and subsequent calculation of the respective PCR efficiency. Primer efficiency was calculated with LinRegPCR (RAMAKERS *et al.* 2003). Mean Ct were calculated from the triplicates and used for calculations of expression ratios according to PFAFFL (2001) with primer specific efficiencies. The Ct values for the amplicons derived from the ß-actin mRNA were used as reference for normalization. PCR conditions were as follows: 50 °C for 10 min, 95 °C for 5 min, followed by 40 cycles at 95 °C for 10 s and at 60 °C for 30 s. After melting curve analysis, statistical analysis was carried out using the Relative Expression Software Tool (REST) (PFAFFL 2001).

3.3 Results

3.3.1 Concentration of soluble proteins

In the first approach (see Table 3.1), most protein concentrations in the small intestine samples of fed bugs seemed to be higher than those of the respective unfed control (Figure 3.1). In some groups, these feeding-induced increases were only statistically different in two out of five comparisons, in the short-control group at 2 and 5 daf ($p<0.001$ and 0.002,

respectively), in the short-surface group at 5 and 10 daf (p=0.004 and 0.046, respectively) and in the long-trypo group also at these dates (both p<0.001). However, in the small intestine samples of the short-trypo group, these concentrations were significantly higher over the whole period of dissections (p<0.001 to 0.011) and in the long-control at 2, 3, 5 and 10 daf (p<0.001 to 0.037).

Also in the rectum, protein concentration of fed bugs was mainly higher than in the respective unfed nymphs (Figure 3.1). In the short-control group they were statistically significantly increased at 2, 5 and 15 daf (p=0.012 and twice <0.001, respectively), in the short-surface group at 5, 10 and 15 daf (p<0.001, <0.001 and 0.016, respectively) and in the short-trypo group at 3, 5, 10 and 15 daf (p<0.001 to 0.044). In comparison to the respective unfed nymphs, the protein concentration of the long-control group was statistically significantly higher at 2, 3, 5 and 10 daf (p<0.001 to 0.008) and in the long-trypo group at 3 and 15 daf (p=0.023 and 0.047, respectively).

In the second approach (see Table 3.1), the overall protein concentration was lower than in the first approach, but a feeding-induced increase of the protein concentration in the small intestine and rectum samples was also observed (Figure 3.2, consider other scaling). For the small intestine samples, protein concentration of the short-surface group bugs was statistically significantly increased at 2 and 3 daf (p<0.001 and 0.004, respectively). In the short-control group (p<0.001 to 0.002), the short-naked-trypo group (always p<0.001) and the short-epi group (p=0.004, 0.013) concentrations were significantly higher at all dissections, i.e. 2, 3 and 5 daf.

For rectum samples, protein concentrations of the short-control group (always p<0.001) and short-naked-trypo group (p<0.001 to 0.011) were statistically significantly higher at all three dissections (Figure 3.2). In comparison to the respective unfed control nymphs (short-control group), short-surface group nymphs possessed a feeding-induced increased protein concentration at 3 and 5 daf (p=0.006 and <0.001, respectively), short-epi group nymphs only at 5 daf (p=0.03) and short-trypo group nymphs only at 2 daf (p<0.001).

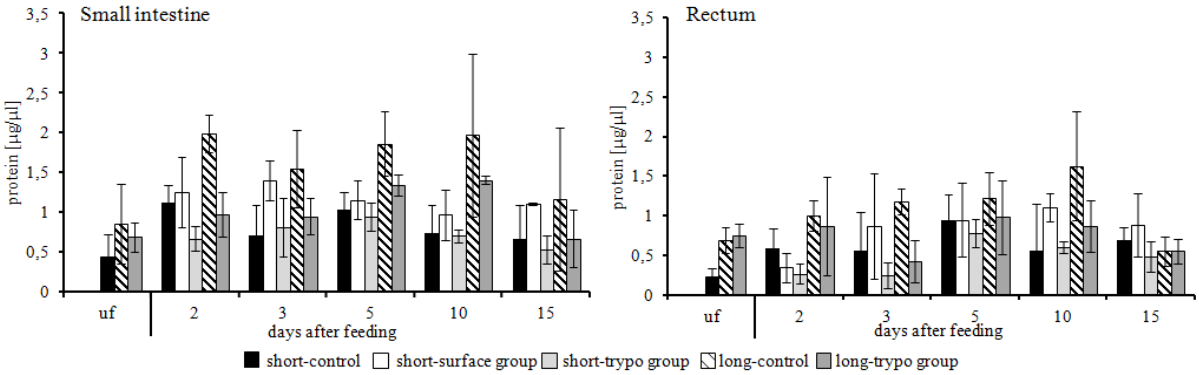

Figure 3.1: Protein concentrations in small intestine and rectum of the different groups in the first approach.
Mean and standard deviation from 3 independent samples. Measurements were done with samples of unfed (uf) fifth instar nymphs as well as 2, 3, 5, 10 and 15 days after feeding.

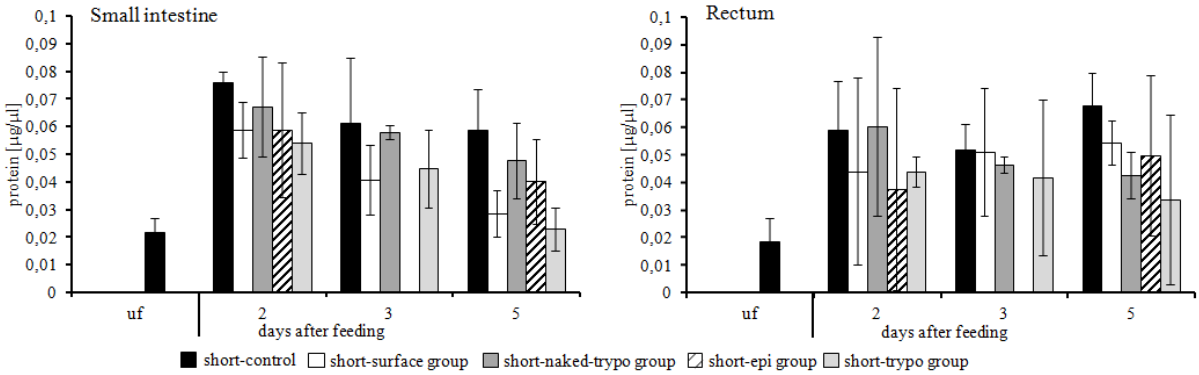

Figure 3.2: Protein concentrations in small intestine and rectum of the different groups in the second approach.
Mean and standard deviation from 3 independent samples. Measurements were done with samples of unfed (uf) fifth instar nymphs as well as 2, 3 and 5 days after feeding.

3.3.2 pH-dependence of bacteriolytic activity

To control whether or not the bacteriolytic activites of the samples were positively correlated with the protein concentration, activity (ΔOD) was plotted against the respective protein concentration for each pH between 3.0 and 8.0 (Figures S8.1.1 and S8.1.2, Suppl.). The activity (ΔOD) for each pH-condition was uniformly distributed in the graphs. Therefore, no correlation between the protein concentration and the level of bacteriolytic activity was evident. However, the protein concentration was used as robust reference for the determination of the specific bacteriolytic activity for comparisons of samples of the same feeding state (see 3.3.3).

In the characterization of the pH-optimum of the bacteriolytic activity against *Micrococcus lysodeikticus* of small intestine and the rectum samples, activity in the rectum samples was generally lower than in the small intestine samples (Figures 3.3 and 3.4). In the first ap-

proach (see Table 3.1), the following comparisons with the activities at pH 6.0 were statistically significantly different. In the small intestine sample of the short-control the activity was statistically significantly higher than at pH 5.0 at 3 daf and at pH 7.0 at 5 daf ($p=0.022$ and <0.001, respectively) (Figure 3.3). In the short-trypo group, this was evident for pH 7.0 in the small intestine samples over the whole post-feeding period ($p<0.001$ to 0.017) and in the rectum samples not only at pH 5.0 but also at pH 7.0 at 3, 5, 10 and 15 daf ($p<0.001$ to 0.007). The short-surface group nymphs also possessed significantly higher post-feeding activities at pH 6.0 than at pH 7.0 in the small intestine samples ($p=0.002$ to 0.044) and at 5, 10 and 15 daf ($p<0.001$ to 0.027) in the rectum samples also at pH 5.0. Only in the long-control group, the bacteriolytic activity of small intestine samples of unfed bugs was significantly lower at pH 5.0 in comparison to pH 6.0 ($p=0.019$) at 3, 5 and 10 daf ($p<0.001$ to 0.019). In the rectum samples, the same result was observed for unfed bugs ($p=0.003$) in comparison to pH 5.0 and at 10 daf ($p=0.034$) in comparison to pH 7.0. In the long-trypo group nymphs, lysis of bacteria by samples of the small intestine was significantly higher than at pH 5.0 at 3, 5 and 10 daf ($p=0.001$ to 0.005). In rectum samples, significant differences were calculated for unfed bugs ($p=0.005$) as well as 5, 10 and 15 daf ($p=0.002$ to 0.011) in comparison to pH 5.0 and pH 7.0, respectively.

In the second approach (see Table 3.1), the following bacteriolytic activities were always statistically significantly higher at pH 6.0 than at pH 5.0, not at pH 7.0. In short-control nymphs, samples of small intestines of unfed bugs ($p<0.001$) and rectum samples at 2 daf ($p<0.001$) showed this difference (Figure 3.4) and in short-trypo group nymphs also small intestine samples of unfed bugs and at 5 daf ($p<0.001$ and 0.04). These comparisons were also statistically significantly different in nymphs of the short-surface group ($p<0.001$ and 0.009, respectively). In the rectum samples of nymphs of this group, this occurred at 2, 3 and 5 daf ($p<0.001$ to 0.045). For the short-naked-trypo group, activities in small intestine samples of unfed bugs ($p<0.001$) as well as 2 and 5 daf ($p=0.037$ and 0.034) and in rectum samples at 3 daf ($p=0.008$) were significantly higher. The short-epi group bugs possessed an increased activity at pH 6.0 in the small intestine samples of unfed bugs ($p<0.001$) as well as at 5 daf ($p=0.026$) compared to the activities at pH 5.0. For further characterization of bacteriolytic activity, measurements at pH 6.0 were used for comparison of the respective activities of the different groups according to the feeding state.

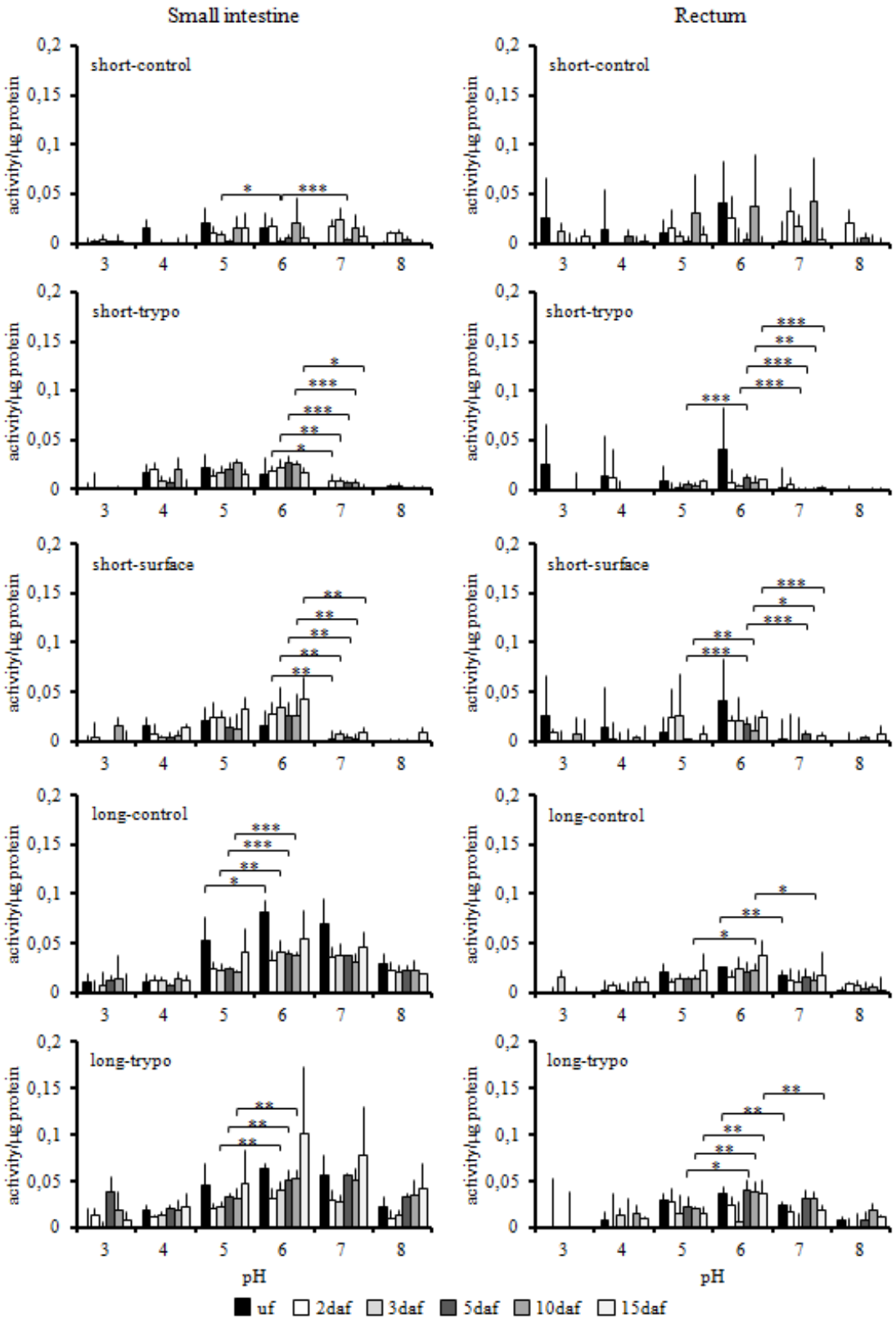

Figure 3.3: Activities/µg protein at different pH in the first approach.
pH-dependant activities/µg protein of short-control, short-trypo, short-surface, long-control and long-trypo groups. Mean of duplicates from 3 independent samples, to which material from always 3 bugs was pooled. Measurements were done over a 30 min period with samples of unfed (uf) fifth instar nymphs as well as 2, 3, 5, 10 and 15 days after feeding. Significant differences to pH 6.0 are indicated by * for $p<0.05$, ** for $p<0.01$ and *** for $p<0.001$.

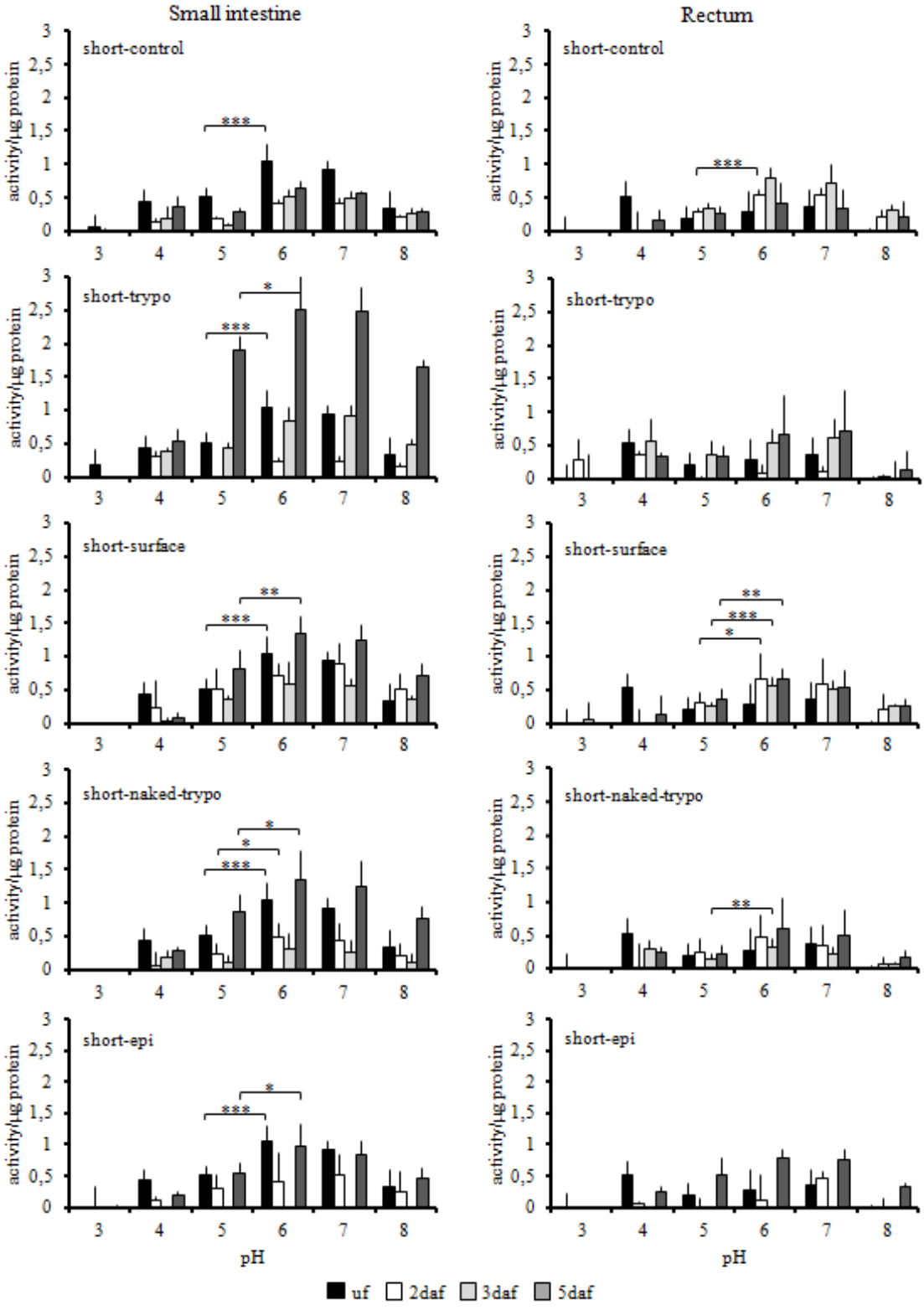

Figure 3.4: Activities/µg protein at different pH in the second approach.
pH-dependant activities/µg protein of short-control, short-trypo, short-surface, short-naked-trypo and short-epi groups. Mean of duplicates from 3 independent samples, to which material from always 3 bugs was pooled. Measurements were done over a 30 min period with samples of unfed (uf) fifth instar nymphs as well as 2, 3 and 5 days after feeding. Significant differences to pH 6.0 are indicated by * for $p<0.05$, ** for $p<0.01$ and *** for $p<0.001$.

3.3.3 Bacteriolytic activities in the small intestine and rectum at the optimal pH

For the comparison of the bacteriolytic activities of the individual samples at the optimal pH, activities were also calculated as activity/µg protein (Figure 3.5). Focusing on the samples of the small intestine of the first approach, the bacteriolytic activity of unfed short-control nymphs was significantly lower in comparison to unfed nymphs of the long-control group ($p<0.001$). In the comparison of the activities after feeding of the two control groups, chicken blood fed fifth instar nymphs of the long-control group possessed a significantly higher activity than rat blood fed nymphs of the short-control group ($p<0.001$ to 0.008). Short-surface group as well as short-trypo group nymphs showed a higher lysis of bacteria at 3, 5 and 15 daf compared to the respective control group ($p=0.002$ to 0.003 and <0.001 to 0.042, respectively). In long-control and long-trypo group nymphs the activity in the small intestine samples was statistically significantly higher at 5, 10 and 15 daf in comparison to unfed nymphs ($p=0.003$ to 0.049 and 0.003 to 0.049, respectively). In nymphs of the long-trypo group, the activity at 5 and 10 daf was significantly higher than in the respective control ($p=0.012$ and 0.008, respectively).

Considering the activities of the rectum samples, nymphs of the short-surface group as well as the short-trypo group possessed a higher activity at 5 and 15 daf ($p=0.002$, <0.001, 0.011 and 0.003, respectively) in comparison to unfed bugs of the short-control group (Figure 3.5). In the comparison of the bacteriolytic activities of the two control groups, a significantly less bacteriolysis occurred in samples of rat blood fed nymphs of the short-control group than of chicken blood fed nymphs of the long-control group at 5 and 15 daf ($p=0.008$ and <0.001, respectively). Chicken blood fed long-control bugs showed a significantly feeding-induced increased lysis of bacteria at 10 ($p=0.009$) and 15 daf ($p=0.006$). In nymphs of the long-trypo group, activities at 2, 5, 10 and 15 daf were statistically significantly higher than in non-infected unfed bugs of the long-control group ($p=0.025$, <0.001, <0.001 and 0.001, respectively). The bacteriolytic activity in samples of long-trypo group nymphs was significantly increased at 5 and 10 daf ($p=0.008$ and 0.007) compared to non-infected nymphs at these days after feeding.

In the second approach (see Table 3.1), the activities/µg protein in the small intestine samples of unfed fifth instars were significantly higher than at 2 and 3 daf for the short-control group (always $p<0.001$), short-surface group ($p=0.002$ and 0.018), short-naked-trypo group ($p=0.002$ and <0.001) and short-trypo group ($p<0.001$ and 0.001) (Figure 3.6). Nymphs infected with blood trypomastigotes (short-trypo group) possessed a significantly higher

activity at 5 daf than unfed nymphs (p<0.001). At 2 and 5 daf of surface coats (short-surface group), the lysis of bacteria by samples of the small intestine was significantly higher than in the short-control group (p=0.002 and <0.001, respectively). It was significantly lower in nymphs of the short-trypo group than in the short-control group (p<0.001). Beginning at 3 daf, short-trypo group nymphs showed an increased activity in the small intestine samples (p=0.004) compared to the non-infected control (short-control group) with a maximum at 5 daf (p<0.001). In comparison to short-trypo group nymphs, at 5 daf the bacteriolytic activity in all other groups was significantly lower (p<0.001 to 0.003).

In the rectum of short-control group nymphs, at 3 daf the activity was significantly higher than in unfed nymphs (p=0.005) (Figure 3.6). At the same day, in short-surface group nymphs (p=0.022), short-naked-trypo group nymphs (p<0.001) and short-trypo group nymphs (p=0.034), the activities were significantly lower than in nymphs of the non-infected control (short-control group). In rectum samples of the short-epi group, the activity was significantly lower at 2 daf than in unfed nymphs (p=0.012). At 5 daf, it was significantly higher in short-epi group nymphs than in nymphs of the short-control group (p=0.018). At 2 daf, significantly less bacteria were lysed in the assay by samples of short-trypo group nymphs than of the short-control group (p<0.001).

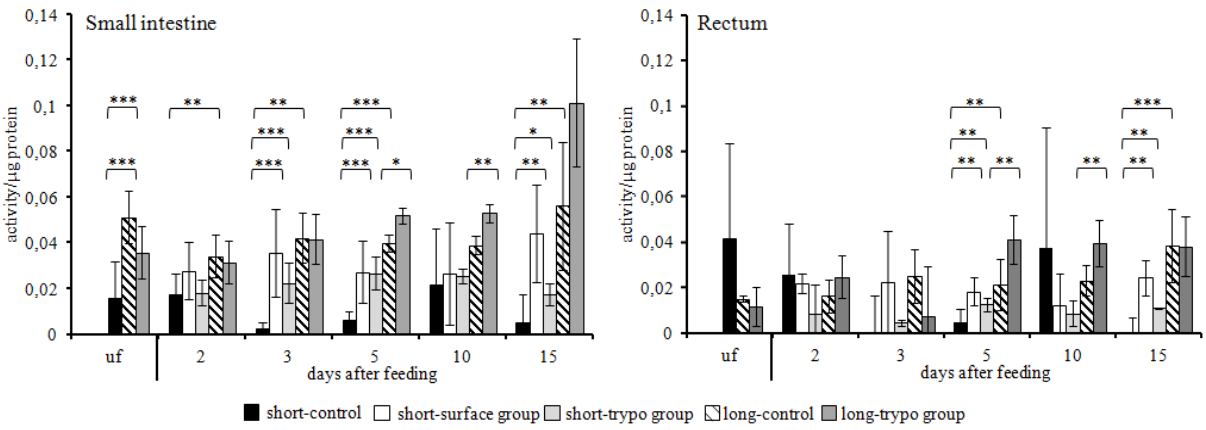

Figure 3.5: Activities/µg protein in small intestine and rectum of the different groups in the first approach.
Mean and standard deviation from 3 independent samples. Measurements were done with samples of unfed (uf) fifth instar nymphs as well as 2, 3, 5, 10 and 15 days after feeding. Significant differences are indicated by * for p<0.05, ** for p<0.01 and *** for p<0.001.

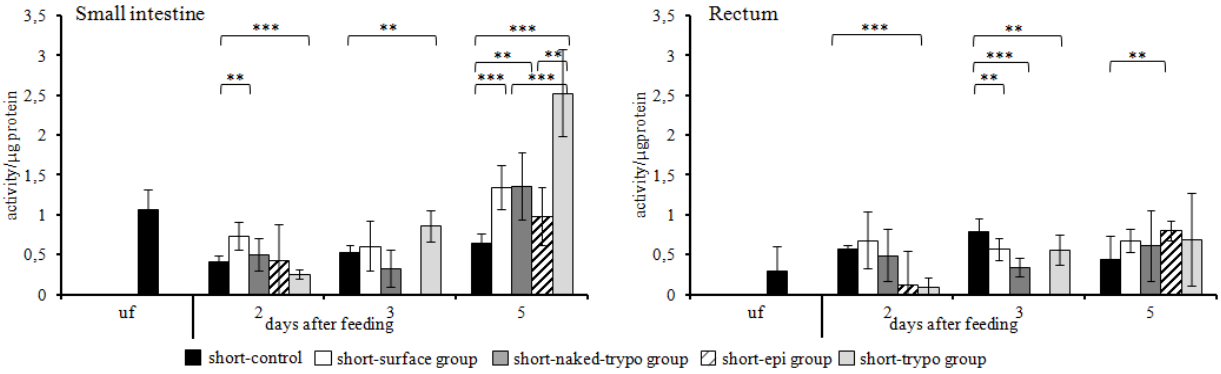

Figure 3.6: Activities/µg protein in small intestine and rectum of the different groups in the second approach.
Mean and standard deviation from 3 independent samples. Measurements were done with samples of unfed (uf) fifth instar nymphs as well as 2, 3 and 5 days after feeding. Significant differences are indicated by * for $p<0.05$, ** for $p<0.01$ and *** for $p<0.001$.

3.3.4 Protein pattern and bacteriolytic activity of small intestine contents after SDS-PAGE

The pattern of bacteriolytic compounds of small intestine contents was investigated by SDS-PAGE and zymography. Electrophoretic separation of samples from both control groups representing chicken blood fed (long-control group) and rat blood fed (short-control group) bugs at different times after feeding showed a complex banding pattern under non-reducing conditions (Figure 3.7). The majority of proteins was located at about 13 kDa. According to the ImageMaster™ 1D analysis, about 42 % and 49 % of total protein concentrations, respectively, were detected there in samples of unfed bugs of short- and long-control groups. At 2, 3 and 5 daf, these abundant protein bands represented 54 %, 50 %, 39 % and 39 % and about 65 % and 68 % of all detected proteins of chicken and rat fed nymphs, respectively. For chicken blood fed bugs at 2 daf, an abundant protein band was detected at about 25 kDa representing 20 % of the total protein concentration.

After zymogram incubation at pH 6.0, lysis bands appeared corresponding to the most abundant protein bands at 13 kDa. For chicken blood fed bugs at 2 daf, a weak additional lysis zone occurred at about 25 kDa (Figure 3.7).

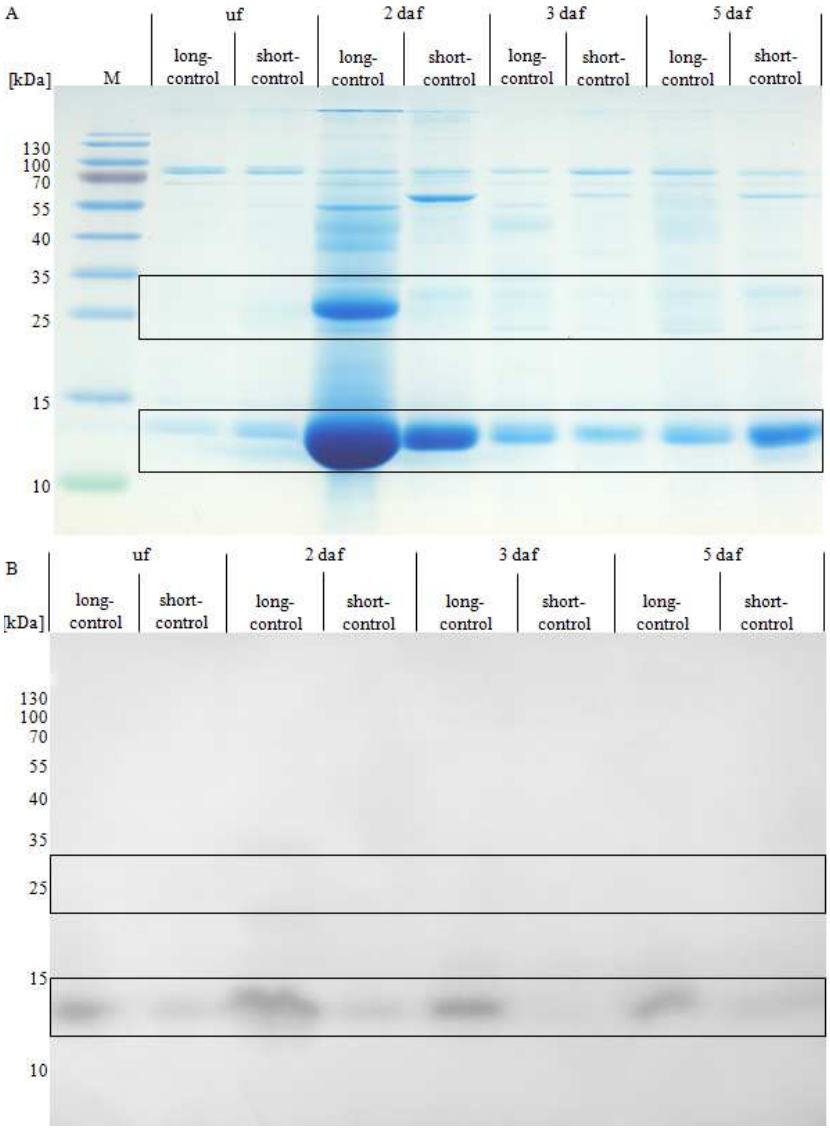

Figure 3.7: Protein profiles and zymography of small intestine contents of long-control and short-control under non-reducing conditions.
Protein profiles of each 15 µl samples of unfed (uf) *T. infestans* and at different days after feeding (2, 3, 5) after non-reducing SDS-PAGE (A) and zymography after an incubation over night at pH 6.0 (B) of the first approach. M: marker proteins. Boxes indicate lysis zones. Zymograms were processed in a black-white conversion to enable the recognition of weak lysis regions.

Separating proteins of small intestine contents of the short-trypo group, short-surface group and the corresponding control samples (short-control group) at different time points after feeding by SDS-PAGE and zymography, the majority of proteins were located at about 13 kDa in all groups (Figure 3.8). Unfed bugs contained less protein than the other groups, but this band represented about 56 % of the total protein concentration. In control samples from 2, 3 and 5 daf, about 56 %, 37 % and 53 %, respectively, of the total protein concentration were present there. In short-trypo group samples from 2, 3 and 5 daf, about 42 %, 52 % and 57 % of the proteins concentrated at about 13 kDa, respectively. For short-surface group samples, the abundance was 37 % at 2 daf and 38 % at 5 daf (Figure 3.8). After zymography at pH 6.0 using *M. lysodeikticus* as substrate, lysis bands appeared at about 13 kDa in all groups and at all time points (Figure 3.8).

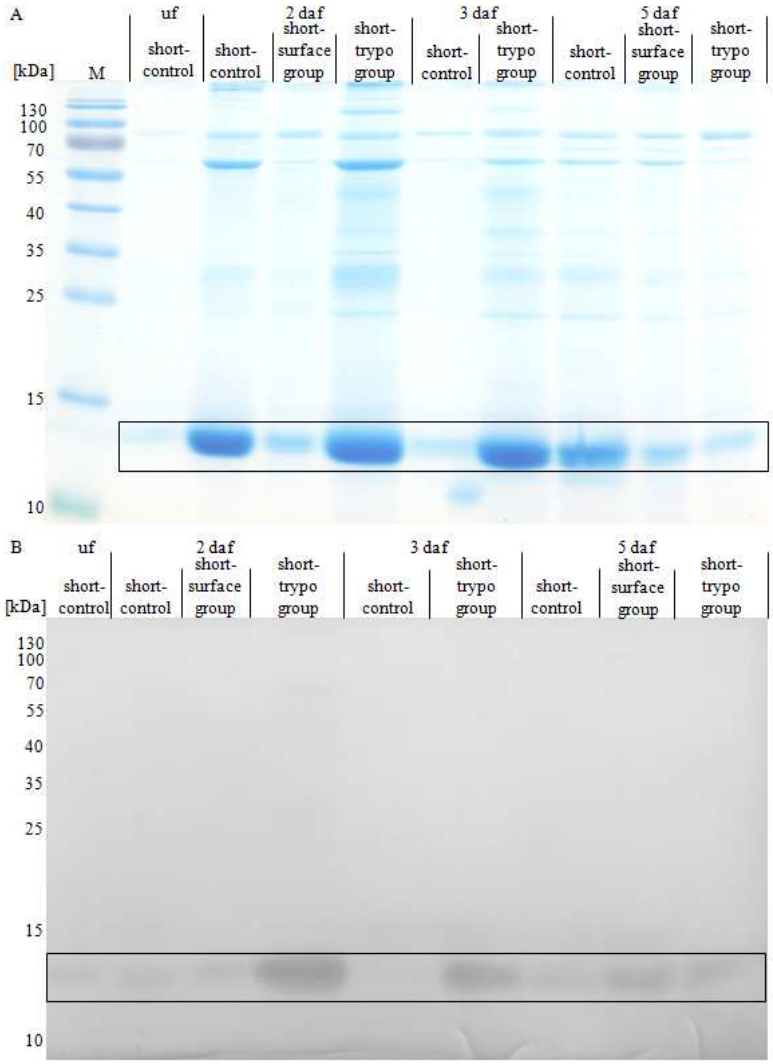

Figure 3.8: Protein profiles and zymography of small intestine contents of short-term groups under non-reducing conditions.
Protein profiles of each 15 µl samples of short-trypo group, short-surface group and the respective control (short-control) of unfed (uf) *T. infestans* and at different days after feeding (2, 3, 5) after non-reducing SDS-PAGE (A) and zymography after an incubation over night at pH 6.0 (B) of the second approach. M: marker proteins. Boxes indicate lysis zones. Zymograms were processed in a black-white conversion to enable the recognition of weak lysis regions.

3.3.5 Protein identification by mass spectrometry

Small intestine proteins of the different groups were separated by non-reducing SDS-PAGE and bands at about 13 kDa and one band at about 25 kDa, showing bacteriolytic activity (see 3.3.4), were subjected to mass spectrometric analysis.

In the bacteriolytically active 13 kDa bands of long-control group samples, TiLys1 was identified. For the unfed long-control group, TiLys1 was identified with 2 peptides and sequence coverage of 20.1 % (Table 3.2). In long-control samples of the 25 kDa band at 2 daf, cathepsin D1 (2 peptides, 8.2 % sequence coverage), cathepsin B1 (3 peptides, 12.7 % sequence coverage), cathepsin B2 (2 peptides, 7.5 % sequence coverage) and cathepsin L-like protease (2 peptides, 8.5 % sequence coverage) were identified in line with histone H3 (3 peptides, 19.9 % sequence coverage) (Table 3.2). For long-control group nymphs at 3 daf, 2 peptides for TiLys1 covered 20.1 % of the deduced amino acid sequence (Table 3.2). Beside

TiLys1, cathepsin D1 and a salivary lipocalin were identified as *T. infestans* proteins. At 5 daf, TiLys1 was identified with 2 peptides and sequence coverage of 20.1 % in line with cathepsin D1, cathepsin L-like protease, ribosomal protein P1, ribosomal protein P2 and a salivary lipocalin (Table 3.2).

In addition, many chicken proteins were identified in samples from all long-term groups (Tables S8.1.10 to S8.1.16, Suppl.). In both samples from the long-control group at 3 and 5 daf, chicken lysozyme C was identified with 4 peptides and a sequence coverage of 35.4 % (Tables S8.1.13 and S8.1.15, Suppl.).

Table 3.2: Mascot identification data for *T. infestans* proteins in the 13 kDa SDS-gel band of unfed long-control group and long-control group at 3 and 5 days after feeding and for 25 kDa SDS-gel band of long-control at 2 days after feeding.

Experimental group	Feeding state	Accession	Amino-acids	MW [kDa]	Σ peptides†	Σ Cov [%]	Score	Protein
long-control	unfed	Q7YZS5	139	15.6	2	20.1	530.4	TiLys1
long-control	2 daf	E2D6N9	390	43.0	2	8.2	1111.2	Cathepsin D1
long-control	2 daf	Q67EP8	332	36.3	3	12.7	263.5	Cathepsin B1
long-control	2 daf	A6YPD4	136	15.3	3	19.9	137.0	Histone H3
long-control	2 daf	Q67EP7	328	36.5	2	8.5	107.6	Cathepsin L-like protease
long-control	2 daf	A2SZV7	333	36.4	2	7.5	70.4	Cathepsin B2
long-control	3 daf	Q7YZS5	139	15.6	2	20.1	362.7	TiLys1
long-control	3 daf	E2D6N9	390	43.0	4	11.0	305.2	Cathepsin D1
long-control	3 daf	A6YPE6	179	20.0	4	21.8	238.4	Salivary lipocalin
long-control	5 daf	Q7YZS5	139	15.6	2	20.1	272.0	TiLys1
long-control	5 daf	A6YPR0	114	11.7	3	25.4	232.1	Ribosomal protein P2
long-control	5 daf	A6YPE6	179	20.0	3	21.8	185.8	Salivary lipocalin
long-control	5 daf	A6YPP2	116	11.8	3	45.7	176.2	Ribosomal protein P1
long-control	5 daf	Q67EP7	328	36.5	2	6.4	126.6	Cathepsin L-like protease
long-control	5 daf	E2D6N9	390	43.0	3	8.7	99.8	Cathepsin D1

Accession numbers were derived from Uniprot Protein Database (2011). †Not redundant peptides. Sequence coverage of the identified peptides is given as Σ Cov [%]. Significance of the search result is given as score.

In the 13 kDa bands of short-term groups, TiLys1 was identified. In samples derived from unfed short-control, 2 peptides covered 20.14 % of the deduced amino acid sequence of the mature TiLys1 (Table 3.3). In the analysis of short-control group at 2 daf one TiLys1 peptide was also identified at the same molecular mass (data not shown). Analysis of the 13 kDa band of short-surface group at 2 daf resulted in the identification of TiLys1 by 3 peptides, covering 20.9 % of the sequence and a cathepsin L-like protease, cathepsin D1 and ribosomal protein P2 (Table 3.3). In small intestine contents of short-trypo group at 2 daf TiLys1 was

identified by the same 3 peptides. Beside TiLys1, 3 salivary lipocalins, a salivary secreted protein and cathepsin D1 were identified (Table 3.3).

In addition to proteins from *T. infestans*, many rat proteins were identified in samples from the short-control group, short-surface group and short-trypo group (Tables S8.1.1 to S8.1.9, Suppl.). In particular, from this SDS-PAGE rat lysozyme C-1 was identified with 2 peptides and sequence coverage of 17.6 % (Tables S8.1.4 and S8.1.7, Suppl.).

Table 3.3: Mascot identification data for *T. infestans* proteins in the 13 kDa SDS-gel band of unfed short-control nymphs and of the short-surface group and short-trypo group at 2 days after feeding.

Experimental group	Feeding state	Accession	Amino-acids	MW [kDa]	Σ peptides†	Σ Cov [%]	Score	Protein
short-control	unfed	Q7YZS5	139	15.6	2	20.1	100.38	TiLys1
short-surface	2 daf	A6YPR0	114	11.7	3	25.4	245.0	Ribosomal protein P2
short-surface	2 daf	Q7YZS5	139	15.6	3	20.9	136.9	TiLys1
short-surface	2 daf	Q67EP7	328	36.5	2	6.4	78.9	Cathepsin L-like protease
short-surface	2 daf	E2D6N9	390	43.0	2	4.4	72.2	Cathepsin D1
short-trypo	2 daf	Q7YZS5	139	15.6	3	20.9	356.13	TiLys1
short-trypo	2 daf	A6YPI9	129	14.6	3	37.2	124.65	Salivary secreted protein
short-trypo	2 daf	A6YPE8	179	19.9	2	14.0	104.91	Salivary lipocalin
short-trypo	2 daf	E2D6N9	390	43.0	5	13.9	103.96	Cathepsin D1
short-trypo	2 daf	A6YPE6	179	20.0	2	14.0	77.48	Salivary lipocalin
short-trypo	2 daf	A6YPE9	179	20.0	2	14.0	66.53	Salivary lipocalin

Accession numbers were derived from Uniprot Protein Database (2011). †Not redundant peptides. Sequence coverage of the identified peptides is given as Σ Cov [%]. Significance of the search result is given as score.

3.3.6 Temporal expression profile of *TiLys1* and *TiLys2* in the small intestine of non-infected and short-term *T. cruzi*-infected *T. infestans*

Real-time qPCR was used to analyze the expression profiles of *TiLys1* and *TiLys2* in the small intestine of non-infected and short-term *T. cruzi*-infected fifth instars of *T. infestans*. In addition, relative expression levels of both lysozyme genes were quantified after feeding of nymphs on chickens or rats. Threshold cycle (Ct) values of *TiLys2* were always lower than of *TiLys1* (data not shown), i.e. the expression level of *TiLys2* was generally higher than those of *TiLys1* in all groups. In comparison to unfed bugs the expression of *TiLys1* was 32-fold higher at 15 daf on chicken (p=0.036) (Figure 3.9). At 10 and 15 daf on chicken, the transcription level of *TiLys2* was significantly up-regulated by the factor 8.8 (p=0.038) and 68.6 (p=0.001), respectively, in comparison to unfed bugs. The transcript level of *TiLys1* in rat blood fed bugs was significantly increased at 3 daf by the factor 8.4 (p=0.036), while the expression of

TiLys2 was not affected by feeding on rats (Figure 3.10A). Comparison of transcript levels of rat blood fed and chicken blood fed bugs for each time point showed a reduction of *TiLys2* expression by 25 % (p=0.034) in rat blood fed bugs at 5 daf (Figure 3.10B).

After short-term *T. cruzi*-infection, transcription of *TiLys1* was not significantly up-regulated referring to unfed bugs, but that of *TiLys2* was increased 5.8-fold at 5 daf (p=0.001) (Figure 3.11A). Comparison of the transcript levels of *TiLys1* and *TiLys2* of short-term *T. cruzi*-infected bugs with the respective expression levels in nymphs of the non-infected control group for each time point showed a reduction of *TiLys1* expression by 99 % at 3 daf compared to the non-infected control group (p=0.05) and a 13-fold increased *TiLys2* transcript level at 5 daf in the short-term *T. cruzi*-infected group (p=0.05) (Figure 3.11B).

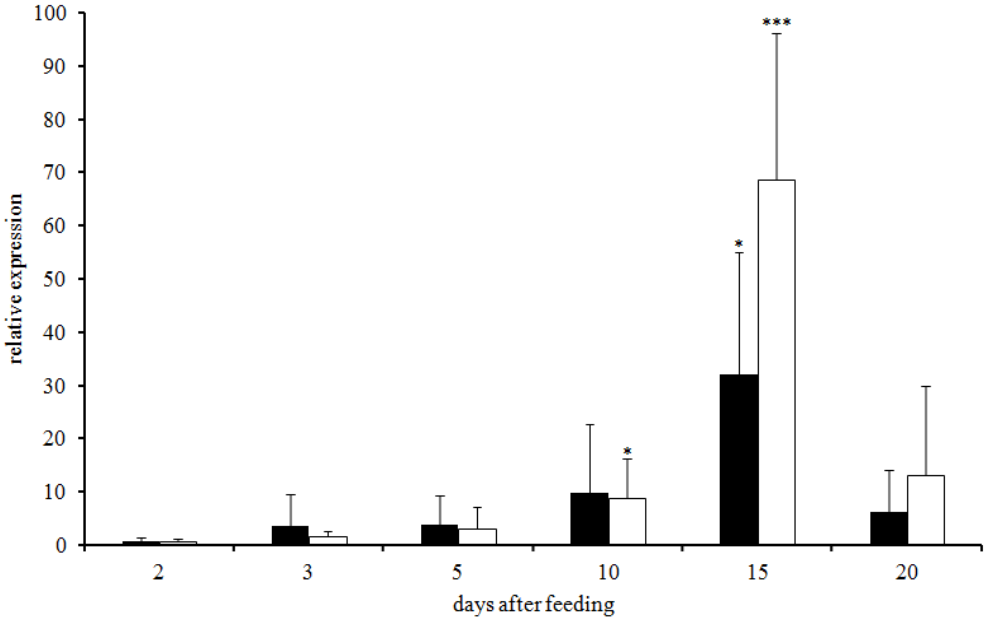

Figure 3.9: Temporal expression of *TiLys1* and *TiLys2* in the small intestine of chicken blood fed *T. infestans* referring to the amount of transcripts of unfed bugs.
Differences of expression levels of *TiLys1* (black bars) and *TiLys2* (white bars) at different days after feeding are given as mean ratios and standard errors (n = 3). Significance of transcript increase after feeding is indicated above bars by * ($p \leq 0.05$) and *** ($p \leq 0.001$).

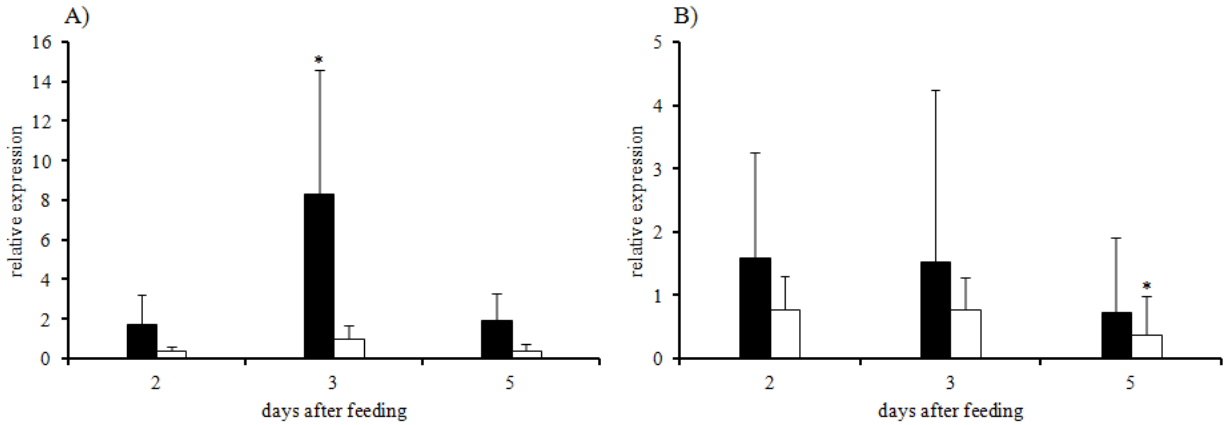

Figure 3.10: Temporal expression of *TiLys1* and *TiLys2* in the small intestine of rat blood fed *T. infestans* A) referring to the amount of transcripts of unfed bugs and B) referring to chicken blood fed bugs.
Differences of expression levels of *TiLys1* (black bars) and *TiLys2* (white bars) at different days after feeding are given as mean ratios and standard errors (n = 3). Significance of transcript increase after feeding is indicated above bars by * ($p \leq 0.05$).

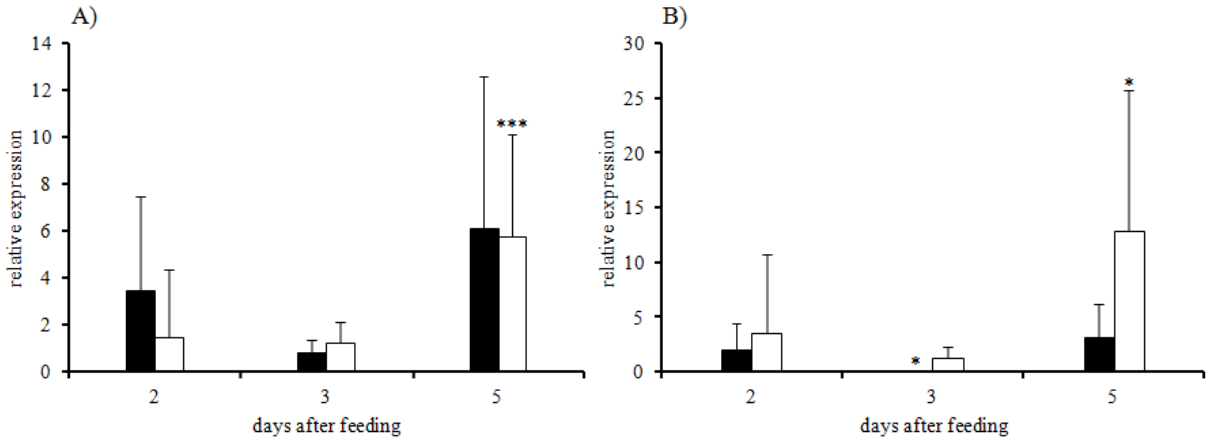

Figure 3.11: Temporal expression of *TiLys1* and *TiLys2* in the small intestine of short-term *T. cruzi*-infected *T. infestans* referring to the amount of transcripts of A) unfed bugs and B) the non-infected control group.
Differences of expression levels of *TiLys1* (black bars) and *TiLys2* (white bars) at different days after infection are given as mean ratios and standard errors (n = 3). Significance of transcript increase after feeding is indicated above bars by * ($p \leq 0.05$) and *** ($p \leq 0.001$).

3.4 Discussion

3.4.1 Concentration of soluble proteins and bacteriolytic activity in the small intestine and rectum of non-infected and *T. cruzi*-infected *T. infestans*

Fifth instar nymphs of the *T. infestans* strain "Chile" ingest on average 400 mg blood and excrete about 60 % of the weight of this bloodmeal within 24 h (EICHLER 1998). Since no proteolysis occurs in the stomach (WIGGLESWORTH 1977; AZAMBUJA *et al.* 1983; GARCIA 1987), the ingested blood increases the protein concentration in the stomach about 20-fold after feeding. Protein concentration decreases slowly until 6 daf and then rapidly until 35 daf

(EICHLER 1998). Since the bloodmeal is passed in small portions to the small intestine (KOLLIEN & SCHAUB 2000), the protein concentration increases 3.3-fold to reach a maximum at 23 daf. This maximum decreases until 35 daf. Here, the concentration is still 2-fold higher compared to unfed *R. prolixus* (EICHLER 1998; RIBEIRO & PEREIRA 1984).

The present investigation covered also these feeding-induced changes, but focused on the analysis of protein concentrations in the small intestine and rectum of short- and long-term *T. cruzi*-infected bugs, considering also the ingestion of trypanosomal surface coats. An initial increase of the protein concentration in small intestine at 2 daf, ranging from 1.4 to 3.5-fold, in non-infected nymphs reflects the already known phenomenon, and was also evident in the nymphs of the other groups. The concentration of soluble proteins in short-surface group nymphs was not higher as the concentration in nymphs of the short-naked-trypo group. Therefore, the protein concentration was not remarkably affected by the additional ingestion of *T. cruzi* proteins.

The first detailed investigation of bacteriolytic activity in different regions of the gut of *R. prolixus* indicated a pH-dependency of immune responsive factors (RIBEIRO & PEREIRA 1984). Using the $Gram^+$ bacterium *M. lysodeikticus* as substrate and a sodium acetate buffered system (pH 5.0-7.5), the highest activity in stomach and small intestine homogenates occurred between pH 5.0 and pH 6.0. In the present investigation, a universal buffer system enabled measurements between pH 3.0 and pH 8.0 with a constant ionic strength. Small intestine contents and recta showed the maximal activity at pH 6.0. Thus, the bacteriolytic activity was similar in both species of triatomines. In microelectrode measurements, the pH-values in the anterior, middle and posterior part of the small intestine of unfed bugs were 6.3, 6.7 and 6.6, respectively (Figure S9.1.6, Suppl.). After feeding, the pH-values ranged between 6.7 and 5.3. Therefore, the determined optimal pH-conditions of bacteriolytic activity are similar to the pH milieu *in situ*, and the comparisons of the bacteriolytic activities in the small intestine and rectum samples of *T. infestans* focused on pH 6.0.

The bacteriolytic activity in small intestine and rectum samples did not correlate to protein concentrations (Figures S8.1.1 and S8.1.2, Suppl.). Thus, the bacteriolytic compounds are present at similar amounts, or different amounts may potentially not be determined with the applied methodology. The high concentrations of proteins at about 13 kDa (see 3.3.4 and 3.4.3) seemed to be mainly caused by hemoglobin degradation products derived from the bugs' blood meal.

A so far unknown phenomenon appeared in the comparisons of activities in nymphs of the two control groups. In nymphs fed on chicken blood, the small intestine contents pos-

sessed a significantly higher bacteriolytic activity than in nymphs fed on rat blood (Figure 3.4). Some major constituents of the blood – carbohydrates, lipids – are similar in most host animals of triatomines. Proteins are the most abundant nutrients in the blood and dissimilar distributed in whole blood, erythrocytes or plasma alone. Mammalian blood, e.g. human blood, contains 36.8 g protein/100 ml erythrocytes and 7.41 g protein/100 ml plasma. However, chicken blood contains only 29 g protein/100 ml erythrocytes and 3.6 g protein/100 ml plasma (summarized by LEHANE 2005). Much stronger is the difference in the levels of nucleic acids, since birds possess nucleated erythrocytes. Total phosphorus as well as certain organic and inorganic fractions in cells and serum are affected by the age of the hen, especially at the moulting season and at the time of egg production (HELLER & PAUL 1934). In future investigations mammalian blood should be supplemented with nuclei or nucleic acids to recognize whether or not this specific difference causes the increased activity after feeding of the blood of chicken.

Not only such host-blood derived effects but also feeding-induced changes affect the bacteriolytic activity (MEISER 2009). Since small intestine samples of chicken blood fed nymphs (long-control group) as well as nymphs of the long-trypo group showed a significantly increased lysis of *M. lysodeikticus* at the same time points (5, 10 and 15 daf) in comparison to unfed nymphs, increased activity of long-trypo group nymphs is most probably caused by the ingested blood. However, the statistically significantly increased bacteriolytic activity of long-trypo group nymphs in comparison to the respective control at the same time points indicates an effect of the infection, perhaps by the increased trypanosome population after blood ingestion (KOLLIEN & SCHAUB 1997, 1998b).

An effect of *T. cruzi* on the bacteriolytic activity is also indicated by the short-term infections. In our attempts to analyze the inductive compound of blood trypomastigotes we focused on the surface coat. The surface of *T. cruzi* is covered by mucins, which contribute to parasite protection and to the establishment of a persistent infection in mammals (BUSCAGLIA *et al.* 2006). Mucin-encoding genes comprise about 1 % of the parasite genome and about 6 % of all predicted *T. cruzi* genes, indicating the high relevance of mucins. *T. cruzi* mucins can be divided into two major types: those present on the surface of epimastigotes in the vector and those present on the surface of blood trypomastigotes in the mammalian host. The structural difference between the mucins extracted from epimastigotes and blood trypomastigotes resides in the lipid portion of the glycosylphosphatidylinositol-(GPI) anchor. In blood trypomastigotes, it partially switches from an alkylacylglycerol to a ceramide (SERRANO *et al.* 1995). The biological role of this modification is unknown, but it might modulate the rate of

mucin shedding (SCHENKMAN *et al.* 1993). In particular in the epimastigote stage, the 35-50 kDa mucins have a protective role against proteases, which are present in the intestinal tract of the insect vector (MORTARA *et al.* 1992). In metacyclic trypomastigotes, mucins have additional roles in the attachment to and invasion of mammalian host cells, and mucins purified from metacyclic trypomastigotes, but not from epimastigotes, bind to these host cells (YOSHIDA *et al.* 1989; RUIZ *et al.* 1993).

In the present investigation, the bacteriolytic activity of small intestine contents of short-term infected bugs (short-trypo group) and of bugs fed with blood containing purified surface coats (short-surface group) were higher than of uninfected controls and of nymphs after ingestion of epimastigotes. Therefore, the variant surface glycoproteins of intact *T. cruzi* bloodstream trypomastigotes, which were ingested by short-term infected bugs, and the purified surface coats caused an increased immune response. Nymphs fed with blood containing blood trypomastigotes after shedding of the surface coat showed no immune response in the small intestine until 3 daf. This fact underlines the importance of the surface coat for the activation of an early immune response in the intestine of the vector. A feeding of bugs on rats infected with African salivarian trypanosomes, e.g. *Trypanosoma brucei brucei*, might elucidate a species-specific induction by *T. cruzi*.

Intestinal immunity response in triatomines is not only present in the midgut, but also induced in the rectum (WHITTEN *et al*. 2007). In the present investigation, at 5 daf a statistically significantly increased bacteriolytic activity occurred in nymphs of the short-trypo group and short-naked-trypo group. Since no trypanosomes were detectable at 5 daf in the rectum of short-term infected and short-naked-trypo group bugs (data not shown), the induction might be caused by bacteria swept out of the Malpighian tubules (SCHAUB & SCHNITKER 1988) or due to a systemic immune response, which is not restricted to one section of the gut.

3.4.2 Pattern of bacteriolytic activity in the small intestine and identification of responsible proteins by mass spectrometry

The bacteriolytic activity in *R. prolixus* intestinal tract was attributed to be lysozyme activity (RIBEIRO & PEREIRA 1984). Using a recombinant lysozyme of *T. brasiliensis* (TbLys1), lysis occurred at 14 kDa and optimally at pH 5.5 in zymograms (WANIEK *et al.* 2009b). In the present investigation, in zymography the major bacteriolytic activity for short-control, long-control as well as for short-trypo and short-surface groups occurred at about 13 kDa. This molecular mass is corresponding to the size of mature *T. infestans* lysozymes (Table 3.4).

Table 3.4: Physico-chemical characteristics of the pro-form and the mature protein of *T. infestans* lysozymes.

	Pro-protein				Mature protein			
	MW [kDa]	pI	Asp+Glu*	Arg+Lys*	MW [kDa]	pI	Asp+Glu*	Arg+Lys*
TiLys1	15.65	9.07	14	21	13.81	9.16	13	20
TiLys2	15.68	5.61	15	13	13.86	5.59	14	12
TiLys3	15.57	6.79	16	16	13.70	6.96	15	15

*Quantity of respective amino acids.

For *T. infestans*, all so far described lysozymes were characterized as c-type lysozymes, attacking cell wall peptidoglycans of especially $Gram^+$ bacteria (KOLLIEN *et al.* 2003; BALCZUN *et al.* 2008; KLENNER 2008). In future investigations, the expression of *TiLys3* in the small intestine should be verified and the amino acid sequence of TiLys3 should be included in mass spectrometric data analysis. The catalytic mechanism of these lysozymes involves two steps. In the first step, a covalent glycosyl-enzyme intermediate results via the catalytic Asp residue. This intermediate is hydrolyzed in the second step, while the carboxylic groups on the side chain of Glu act as a catalytic acid/base (VOCADLO *et al.* 2001). These functionally important residues Glu and Asp are present at positions 50 and 68 in TiLys1 and TiLys3 mature proteins, respectively. Both lysozymes possess an exchange of Asn65 to Asp as well as exchanges of the polar Ser106 and Thr107 to a polar Tyr and a non-polar Gly, respectively. The lysozyme of *T. brasiliensis* possesses the same characteristics indicating a similar pH-optimum (ARAUJO *et al.* 2006).

According to mass spectrometric data analysis, TiLys1 was present in bacteriolytic active bands at about 13 kDa (Tables 3.2 and 3.3). In groups fed on chicken or rats, corresponding lysozymes of these hosts were identified additionally to TiLys1 (Tables S8.1.1-S8.1.16, Suppl.). The relevance of host blood derived lysozymes in total bacteriolytic activity in zymograms of small intestine contents is rather negligible, since in zymograms of chicken blood serum no lysis about 13 kDa occured (data not shown). Moreover, unfed bugs showed a bacteriolytic activity against *M. lysodeikticus*, and hence the activity in fed bugs is presumably not caused by chicken lysozyme, but most likely by TiLys1.

Beside the lysozymes, peptides of different *T. infestans* cathepsins were identified in the 13 kDa SDS-gel band (Figures S8.1.3 and S8.1.4, Suppl.). However, the molecular mass of mature triatomine cathepsins is about 23-29 kDa and thus considerably higher than the molecular mass of lysozymes. Therefore, only protein fragments of these cathepsins were identified, and a functional synergism in zymogram activity with TiLys1 is unlikely. These cathepsin fragments most likely seemed to be naturally occurring remnants of cathepsin turn-

over. Mature cathepsins D (TiCatD and TiCatD2) were isolated from an SDS-gel band at about 28 kDa (Figure 9.1.3). Mature proteins of cathepsin B (TiCatB1) and cathepsin L (TiCatL1) possess molecular masses of about 27 kDa and 23 kDa, respectively (KOLLIEN *et al*. 2004). In the zymogram of small intestines of the long-control group at 2 daf, a slight lysis zone at about 25 kDa occurred, and TiCatB, TiCatD and TiCatL were identified (Table 3.2). After *T. cruzi*-infection of *R. prolixus*, cathepsin D activity was increased in the contents of the small intestine (BORGES *et al*. 2006). Since lysozymes and cathepsin D-like proteases seem to act synergistically in the digestion of bacteria in the gut of larvae of the housefly (ESPINOZA-FUENTES & TERRA 1987; REGEL *et al*. 1998; PADILHA *et al*. 2009), a possible involvement of cathepsin D in intestinal immune responses to *T. cruzi*-infection should be investigated by qRT-PCR in future studies.

Analysis of the 13 kDa SDS-gel bands of small intestine contents of the short-surface group at 2 daf and of the long-control group at 2 and 5 daf also identified the ribosomal proteins P1 and P2 and histone H3 from *T. infestans*, respectively. These proteins are intracellular proteins, whose presence in the small intestine contents was surprising. However, their presence was probably caused by destruction of cells while extracting the contents of the small intestines or by the cell renewal of the small intestine epithelium in which old cells are passed into the lumen of the small intestine.

Although both intestinal lysozymes of *T. infestans* were described as digestive lysozymes (URSIC-BEDOYA *et al.* 2008), TiLys1 seems to possess mainly an immune related function, which is induced after feeding and significantly higher after ingestion of *T. cruzi*. It should be emphasized that especially the ingestion of blood trypomastigotes induces an immunological response. Therefore, the presence of surface coat possessing parasite stages or the presence of shed surface coats seem to up-regulate the humoral immune response in *T. infestans* small intestine after feeding. In comparison to the non-infected control group, long-term infected bugs showed a statistically significantly higher bacteriolytic activity at 5 and 10 daf. Since a *T. cruzi*-infection supports the development of non-symbiotic germs in *T. infestans* (EICHLER 1998), an immune suppressive effect of long-term *T. cruzi*-infections seems to be possible.

3.4.3 Transcriptional profile of *TiLys1* and *TiLys2*

According to the changes of bacteriolytic activities, blood ingestion and *T. cruzi* might regulate the expression of genes encoding lysozymes. The inducing effect of feeding on the

expression level was evident in the anterior midgut regions, cardia and stomach of fifth instar nymphs of *T. infestans*, dissected unfed and at 5, 10 and 15 daf, but not in the small intestine (KOLLIEN *et al*. 2003). These differences were also evident in fifth instar nymphs of *Triatoma brasiliensis* dissected additionally at 1 and 3 daf (ARAUJO *et al*. 2006). Considering only the whole intestinal tract of unfed adult *R. prolixus* and at 2, 7 and 14 daf, the feeding did not induce significant changes of expression levels of the two lysozyme encoding genes, *RpLys-A* and *RpLys-B* (URSIC-BEDOYA et al. 2008).

In the present investigations fifth instars of *T. infestans* were fed on rats (short-control group) and dissected unfed and 2, 3 and 5 daf or fed on chicken (long-control group) and dissected additionally at 10, 15 and 20 daf. Focusing on the small intestine and the two lysozymes, the expression level of *TiLys1* was significantly higher in nymphs 3 daf on rats and 15 daf on chicken than in unfed nymphs, while that of *TiLys2* was significantly higher at 10 and 15 daf on chicken and 5 daf on rats. This regulation of *TiLys1* and *TiLys2* might be part of the response of the intestinal tissue to increasing populations of symbiotic or other bacteria, activated by stimuli received elsewhere in the insects' body – or as shown in the present study – due to feeding.

Effects of *T. cruzi* on the expression of genes encoding lysozymes have only be considered previously in *R. prolixus* (URSIC-BEDOYA et al. 2008). While *RpLys-A* expression was up-regulated 7 and 14 days after ingestion of blood trypomastigotes, the transcriptional profile of *RpLys-B* remained similar after feeding non-infected or infected blood. In addition, the transcriptional level of *RpLys-A* was also up-regulated in the midgut of non-infected *R. prolixus* after inoculation of bacteria into the haemolymph (URSIC-BEDOYA *et al.* 2008). The amino acid sequence of RpLys-A is more similar to TiLys1 (79 %) and less similar to TiLys2 (61 %). RpLys-B is more divergent and has 53 % similarity to TiLys2 and only 49 % similarity to TiLys1 (Figure 3.12). The high sequence similarity of RpLysA and TiLys1 suggests a similar function in parasite interaction in the small intestine of *R. prolixus* and *T. infestans*. However, in the present study, the *TiLys2* transcript level was significantly increased at 5 daf in short-term infected nymphs, while *TiLys1* expression was down-regulated and not up-regulated at 3 days after *T. cruzi*-ingestion. Since the expression of *TiLys2* was induced following *T. cruzi* challenge, this lysozyme might be the functional counterpart of RpLys-A in *T. infestans*, despite of the higher sequence identity of TiLys1 and RpLys-A.

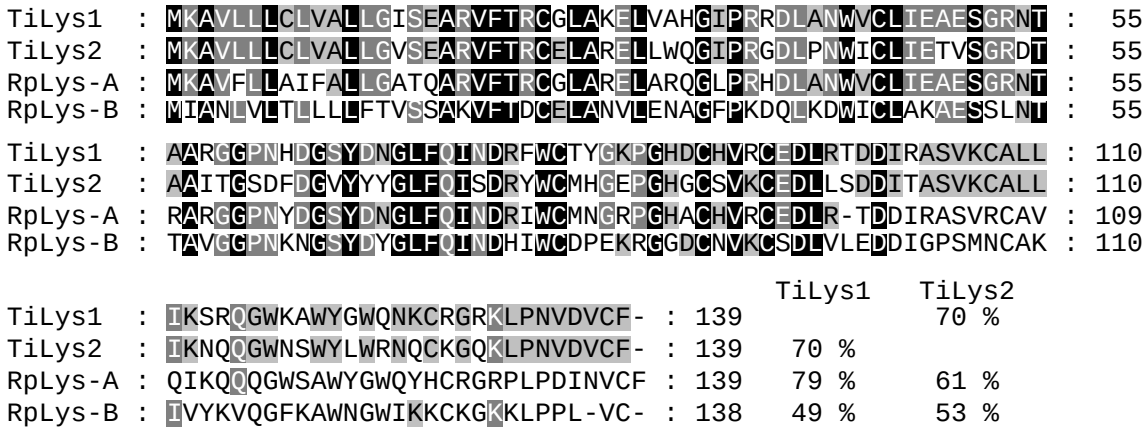

Figure 3.12: Multiple sequence alignment of lysozymes of different triatomines.
Identical amino acid residues conserved in all sequences are black shaded; amino acid residues conserved in two or three of four sequences are grey shaded. Percentages display identities to TiLys1 and TiLys2. The following GenBank sequences were used for comparison: *R. prolixus* Lys-A (**ABX11553**); *R. prolixus* Lys-B (**ABX11554**); *T. infestans* Lys1 (**AY253830**); *T. infestans* Lys2 (**ABI94387.1**).

In the analysis of the expression levels of the three independent biological samples, high standard errors were evident (Figures 3.9-3.11). Since the presence of PCR inhibitors was excluded and the robustness of the qRT-PCR setup was evaluated by using different combinations of concentration of template RNA and oligonucleotides (data not shown), the strong variations most probably reflect biological differences. One reason might be the number of symbionts which colonize the intestinal tract of triatomines. These are essential for a proper development of the nymphal stages and fertility of the adults (summarized by EICHLER & SCHAUB 2002; VALLEJO *et al.* 2009). After feeding *T. infestans* N2 with an appropriate number of symbionts, symbiotic populations in the small intestine can be detected at 2 daf for the first time (EICHLER 1998). Afterwards, symbiont population continuously rises up until 7 daf. Up to 20 daf, no additional increase of the population size is detectable. These symbionts develop up to high densities in the cardia and the stomach, but are killed in the small intestine, most probably due to the action of antimicrobial factors – like lysozymes – or digestive conditions. Since the symbiont density is variable between different individuals (EICHLER 1998), differences in expression levels of *TiLys1* and *TiLys2* within the different biological replicas might be explained by variable intensities of immune responses and/or partly by interaction with symbionts.

Most recently, up-regulation of *defensin1* transcription level in *Triatoma brasiliensis* at 20 days after ingestion of *in vitro* cultured *T. cruzi* suggested defensin1 to have a role in *T. cruzi* control (WANIEK *et al*. 2011). A synergistic function of lysozymes and defensins in *T. infestans* after short-term *T. cruzi*-infection should be considered. In *T. infestans* bacteri-

olytic activity of short-term infected and surface coat fed nymphs was significantly increased up to 5 daf. Thus, the immune response to *T. cruzi*-infection seems not to be regulated by the transcription level of neither *TiLys1* nor *TiLys2* but rather by the activity of low abundant TiLys1, whose presence was verified by mass spectrometric analysis. However, former studies focused on the long-term effect of *T. cruzi*-infection of *R. prolixus* or *T. brasiliensis* on either lysozymes or defensin (URSIC-BEDOYA *et al.* 2008; WANIEK *et al*. 2011), whereas the present study considered the initial effect of a short-term *T. cruzi*-infection. Therefore, further investigations have to include the effects on *TiLys1* and *TiLys2* relative expression levels up to 20 days after *T. cruzi*-infection.

The increase of the bacteriolytic activity by the surface coats offers the possibility for a molecular biologic identification of the intracellular pathway related to the immune response. So far, this has been considered in *Drosophila* after artificial infection with *Crithidia fasciculata* or *C. bombi*. These insect trypanosomatids which naturally infect seed sucking Hemiptera or bumblebees, respectively, induced the production of eight antimicrobial peptides including defensin, cecropin, attacin, drosocin, metchnikovin, drosomycin, diptericin and a matured prodomain of attacin C (BOULANGER *et al*. 2001). These peptides indicate inductions of the immune deficiency (IMD) and Toll pathway. Usually lipopolysaccharide (LPS), a cell wall compound of $Gram^-$ bacteria, is recognized by the receptors in the immune deficiency (IMD) pathway and leads to the induction of antimicrobial peptides like cecropin, drosocin and diptericin. The presence of fungi and $Gram^+$ bacteria activates the Toll pathway in *Drosophila*, resulting in the synthesis of drosomycin (summarized by BOULANGER *et al.* 2006). So far, genes encoding the IMD and Toll pathway were detected in the triatomine *R. prolixus* (URSIC-BEDOYA & LOWENBERGER 2007), but the inducing pathogen-associated molecular patterns have not been investigated. Usually, these molecules are conserved structures or motifs (MÜLLER *et al*. 2008). In *Brugia malayi* infected *Armigeres subalbatus* mosquitoes, a peptidoglycan recognition protein, C-type lectins and calreticulin were detected in the immune response of the mosquitoes against the filarial infection suggesting that lectins play a role in the detection of nematode infection in mosquitoes (summarized by CASTILLO *et al*. 2011). Since the surface coat of *T. cruzi* does not possess the uniformly composition as in African trypanosomes (summarized by HUTCHINSON *et al*. 2007), different molecules can induce the immune response in the vector. However, which pathway regulates the expression of *TiLys2* after short-term *T. cruzi*-infection in *T. infestans* has to be investigated in future studies.

CHAPTER 4

PATTERN OF BACTERIOLYTIC COMPOUNDS IN THE SMALL INTESTINE OF THE HAEMATOPHAGOUS HEMIPTERA *TRIATOMA INFESTANS*

4. Pattern of bacteriolytic compounds in the small intestine of the haematophagous Hemiptera *Triatoma infestans*

4.1 Introduction

Triatomines are vectors of *Trypanosoma cruzi*, the etiologic agent of Chagas disease in Latin America (SCHAUB 2008). *Triatoma infestans* is one of the most important vectors (SCHOFIELD 1994). Sylvatic populations of this triatomine are closely associated with wild rodents, e.g. guinea pigs. Thereby, bugs presumably colonized houses during domestication of these mammals, and *T. infestans* was dispersed passively over the South American continent, starting with pre-Incan and Incan tribes to the point of economic migration in the last century (BARGUES *et al.* 2006). In the last decade of the 20th century, domestic populations of *T. infestans* were strongly reduced by intensive spraying campaigns (DIAS & SCHOFIELD 1999; GÜRTLER *et al.* 2007) (see 1.1).

Triatomines are obligate bloodsuckers. They ingest large amounts of blood, e.g nymphs can take up 12 times of their own body weight and *T. infestans* fifth instar nymphs engorge about 360 mg blood within a single blood meal (RABINOVICH 1972). Ingested blood passes through the foregut to the midgut. It is stored in the strongly distensible stomach (LACOMBE 1957; KOLLIEN & SCHAUB 2000). There, the blood is concentrated and erythrocytes are lysed (WIGGLESWORTH 1977; AZAMBUJA *et al.* 1983). Subsequently, small portions are transported into the small intestine, where digestion takes place (KOLLIEN & SCHAUB 2000). Complete digestion is a time consuming process, e.g. digestion of twice their own body weight requires about 340 h in *T. infestans* females (LEHANE 1991).

Like many other haematophagous insects, triatomines possess symbionts, supplying them with essential nutritional compounds. While aposymbiosis causes strong pathological effects, bugs possessing symbionts show a normal development to the adult stage (summarized by EICHLER & SCHAUB 2002; VALLEJO *et al.* 2009). To date, mainly Gram^{+} actinomycetes were classified as acting totally symbiotic (summarized by DURVASULA *et al.* 2008; VALLEJO *et al.* 2009) (see 1.2.5). Symbionts are circulating within a population via coprophagy (SCHAUB 1988c; SCHAUB 1989). The number of symbionts in the stomach increases up to 18-fold after feeding (EICHLER & SCHAUB 2002). After passage of the stomach content to the small intestine, 99.9 % of the symbiont population is killed (EICHLER & SCHAUB 2002). Therefore, symbiont density in the intestine seems to be regulated by antimicrobial compounds (KOLLIEN *et al.* 2003; ARAUJO *et al.* 2006).

In addition to symbionts, air-borne microorganisms are taken up by coprophagy, but also during the moulting process in which amounts of air are ingested to increase body volume (KOLLIEN *et al.* 2003; MÜLLER *et al.* 2008). Thereby, co-infections with different microorganisms occur (FIGUEIREDO *et al.* 1990; EICHLER *et al.* 1996; MORAES *et al.* 2001; AZAMBUJA *et al.* 2004; VALLEJO *et al.* 2009). After ingestion of blood artificially enriched with high densities of air-borne bacteria, many nymphs die within 3 days (SCHAUB, unpublished). This might point to an antimicrobial control of bacteria growth.

Bacteriolytic activity in homogenates of the intestinal tract of the triatomine *R. prolixus* was suggested to be lysozyme-like activity (RIBEIRO & PEREIRA 1984). The expression rates of genes encoding lysozymes and defensin in the stomach are increased after feeding up to 15-fold and 12-fold, respectively (KOLLIEN *et al.* 2003; ARAUJO *et al.* 2006). In the small intestine, the expression levels of lysozyme and defensin determined by *in situ* hybridization are much lower than in the stomach (ARAUJO *et al.* 2006). So far, in *T. infestans* three lysozyme encoding genes have been identified by sequencing (KOLLIEN *et al.* 2003; BALCZUN *et al.* 2008; KLENNER 2008). TiLys1 and TiLys2 are expressed in the digestive tract and possess an amino acid sequence identity of 70 % (KOLLIEN *et al.* 2003; BALCZUN *et al.* 2008). These two lysozymes belong to c-type lysozymes, and each is expressed as a pro-lysozyme, consisting of a hydrophobic signal peptide and a mature protein. In contrast to TiLys1, TiLys2 has a low theoretical isoelectric point, and the two typically occurring glutamate and aspartate residues of the catalytic site are replaced by valine and tyrosine, respectively (BALCZUN *et al.* 2008). The mRNA encoding the third lysozyme was isolated from the salivary gland D3 of *T. infestans* (KLENNER 2008) and the expression in the gut remains to be determined.

Whereas the mRNA encoding these lysozymes has been characterized in detail, the presence of these proteins in the intestine has not been proven up to date. In the present study, we separated intestinal proteins of *T. infestans* via anion exchange chromatography to enrich low abundant proteins in small intestine homogenates of unfed fifth instar nymphs. The bacteriolytic activity of the fractions was determined and respective proteins were identified via subsequent mass spectrometry. Furthermore, the pattern of bacteriolytic compounds was investigated by zymography.

4.2 Methods

4.2.1 Sample preparation

At 40 days after feeding (daf) of N4, small intestines of 320 starved N5 were dissected. Eight times, fourty intestines were pooled and pestled in 150 µl buffer A (20 mM Tris, pH 7.0). The samples were centrifuged for 15 min at 13,000 *g* (4 °C). Remaining perturbing particles in the supernatants were removed by an additional centrifugation through a 0.2 µm filter (Pall Life Sciences, Port Washington, NY, USA) using the same conditions.

4.2.2 Enrichment of intestinal proteins, zymography and mass spectrometry

An anion exchange column SOURCE 15Q 4.6/100 PE (GE Healthcare, Freiburg, Germany) was equilibrated with buffer A and samples were loaded on the column. Within 30 min, bound protein was eluted by a continuously increasing linear gradient of buffer B (20 mM Tris, pH 7.0, 1 M NaCl) from 0 % to 75 % resulting in a gradient of 0-750 mM NaCl and finally 1 M NaCl and a flow rate of 500 µl/min. Fractions of 250 µl were collected. Anti-bacterial activity of each fraction was determined usin a liquid assay (see 2.2.1). Subsequent fractions at the peak of bacteriolytic activity were pooled to three independent samples (I-III). To exclude an overload of the column with proteins in the first separation, the flow-through of five replica was concentrated at 4 °C and 13,000 *g* in ultra filtration tubes with a 4 kDa exclusion limit (Intersep, Witten, Germany), and the buffer was exchanged by buffer A.

Flow-through was loaded again on the column and eluted under the same conditions in a second separation including the determination of the protein content of the elution. The three samples I-III were concentrated, buffer was exchanged as described above and loaded again on the column in a third separation. To enhance separation of proteins, they were eluted by a salt gradient increasing continuously from 0-350 mM NaCl within 30 min and finally 1 M NaCl. To increase the protein concentration for a subsequent separation, fractions with bacteriolytic activity of five replica were pooled to one sample. After concentration and buffer exchange (see above), separation was performed using the same salt gradient to elute the proteins.

The flow-through and the pooled fractions of bacteriolytic activity from the fourth separation were used to determine bacteriolytic activity at different pH-values and for zymography and mass spectrometry (see 2.2.1-2.2.5).

4.3 Results

4.3.1 Antibacterial activity of the purified compounds

Bacteriolytic activity was determined by measurement of the change in optical density at 415 nm of 0.3 % *Micrococcus lysodeikticus* liquid assays. The flow-through induced a lysis of the cells within 30 min at pH 4.0. At other pH-values no cell lysis occurred (see 4.3.2). Bacteriolytic activity at pH 4.0 accounted for 23 % of the highest activities of the pooled sample of bacteriolytic fractions at pH 6.0 and pH 7.0 (see 4.3.2). Samples of bacteriolytic fractions showed a pH-dependant activity. No lysis occurred at pH 3.0, but about 18 %, 60 % and 58 % of the highest lysis at pH 6.0 and pH 7.0 (100 %) occurred at pH 4.0, pH 5.0 and pH 8.0, respectively. In a zymogram incubated at pH 6.0, lysis of *M. lysodeikticus* occurred at about 13 kDa for flow-through and fractions with bacteriolytic activity (data not shown) similar to the zymogram of samples of non-infected bugs (see 3.3.3).

4.3.2 Proteins in the small intestine homogenates

Proteins in the flow-through eluted from the first anion exchange chromatographies possessed bacteriolytic activity (Figure 4.1). An overload of the column could be excluded (see 4.2.2), as no further proteins were eluted by an increasing salt gradient after a concentration of the flow-through of five replica, buffer exchange and subsequent chromatography (Figure S8.2.1, Suppl.).

In the first separations, proteins possessing bacteriolytic activity mainly eluted between 137 mM NaCl and 325 mM NaCl (Figure 4.1). Fractions eluting at about 137 mM NaCl (50-225 mM NaCl), 250 mM NaCl (225-275 mM NaCl) and 325 mM NaCl (275-375 mM NaCl) were also pooled and processed for a third chromatography, and the proteins were eluted using a salt gradient of 0-350 mM NaCl within 30 min (Figure S8.2.2, Suppl.). The protein profile of these separations differed and showed slightly increased concentrations at different peaks between 137-325 mM NaCl and at 1 M NaCl (Figure S8.2.2, Suppl.). However, in relation to the first separations none of the later fractions possessed a bacteriolytic activity. Therefore, all fractions of bacteriolytic activity were pooled and concentrated for a fourth chromatography, but even with the higher protein concentration, no bacteriolytic activity was detectable (Figure S8.2.3, Suppl.).

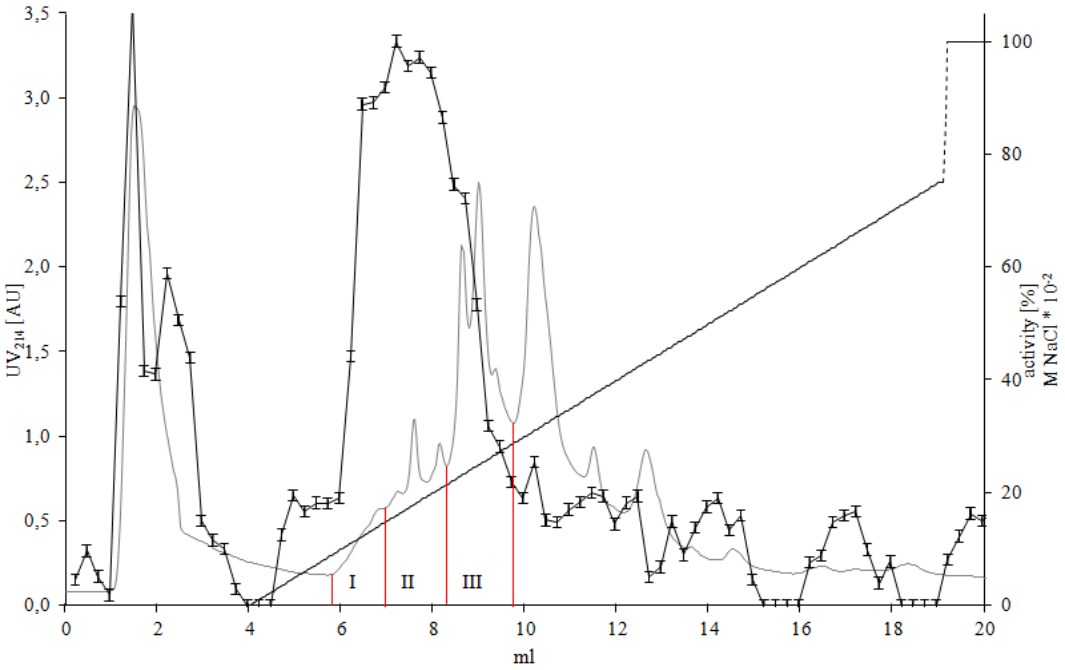

Figure 4.1: First chromatographic separations of bacteriolytic compounds from small intestine homogenates of *T. infestans*.
In the anion exchange chromatography, supernatant of small intestine homogenate was separated on a SOURCE 15Q column equilibrated with 20 mM Tris, pH 7.0. Proteins (grey line) were eluted by a linear gradient of 0-750 mM NaCl and finally 1 M NaCl (dotted line). Lysis of *Micrococcus lysodeikticus* by the respective fraction is presented as percentage of the maximal activity (black line). Standard deviations were calculated from activity of three independent separations. Red lines border the subsequent fractions used for the next separation (samples I-III).

4.3.3 Identified peptides after mass spectrometry

After tandem mass spectrometric analysis of the flow-through protein and fractions with bacteriolytic activity against *M. lysodeikticus*, 26 proteins of the flow-through were identified (Tables S8.2.1-S8.2.3, Suppl.), 17 of them as proteins from *T. infestans* (Table 4.1) the others from *Gallus gallus* (Tables S8.2.4-S8.2.6, Suppl.). Almost 90 % of the *T. infestans* proteins were salivary proteins, about two third salivary lipocalins and in addition a NAD-binding glycerol-3-phosphate dehydrogenase and a Ca^{2+}-binding protein.

In the eluted fractions, 7 of 17 proteins were also present in the flow-through; 58.8 % of all identified proteins originated from *T. infestans* (Table 4.2), and 70.5 % of them were salivary proteins. For the digestive carboxypeptidase I, cathepsin B and L, six, three and three peptides (covered 14.6 %, 12.9 % and 10.7 %) of the respective enzyme were identified. Two specific peptides covered 12.2 % of the deduced amino acid sequence of the mature TiLys1 protein (Figure 4.2). Additionally, trialysin as antibacterial pore-forming compound of the

bugs' saliva was identified with two peptides covering 16.1 % of its amino acid sequence (Figure 4.3).

Table 4.1: Mascot identification data for *T. infestans* proteins in the flow-through of the chromatographic separation.

Accession	Amino-acids	MW [kDa]	Σ Identified peptides†	Σ Coverage [%]	Score	Protein
A6YPU2	175	19.9	9	41.7	3308.4	Putative salivary secreted protein
B4XU24	355	39.0	17	43.4	3113.7	Glycerol-3-phosphate dehydrogenase
A6YPE6	179	20.0	6	29.6	625.9	Salivary lipocalin
A6YPP6	193	22.3	6	32.1	412.2	Salivary lipocalin
Q18NS6	178	19.5	4	28.7	399.5	Platelet inhibitor triplatin-2
A6YPL3	199	22.3	5	26.6	381.8	Salivary lipocalin
A6YPE9	179	20.0	5	25.1	359.4	Salivary lipocalin
A6YPR4	197	21.6	4	17.8	356.7	Lipocalin-like Ti65
A6YPG6	182	20.4	3	13.7	136.6	Salivary lipocalin
A6YPH4	175	19.2	2	17.7	318.4	Salivary lipocalin
A6YPE8	179	19.9	5	25.1	309.1	Salivary lipocalin
A6YPH2	202	22.7	3	13.4	304.4	Salivary lipocalin
A6YPT7	154	15.9	2	18.2	137.8	Superoxide dismutase [Cu-Zn]
A6YPN6	202	22.4	2	9.4	98.0	Salivary lipocalin
A6YPG4	184	20.3	2	13.1	95.5	Calponin
A6YPK2	178	20.5	2	14.1	85.0	Ca^{2+}-binding protein
A6YPH0	185	20.5	2	12.4	75.2	Salivary lipocalin

Accession numbers were derived from Uniprot Protein Database (2011). Sequence coverage of the identified peptides is given as Σ Coverage. Significance of the search result is given as score. †Not redundant peptides.

Table 4.2: Mascot identification data for *T. infestans* proteins in bacteriolytic active fractions of the chromatographic separation.

Accession	Amino-acids	MW [kDa]	Σ Identified peptides†	Σ Coverage [%]	Score	Protein
Q101N9	474	53.9	6	14.6	656.5	Serine carboxypeptidase 1
A6YPH1	169	18.6	9	61.0	586.7	Thymosin beta
A6YPG8	193	20.3	8	33.7	449.3	DJ-1
A6YPT7*	154	15.9	4	31.2	421.6	Superoxide dismutase [Cu-Zn]
Q67EP7	328	36.5	3	10.7	421.2	Cathepsin L-like protease
B4XU24*	355	39.0	6	18.3	419.7	Glycerol-3-phosphate dehydrogenase
A6YPK2*	178	20.5	5	28.1	302.6	Ca^{2+}-binding protein
A6YPG4*	184	20.3	5	32.6	279.9	Calponin
A6YPI9	129	14.6	4	45.7	276.7	Salivary secreted protein
A6YPU2*	175	19.9	2	16.6	209.4	Putative salivary secreted protein
A6YPR1	214	24.3	3	15.9	166.8	Putative rab11
A6YPR4*	197	21.6	3	17.8	152.1	Lipocalin-like Ti65
A6YPL3*	199	22.3	2	10.6	126.5	Salivary lipocalin
A6YPU0	178	20.4	3	28.7	115.5	Actin-related protein Arp2/3$^{\Delta}$
Q8T0Z4	205	22.2	2	16.1	113.1	Trialysin
A2SZV7	333	36.4	3	12.9	107.7	Cathepsin B-like protease
Q7YZS5	139	15.6	2	12.2	85.3	TiLys1

Accession numbers were derived from Uniprot Protein Database (2011). Sequence coverage of the identified peptides is given as Σ Coverage. Significance of the search result is given as score. *Identical peptides were also identified in the flow-through. †Not redundant peptides. $^{\Delta}$Complex subunit ARPC3.

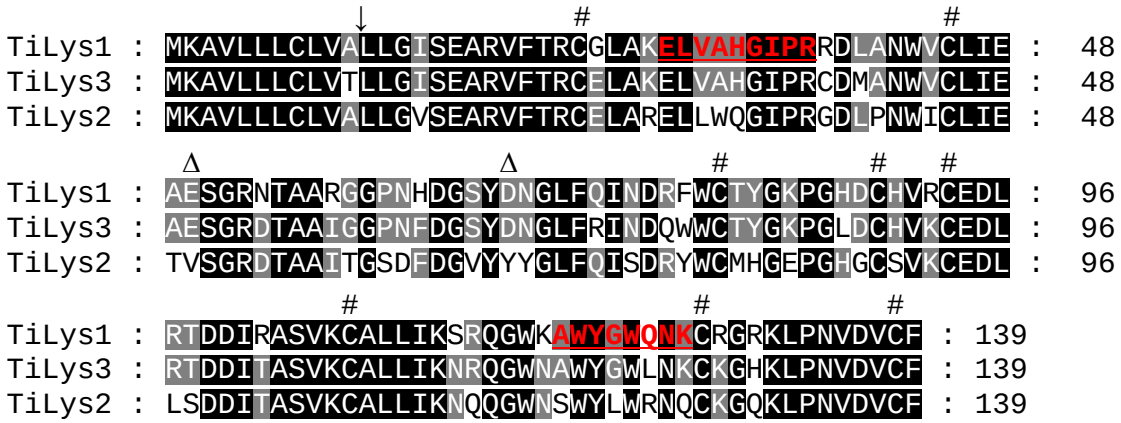

Figure 4.2: Multiple sequence alignment of TiLys1, TiLys2 and TiLys3.
The predicted signal peptide cleavage site is marked by an arrow. The conserved cysteine residues presumably forming disulphide bridges are marked (#). Functionally important residues of glutamate (E) and aspartate (D) are indicated by Δ. Identical amino acid residues conserved in all or two of three sequences are black or grey shaded, respectively. Peptides identified for TiLys1 by mass spectrometry are underlined and printed red.

```
MSKFWLLLLLVAAFQFAHSYPAAEYELDETTNDEVRQFIGDGYFEDEGDDGD  52
EERFKIKPGKVLDKFGKIVSKVLKQLKKVSAVAKVAMKKGAALLKKMGVKIS 104
PLKCEENTCKSCVIFKIPTENSFCLTIRFMKTNIATYLVVAGEINRKSKFEE 156
KLKLGNMPRCVNVEGFIGKVCMKGIEGHAKSSSGQANVNFCLGLVAEKFGVG 208
AKLCGIYANKKVRVKISPQLFPGATSLDGDIVKLDDNGEDATTLDVDEVEID 260
```

Figure 4.3: Putative amino acid sequence of trialysin.
The sequence was derived from GenBank query **AF427487** (AMINO *et al.* 2002). Peptides identified for trialysin by mass spectrometry are underlined and printed red.

4.4 Discussion

Whereas proteins in the saliva of different triatomines have been identified (RIBEIRO *et al*. 1998; AMINO *et al*. 2002; ASSUMPÇÃO *et al*. 2008; MEISER *et al*. 2010), the digestive tract has not been considered before. Results obtained from the separation of small intestine homogenates via anion exchange chromatography allowed the determination of bacteriolytic compounds in the eluted fractions. Subsequently, the bacteriolytic compounds were identified using mass spectrometry. In both, flow-through and bacteriolytically active fractions, salivary lipocalins were detected (Tables 4.1 and 4.2). These salivary lipocalins were described on transcript level and suggested to act as a factor for evasion or tolerance of the host defense response (ASSUMPCAO *et al.* 2008). The mass spectrometric identification of these proteins indicates a stable presence of proteins of the saliva in the small intestine even at 40 daf or a so far unknown expression of the responsive genes also in the intestine, as indicated by the ge-

nome project in *R. prolixus* (RIBEIRO *et al*. unpublished). Compared to other proteins, salivary lipocalins were present in both samples. Beside salivary lipocalins, superoxide dismutase [Cu-Zn], glycerol-3-phosphate dehydrogenase and Ca^{2+}-binding protein were identified in both samples (Table 4.2). The presence of these proteins in the flow-through as well as in the bacteriolytically active fractions can possibly be explained by different isoforms or degradation products, interactions with other proteins or different posttranslational modifications.

In chromatography, the flow-through initially possessed a bacteriolytic activity against *M. lysodeikticus* at pH 6.0. After further chromatographic separation, the bacteriolytic activity faded (Figure S8.2.1, Suppl.). The loss of activity can be explained by the presence of hemoglobin degradation products. Bovine hemoglobin fragments in the tick *Boophilus microplus* are antibacterially active against *M. lysodeikticus* (FOGAÇA *et al*. 1999). In *T. infestans* degradation products of chicken hemoglobin were detected in the flow-through (Table S8.2.1, Suppl.), which further supports this suggestion. In fractions of the first separations the bacteriolytic activity remained stable. In these fractions, highest activity occurred at pH 6.0. This pH is typical for the small intestine of *T. infestans* (see Chapter 9), and enables the highest bacteriolytic activity.

The present study also identified trialysin in the bacteriolytically active fractions (Table 4.1). The presence of trialysin was shown in the salivary glands (AMINO *et al.* 2002). The protein was characterized as pore-forming antibacterial protein with a molecular mass of 22.2 kDa. Trialysin was able to lyse bacteria as well as trypanosomes. A protective function against trypanosome infection of the salivary glands was already suggested by AMINO *et al.* (2002). The absent lysis in the zymograms at the respective molecular mass suggests that trialysin in the bacteriolytic active fractions is not present in its active form. Whether trialysin origins from the salivary glands or small intestine needs to be considered in future investigations. Elucidating also a function in the digestive tract is furthermore essential.

Other known antibacterial compounds in the intestine of triatomines – including the 4-5 kDa defensins and attacin-like proteins of 20-23 kDa (BULET *et al*. 1993; ARAUJO *et al*. 2006; URSIC-BEDOYA *et al*. 2011) – were not identified via mass spectrometry. These proteins were not detected in the flow-through or in the pooled fractions. In contrast to attacin-like proteins, the predicted amino acid sequence of defensin (GenBank accession **ABD61004**) is rich in cysteines. Theoretic tryptic digestion results in seven peptides, each possessing one or more cysteine residues. Unfortunately, the identification of cysteine containing peptides is almost impossible in mass spectrometry without reduction and alkylation during sample preparation. Therefore, defensin could not be identified in the here investigated samples. The

presence of defensin in small intestine homogenates of *T. infestans* needs to be validated in future studies using reduced and alkylated samples.

Bacteriolytic activity is usually suggested to depend on lysozymes (HULTMARK 1996). In Diptera, the c-type lysozymes have been divided into immunity-related lysozymes, protecting the intestinal tract against bacterial infections, and digestive lysozymes (REGEL *et al.* 1998). The latter share common features with the digestive lysozymes of vertebrate ruminants, e.g. activity optima at low pH-values and at physiological ionic strength and a resistance to proteolytic digestive enzymes (PRAGER 1996). For triatomines, the lysozymes TiLys1 and TiLys2 (KOLLIEN *et al*. 2003; BALCZUN *et al*. 2008) were suggested to act mainly as digestive enzymes due to sequence homologies with the respective lysozymes of Diptera (URSIC-BEDOYA *et al.* 2008). TiLys1 was the first lysozyme described at the transcript level from the intestinal tract of *T. infestans* (KOLLIEN *et al.* 2003). Later, molecular biological investigations identified another intestinal lysozyme (TiLys2) of this haematophagous insect (BALCZUN *et al.* 2008). A third one was found to be expressed in the insects' salivary glands D3 (KLENNER 2008). In *Triatoma brasiliensis*, a lysozyme gene (*TbLys1*), expressed in the intestinal tract and fat body was described (ARAUJO *et al*. 2006). The expression of *TbLys1* in the small intestine was 60-300 times higher than in the stomach, rectum and fat body. In immune-stimulated *R. prolixus*, fat body and intestine contained mRNA encoding two lysozymes (*RpLys-A* and *RpLys-B*) (URSIC-BEDOYA *et al.* 2008). While *RpLys-B* is predominantly expressed in the fat body, *RpLys-A* is mainly expressed in the midgut after *T. cruzi*-ingestion. In RpLys-A, 79 % of the deduced amino acid sequence are identical with TiLys1 and only 49 % with RpLys-B (Figure 3.12). *T. infestans* lysozymes have so far only been investigated once in zymograms of small intestine homogenates (MEISER 2009), while mass spectrometry analysis focused on *T. infestans* cathepsins (see Chapter 9). In zymograms of the present investigation, lysis occurred at about 13 kDa for both, flow-through and bacteriolytic active fractions after incubation at pH 6.0. This molecular mass corresponds to the size of TiLys1 mature protein (13.81 kDa), but no lysozyme was identified in the flow-through by mass spectrometry.

So far, transcripts of *TiLys3* were only identified in the salivary glands and not in the small intestine of *T. infestans* (KLENNER 2008). Thus, TiLys3 was excluded in the classification of the mass spectrometric data. Theoretical tryptic digestion of TiLys1 and TiLys3 leads to several specific peptides, six identical and three peptides with one or two replacements of amino acids for the both lysozymes (data not shown). One of these six identical peptides was identified by mass spectrometry. To generate the second identified peptide by tryptic diges-

tion of TiLys3, exchange of two amino acids would be necessary – one within the peptide sequence and another one amino acid directly before the N-terminus of the peptide – to generate a cleavage site for trypsin. Thus, the second identified peptide seemed to be specific for TiLys1 and enabled the identification of TiLys1 in the bacteriolytic active fractions.

Due to the different theoretical isoelectric points (pI) of TiLys1 (pI 9.1), TiLys2 (pI 5.6) and TiLys3 (pI 6.8) calculated by expasy pI tool (2011), a separation of the three lysozymes via anion exchange chromatography seemed to be possible. TiLys1 was predicted to be present in the flow-through. However, mass spectrometric data analysis proved the presence of TiLys1 in the bacteriolytic active fractions eluting between 50 mM NaCl and 375 mM NaCl (Figure 4.1 and Table 4.1). This difference might be caused by posttranslational modifications. Information on N-terminal acetylation or phosphorylation of the three lysozymes is lacking. Both modifications affect the surface charge of proteins and therefore the binding capacities to the anion exchange column. Usually, the N-terminus possesses a pk_s of 8. Using an anion exchange chromatographic approach around pH 7.0, the N-terminus is predominantly charged positive. Each N-terminal acetylation results in reducing the protein net charge by 1, and a phosphorylation is causing more negative charges, depending on the pH. A highly negative charged protein is eluted later from the column than a protein charged positive.

In the present study, the intestinal lysozyme TiLys1 was identified by mass spectrometry (see 3.4.3) after tryptic digestion and chromatographic separation of small intestine homogenates in the bacteriolytic active fractions (Table 4.1). Since the evidence of lysozyme was so far only proved on transcript level, this study verifies its presence for the first time *in vivo*. The protein is present in the small intestine of *T. infestans* even at 40 daf of N4, suggesting a permanent lysozyme titer, despite the inducible expression after feeding (see 3.3.6). For the other intestinal *T. infestans* lysozyme, TiLys2, only one peptide was found after mass spectrometry. Thus, TiLys2 could not be definitely identified in the present study, but its presence in the small intestine cannot be excluded.

CHAPTER 5

GENERAL DISCUSSION

5. General discussion

5.1 Material and methodological problems

Before the results of the individual chapters of this thesis are discussed comparatively, material as well as methodological problems will be addressed. For the present investigations simultaneous rearing of high numbers of nymphs was required to obtain large amounts of small intestine contents or small intestine and rectum homogenates. Especially the infection of large numbers of bugs for short-trypo group and the feeding of nymphs with high numbers of surface coats or either naked trypomastigotes was complicated. Therefore nude rats were included, which develop high parasitaemias, but the risk is high that this rat strain, characterized by an absent spleen, dies before the maximum of parasitism is reached (SCHAUB *et al.* 2001). Therefore, even more batches of standardized nymphs were required.

Changes of protein pattern in digestive tract samples were problematic. After feeding, the concentrations of proteins from the ingested blood, especially hemoglobin degradation products, were predominantly present in the small intestine (see Chapter 3). These high amounts of hemoglobin degradation products bind to the precolumn and consequently are eluted, which results in high amounts of hemoglobin in the samples. Thereby, the identification accuracy of low abundant peptides is decreased.

A chromatographic separation of small intestine homogenates of pooled fractions with bacteriolytic activity was used to obtain sufficient amounts of low abundant proteins, which were required for the further identification and characterization. To avoid hemoglobin covering, bugs at 40 daf were used for this experimental approach (see Chapter 4). However, mass spectrometric identifications of individual triatomine proteins using fragment spectra were difficult. The main problem was the small number of triatomine database references compared to e.g. the human genome. Since the proteome of *T. infestans* is not completely known, the identification of the proteins was performed by comparisons with 257 entries for *T. infestans* in the TrEMBL Database (2011). For the identification of chicken and rat proteins the Swiss-Prot Database (2010) was used. However, unequivocal identification of TiLys1 was successful after mass spectrometry (see Chapter 3 and 4).

A further methodological problem had to be considered in the characterization of the bacteriolytic activity in the photometric measurements (see Chapters 3 and 4). The bacteriolytic activity of lysozymes can be affected by an increase of the ionic strength resulting in a shift of the pH-optimum to a more acidic pH (summarized by CANÇADO *et al.* 2008). Since

we had chosen a buffer system with a constant ionic strength, pH-optima found for bacteriolytic activity in the small intestine and rectum of *Triatoma infestans* were comparable to pH-optima of other bacteriolytic proteins.

5.2 Pattern of bacteriolytic activities of unfed, short-term and long-term *T. cruzi*-infected *T. infestans*

Insects produce a wide range of antimicrobial peptides indicating the importance of humoral immunity (see 1.4.2). These compounds are secreted not only into the haemocoel but also into the intestinal tract (RIBEIRO & PEREIRA 1984; REGEL *et al*. 1998). Parasites, which are transmitted by insect vectors, occupy a specific niche in the insect. In order to be transmitted to the vertebrate host, they have to establish a relationship in which neither the insect nor the parasite dies (BOULANGER *et al.* 2006), i.e. they have to interact specifically with the immune system. In the *Trypanosoma cruzi*-triatomine interaction, the flagellate cannot simply suppress the immunity, since ingested blood has to be protected from microorganisms and the growth of the essential symbionts has to be enabled. Although 99.9 % of the symbiont population is killed after the passage to the small intestine, some symbionts must survive to enable an infection of other individuals of the population via coprophagy (EICHLER 1998). Investigations of the interactions of symbiotic and non-symbiotic bacteria, fungi and *T. cruzi* require different methodologies. In the present study, biochemical approaches (reverse-phase high-performance liquid chromatography and mass spectrometry analysis) in combination with bacteriolysis *in vitro* assays have been used to characterize the constitutive and inducible immune response after feeding and the interactions with *T. cruzi* in the small intestine and rectum of *T. infestans*.

Comparing bacteriolytic activities in small intestine samples of unfed *T. infestans* (see Chapter 4) and of short-term and long-term *T. cruzi*-infected bugs (see Chapter 3), in both investigations the main bacteriolytic activity occurred at pH 6.0. According to mass spectrometry TiLys1 seems to be the important factor for this activity. The theoretical isoelectric point for TiLys1 (pI 9.07) indicates the environment in which this protein operates. In recent investigations of the small intestine of *T. infestans* after feeding, the pH ranged between pH 5.3 and pH 6.7 (see Chapter 9). Therefore, the pH-environment in the small intestine of *T. infestans* seems to be optimal for bacteriolytic activities of TiLys1.

Beside TiLys1, lysozymes from chicken or rat were identified in bacteriolytic active SDS-gel bands of fed *T. infestans* fifth instar nymphs (see Chapter 3). Since TiLys1 was also identified in unfed bugs (see Chapter 3), the bacteriolytic activity in fed bugs is probably

caused by this protein and may only be supported by mammalian or bird lysozymes. Mass spectrometry of samples obtained at different times after feeding proved for the first time a permanent presence of TiLys1. This correlates with results of previous investigations describing *TiLys1* as a constitutively expressed gene (KOLLIEN *et al.* 2003).

For further characterization of lysozyme activity in the small intestine after short-term *T. cruzi*-infection, heat stability of bacteriolytic activity has to be evaluated. Establishment of a heterologous expression system for TiLys1 and TiLys2 will help to characterize the two intestinal lysozymes in detail. Especially investigation of their direct interaction with trypanosomes will provide a more detailed understanding of their role in the small intestine of *T. infestans*. In addition, the unequivocal localization and quantity of the different lysozymes could be determined by generating specific antibodies using heterologous synthesized proteins. However, although heterologous synthesis of lysozymes of different animals has been done by different groups, the synthesis of *T. infestans* lysozymes is complicated and own investigations with different expression systems were not successful. Former studies focused in the establishment of *TiLys1* gene knock-down through injection of double stranded RNA into the haemocoel of *T. infestans* nymphs (BUSCH 2008; ALBRING 2009). After gene knock-down of *TiLys1*, the population size of the symbiont *Rhodococcus triatomae* increased (ALBRING 2009). To evaluate the relevance of lysozymes in parasite control, future studies should focus on differences in *T. cruzi* population dynamics after gene knock-down of the different intestinal lysozymes.

CHAPTER 6

SUMMARY/ZUSAMMENFASSUNG

6. Summary/Zusammenfassung

6.1 Summary

Triatomines are obligate haematophagous insects transmitting *Trypanosoma cruzi*, the etiological agent of Chagas disease in Latin America. The present investigations focused on the parasite-induced humoral immune response to *T. cruzi*-infection in *Triatoma infestans*. Molecular biological and protein biochemical tools were applied to characterize bacteriolytically active compounds of the immune response to achieve a more detailed understanding of host parasite interactions. Addressing the bacteriolytic activity of either small intestine contents or recta or of separated fractions of small intestine homogenates after high-performance liquid chromatography, the optimal pH-condition for the activity was determined. In addition, factors inducing the intestinal immune response were elucidated by the feeding of mixtures of blood with trypomastigotes, surface coat, blood trypomastigotes without surface coat and epimastigotes. Peptidergic bacteriolytic components were identified through mass spectrometry and transcript levels of intestinal lysozymes *TiLys1* and *TiLys2* were determined by qRT-PCR.

- Investigating small intestine contents, homogenates of small intestines and recta of unfed fifth instars and fed bugs up to 15 days after feeding via photometric assays, the bacteriolytic activity against *Micrococcus lysodeikticus* was highest at pH 6.0.
- The concentration of soluble protein in the small intestine and rectum samples was not positively correlated with the bacteriolytic activity.
- The bacteriolytic activity at pH 6.0 was higher in the small intestine samples compared to the rectum samples.
- In the small intestine samples of short-term *T. cruzi*-infected bugs and bugs fed shed surface coats, bacteriolytic activities were significantly increased up to 5 days after feeding. After ingestion of blood trypomastigotes without surface coat and epimastigotes, the bacteriolytic activity in the small intestine and rectum samples was not changed significantly.
- In the small intestine samples of long-term *T. cruzi*-infected bugs, the bacteriolytic activity was significantly increased 5 and 10 days after feeding compared to non-infected bugs.
- In zymograms, the activity against *M. lysodeikticus* was correlated with proteins of

about 13 kDa. Mass spectrometry identified TiLys1 as possible agent for this activity. After protein separation via high-performance liquid chromatography even 40 days after feeding, TiLys1 was present in small intestine homogenates, suggesting a permanent presence.

- Transcription levels of *TiLys2* in the small intestine after feeding of fifth instar nymphs of *T. infestans* were generally higher than of *TiLys1*.
- After ingestion of chicken or rat blood, *TiLys1* was up-regulated 32-fold at 15 days after feeding or 8.4-fold at 3 days after feeding, respectively. *TiLys2* was up-regulated 8.8 and 68.6-fold at 10 and 15 days after feeding on chicken, respectively, and 5.8-fold at 5 days after feeding on rats. This indicates a specific action of the intestinal immune response to blood of different hosts.
- In short-term *T. cruzi*-infected *T. infestans*, transcription level of *TiLys2* in the small intestine was 13-fold increased at 5 days after feeding compared to unfed nymphs, while that of *TiLys1* was down-regulated at 3 days after feeding, compared to non-infected nymphs.

Both, bacteriolytic activity and expression levels of lysozymes in the small intestine samples of short-term *T. cruzi*-infected fifth instar nymphs showed a significant increase between 3 and 10 days after infection. Therefore, the flagellate induces an early intestinal immune response in *T. infestans* after the passage into the small intestine.

6.2 Zusammenfassung

Triatominen sind obligat hämatophage Insekten, die in Lateinamerika *T. cruzi* übertragen, den Erreger der Chagas Krankheit. Die vorliegenden Untersuchungen erfassten die Parasiten-induzierte Immunantwort nach einer Infektion von *T. infestans* mit *T. cruzi*. Zur Charakterisierung von bakteriolytisch aktiven Komponenten der Immunantwort und zum besseren Verständnis der Wirt-Parasit-Interaktionen wurden molekularbiologische und proteinbiochemische Verfahren eingesetzt. Bei Untersuchungen der bakteriolytischen Aktivität von entweder Dünndarminhalten und Rekta oder aufgetrennten Fraktionen von Dünndarmhomogenaten nach Hochleistungsflüssigkeitschromatographie wurde das pH-Optimum der Aktivität bestimmt. Zusätzlich wurden die auslösenden Faktoren der intestinalen Immunantwort durch Verfütterung von Blut mit Trypomastigoten, Surface coat, Bluttrypomastigoten ohne Surface coat und Epimastigoten erfasst. Peptiderge bakteriolytische Komponenten wurden mittels Massenspektrometrie identifiziert und Transkriptmengen der intestinalen Lysozyme *TiLys1* und *TiLys2* über die qRT-PCR verglichen.

- Bei photometrischen Untersuchungen der bakteriolytischen Aktivität gegen *M. lysodeikticus* an Dünndarminhalten und an Homogenaten des Dünndarms und Homogenaten des Rektums hungriger Wanzen des fünften Nymphenstadiums sowie bei Wanzen bis zu 15 Tagen nach der Fütterung war die Aktivität bei pH 6,0 am höchsten.
- Die Konzentration von löslichen Proteinen war nicht positiv mit der bakteriolytischen Aktivität korreliert.
- Die bakteriolytische Aktivität bei pH 6,0 war in Dünndarmproben stärker als in Rektumproben.
- In Dünndarmproben von frisch *T. cruzi*-infizierten und mit Surface coat gefütterten Wanzen war die bakteriolytische Aktivität bis zu 5 Tage nach der Fütterung signifikant erhöht. Nach der Verfütterung von Bluttrypomastigoten ohne Surface coat und Epimastigoten war die bakteriolytische Aktivität in Dünndarm und Rektum nicht signifikant erhöht.
- In Dünndarmproben von Nymphen mit etablierten *T. cruzi*-Infektionen war die bakteriolytische Aktivität im Vergleich zu nicht-infizierten Wanzen 5 und 10 Tage nach der Fütterung signifikant erhöht.
- In Zymogrammen wurden die stärksten bakteriolytischen Aktivitäten gegen *M. lysodeikticus* Proteinen mit einem Molekulargewicht von 13 kDa zugeordnet. Mit-

tels Massenspektrometrie wurde TiLys1 als möglicher verantwortlicher Faktor identifiziert. Auch 40 Tage nach der Fütterung wurde TiLys1 in Dünndarmhomogenaten nach der Auftrennung mittels Hochleistungsflüssigkeitschromatographie nachgewiesen. Dies belegt die permanente Präsenz des Proteins.

- Die Transkriptmenge von *TiLys2* lag im Dünndarm des fünften Nymphenstadiums von *T. infestans* nach der Fütterung generell über der von *TiLys1*.
- 15 bzw. 3 Tage nach Verfütterung von Hühner- bzw. Rattenblut war die Transkriptmenge von *TiLys1* 32- bzw. 8,4-mal höher als die von ungefütterten Wanzen. Die Transkriptmenge von *TiLys2* war 10 und 15 Tage nach der Aufnahme von Hühnerblut 8,8- bzw. 68,6-mal höher, 5 Tage nach der Aufnahme von Rattenblut 5,8-mal. Dies deutet auf eine Wirtsblut-spezifische Immunantwort des intestinalen Gewebes hin.
- Im Dünndarm der frisch infizierten Wanzen war 5 Tage nach der Fütterung die Transkriptmenge von *TiLys2* 13-mal höher als bei ungefütterten Wanzen, die von *TiLys1* jedoch 3 Tage nach der Fütterung signifikant niedriger als die von nicht-infizierten Wanzen.

Beim Vergleich der bakteriolytischen Aktivität und der Transkriptmengen der Lysozyme in Dünndarmproben von frisch infizierten Wanzen des 5. Nymphenstadiums ist ein signifikanter Anstieg zwischen 3 und 10 Tagen nach der Infektion hervorzuheben. Demnach induziert der Flagellat eine relativ frühe intestinale Immunantwort in *T. infestans*.

CHAPTER 7

REFERENCES

7. References

ABRAHAM, EP (1939) Some properties of egg-white lysozyme. *Biochemical journal* 33: 622-630

AGUILAR, VHM, ABAD-FRANCH, F, RACINES, VJ and PAUCAR, CA (1999) Epidemiology of Chagas disease in Ecuador. A brief review. *Memórias do Instituto Oswaldo Cruz* 94: 387-393

ALBRING, A (2009) *RNA-Interferenz zum Knockdown von Lysozym- und Defensin-Genen bei* Triatoma infestans. Diplomarbeit, Fakultät für Biologie und Biotechnologie, Ruhr-Universität Bochum

ALVARENGA, NJ, BRONFEN, E (1997) The metacyclogenesis of *Trypanosoma cruzi* as a parameter of parasite interaction with the triatomid vector. *Revista da Sociedade Brasileira de Medicina Tropical* 30: 247-250

AMINO, R, MARTINS, RM, PROCOPIO, J, HIRATA, IY, JULIANO, MA and SCHENKMAN, S (2002) Trialysin, a novel pore-forming protein from the saliva of hematophagous insects activated by limited proteolysis. *The journal of biological chemistry* 277: 6207-6213

ANDERSON, RS and COOK, ML (1979) Induction of lysozyme like activity in the haemolymph and hemocytes of an insect, *Spodoptera eridania*. *Journal of invertebrate pathology* 33: 197-203

ANWYL, R (1972) The structure and properties of an abdominal stretch receptor in *Rhodnius prolixus*. *Journal of insect physiology* 18: 2143-2153

ARAUJO, CA, WANIEK, PJ, STOCK, P, MAYER, C, JANSEN, AM and SCHAUB, GA (2006) Sequence characterization and expression patterns of defensin and lysozyme encoding genes from the gut of the reduviid bug *Triatoma brasiliensis*. *Insect biochemistry and molecular biology* 36: 547-560

ARAUJO, HC, CAVALCANTI, MG, SANTOS, SS, ALVES, LC and BRAYNER, FA (2008) Hemocytes ultrastructure of *Aedes aegypti* (Diptera: Culicidae). *Micron: the international research and review journal for microscopy* 39: 184-189

ARMAGANIJAN, L and MORILLO, CA (2010) Chagas disease: 101 years of solitude! Time for action. *Stroke* 41: 2453-2454

ASCHNER, M (1931) Die Bakterienflora der Pupiparen (Diptera). *Zeitschrift für Morphologie und Ökologie der Tiere* 20: 368-442

ASSUMPCAO, TC, FRANCISCHETTI, IM, ANDERSEN, JF, SCHWARZ, A, SANTANA, JM and RIBEIRO, JM (2008) An insight into the sialome of the blood-sucking bug *Triatoma infestans*, a vector of Chagas' disease. *Insect biochemistry and molecular biology* 38: 213-232

AUFDERHEIDE, AC, SALO, W, MADDEN, M, STREITZ, J, BUIKSTRA, J, GUHL, F, ARRIAZA, B, RENIER, C, WITTMERS, LE, FORNACIARI, G and ALLISON, M (2004) A 9,000-year record of Chagas' disease. *Proceedings of the National Academy of Sciences of the United States of America* 101: 2034-2039

AZAMBUJA, P, GUIMARAES, JA and GARCIA, ES (1983) Haemolytic factor from the crop of *Rhodnius prolixus*: evidence and partial characterization. *Journal of insect physiology* 29: 833-837

AZAMBUJA, P, MELLO, CB, D'ESCOFFIER, LN and GARCIA, ES (1989) *In vitro* cytotoxicity of *Rhodnius prolixus* hemolytic factor and mellitin towards different trypanosomatids. *Brazilian journal of medical and biological research* 22: 597-599

AZAMBUJA, P, FEDER, D and GARCIA, ES (2004) Isolation of *Serratia marcescens* in the midgut of *Rhodnius prolixus*: impact on the establishment of the parasite *Trypanosoma cruzi* in the vector. *Experimental parasitology* 107: 89-96

BAINES, S (1956) The role of the symbiotic bacteria in the nutrition of *Rhodnius prolixus* (Hemiptera). *The journal of experimental biology* 33: 533-541

BALCZUN, C, KNORR, E, TOPAL, H, MEISER, CK, KOLLIEN, AH and SCHAUB, GA (2008) Sequence characterization of an unusual lysozyme gene expressed in the intestinal tract of the reduviid bug *Triatoma infestans* (Insecta). *Parasitology research* 102: 229-232

BALCZUN, C, SIEMANOWSKI, J, PAUSCH, JK, HELLING, S, MARCUS, K, STEPHAN, C, MEYER, HE, SCHNEIDER, T, CIZMOWSKI, C, OLDENBURG, M, MEISER, CK, SCHUHMANN, W, SCHMIDT, S and SCHAUB, GA (2012) Intestinal aspartate proteases of the haematophagous bug *Triatoma*

infestans (Reduviidae): sequence characterisation, expression pattern and characterisation of proteolytic activity. *Insect biochemistry and molecular biology*

BAPTIST, BA (1941) The morphology and physiology of the salivary glands of Hemiptera-Heteroptera. *Quarterly journal of microscopical science* 83: 91-139

BARGUES, MD, KLISIOWICZ, DR, PANZERA, F, NOIREAU, F, MARCILLA, A, PEREZ, R, ROJAS, MG, O'CONNOR, JE, GONZALEZ-CANDELAS, F, GALVAO, C, JURBERG, J, CARCAVALLO, RU, DUJARDIN, JP and MAS-COMA, S (2006) Origin and phylogeography of the Chagas disease main vector *Triatoma infestans* based on nuclear rDNA sequences and genome size. *Infections, genetics and evolution: journal of molecular epidemiology and evolutionary genetics in infectious diseases* 6: 46-62

BARROS, VC, ASSUMPCAO, JG, CADETE, AM, SANTOS, VC, CAVALCANTE, RR, ARAUJO, RN, PEREIRA, MH and GONTIJO, NF (2009) The role of salivary and intestinal complement system inhibitors in the midgut protection of triatomines and mosquitoes. *PLoS One* 4: e6047

BARTH, R (1954) Estudos anatômicos e histólogicos sôbre a subfamília Triatominae (Heteroptera, Reduviidae). IV. parte O comlexo das glândulas salivares de *Triatoma infestans*. *Memórias do Instituto Oswaldo Cruz* 52: 517-585

BEARD, CB, CORDON-ROSALES, C and DURVASULA, RV (2002) Bacterial symbionts of the Triatominae and their potential use in control of Chagas disease transmission. *Annual review of entomology* 47: 123-141

BECKEL, WE and FRIEND, WG (1964) The relation of abdominal distension and nutrition to moulting in *Rhodnius prolixus* (Hemiptera). *Canadian journal of zoology* 42: 71-78

BENNETT-CLARK, HC (1963) Negative pressures produced in the cibarial pump of the blood sucking bug, *Rhodnius prolixus*. *Journal of experimental biology* 40: 223-229

BEN-YAKIR, D (1987) Growth retardiation of *Rhodnius prolixus* symbionts by immunizing host against *Nocardia* (*Rhodococcus*) *rhodnii*. *Journal of insect physiology* 33: 379-383

BERN, C and MONTGOMERY, SP (2009) An estimate of the burden of Chagas disease in the United States. *Clinical infectious diseases* 49: e52-54

BEWIG, F and SCHWARTZ, W (1954) Untersuchungen über die Symbiose der Triatomiden *Rhodnius prolixus* Stål und *Triatoma infestans*. *Naturwissenschaften* 41: 435

BILLINGSLEY, PF and DOWNE, AER (1985) Cellular localization of aminopeptidase in the midgut of *Rhodnius prolixus* Stål (Hemiptera, Reduviidae) during blood digestion. *Cell and tissue research* 241: 421-428

BILLINGSLEY, PF and DOWNE, AER (1986) The surface morphology of the midgut cells of *Rhodnius prolixus* Stål (Hemiptera, Reduviidae) during blood digestion. *Acta tropica* 43: 355-366

BILLINGSLEY, PF and DOWNE, AER (1988) Ultrastructural localization of cathepsin B in the midgut of *Rhodnius prolixus* Stål (Hemiptera, Reduviidae) during blood digestion. *International journal of insect morphology & embryology* 17: 295-302

BILLINGSLEY, PF and DOWNE, AER (1989) Changes in the anterior midgut cells of adult female *Rhodnius prolixus* (Hemiptera, Reduviidae) after feeding. *Journal of medical entomology* 26: 104-108

BOISBOUVIER, J, PROCHNICKA-CHALUFOUR, A, NIETO, AR, TORRES, JA, NANARD, N, RODRIGUEZ, MH, POSSANI, LD and DELEPIERRE, M (1998) Structural information on a cecropin-like synthetic peptide, Shiva-3 toxic to the sporogonic development of *Plasmodium berghei*. *European journal of biochemistry* 257: 263-273

BORGES, EC, MACHADO, EM, GARCIA, ES and AZAMBUJA, P (2006) *Trypanosoma cruzi*: effects of infection on cathepsin D activity in the midgut of *Rhodnius prolixus*. *Experimental parasitology* 112: 130-133

BOULANGER, N, BULET, P and LOWENBERGER, C (2006) Antimicrobial peptides in the interactions between insects and flagellate parasites. *Trends Parasitol* 22: 262-268

BRACK, C (1968) Electron microscopic studies on the life cycle of *Trypanosoma cruzi* with special reference to developmental forms in the vector *Rhodnius prolixus*. *Acta tropica* 25: 289-356

BRADFORD, MM (1976) A rapid and sensitive method for the quantitation of microgram quantities of protein utilizing the principle of protein-dye binding. *Analytical biochemistry* 72: 248-254

BRECHER, G and WIGGLESWORTH, VB (1944) The transmission of *Actinomyces rhodnii* Erikson in *Rhodnius prolixus* Stål (Hemiptera) and its influence on the growth of the host. *Parasitology* 35: 220-224

BRENER, Z (1973) Biology of *Trypanosoma cruzi*. *Annual review in microbiology* 27: 347-382

BREY, PT and HULTMARK, D (1998) *Molecular mechanisms of immune responses in insects*. Chapman and Hall, London.

BRIGGS, JD and ROCKSTEIN, M (1964) *Immunological responses.* Academic Press, New York.

BRITTON, HTS and ROBINSON, RA (1931) Universal buffer solution and the dissociation constant of veronal. *Journal of the chemical society* 198: 1456-1462

BROOKS, MA (1963) Symbiosis and aposymbiosis in arthropods. In: "*Symbiotic association. Thirteenth symposium of the Society for General Microbiology held at the Royal Institution, London April 1963.*" Cambridge University Press, Cambridge, pp. 200-231

BULET, P, DIMARCQ, JL, HETRU, C, LAGUEUX, M, CHARLET, M, HEGY, G, VAN DORSSELAER, A and HOFFMANN, JA (1993) A novel inducible antibacterial peptide of *Drosophila* carries an O-glycosylated substitution. *The journal of biological chemistry* 268: 14893-14897

BULET, P, HETRU, C, DIMARCQ, JL and HOFFMANN, D (1999) Antimicrobial peptides in insects; structure and function. *Developmental & comparative immunology* 23: 329-344

BURLEIGH, BA and ANDREWS, NW (1995) The mechanisms of *Trypanosoma cruzi* invasion of mammalian cells. *Annual review of microbiology* 49: 175-200

BUSCAGLIA, CA, CAMPO, VA, FRASCH, ACC and DI NOIA, JM (2006) *Trypanosoma cruzi* surface mucins: host-dependent coat diversity. *Nature reviews microbiology* 4: 229-236

BUSCH, I (2008) *Ausschaltung des Lysozyms im Darmtrakt von* Triatoma infestans *(Reduviidae, Insecta) über RNAi.* Diplomarbeit, Fakultät für Biologie und Biotechnologie, Ruhr-Universität Bochum

CAMARGO, EP (1964) Growth and differentiation in *T. cruzi*. I Origin of metacyclic trypanosomes in liquid media. *Revista do Instituto de Medicina Tropical de São Paulo* 12: 93-100

CANÇADO, FC, CHIMOY EFFIO, P, TERRA, WR and MARANA, SR (2008) Cloning, purification and comparative characterization of two digestive lysozymes from *Musca domestica* larvae. *Brazilian journal of medical and biological research* 41: 969-977

CAROD-ARTAL, FJ and GASCON, J (2010) Chagas disease and stroke. *Lancet neurology* 9: 533-542

CARVALHO-PINTO, CJ, GRISARD, EC, LOROZA, ES and STEINDEL, M (2000) Ecological and behavioral aspects of *Triatoma klugi*, a new triatome species recently described from Rio Grande do Sul State, Brazil. *Memórias do Instituto Oswaldo Cruz* 95: 336-337

CASTEELS, P, AMPE, C, JACOBS, F, VAECK, M and TEMPST, P (1989) Apidaecins: antibacterial peptides from honeybees. *The EMBO journal* 8: 2387-2391

CASTEELS, P, AMPE, C, RIVIERE, L, VAN DAMME, J, ELICONE, C, FLEMMING, M, JACOBS, F and TEMPST, P (1990) Isolation and characterization of abaecin, a major antibacterial response peptide in the honeybee (*Apis mellifera*). *European journal of biochemistry* 187: 381-386

CASTILLO, JC, REYNOLDS, SE AND ELEFTHERIANOS, I (2011) Insect immune responses to nematode parasites. *Trends in Parasitology* 27: 537-547

CASTRO, DP, MORAES, CS, GARCIA, ES and AZAMBUJA, P (2007a) Inhibitory effects of D-mannose on trypanosomatid lysis induced by *Serratia marcescens*. *Experimental parasitology* 115: 200-204

CASTRO, DP, SEABRA, SH, GARCIA, ES, DE SOUZA, W and AZAMBUJA, P (2007b) *Trypanosoma cruzi*: ultrastructural studies of adhesion, lysis and biofilm formation by *Serratia marcescens*. *Experimental parasitology* 117: 201-207

CAVANAGH, P and MARSDEN, PD (1969) Bacteria isolated from the gut of some reduviid bugs. *Transactions of the Royal Society of Tropical Medicine and Hygiene* 63: 415-416

CHAGAS, C (1909) Über eine neue Trypanosomiasis des Menschen. *Memórias do Instituto Oswaldo Cruz* 1: 159-218

CHAGAS, C (1922) The discovery of *Trypanosoma cruzi* and of American Trypanosomiasis. *Memórias do Instituto Oswaldo Cruz* 15: 3-11

CHALK, R, TOWNSON, H, NATORI, S, DESMOND, H and HAM, PJ (1994) Purification of an insect defensin from the mosquito, *Aedes aegypti*. *Insect biochemistry and molecular biology* 24: 403-410

CHIANG, RG and DAVEY, KG (1988) A novel receptor capable of monitoring applied pressure in the abdomen of an insect. *Science* 241: 1665-1667

COCIANCICH, S, DUPONT, A, HEGY, G, LANOT, R, HOLDER, F, HETRU, C, HOFFMANN, JA and BULET, P (1994) Novel inducible antibacterial peptides from a hemipteran insect, the sap-sucking bug *Pyrrhocoris apterus*. *The biochemical journal* 300: 567-575

CONTRERAS, VT, NAVARRO, MC, DE LIMA, AR, DURAN, F, ARTEAGA, R and FRANCO, Y (2002) Early and late molecular and morphologic changes that occur during the *in vitro* transformation of *Trypanosoma cruzi* metacyclic trypomastigotes to amastigotes. *Biological research* 35: 47-58

CYTRYNSKA, M, ZDYBICKA-BARABAS, A, JABLONSKI, P and JAKUBOWICZ, T (2001) Detection of antibacterial polypeptide activity *in situ* after sodium dodecyl sulfate-polyacryl-amide gel electrophoresis. *Analytical biochemistry* 299: 274-276

DAFFRE, S, KYLSTEN, P, SAMAKOVLIS, C and HULTMARK, D (1994) The lysozyme locus in *Drosophila melanogaster*: an expanded gene family adapted for expression in the digestive tract. *Molecular & general genetics* 242: 152-162

DAN, A, PEREIRA, MH, PESQUERO, JL, DIOTAIUTI, L and BEIRÃO, PS (1999) Action of the saliva of *Triatoma infestans* (Heteroptera: Reduviidae) on sodium channels. *Journal of medical entomology* 36: 875-879

DATEN-CONSULT (2011) http://daten-consult.de/forms/ttestunabh.html. called on 11.05.2011

DENISOV, V, STRONG, W, WALDER, A, GINRICH, J AND WINTZ, H (2008) Development and validation of RQI: an RNA quality indicator for the Experion™ automated electrophoresis system. *Bio-Rad tech note*: 5761

DIAS, E, LARANJA, FS, MIRANDA, A and NOBREGA, G (1956) Chagas' disease; a clinical, epidemiologic, and pathologic study. *Circulation* 14: 1035-1060

DIAS, J and SCHOFIELD, C (1999) The evolution of Chagas disease (American trypanosomiasis) control after 90 years since Carlos Chagas discovery. *Memórias do Instituto Oswaldo Cruz* 94 (Suppl. 1): 103-121

DIAS, JCP (1984) Acute Chagas` disease. *Memórias do Instituto Oswaldo Cruz* 79 (Suppl.1): 85-91

DIAS, JCP (1989) The indeterminate form of human chronic Chagas' disease. A clinical epidemiological review. *Revista da Sociedade Brasileira de Medicina Tropical* 22: 147-156

DIAS, JCP (1995) Natural history of Chagas`disease. *Arquivos brasileiros de cardiologia* 65: 359-366

DIMARCQ, JL, HOFFMANN, D, MEISTER, M, BULET, P, LANOT, R, REICHHART, JM and HOFFMANN, JA (1994) Characterization and transcriptional profiles of a *Drosophila* gene encoding an insect defensin. A study in insect immunity. *European journal of biochemistry* 221: 201-209

DIMARCQ, JL, BULET, P, HETRU, C and HOFFMANN, JA (1998) Cysteine-rich antimicrobial peptides in invertebrates. *Biopolymers* 47: 465-477

DOCAMPO, R (2007) Recent advances in chemotherapy of American trypanosomiasis. In: Sociedade de Pediatra do Estado de Rio de Janeiro (SOPERJ) (eds) "*Update of American trypanosomiasis and leishmaniasis control and research: Final report.*" Pan American Health Organisation/World Health Organisation (PAHO/WHO), Washington, pp. 83-89

DOUGLAS, AE (1989) Mycetocyte symbiosis in insects. *Biological reviews* 64: 409-434

DUNCAN, JT (1926) On a bactericidal principle present in the alimentary canal of insects and arachnids. *Parasitology* 18: 238-252

DURVASULA, RV, SUNDARAM, RK, KIRSCH, P, HURWITZ, I, CRAWFORD, CV, DOTSON, E and BEARD, CB (2008) Genetic transformation of a corynebacterial symbiont from the Chagas disease vector *Triatoma infestans*. *Experimental parasitology* 119: 94-98

EBERT, F and SCHAUB, G (1983) The characterization of Chilean and Bolivian *Trypanosoma cruzi* stocks from *Triatoma infestans* by isoelectrofocusing. *Zeitschrift für Parasitenkunde* 69: 283-290

EICHLER, S (1998) *Interaktionen von Triatominen mit ihren Symbionten und Trypanosomatiden.* Dissertation, Fakultät für Biologie und Biotechnologie, Ruhr-Universität Bochum

EICHLER, S and SCHAUB, GA (2002) Development of symbionts in triatomine bugs and the effects of infections with trypanosomatids. *Experimental parasitology* 100: 17-27

EICHLER, S, REINTJES, N, JUNG, M, YASSIN, AF, SCHAAL, KP, JUNQUEIRA, A, COURA, JR and SCHAUB, GA (1996) Identification of bacterial isolates and symbionts from wild populations of *Triatoma infestans* and *T. sordida*. *Memórias do Instituto Oswaldo Cruz* 91 (Suppl.): 125

EKENGREN, S and HULTMARK, D (1999) *Drosophila* cecropin as an antifungal agent. *Insect biochemistry and molecular biology* 29: 965-972

EL-SAYED, NM, MYLER, PJ, BARTHOLOMEU, DC, NILSSON, D, AGGARWAL, G, TRAN, AN, ELODIE GHEDIN, WORTHEY, EA, DELCHER, AL, BLANDIN, G, WESTENBERGER, SJ, CALER, E, CERQUEIRA, GC, BRANCHE, C, HAAS, B, ANUPAMA, A, ARNER, E, ASLUND, L, ATTIPOE, P, BONTEMPI, E, BRINGAUD, F, BURTON, P, CADAG, E, CAMPBELL, DA, CARRINGTON, M, CRABTREE, J, DARBAN, H, DA SILVEIRA, JF, DE JONG, P, EDWARDS, K, ENGLUND, PT, FAZELINA, G, FELDBLYUM, T, FERELLA, M, FRASCH, AC, GULL, K, HORN, D, HOU, L, HUANG, Y, KINDLUND, E, KLINGBEIL, M, KLUGE, S, KOO, H, LACERDA, D, LEVIN, MJ, LORENZI, H, LOUIE, T, MACHADO, CR, MCCULLOCH, R, MCKENNA, A, MIZUNO, Y, MOTTRAM, JC, NELSON, S, OCHAYA, S, OSOEGAWA, K, PAI, G, PARSONS, M, PENTONY, M, PETTERSSON, U, POP, M, RAMIREZ, JL, RINTA, J, ROBERTSON, L, SALZBERG, SL, SANCHEZ, DO, SEYLER, A, SHARMA, R, SHETTY, J, SIMPSON, AJ, SISK, E, TAMMI, MT, TARLETON, R, TEIXEIRA, S, VAN AKEN, S, VOGT, C, WARD, PN, WICKSTEAD, B, WORTMAN, J, WHITE, O, FRASER, CM, STUART, KD and ANDERSSON, B (2005) The genome sequence of *Trypanosoma cruzi*, etiologic agent of Chagas' disease. *Science* 309: 409-415

ENGSTRÖM, Å, ENGSTRÖM, P, TAO, ZJ, CARLSSON, A and BENNICH, H (1984a) Insect immunity. The primary structure of the antibacterial protein attacin F and its relation to two native attacins from *Hyalophora cecropia*. *The EMBO journal* 3: 2065-2070

ENGSTRÖM, P, CARLSSON, A, ENGSTRÖM, Å, TAO, ZJ and BENNICH, H (1984b) The antibacterial effect of attacins from the silk moth *Hyalophora cecropia* is directed against the outer membrane of *Escherichia coli*. *The EMBO journal* 3: 3347-3351

ESPINOZA-FUENTES, FP, TERRA, WR (1987) Physiological adaptations for digesting bacteria. Water fluxes and distribution of digestive enzymes in *Musca domestica* larval midgut. *Insect biochemistry* 17: 809-817

EXPASY (2011) http://web.expasy.org/compute_pi/ (19.09.2011).

FEHLBAUM, P, BULET, P, MICHAUT, L, LAGUEUX, M, BROEKAERT, WF, HETRU, C and HOFFMANN, JA (1994) Insect immunity. Septic injury of *Drosophila* induces the synthesis of a potent antifungal peptide with sequence homology to plant antifungal peptides. *The journal of biological chemistry* 269: 33159-33163

FEHLBAUM, P, BULET, P, CHERNYSH, S, BRIAND, JP, ROUSSEL, JP, LETELLIER, L, HETRU, C and HOFFMANN, JA (1996) Structure-activity analysis of thanatin, a 21-residue inducible insect defense peptide with sequence homology to frog skin antimicrobial peptides. *Proceedings of the National Academy of Sciences of the United States of America* 93: 1221-1225

FERREIRA, C, RIBEIRO, AF, GARCIA, EDS and TERRA, WR (1988) Digestive enzymes trapped between and associated with the double plasma membranes of *Rhodnius prolixus* posterior midgut cells. *Insect biochemistry* 18: 521-530

FERREIRA, RA, LAZZARI, CR, LORENZO, MG and PEREIRA, MH (2007) Do haematophagous bugs assess skin surface temperature to detect blood vessels? *PLoS one* 2: e932; 6pp

FIGUEIREDO, AR, PEREGRINO DA SILVA, MA, HOFER, E, DE MORAES, AML, OLIVEIRA, PC and COURA, JR (1990) Microorganisms of the Triatominae vectors of *Trypanosoma cruzi*. Microorganismos de triatomíneos vetores do *Trypanosoma cruzi*. III-Isolamento e caracterizaçao de bactérias e fungos do trato digestivo de *P. megistus* negativos e positivos para *T. cruzi*. *Memórias do Instituto Oswaldo Cruz* 85: 114

FISCHER, K (1989) *Isolierung und Identifizierung von Darmbakterien aus* Panstrongylus megistus, Triatoma infestans *und* Rhodnius prolixus *(Reduviidae, Hemiptera) und ihr Einfluss auf die Entwicklung dieser Raubwanzen.* Diplomarbeit, Fakultät für Biologie, Universität Freiburg

FLORES, GB and LAZZARI, CR (1996) The role of the antennae in *Triatoma infestans*: orientation towards thermal sources. *Journal of insect physiology* 42: 433-440

FLYG, C, KENNE, K and BOMAN, HG (1980) Insect pathogenic properties of *Serratia marcescens*: phage-resistant mutants with a decreased resistance to *Cecropia* immunity and a decreased virulence to *Drosophila*. *Journal of general microbiology* 120: 173-181

FOGAÇA, AC, DA SILVA, PI, MIRANDA, MT, BIANCHI, AG, MIRANDA, A, RIBOLLA, PE AND DAFFRE, S (1999) Antimicrobial activity of a bovine hemoglobin fragment in the tick *Boophilus microplus*. *Journal of biological chemistry* 274: 25330-25334

GALVÃO, C, CARCAVALLO, R, DA SILVA ROCHA, D and JURBERG, J (2003) A checklist of the current valid species of the subfamily Triatominae Jeannel, 1919 (Hemiptera, Reduviidae) and their geographical distribution, with nomenclatural and taxonomic notes. *Zootaxa* 202: 1-36

GANZ, T and LEHRER, RI (1995) Defensins. *Pharmacology and therapeutics* 66: 191-205

GARCIA, ES (1987) The digestion of Triatominae. In: Brenner, RR and Stoka, A (eds) "*Chagas' disease vector. Vol. 2. Anatomic and physiological aspects.*" CRC Press, Boca Raton, Florida, pp. 47-59

GARCIA, ES and GARCIA, MLM (1977) Control of protease secretion in intestine of fifth instar larvae of *Rhodnius prolixus*. *Journal of insect physiology* 23: 247-251

GARCIA, ES and GILLIAM, FC (1980) *Trypanosoma cruzi* development is independent of protein digestion in the gut of *Rhodnius prolixus*. *Journal for parasitology* 66:1052-1053

GARCIA, ES and GUIMARAES, JA (1979) Proteolytic enzymes in the *Rhodnius prolixus* midgut. *Experientia* 35: 305-306

GARCIA, ES, RATCLIFFE, NA, WHITTEN, MM, GONZALEZ, MS and AZAMBUJA, P (2007) Exploring the role of insect host factors in the dynamics of *Trypanosoma cruzi-Rhodnius prolixus* interactions. *Journal of insect physiology* 53: 11-21

GARCIA, ES, GENTA, FA, AZAMBUJA, P and SCHAUB, GA (2010) Interactions of intestinal compounds of triatomines and *Trypanosoma cruzi*. *Trends in parasitology* 26: 499-505

GASCON, J, BERN, C and PINAZO, MJ (2010) Chagas disease in Spain, the United States and other non-endemic countries. *Acta tropica* 115: 22-27

GAUNT, M and MILES, M (2000) The ecotopes and evolution of triatomine bugs (Triatominae) and their associated trypanosomes. *Memórias do Instituto Oswaldo Cruz* 95: 557-565

GEIGY, R, HALFF, LA and KOCHER, V (1953) Studies on physiological relations between a carrier of Chagas' disease, *Triatoma infestans* and its intestinal symbionts. *Schweizerische medizinische Wochenschrift* 83: 928-930

GOODCHILD, AJ (1955) The bacteria associated with *Triatoma infestans* and some other species of Reduviidae. *Parasitology* 45: 441-448

GORLA, DE, DUJARDIN, JP and SCHOFIELD, CJ (1997) Biosystematics of Old World Triatominae. *Acta tropica* 63: 127-140

GÖTZ, P (1988) Immunreaktion bei Wirbellosen, insbesondere Insekten. *Verhandlungen der Deutschen Zoologischen Gesellschaft* 81: 113-129

GÖTZ, P and VEY, A (1974) Humoral encapsulation in Diptera (Insecta): defence reactions in *Chironomus* larvae against fungi. *Parasitology* 68: 193-205

GRINDE, B, JOLLÈS, J and JOLLÈS, P (1988) Purification and characterization of two lysozymes from rainbow trout (*Salmo gairdneri*). *European journal of biochemistry* 173: 269-273

GRUNCLOVÀ, L, FOUQUIR, H, HYPSA, V and KOPÀCEK, P (2003) Lysozyme from the gut of the soft tick *Ornithodoros moubata*: the sequence, phylogeny and post-feeding regulation. *Developmental & comparative immunology* 27: 651-660

GUERENSTEIN, PG and GUERIN, PM (2001) Olfactory and behavioural responses of the blood-sucking bug *Triatoma infestans* to odours of vertebrate hosts. *The journal of experimental biology* 204: 585-597

GUERRI-GUTTENBERG, RA, GRANA, DR, AMBROSIO, G and MILEI, J (2008) Chagas cardiomyopathy: Europe is not spared! *European heart journal* 29: 2587-2591

GÜRTLER, RE, KITRON, U, CECERE, MC, SEGURA, EL and COHEN, JE (2007) Sustainable vector control and management of Chagas disease in the Gran Chaco, Argentina. *Proceedings of the National Academy of Sciences of the United States of America* 104: 16194-16199

GUHL, F, JARAMILLO, C, VALLEJO, GA, YOCKTENG, R, CARDENAS-ARROYO, F, FORNACIARI, G, ARRIAZA, B and AUFDERHEIDE, AC (1999) Isolation of *Trypanosoma cruzi* DNA in 4,000-

year-old mummified human tissue from northern Chile. *American journal of physical anthropology* 108: 401-407

GULLAN, PJ and CRANSTON, PS (1994) *The insects: an outline of entomology*. Chapman and Hall, London.

GUMPERT, J (1962) Untersuchungen über die Symbiose von Tieren mit Pilzen und Bakterien. X. Die Symbiose der Triatominen. 2. Infektion symbiontenfreier Triatominen mit symbiontischen und saprophytischen Mikroorganismen und gemeinsame Eigenschaften der symbiontischen Stämme. *Zeitschrift für allgemeine Mikrobiologie* 2: 290-302

GUMPERT, J and SCHWARTZ, W (1962) Untersuchungen über die Symbiose von Tieren mit Pilzen und Bakterien. X. Die Symbiose der Triatominen. 1. Aufzucht symbiontenhaltiger und symbiontenfreier Triatominen und Eigenschaften der bei Triatominen vorkommenden Mikroorganismen. *Zeitschrift für allgemeine Mikrobiologie* 2: 209-225

HALL, BF and JOINER, KA (1991) Strategies of obligate intracellular parasites for evading host defences. *Immunology today* 12: A22-27

HARDT, M, GUO, Y, HENDERSON, G and LAINE, RA (2003) Zymogram with Remazol brilliant blue-labeled *Micrococcus lysodeikticus* cells for detection of lysozymes: example of a new lysozyme activity in Formosan termite defense secretions. *Analytical biochemistry* 312: 73-76

HARIDASS, ET and ANANTHAKRISHNAN, TN (1980) Bionomics and behaviour of the reduviid bug, *Triatoma rubrofasciata* (de Geer), the vector of *Trypanosoma* (*Megatrypanum*) *conorhini* (Donovan), in India (Insecta: Heteroptera). *Proceedings of the Indian National Science Academy. Part B, Biological sciences* 46: 884-891

HARINGTON, JS (1960) Studies on *Rhodnius prolixus*: growth and development of normal and sterile bugs, and the symbiotic relationship. *Parasitology* 50: 279-286

HELLER, VG and PAUL, H (1934) Changes in the blood calcium and phosphorus partition during the life cycle of the chicken. *The Journal of biological chemistry* 106: 357-364

HILL, P, CAMPBELL, JA and PETRIE, IA (1976) *Rhodnius prolixus* and its symbiotic actinomycete: a microbiological, physiological and behavioural study. *Proceedings of the Royal Society of London. Series B, Biological sciences* 194: 501-525

HINDE, R (1971) The control of the mycetome symbiotes of the aphids *Brevicoryne brassicae*, *Myzus persicae*, and *Macrosiphum rosae*. *Journal of insect physiology* 17: 1791-1800

HOFFMANN, T (1992) *Untersuchung zur bakteriellen Darmflora von* Panstrongylus megistus, Triatoma klugi *und* Triatoma brasiliensis *(Reduviidae, Hemiptera) und Identifizierung symbiontischer Aktinomyceten.* Diplomarbeit, Fakultät für Biologie, Ruhr-Universität Bochum

HÖLSCHER, C, MOHRS, M, DAI, WJ, KÖHLER, G, RYFFEL, B, SCHAUB, GA, MOSSMANN, H AND BROMBACHER, F (2000) Tumor necrosis Factor alpha-mediated toxic shock in *Trypanosoma cruzi*-infected interleukin 10-deficient mice. *Infection and immunity* 68: 4075-4083

HÖLSCHER, C, HARTMANN, R, MOSSMANN, H and SCHAUB, GA (2003) Effects of the isolation methodology on protein profiles of blood trypomastigotes of *Trypanosoma cruzi*. *Parasitology* 126: 41-51

HOTEZ, PJ, MOLYNEUX, DH, FENWICK, A, KUMARESAN, J, SACHS, SE, SACHS, JD and SAVIOLI, L (2007) Control of neglected tropical diseases. *The New England journal of medicine* 357: 1018-1027

HOUSEMAN, J (1978) A thiol-activated digestive proteinase from adults of *Rhodnius prolixus* Stal (Hemiptera-Reduviidae). *Can J Zool* 56: 1140-1143

HOUSEMAN, JG and DOWNE, AER (1981) Exoproteinase activity in the posterior midgut of *Rhodnius prolixus* Stål (Hemiptera, Reduviidae). *Insect biochemistry* 11: 579-582

HOUSEMAN, JG and DOWNE, AER (1982) Characterization of an acidic proteinase from the posterior midgut of *Rhodnius prolixus* Stål (Hemiptera, Reduviidae). *Insect biochemistry* 12: 651-655

HOUSEMAN, JG and DOWNE, AER (1983a) Activity cycles and the control of four digestive proteinases in the posterior midgut of *Rhodnius prolixus* Stål (Hemiptera, Reduviidae). *Journal of insect physiology* 29: 141-148

HOUSEMAN, JG and DOWNE, AER (1983b) Cathepsin D-like activity in the posterior midgut of the hemipteran insects. *Comparative biochemistry and physiology B, Comparative biochemistry* 75: 509-512

HOUSEMAN, JG, DOWNE, AER and MORRISON, PE (1985) Similarities in digestive proteinase production in *Rhodinius prolixus* (Hemiptera, Reduviidae) and *Stomoxys calcitrans* (Diptera, Muscidae). *Insect biochemistry* 15: 471-474

HULTMARK, D (1996) *Insect lysozymes.* Birkhäuser Verlag, Basel.

HULTMARK, D, ENGSTROM, A, BENNICH, H, KAPUR, R and BOMAN, HG (1982) Insect immunity: isolation and structure of cecropin D and four minor antibacterial components from *Cecropia* pupae. *European journal of biochemistry* 127: 207-217

HULTMARK, D, ENGSTROM, A, ANDERSSON, K, STEINER, H, BENNICH, H and BOMAN, HG (1983) Insect immunity. Attacins, a family of antibacterial proteins from *Hyalophora cecropia*. *The EMBO journal* 2: 571-576

HUTCHINSON, OC, PICOZZI, H, JONES, NG, MOTT, H, SHARMA, R, WELBURN, SC and CARRINGTON, M (2007) Variant Surface Glycoprotein gene repertoires in *Trypanosoma brucei* have diverged to become strain-specific. *BMC Genomics* 8: 234

JAYNES, JM, BURTON, CA, BARR, SB, JEFFERS, GW, JULIAN, GR, WHITE, KL, ENRIGHT, FM, KLEI, TR and LAINE, RA (1988) *In vitro* cytocidal effect of novel lytic peptides on *Plasmodium falciparum* and *Trypanosoma cruzi*. *FASEB journal* 2: 2878-2883

JOLLÈS, J, SCHOENTGEN, F, CROIZIER, G and JOLLÈS, P (1979) Insect lysozymes from three species of Lepidoptera: their structural relatedness to the C (chicken) type lysozyme. *Journal of molecular evolution* 14: 267-271

JUNG, M (1995) *Auswirkungen der Infektion mit verschiedenen Bakterien auf die Entwicklung der Raubwanze* Triatoma infestans *(Reduviidae, Hemiptera).* Diplomarbeit, Fakultät für Biologie, Ruhr-Universität Bochum

KINOSHITA, T and INOUE, K (1977) Bactericidal activity of the normal, cell-free hemolymph of silkworms (*Bombyx mori*). *Infection and immunity* 16: 32-36

KLENNER, L (2008) *Biochemische und molekularbiologische Charakterisierung antibakterieller Faktoren aus den Speicheldrüsen von* Triatoma infestans *(Reduviidae, Insecta).* Diplomarbeit, Fakultät für Biologie und Biotechnologie, Ruhr-Universität Bochum

KOLLIEN, AH and SCHAUB, GA (1997) *Trypanosoma cruzi* in the rectum of the bug *Triatoma infestans*: effects of blood ingestion of the vector and artificial diuresis. *Parasitology research* 83: 781-8

KOLLIEN, AH and SCHAUB, GA (1998a) The development of *Trypanosoma cruzi* (Trypanosomatidae) in the reduviid bug *Triatoma infestans* (Insecta): influence of starvation. *The journal of eukaryotic microbiology* 45: 59-63

KOLLIEN, AH and SCHAUB, GA (1998b) *Trypanosoma cruzi* in the rectum of the bug *Triatoma infestans*: effects of blood ingestion by the starved vector. *The American journal of tropical medicine and hygiene* 59: 166-170

KOLLIEN, AH and SCHAUB, GA (2000) The development of *Trypanosoma cruzi* in Triatominae. *Parasitology today* 16: 381-387

KOLLIEN, AH, FECHNER, S, WANIEK, PJ and SCHAUB, GA (2003) Isolation and characterization of a cDNA encoding for a lysozyme from the gut of the reduviid bug *Triatoma infestans*. *Archives of insect biochemistry and physiology* 53: 134-145

KOLLIEN, AH, WANIEK, PJ, NISBET, AJ, BILLINGSLEY, PF and SCHAUB, GA (2004) Activity and sequence characterization of two cysteine proteases in the digestive tract of the reduviid bug *Triatoma infestans*. *Insect molecular biology* 13: 569-579

KYLSTEN, P, SAMAKOVLIS, C and HULTMARK, D (1990) The cecropin locus in *Drosophila*; a compact gene cluster involved in the response to infection. *The EMBO journal* 9: 217-224

LACKIE, AM (1988a) Haemocyte behavior. *Advances in insect physiology* 21: 97-111

LACKIE, AM (1988b) Immune mechanisms in insects. *Parasitology today* 4: 98-103

LACOMBE, D (1957) Anatomical and histological studies of the subfamily Triatominae (Heteroptera, Reduviidae). VII. Anatomical study of the intestinal duct of *Triatoma infestans*. *Memórias do Instituto Oswaldo Cruz* 55: 69-111

LACOMBE, D (1999) Anatomia e histologia das glândulas salivares das Triatomíneos. *Memórias do Instituto Oswaldo Cruz* 94: 557-564

LAEMMLI, UK (1970) Cleavage of structural proteins during the assembly of head of bacteriophage T4. *Nature* 227: 680-685

LAKE, P and FRIEND, WG (1967) A monoxenic relationship, *Nocardia rhodnii* Erikson in the gut of *Rhodnius prolixus* Stål (Hemiptera, Reduviidae). *Proceedings of the Entomological Society of Ontario* 98: 53-57

LAMBERT, J, KEPPI, E, DIMARCQ, JL, WICKER, C, REICHHARD, JM, DUNBAR, B, LEPAGE, P, VAN DORSSELAER, A, HOFFMANN, JA and FOTHERGILL, J (1989) Insect immunity: isolations from immune blood of the dipteran *Phormia terranovae* of two insect antibacterial peptides with sequence homology to rabbit lung macrophage bactericidal peptides. *Proceedings of the National Academy of Sciences of the United States of America* 86: 262-266

LAVINE, MD and STRAND, MR (2002) Insect hemocytes and their role in immunity. *Insect biochemistry and molecular biology* 32: 1295-1309

LAVOIPIERRE, MM, DICKERSON, G and GORDON, RM (1959) Studies on the methods of feeding of blood-sucking arthropods. I. The manner in which triatomine bugs obtain their blood-meal, as observed in the tissues of the living rodent, with some remarks on the effects of the bite on human volunteers. *Annals of tropical medicine and parasitology* 53: 235-250

LAZZARI, CR (1992) Circadian organization of locomotion activity in the haematophagous bug *Triatoma infestans*. *Journal of insect physiology* 38: 895-903

LAZZARI, CR and NÚÑEZ, JA (1989) The response to radiant heat and the estimation of the temperature of distant sources in *Triatoma infestans*. *Journal of insect physiology* 35: 525-529

LEE, WJ and BREY, PT (1995) Isolation and characterization of the lysozyme-encoding gene from the silkworm *Bombyx mori*. *Gene* 161: 199-203

LEHANE, MJ (1991) Managing the blood meal. In: Lehane, MJ (ed) "*Biology of blood-sucking insects.*" Harper Collins Academic, London, pp. 79-110

LEHANE, MJ (2005) Managing the blood meal. In: Lehane, MJ (ed) 2nd edn. "*The biology of blood-sucking in insects.*" University Press, Cambridge, pp. 85-115

LENT, H and WYGODZINSKY (1979) Revision of the Triatominae (Hemiptera, Reduviidae), and their significance as vectors of Chagas' disease. *Bulletin of the American Museum of Natural History* 163: 123-520

LLEWELLYN, MS and MILES, MA (2010) Outlook Chagas disease: who, how, what and where? *Nature* 465: 8-9

LOPEZ, L, MORALES, G, URSIC, R, WOLFF, M and LOWENBERGER, C (2003) Isolation and characterization of a novel insect defensin from *Rhodnius prolixus*, a vector of Chagas disease. *Insect biochemistry and molecular biology* 33: 439-447

LOPEZ-ORDOÑEZ, T, RODRIGUEZ, MH and HERNANDEZ-HERNANDEZ, FD (2001) Characterization of a cDNA encoding a cathepsin L-like protein of *Rhodnius prolixus*. *Insect molecular biology* 10: 505-511

LORENZO, AN, KENIFSTEIN, A and LAZZARI, CR (1991) Daily dynamics and factors affecting aggregation in *Triatoma infestans*. *Memórias do Instituto Oswaldo Cruz* (Suppl. 1) 86: 246

LOWENBERGER, C (2001) Innate immune response of *Aedes aegypti*. *Insect biochemistry and molecular biology* 31: 219-229

LOWENBERGER, CA, FERDIG, MT, BULET, P, KHALILI, S, HOFFMANN, JA and CHRISTENSEN, BM (1996) *Aedes aegypti*: induced antibacterial proteins reduce the establishment and development of *Brugia malayi*. *Experimental parasitology* 83: 191-201

LOWENBERGER, CA, KAMAL, S, CHILES, J, PASKEWITZ, S, BULET, P, HOFFMANN, JA and CHRISTENSEN, BM (1999) Mosquito-*Plasmodium* interactions in response to immune activation of the vector. *Experimental parasitology* 91: 59-69

MALKE, H (1965) Über das Vorkommen von Lysozym in Insekten. *Zeitschrift für allgemeine Mikrobiologie* 5: 42-47

MATHERS, CD, EZZATI, M and LOPEZ, AD (2007) Measuring the burden of neglected tropical diseases: the global burden of disease framework. *PLoS neglected tropical diseases* 1: e114

MATOVA, N and ANDERSON, KV (2006) Rel/NF-kappaB double mutants reveal that cellular immunity is central to *Drosophila* host defense. *Proceedings of the National Academy of Sciences of the United States of America* 103: 16424-16429

MATSUYAMA, K and NATORI, S (1988) Purification of three antibacterial proteins from the culture medium of NIH-Sape-4, an embryonic cell line of *Sacrophaga peregrina*. *The journal of biological chemistry* 263: 17112-17116

MATTOCK, N and PINK, R (2005) Special programme for research and training in tropical diseases. Making health research work for poor people: progress 2003-2004: tropical disease research. In: "*Seventeenth programme report, TDR."* World Health Organisation, Geneva. p. 98

MEDEIROS, MB, GUERRA, JA and LACERDA, MV (2008) Meningoencephalitis in a patient with acute Chagas disease in the Brazilian Amazon. *Revista da Sociedade Brasiliera de Medicina Tropical* 41: 520-521

MEIRELLES, RM, RODRIGUES, IS, STEINDEL, M and SOARES, MJ (2003) Ultrastructure of the salivary glands of *Rhodnius domesticus* Neiva & Pinto, 1923 (Hemiptera: Reduviidae). *Journal of submicroscopic cytology and pathology* 35: 199-207

MEISER, CK (2009) *Bacteriolytic and anticoagulant proteins in the saliva and intestine of blood sucking bugs (Triatominae, Insecta).* Dissertation, Fakultät für Biologie und Biotechnologie, Ruhr-Universität Bochum

MEISER, CK, PIECHURA, H, MEYER, HE, WARSCHEID, B, SCHAUB, GA, BALCZUN, C (2010) A salivary serine protease of the haematophagous reduviid *Panstrongylus megistus*: sequence characterization, expression pattern and characterization of proteolytic activity. *Insect molecular biology* 19: 409-421

MOHRIG, W and MESSNER, B (1968) Immunreaktionen bei Insekten. II. Lysozym als antimikrobielles Agens im Darmtrakt von Insekten. *Biologisches Zentralblatt* 87: 705-718

MONCAYO, A (2003) Chagas disease: current epidemiological trends after the interruption of vectorial and transfusional transmission in the Southern Cone countries. *Memórias do Instituto Oswaldo Cruz* 98: 577-591

MONCAYO, A and SILVEIRA, AC (2009) Current epidemiological trends for Chagas disease in Latin America and future challenges in epidemiology, surveillance and health policy. *Memórias do Instituto Oswaldo Cruz* 104 (Suppl. 1): 17-30

MORAES, AML, JUNQUEIRA, ACV, COSTA, GL, CELANO, V, OLIVEIRA, PC and COURA, JR (2001) Fungal flora of the digestive tract of 5 species of triatomines vectors of *Trypanosoma cruzi*, Chagas 1909. *Mycopathologia* 151: 41-48

MORISHIMA, I, HORIBA, T, IKETANI, M, NISHIOKA, E and YAMANO, Y (1995) Parallel induction of cecropin and lysozyme in larvae of the silkworm, *Bombyx mori*. *Developmental and comparative immunology* 19: 357-363

MORISHIMA, I, SUGINAKA, S, UENO, T and HIRANO, H (1990) Isolation and structure of cecropins, inducible antibacterial peptides, from the silkworm, *Bombyx mori*. *Comparative biochemistry and physiology. B, Comparative biochemistry* 95: 551-554

MORTARA, RA, DA SILVA, S, ARAGUTH, MF, BLANCO, SA and YOSHIDA, N (1992) Polymorphism of the 35- and 50-kilodalton surface glycoconjugates of *Trypanosoma cruzi* metacyclic trypomastigotes. *Infection and immunity* 60: 4673-8

MÜHLPFORDT, H (1959) Der Einfluß der Darmsymbionten von *Rhodnius prolixus* auf *Trypanosoma cruzi*. *Zeitschrift für Tropenmedizin und Parasitologie* 10: 314-327

MÜLLER, U, VOGEL, P, ALBER, G and SCHAUB, GA (2008) The innate immune system of mammals and insects. *Contributions to microbiology* 15: 21-44

NILSEN, IW, OVERBO, K, SANDSDALEN, E, SANDAKER, E, SLETTEN, K and MYRNES, B (1999) Protein purification and gene isolation of chlamysin, a cold-active lysozyme-like enzyme with antibacterial activity. *FEBS Letters* 464: 153-158

NOIREAU, F, CORTEZ, MG, MONTEIRO, FA, JANSEN, AM and TORRICO, F (2005) Can wild *Triatoma infestans* foci in Bolivia jeopardize Chagas disease control efforts? *Trends in parasitology* 21: 7-10

NÚÑEZ, JA (1982) Food source orientation and activity in *Rhodnius prolixus* Stål (Hemiptera, Reduviidae). *Bulletin of entomological research* 72: 253-262

NUSSENZVEIG, RH, BENTLEY, DL and RIBEIRO, JM (1995) Nitric oxide loading of the salivary nitric-oxide-carrying hemoproteins (nitrophorins) in the blood-sucking bug *Rhodnius prolixus*. *The journal of experimental biology* 198: 1093-1098

O'CALLAGHAN, M, GARNHAM, ML, NELSON, TL, BAIRD, D and JACKSON, TA (1996) The pathogenicity of *Serratia* strains to *Lucilia sericata* (Diptera, Calliphoridae). *Journal of invertebrate pathology* 68: 22-27

PADILHA, MH, PIMENTEL, AC, RIBEIRO, AF, TERRA, WR (2009) Sequence and function of lysosomal and digestive cathepsin D-like proteinases of *Musca domestica* midgut enzymes. *Insect biochemistry and molecular biology* 39: 782-791

PAHO (2006) *Estimacion cuantitativa de la enfermedad de Chagas en las Americas*. Organización Panamericana de la Salud. Montevideo, Uruguay

PASKEWITZ, SM, LI, B and KAJLA, MK (2008) Cloning and molecular characterization of two invertebrate-type lysozymes from *Anopheles gambiae*. *Insect molecular biology* 17: 217-225

PAUSCH, JK, BALCZUN, C and SCHAUB, GA (in press) Interactions of *Trypanosoma cruzi*, the etiologic agent of Chagas disease, and triatomines (Reduviidae): a review. *Mitteilungen der Deutschen Gesellschaft für allgemeine und angewandte Entomologie* Band 18

PEREIRA, MH, GONTIJO, NF, GUARNERI, AA, SANT'ANNA, MR and DIOTAIUTI, L (2006) Competitive displacement in Triatominae: the *Triatoma infestans* success. *Trends in parasitology* 22: 516-520

PERKINS, DN, PAPPIN, DJC, CREASY, DM and COTTRELL, JS (1999) Probability-based protein identification by searching sequence databases using mass spectrometry data. *Electrophoresis* 20: 3551-3567

PFAFFL, MW (2001) A new mathematical model for relative quantification in real-time RT-PCR. *Nucleic acids research* 29: e45

PINTO, AY, VALENTE, SA, DA VALENTE V, FERREIRA JUNIOR, AG and COURA, JR (2008) Acute phase of Chagas disease in the Brazilian Amazon region: study of 233 cases from Pará, Amapá and Maranhão observed between 1988 and 2005. *Revista da Sociedade Brasiliera Medicina Tropical* 41: 602-614

POSSANI, LD, ZURITA, M, DELEPIERRE, M, HERNANDEZ, FH and RODRIGUEZ, MH (1998) From noxiustoxin to Shiva-3, a peptide toxic to the sporogonic development of *Plasmodium berghei*. *Toxicon* 36: 1683-1692

PRAGER, EM (1996) Adaptive evolution of lysozyme: changes in amino acid sequence, regulation of expression and gene number. In: Jolles, P (ed) "*Lysozymes: model enzymes in biochemistry and biology*." Birkhäuser Verlag, Basel, pp. 323-345

RABINOVICH, JE (1972) Vital statistics of Triatominae (Hemiptera: Reduviidae) under laboratory conditions. I. *Triatoma infestans* Klug. *Journal of medical entomology* 9: 351-70

RAMAKERS, C, RUIJTER, JM, DEPREZ, RH and MOORMAN, AF (2003) Assumption-free analysis of quantitative real-time polymerase chain reaction (PCR) data. *Neuroscience letters* 339: 62-66

RASSI, A, RASSI, A and MARIN-NETO, JA (2010) Chagas disease. *Lancet* 375: 1388-1402

REES, JA, MONIATTE, M and BULET, P (1997) Novel antibacterial peptides isolated from an European bumblebee *Bombus pascuorum* (Hymenoptera, Apoidea). *Insect biochemistry and molecular biology* 27: 413-422

REGEL, R, MATIOLI, SR and TERRA, WR (1998) Molecular adaption of *Drosophila melanogaster* lysozymes to a digestive function. *Insect biochemistry and molecular biology* 28: 309-319

REINTJES, N (1993) *Identifizierung der Darmbakterien von* Triatoma infestans *(Reduviidae, Hemiptera) und ihre Auswirkungen auf die Raubwanze.* Diplomarbeit, Fakultät für Biologie, Ruhr-Universität Bochum

RIBEIRO, JMC and PEREIRA, MEA (1984) Midgut glycosidases of *Rhodnius prolixus*. *Insect biochemistry* 14: 103-108

RIBEIRO, JMC, SCHNEIDER, M, ISAIAS, T, JURBERG, J, GALVÃO, C and GUIMARÃES, JA (1998) Role of salivary antihemostatic components in blood feeding by triatomine bugs (Heteroptera). *Journal of medical entomology* 35: 599-610

RODRIGUEZ, MC, ZAMUDIO, F, TORRES, JA, GONZALEZ-CERON, L, POSSANI, LD and RODRIGUEZ, MH (1995) Effect of a cecropin-like synthetic peptide (Shiva-3) on the sporogonic development of *Plasmodium berghei*. *Experimental parasitology* 80: 596-604

ROGL, A (2001) *Untersuchungen der Darmflora von* Triatoma vitticeps *(Reduviidae, Hemiptera) und der Leistung der Triatominen Symbionten.* Diplomarbeit, Fakultät für Biologie, Ruhr-Universität Bochum

RUIZ, RC, RIGONI, VL, GONZALEZ, J and YOSHIDA, N (1993) The 35/50 kDa surface antigen of *Trypanosoma cruzi* metacyclic trypomastigotes, an adhesion molecule involved in host cell invasion. *Parasite immunology* 15: 121-125

SACKS, D and SHER, A (2002) Evasion of innate immunity by parasitic protozoa. *Nature immunology* 3: 1041-1047

SAITO, A, UEDA, K, IMAMURA, M, ATSUMI, S, TABUNOKI, H, MIURA, N, WATANABE, A, KITAMI, M and SATO, R (2005) Purification and cDNA cloning of a cecropin from the longicorn beetle, *Acalolepta luxuriosa*. *Comparative biochemistry and physiology Part B, Biochemistry & molecular biology* 142: 317-323

SALT, G (1970) *The cellular defense reactions of insects. Cambridge monographs in experimental biology No. 16.* Cambridge University Press, London.

SANT'ANNA, MRV, DIOTAIUTI, L, DE FIGUEIREDO GONTIJO, A, DE FIGUEIREDO GONTIJO, N and PEREIRA, MH (2001) Feeding behaviour of morphologically similar *Rhodnius* species: influence of mechanical characteristics and salivary function. *Journal of insect physiology* 47: 1459-1465

SANTOS, A, RIBEIRO, JM, LEHANE, MJ, GONTIJO, NF, VELOSO, AB, SANT'ANNA, MR, NASCIMENTO ARAUJO, R, GRISARD, EC and PEREIRA, MH (2007) The sialotranscriptome of the blood-sucking bug *Triatoma brasiliensis* (Hemiptera, Triatominae). *Insect biochemistry and molecular biology* 37: 702-712

SCHAUB, GA (1988a) Developmental time and mortality in larvae of the reduviid bugs *Triatoma infestans* and *Rhodnius prolixus* after coprophagic infection with *Blastocrithidia triatomae* (Trypanosomatidae). *Journal of invertebrate pathology* 51: 23-31

SCHAUB, GA (1988b) Developmental time and mortality of larvae of *Triatoma infestans* infected with *Trypanosoma cruzi*. *Transactions of the Royal Society of Tropical Medicine and Hygiene* 82: 94-96

SCHAUB, GA (1988c) Direct transmission of *Trypanosoma cruzi* between vectors of Chagas' disease. *Acta Tropica* 45: 11-19

SCHAUB, GA (1989) *Trypanosoma cruzi*: quantitative studies of development of two strains in small intestine and rectum of the vector *Triatoma infestans*. *Experimental parasitology* 68: 260-273

SCHAUB, GA (1990) Membrane feeding for infection of the reduviid bug *Triatoma infestans* with *Blastocrithidia triatomae* (Trypanosomatidae) and pathogenic effects of the flagellate. *Parasitology research* 76: 306-310

SCHAUB, GA (1991) Rapid isolation of metacyclic trypomastigotes of *Trypanosoma cruzi* from feces and urine of the vector. *Acta tropica* 50: 51-58

SCHAUB, GA (2008) Kissing bugs. In: Mehlhorn, H (ed) 3rd edn. "*Encyclopedic reference of parasitology, Vol.1. Biology, Structure, Function*", vol. 1. Springer-Verlag, Heidelberg, pp. 684-686

SCHAUB, GA (2009) Interactions of trypanosomatids and triatomines. *Advances in insect physiology* 37: 177-242

SCHAUB, GA and LÖSCH, P (1988) *Trypanosoma cruzi*: origin of metacyclic trypomastigotes in the urine of the vector *Triatoma infestans*. *Experimental parasitology* 65: 174-186

SCHAUB, GA and LÖSCH, P (1989) Parasite/host-interrelationships of the trypanosomatids *Trypanosoma cruzi* and *Blastocrithidia triatomae* and the reduviid bug *Triatoma infestans*: influence of starvation of the bug. *Annuals of tropical medicine and parasitology* 83: 215-223

SCHAUB, GA and POSPISCHIL, R (1995) Chagas (Teil 2) - Epidemiologie, Vektorbiologie und Bekämpfung. *Reisemedizin* No. 2: 19-20

SCHAUB, GA and SCHNITKER, A (1988) Influence of *Blastocrithidia triatomae* (Trypanosomatidae) on the reduviid bug *Triatoma infestans*: alterations in the Malpighian tubules. *Parasitology research* 75: 88-97

SCHAUB, GA and WUNDERLICH, F (1985) Die Chagas-Krankheit. *Biologie in unserer Zeit* 15: 42-51

SCHAUB, GA, HÖLSCHER, C and MOSSMANN, H (2001) Development of high numbers of blood trypomastigotes of *Trypanosoma cruzi* in nude rats. *Parasitology research* 87: 245-247

SCHAUB, GA, MEISER, CK and BALCZUN, C (2011) Interactions of *Trypanosoma cruzi* and triatomines. In: Mehlhorn, H (ed) "*Progress in the fight against parasitic diseases.*" Springer Verlag, Heidelberg, pp. 155-178

SCHENKMAN, S, FERGUSON, MA, HEISE, N, DEALMEIDA, ML, MORTARA, RA and YOSHIDA, N (1993) Mucin-like glycoproteins linked to the membrane by glycosylphosphatidylinositol

anchor are the major acceptors of sialic acid in a reaction catalyzed by transsialidase in metacyclic forms of *Trypanosoma cruzi*. *Molecular and biochemical parasitology* 59: 293-303

SCHMUNIS, GA (2007) Epidemiology of Chagas disease in non-endemic countries: the role of international migration. *Memórias do Instituto Oswaldo Cruz* 102 (Suppl. 1): 75-85

SCHNEIDER, M and DORN, A (2001) Differential infectivity of two *Pseudomonas* species and the immune response in the milkweed bug *Oncopeltus fasciatus* (Insecta: Hemiptera). *Journal of invertebrate pathology* 78: 135-140

SCHOFIELD, CJ (1994) *Triatominae. Biology & control.* Eurocommunica Publications, West Sussex, UK.

SCHOFIELD, CJ (2000) *Trypanosoma cruzi*-the vector-parasite paradox. *Memórias do Instituto Oswaldo Cruz* 95: 535-544

SCHOFIELD, CJ and DIAS, JCP (1999) The Southern Cone Initiative against Chagas Disease. *Advances in parasitology* 42: 1-27

SCHOFIELD, CJ and GALVAO, C (2009) Classification, evolution, and species groups within the Triatominae. *Acta tropica* 110: 88-100

SCHUSTER, JP and SCHAUB, GA (2000) *Trypanosoma cruzi*: skin-penetration kinetics of vector-derived metacyclic trypomastigotes. *International journal for parasitology* 30: 1475-1479

SERRANO, AA, SCHENKMAN, S, YOSHIDA, N, MEHLERT, A, RICHARDSON, JM and FERGUSON, MAJ (1995) The lipid structure of the glycosylphosphatidylinositol-anchored mucin-like sialic acid acceptors of *Trypanosoma cruzi* changes during parasite differentiation from epimastigotes to infective metacyclic trypomastigote forms. *The journal of biological chemistry* 270: 27244-27253

SHAHABUDDIN, M, FIELDS, I, BULET, P, HOFFMANN, JA and MILLER, LH (1998) *Plasmodium gallinaceum*: differential killing of some mosquito stages of the parasite by insect defensin. *Experimental parasitology* 89: 103-112

SOARES, RP, DAS GRAÇAS EVANGELISTA, L, LARANJA, LS and DIOTAIUTI, L (2000) Population dynamics and feeding behavior of *Triatoma brasiliensis* and *Triatoma pseudomaculata*, main vectors of Chagas disease in Northeastern Brazil. *Memórias do Instituto Oswaldo Cruz* 95: 151-155

SWISS PROT (2010) Protein Database http://www.uniprot.org/. called on 19.09.2011

TANIAI, K, KATO, Y, HIROCHIKA, H and YAMAKAWA, M (1992) Isolation and nucleotide sequence of cecropin B cDNA clones from the silkworm, *Bombyx mori*. *Biochimica et biophysica acta* 1132: 203-206

TANOWITZ, HB, KIRCHHOFF, LV, SIMON, D, MORRIS, SA, WEISS, LM and WITTNER, M (1992) Chagas' disease. *Clinical microbiology reviews* 5: 400-419

TERRA, WR, FERREIRA, C and GARCIA, ES (1988) Origin, distribution, properties and functions of the major *Rhodnius prolixus* midgut hydrolases. *Insect biochemistry* 18: 423-434

TREMBL (2011) Protein Database http://www.uniprot.org/. called on 19.09.2011

TRENCZEK, T (1992) Immunität bei Insekten? *Biologie in unserer Zeit* 22: 212-217

TYLER, KM and ENGMAN, DM (2001) The life cycle of *Trypanosoma cruzi* revisited. *International journal for parasitology* 31: 472-481

UNIPROT (2011) Protein Database http://www.uniprot.org/. called on 19.09.2011

URSIC-BEDOYA, RJ and LOWENBERGER, CA (2007) *Rhodnius prolixus*: identification of immune-related genes up-regulated in response to pathogens and parasites using suppressive subtractive hybridization. *Developmental & comparative immunology* 31: 109-120

URSIC-BEDOYA, RJ, NAZZARI, H, COOPER, D, TRIANA, O, WOLFF, M and LOWENBERGER, C (2008) Identification and characterization of two novel lysozymes from *Rhodnius prolixus*, a vector of Chagas disease. *Journal of insect physiology* 54: 593-603

URSIC-BEDOYA, RJ, BUCHHOP, J, JOY, JB, DURVASULA, R, LOWENBERGER, C (2011) Prolixicin: a novel antimicrobial peptide isolated from *Rhodnius prolixus* with differential activity against bacteria and *Trypanosoma cruzi*. *Insect molecular biology* 20: 775-786

VALLEJO, GA, GUHL, F and SCHAUB, GA (2009) Triatominae-*Trypanosoma cruzi*/*T. rangeli*: Vector-parasite interactions. *Acta tropica* 110: 137-147

VICKERMAN, K (1985) Developmental cycles and biology of pathogenic trypanosomes. *British medical bulletin* 41: 105-114

VITTA, AC, FIGUEIRAS, AN, LAZZARI, CR, DIOTAIUTI, L and LORENZO, MG (2002) Aggregation mediated by faeces and footprints in *Triatoma pseudomaculata* (Heteroptera: Reduviidae), a Chagas disease vector. *Memórias do Instituto Oswaldo Cruz* 97: 865-867

VIZIOLI, J, RICHMAN, AM, UTTENWEILER-JOSEPH, S, BLASS, C and BULET, P (2001) The defensin peptide of the malaria vector mosquito *Anopheles gambiae*: antimicrobial activities and expression in adult mosquitoes. *Insect biochemistry and molecular biology* 31: 241-248

VOCADLO, D, DAVIES, G, LAINE, R and WITHERS, S (2001) Catalysis by hen egg-white lysozyme proceeds via a covalent intermediate. *Nature* 412: 835-838

WAKSMAN, SA (1940) On the classification of actinomycetes. *Journal of bacteriology* 39: 549-558

WANG, L, LI, Z, DU, C, CHEN, W and PANG, Y (2007) Characterization and expression of a cecropin-like gene from *Helicoverpa armigera*. *Comparative biochemistry and physiology. Part B, Biochemistry & molecular biology* 148: 417-425

WANIEK, PJ, HENDGEN-COTTA, UB, STOCK, P, MAYER, C, KOLLIEN, AH and SCHAUB, GA (2005) Serine proteinases of the human body louse (*Pediculus humanus*): sequence characterization and expression patterns. *Parasitology research* 97: 486-500

WANIEK, PJ, CASTRO, HC, SATHLER, PC, MICELI, L, JANSEN, AM and ARAUJO, CA (2009a) Two novel defensin-encoding genes of the Chagas disease vector *Triatoma brasiliensis* (Reduviidae, Triatominae): gene expression and peptide-structure modeling. *Journal of insect physiology* 55: 840-848

WANIEK, PJ, MENDONÇA-LIMA, L, MENEZES, GB, JANSEN, AM and ARAÚJO, CAC (2009b) Recombinant expression and characterization of a lysozyme from the midgut of *Triatoma brasiliensis* (Hemiptera, Reduviidae) in comparison with intestinal muramidase activity. *Physiological entomology* 34: 309-317

WANIEK, PJ, JANSEN, AM and ARAÚJO, CAC (20011) *Trypanosoma cruzi* infection modulates the expression of *Triatoma brasiliensis def1* in the midgut. *Vector borne and zoonotic diseases* 11: 845-847

WENK, P and RENZ, A (2003) *Parasitologie*. Georg Thieme Verlag, Stuttgart.

WEURMAN, C (1946) Investigations concerning the symbionts of bacteria in *Triatoma infestans* (Klug). *Acta Leiden* 18: 307-319

WHITTEN, M, SUN, F, TEW, I, SCHAUB, G, SOUKOU, C, NAPPI, A and RATCLIFFE, N (2007) Differential modulation of *Rhodnius prolixus* nitric oxide activities following challenge with *Trypanosoma rangeli*, *T. cruzi* and bacterial cell wall components. *Insect biochemistry and molecular biology* 37: 440-452

WHO (2002) *Control of Chagas disease. Second report of the WHO Expert Commitee*. WHO, Geneva.

WHO (2008) Chagas disease: control and elimination, Report of the secretariat. www.who.int/gb/ebwha/pdf.../B124_17-en.pdf. called on 11.05.2011

WHO (2011) http://www.who.int/mediacentre/factsheets/fs340/en/index.html. called on 11.05.2011

WIGGLESWORTH, VB (1929) Digestion in tsetse fly. A study of structure and function. *Parasitology* 21: 288-321

WIGGLESWORTH, VB (1940) Local and general factors in the development of "pattern" in *Rhodnius prolixus* (Hemiptera). *The journal of experimental biology* 17: 180-200

WIGGLESWORTH, VB (1977) Digestion and nutrition. In: Wigglesworth, VB (ed) 7 edn. "*The principles of insect physiology*." Chapman and Hall, London, pp. 476-552

WINNEBECK, EC, MILLAR, CD and WARMAN, GR (2010) Why does insect RNA look degraded? *Journal of insect science* 10: 1-7

WIRTZ, HP (1987) Eindringen der Mundwerkzeuge von Raubwanzen durch eine Membran (Hemiptera: Reduviidae). *Entomologia generalis* 12: 147-153

YASSIN, AF (2005) *Rhodococcus triatomae* sp. nov., isolated from a blood-sucking bug. *International journal of systematic and evolutionary microbiology* 55: 1575-1579

YASSIN, AF AND SCHAAL, KP (2005) Reclassification of *Nocardia corynebacterioides* Serrano *et al*. 1972 (Approved Lists 1980) as *Rhodococcus corynebacterioides* comb. nov.. *International journal of systematic and evolutionary microbiology* 55: 1345-1348

YOSHIDA, N, MORTARA, RA, ARAGUTH, MF, GONZALEZ, JC and RUSSO, M (1989) Metacyclic neutralizing effect of monoclonal antibody 10D8 directed to the 35- and 50-kilodalton surface glycoconjugates of *Trypanosoma cruzi*. *Infection and immunity* 57: 1663-1667

ZELEDÓN, R and RABINOVICH, JE (1981) Chagas' disease: an ecological appraisal with special emphasis on its insect vectors. *Annual review of entomology* 26: 101-133

ZELEDÓN, R, BOLAÑOS, R and ROJAS, M (1984) Scanning electron microscopy of the final phase of the life cycle of *Trypanosoma cruzi* in the insect vector. *Acta tropica* 41: 39-43

ZINGALES, B, ANDRADE, SG, BRIONES, MR, CAMPBELL, DA, CHIARI, E, FERNANDES, O, GUHL, F, LAGES-SILVA, E, MACEDO, AM, MACHADO, CR, MILES, MA, ROMANHA, AJ, STURM, NR, TIBAYRENC, M and SCHIJMAN, AG (2009) A new consensus for *Trypanosoma cruzi* intraspecific nomenclature: second revision meeting recommends TcI to TcVI. *Memórias do Instituto Oswaldo Cruz* 104: 1051-1054

ZOR, T and SELINGER, Z (1996) Linearization of the Bradford protein assay increases its sensitivity: theoretical and experimental studies. *Analytical biochemistry* 236: 302-308

CHAPTER 8

SUPPLEMENTAL DATA

8. Supplemental data

8.1 Supplemental data for chapter 3

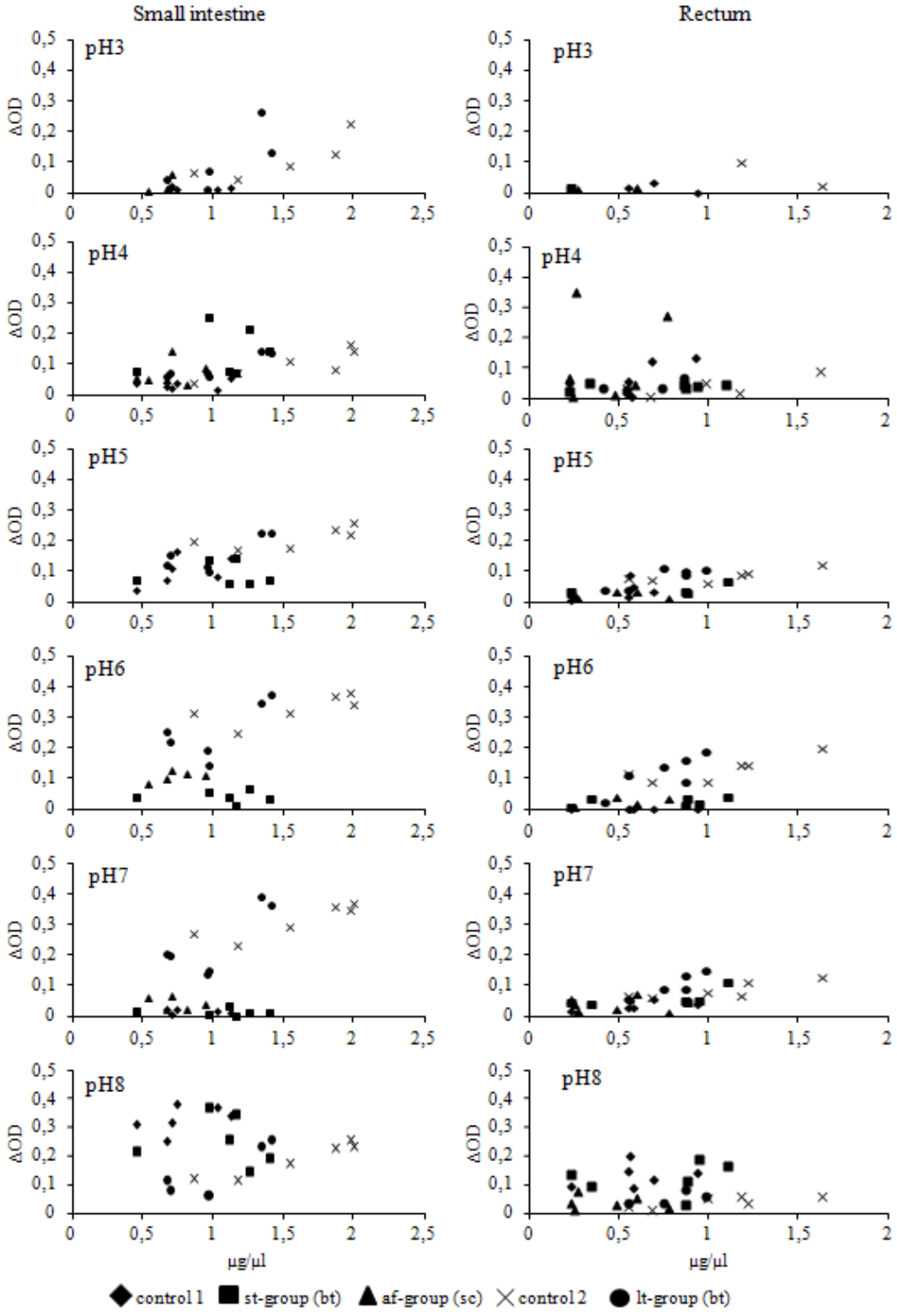

Figure S8.1.1: Bacteriolytic activities (ΔOD) plotted against the respective protein concentration in small intestine and rectum of the different groups in the first approach. Mean from 3 independent samples. Measurements were done over a 30 min period. Plots contain data points of unfed (uf) fifth instar larvae as well as 2, 3, 5, 10 and 15 days after feeding.

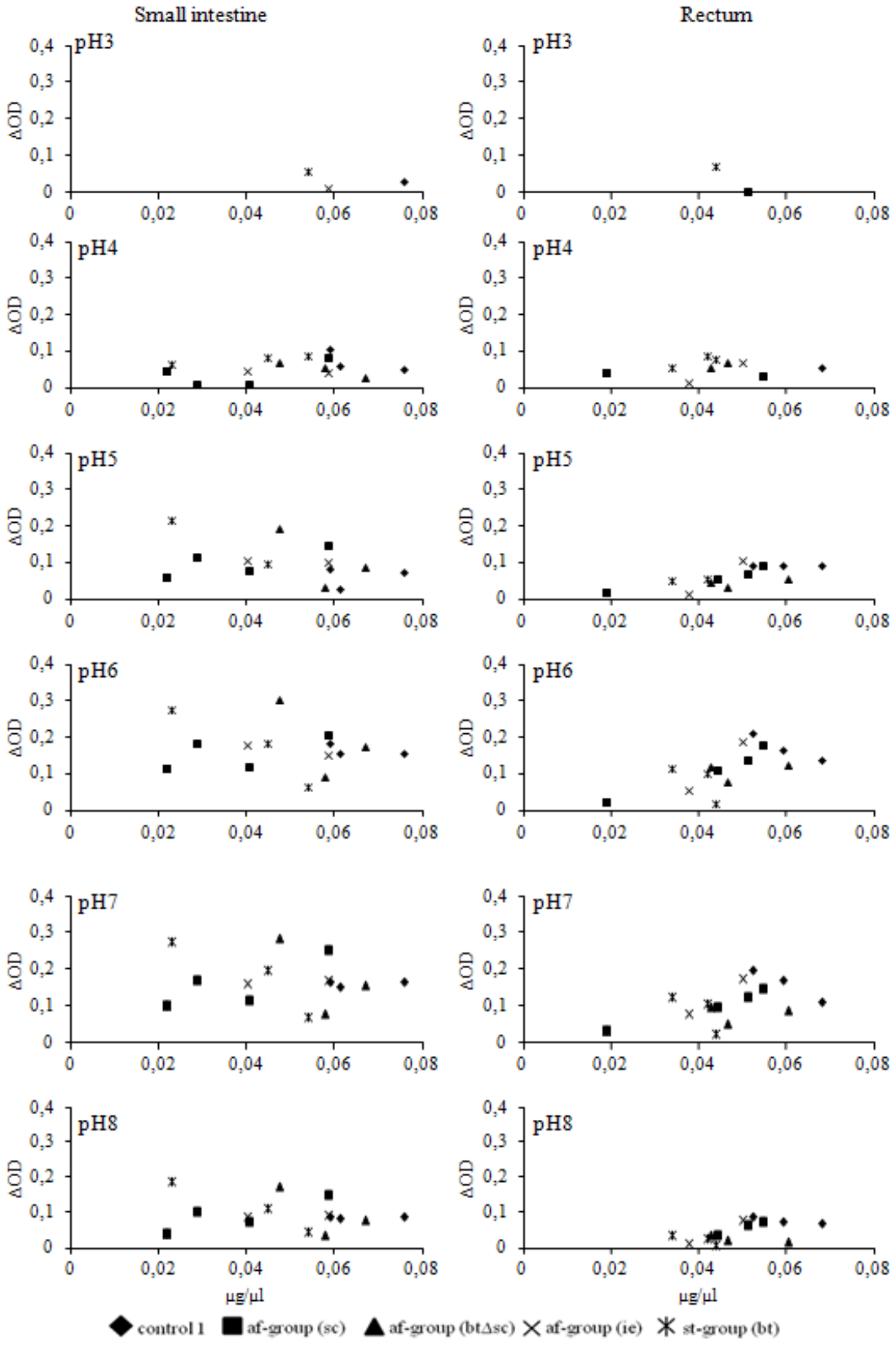

Figure S8.1.2: Bacteriolyic activities (ΔOD) plotted against the respective protein concentration in small intestine and rectum of the different groups in the second approach.

Mean from 3 independent samples. Measurements were done over a 30 min period. Plots contain data points of unfed (uf) fifth instar larvae as well as 2, 3 and 5 days after feeding.

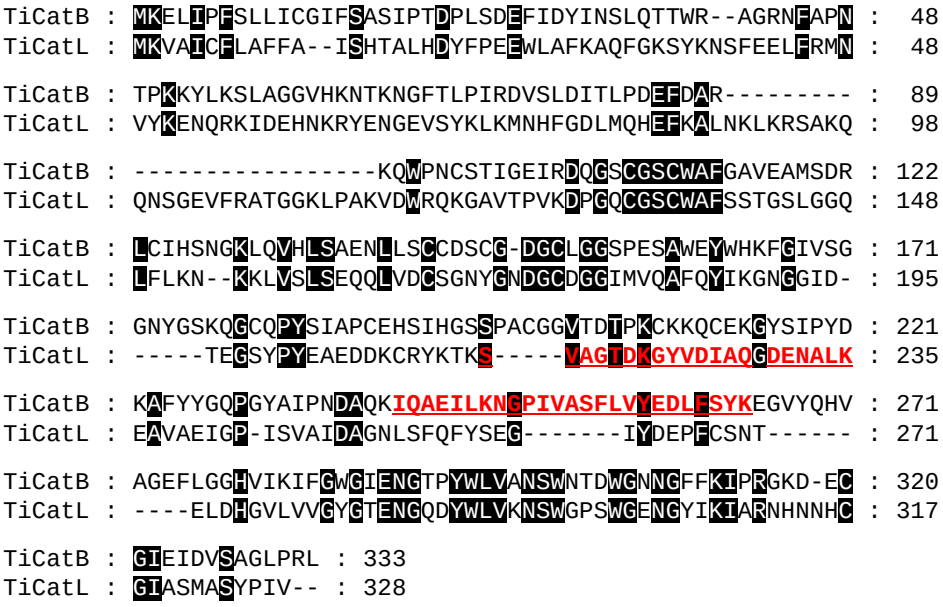

Figure S8.1.3: Multiple sequence alignment of the amino acid sequences of *T. infestans* cathepsin B and L using CLUSTALX (v2.0).

Peptides identified by mass spectrometry are underlined and marked red. Identical amino acid residues conserved in all sequences are black shaded. The GenBank sequences used for this alignment are: *T. infestans* cathepsin B-like cysteine proteinase (TiCatB) (**ABD35300**) and cathepsin L-like proteinase (TiCatL) (**AAR12010**).

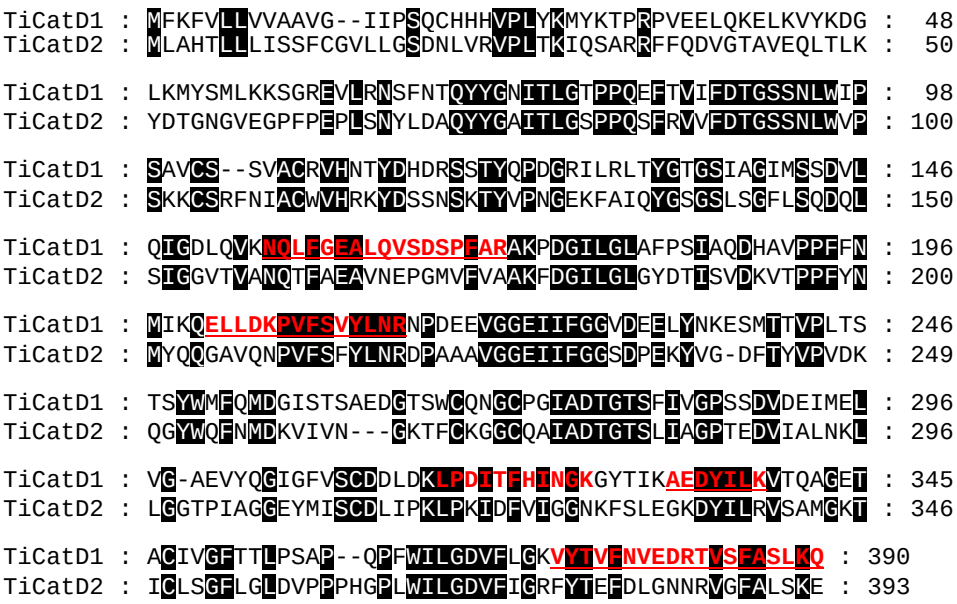

Figure S8.1.4: Multiple sequence alignment of the amino acid sequences of *T. infestans* cathepsin D and D2 using CLUSTALX (v2.0).

Peptides identified by mass spectrometry are underlined and marked red. Identical amino acid residues conserved in all sequences are black shaded. The GenBank sequences used for this alignment are: *T. infestans* cathepsin D1 (TiCatD1) (**ADK47877**) and aspartate protease cathepsin D (TiCatD2) (**AEO94539**).

Table S8.1.1: Mascot identification data (score 9918.13 to 301.72) for a 13 kDa band of small intestines of unfed fifth instars of *T. infestans* (short-control group) after gelelectrophoretic separation.

Protein/Characteristics		Peptide sequences (spectro counts)	
Hemoglobin subunit beta-1			
Accession: P02091	∑ Coverage: 91.7	YFDSFGDLSSASAIMGNPK (80)	LLVVYPWTQR (17)
Aminoacids: 147	Spectral counts: 253	VVAGVASALAHKYH (12)	LLGNMIVIVLGHHLGK (17)
MW [kDa]: 16.0	Score: 9918.1	VVAGVASALAHK (62)	AAVNGLWGK (1)
Calc. pI: 8.1		VNPDDVGGEALGR (26)	EFTPCAQAAFQK (2)
		KVINAFNDGLK (14)	VINAFNDGLK (16)
		GTFAHLSELHCDK (2)	LHVDPENFR (3)
		VHLTDAEK (1)	
Hemoglobin subunit beta-2			
Accession: P11517	∑ Coverage: 89.8	VNADNVGAEALGR (7)	LLVVYPWTQR (17)
Aminoacids: 147	Spectral counts: 172	FGDLSSASAIMGNPQVK (18)	LLGNMIVIVLGHHLGK (17)
MW [kDa]: 16.0	Score: 6147.1	VVAGVASALAHKYH (12)	ATVSGLWGK (1)
Calc. pI: 8.8		VVAGVASALAHK (62)	EFTPCAQAAFQK (2)
		KVINAFNDGLK (14)	VINAFNDGLK (16)
		GTFAHLSELHCDK (2)	LHVDPENFR (3)
		VHLTDAEK (1)	
Hemoglobin subunit alpha-1/2			
Accession: P01946	∑ Coverage: 71.8	FLASVSTVLTSK (70)	MFAAFPTTK (42)
Aminoacids: 142	Spectral counts: 187	IGGHGGEYGEEALQR (27)	VLSADDKTNIK (6)
MW [kDa]: 15.3	Score :6110.4	AADHVEDLPGALSTLSDLHAHK (17)	KVADALAK (2)
Calc. pI: 8.0		TYFSHIDVSPGSAQVK (9)	LRVDPVNFK (14)
Keratin, type II cytoskeletal 1			
Accession: Q6IMF3	∑ Coverage: 5.3	FLEQQNQVLQTK (5)	DYQELMNTK (2)
Aminoacids: 625	Spectral counts: 10	TNAENEFVTIK (3)	
MW [kDa]: 64.8	Score: 434.7		
Calc. pI: 7.9			
Keratin, type II cytoskeletal 6A			
Accession: Q4FZU2	∑ Coverage: 6.0	SLDLDSIIAEVK (2)	LALDVEIATYR (1)
Aminoacids: 552	Spectral counts: 8	YEELQITAGR (5)	
MW [kDa]: 59.2	Score: 351.7		
Calc. pI: 7.9			
Keratin, type I cytoskeletal 10			
Accession: Q6IFW6	∑ Coverage: 10.3	QSVEADINGLR (1)	LKYENEVALR (1)
Aminoacids: 526	Spectral counts: 10	LENEIQTYR (2)	SEITELR (1)
MW [kDa]: 56.5	Score: 308.0	YENEVALR (2)	SEITELRR (1)
Calc. pI: 5.2		DAEAWFNEK (1)	LAADDFR (1)
Keratin, type II cytoskeletal 1b			
Accession: Q6IG01	∑ Coverage: 4.2	FLEQQNQVLQTK (5)	NKYEDEINK (1)
Aminoacids: 519	Spectral counts: 7	NKYEDEINKR (1)	
MW [kDa]: 57.2	Score: 303.8		
Calc. pI: 5.6			
Keratin, type II cytoskeletal 5			
Accession: Q6P6Q2	∑ Coverage: 11.3	SLDLDSIIAEVK (2)	NKYEDEINKR (1)
Aminoacids: 576	Spectral counts: 8	YEELQQTAGR (1)	VDALMDEINFMK (1)
MW [kDa]: 61.8	Score: 301.7	LALDVEIATYR (1)	NKYEDEINK (1)
Calc. pI: 7.8		WTLLQEQGTK (1)	

All proteins originated from *R. rattus*. Accession numbers were derived from Uniprot Protein Database (2011). Sequence coverage of the identified peptides is given as Σ Coverage. Significance of the search result is given as score.

Table S8.1.2: Mascot identification data (score 251.73 to 89.82) for a 13 kDa band of small intestines of unfed fifth instars of *T. infestans* (short-control group) after gelelectrophoretic separation.

Protein/Characteristics		Peptide sequences (spectro counts)	
Murinoglobulin-1			
Accession: Q03626	∑ Coverage: 3.4	QLSFSLSAEPIQGPYK (3)	FRVVSMDK (1)
Aminoacids: 1487	Spectral counts: 7	ESVVFVQTDKPVYKPGQSVK (1)	FGVDVK (2)
MW [kDa]: 165.2	Score: 251.7		
Calc. pI: 6.0			
Keratin, type II cytoskeletal 2			
Accession: Q6IG02	∑ Coverage: 7.6	GFSSGSAVVSGGSR (1)	DYQELMNVK (1)
Aminoacids: 685	Spectral counts: 5	LALDVEIATYR (1)	HGDSLKEIK (1)
MW [kDa]: 69.1	Score: 185.1	VDPEIQNVK (1)	
Calc. pI: 7.7			
Keratin, type I cytoskeletal 42			
Accession: Q6IFU7	Calc. pI: 5.2	GQVGGDVNVEMDAAPGVDLSR (1)	LAADDFR (1)
Aminoacids: 452	∑ Coverage: 6.2		
MW [kDa]: 50.2	Spectral counts: 2		
	Score: 107.1		
TiLys1			
Accession: Q7YZS5	∑ Coverage: 20.1	GGPNHDGSYDNGLFQINDR (1)	ELVAHGIPR (2)
Aminoacids: 139	Spectral counts: 3		
MW [kDa]: 15.6	Score: 100.4		
Calc. pI: 8.7			
Keratin, type I cytoskeletal 19			
Accession: Q63279	∑ Coverage: 4.0	LASYLDKVR (1)	LASYLDK (2)
Aminoacids: 403	Spectral counts: 4	LAADDFR (1)	
MW [kDa]: 44.6	Score: 98.0		
Calc. pI: 5.3			
Actin, cytoplasmic 1			
Accession: P60711	∑ Coverage: 6.9	SYELPDGQVITIGNER (1)	AGFAGDDAPR (1)
Aminoacids: 375	Spectral counts: 2		
MW [kDa]: 41.7	Score: 89.8		
Calc. pI: 5.5			

Proteins originated from *T. infestans* or *R. rattus*. *T. infestans* protein is underlined. Accession numbers were derived from Uniprot Protein Database (2011). Sequence coverage of the identified peptides is given as Σ Coverage. Significance of the search result is given as score.

Table S8.1.3: Mascot identification data (score 18731.8 to 287.8) for a 13 kDa band of small intestines of fifth instars of *T. infestans* at 2 days after feeding surface coat of *T. cruzi* (short-surface group) and after gelelectrophoretic separation.

Protein/Characteristics		Peptide sequences (spectro counts)	
Hemoglobin subunit beta-1			
Accession: P02091	∑ Coverage: 96.6	YFDSFGDLSSASAIMGNPK (117)	GTFAHLSELHCDK (3)
Aminoacids: 147	Spectral counts: 604	VNPDDVGGEALGR (44)	LLVVYPWTQR (46)
MW [kDa]: 16.0	Score: 18731.8	VVAGVASALAHKYH (34)	VINAFNDGLK (65)
Calc. pI: 8.1		VVAGVASALAHK (120)	AAVNGLWGK (2)
		LLGNMIVIVLGHHLGK (121)	LHVDPENFR (11)
		KVINAFNDGLK (27)	EFTPCAQAAFQK (2)
		VINAFNDGLKHLDNLK (6)	VHLTDAEK (1)
		AAVNGLWGKVNPDDVGGEALGR (5)	
Hemoglobin subunit alpha-1/2			
Accession: P01946	∑ Coverage: 73.9	AADHVEDLPGALSTLSDLHAHK (109)	LRVDPVNFK (33)
Aminoacids: 142	Spectral counts: 451	FLASVSTVLTSK (90)	MVLSADDKTNIK (1)
MW [kDa]: 15.3	Score: 14666.8	IGGHGGEYGEEALQR (40)	VADALAK (1)
Calc. pI: 8.0		TYFSHIDVSPGSAQVK (43)	KVADALAK (1)
		AADHVEDLPGALSTLSDLHAHKLR (22)	VDPVNFK (1)
		VLSADDKTNIK (10)	FLASVSTVLTSKYR (1)
		MFAAFPTTKTYFSHIDVSPGSAQVK (7)	MFAAFPTTK (92)
Hemoglobin subunit beta-2			
Accession: P11517	∑ Coverage: 96.6	VNADNVGAEALGR (23)	GTFAHLSELHCDK (3)
Aminoacids: 147	Spectral counts: 478	FGDLSSASAIMGNPQVK (20)	LLVVYPWTQR (46)
MW [kDa]: 16.0	Score: 13053.9	VVAGVASALAHKYH (23)	ATVSGLWGK (1)
Calc. pI: 8.8		VVAGVASALAHK (120)	LHVDPENFR (11)
		LLGNMIVIVLGHHLGK (121)	EFTPCAQAAFQK (2)
		KVINAFNDGLK (17)	VINAFNDGLK (65)
		VINAFNDGLKHLDNLK (6)	ATVSGLWGKVNADNVGAEALGR (2)
		HLDNLK (1)	VHLTDAEK (2)
		YFSKFGDLSSASAIMGNPQVK (4)	EFTPCAQAAFQK (1)
Murinoglobulin-1			
Accession: Q03626	∑ Coverage: 7.1	QLSFSLSAEPIQGPYK (6)	QSGVKEEHSFTVMEFVLPR (4)
Aminoacids: 1487	Spectral counts: 40	NLHPLNELFPLAYIEDPKMNR (5)	IMQWQDIKTENGLK (1)
MW [kDa]: 165.2	Score: 966.2	ESVVFVQTDKPVYKPGQSVK (5)	VVSMDKNLHPLNELFPLAYIEDPK (2)
Calc. pI: 6.0		IMQWQDIK (4)	NKESVVFVQTDKPVYKPGQSVK (2)
		FGVDVK (6)	FRVVSMDK (1)
		EEHSFTVMEFVLPR (2)	NLHPLNELFPLAYIEDPK (1)
Alpha-1-inhibitor 3			
Accession: P14046	∑ Coverage: 6.6	QLSFSLSAEPIQGPYK (6)	IMQWQDVK (1)
Aminoacids: 1477	Spectral counts: 32	NLHPLNELFPLAYIEDPKMNR (5)	FRVVSMDK (1)
MW [kDa]: 163.7	Score: 787.7	FGVDVK (6)	QSGVKEEHSFTVMEFVLPR (5)
Calc. pI: 6.0		EEHSFTVMEFVLPR (2)	NLHPLNELFPLAYIEDPK (1)
		ESVVFVQTDKPMYKPGQSVK (3)	VVSMDKNLHPLNELFPLAYIEDPK (2)
Keratin, type II cytoskeletal 6A			
Accession: Q4FZU2	∑ Coverage: 7.4	SLDLDSIIAEVK (2)	YEELQITAGR (2)
Aminoacids: 552	Spectral counts: 7	LALDVEIATYR (2)	GRLDSELR (1)
MW [kDa]: 59.2	Score: 313.8		
Calc. pI: 7.9			
Keratin, type II cytoskeletal 5			
Accession: Q6P6Q2	∑ Coverage: 9.2	SLDLDSIIAEVK (2)	GRLDSELR (1)
Aminoacids: 576	Spectral counts: 7	LALDVEIATYR (2)	LRSEIDNVKK (1)
MW [kDa]: 161.8	Score: 288.3	VDALMDEINFMK (1)	
Calc. pI: 7.8			
Keratin, type I cytoskeletal 10			
Accession: Q6IFW6	∑ Coverage: 15.0	ADLEMQIESLTEELAYLK (1)	LKYENEVALR 3)
Aminoacids: 526	Spectral counts: 13	QSVEADINGLR (1)	LAADDFR (2)
MW [kDa]: 56.5	Score: 238.5	DAEAWFNEK (2)	SEITELR (1)
Calc. pI: 5.2		QSVEADINGLRR (1)	IKEWYEK (1)
		LENEIQTYR (1)	
Keratin, type II cytoskeletal 1			
Accession: Q6IMF3	∑ Coverage: 3.7	FLEQQNQVLQTK (6)	TNAENEFVTIK (1)
Aminoacids: 625	Spectral counts: 7		
MW [kDa]: 64.8	Score: 287.8		
Calc. pI: 7.9			

All proteins originated from *R. rattus*. Accession numbers were derived from Uniprot Protein Database (2011). Sequence coverage of the identified peptides is given as Σ Coverage. Significance of the search result is given as score.

Table S8.1.4: Mascot identification data (score 244.9 to 72.2) for a 13 kDa band of small intestines of fifth instars of *T. infestans* at 2 days after feeding surface coat of *T. cruzi* (short-surface group) and after gelelectrophoretic separation.

Protein/Characteristics		Peptide sequences (spectro counts)	
Ribosomal protein P2			
Accession: A6YPR0	∑ Coverage: 25.4	YVAAYLLAVLGGK (2)	ILSSVGIEADADK (1)
Aminoacids: 114	Spectral counts: 5	ILSSVGIEADADKLNK (2)	
MW [kDa]: 11.7	Score: 244.9		
Calc. pI: 4.9			
Complement C3			
Accession: P01026	∑ Coverage: 4.6	YYQTIEIPPK (2)	AAVFNHFISDGVK (1)
Aminoacids: 1663	Spectral counts: 8	IGLQEVEVK (1)	SSVAVPYVIVPLK (1)
MW [kDa]: 186.3	Score: 186.9	AFYEHAPK (1)	IFTVDNNLLPVGK (1)
Calc. pI: 6.5		AVLFNYREQEK (1)	
Keratin, type II cytoskeletal epidermal			
Accession: Q6IG02	∑ Coverage: 5.0	GFSSGSAVVSGGSR (1)	VDPEIQNVK (1)
Aminoacids: 685	Spectral counts: 4	LALDVEIATYR (2)	
MW [kDa]: 69.1	Score: 185.1		
Calc. pI: 7.7			
Keratin, type I cytoskeletal 14			
Accession: Q6IFV1	∑ Coverage: 8.5	EVATNSELVQSGK (1)	GQVGGDVNVEMDAAPGVDLSR (1)
Aminoacids: 485	Spectral counts: 4	LAADDFR (2)	
MW [kDa]: 52.7	Score: 166.9		
Calc. pI: 5.2			
TiLys1			
Accession: Q7YZS5	∑ Coverage: 20.9	GGPNHDGSYDNGLFQINDR (2)	ELVAHGIPRR (1)
Aminoacids: 139	Spectral counts: 4	ELVAHGIPR (1)	
MW [kDa]: 15.6	Score: 136.9		
Calc. pI: 8.7			
Keratin, type I cytoskeletal 42			
Accession: Q6IFU7	∑ Coverage: 8.4	TKYETELNLR (1)	GQVGGDVNVEMDAAPGVDLSR (1)
Aminoacids: 452	Spectral counts: 4	LAADDFR (2)	
MW [kDa]: 50.2	Score:133.3		
Calc. pI: 5.2			
Lysozyme C-1			
Accession: P00697	∑ Coverage: 17.6	NYNPGDQSTDYGIFQINSR (3)	DLSGYIR (1)
Aminoacids: 148	Spectral counts: 4		
MW [kDa]: 16.7	Score: 147.7		
Calc. pI: 9.1			
Keratin, type I cytoskeletal 17			
Accession: Q6IFU8	∑ Coverage: 6.7	EVATNSELVQSGK (1)	LASYLDKVR (1)
Aminoacids: 433	Spectral counts: 5	LASYLDK (1)	LAADDFR (2)
MW [kDa]: 48.1	Score: 132.3		
Calc. pI: 5.0			
Profilin-1			
Accession: P62963	∑ Coverage: 41.4	DSLLQDGEFTMDLR (1)	EGVHGGLINKK (1)
Aminoacids: 140	Spectral counts: 5	STGGAPTFNVTVTMTAK (1)	TFVSITPAEVGVLVGK (2)
MW [kDa]: 14.9	Score: 109.3		
Calc. pI: 8.3			
Fibronectin			
Accession: P04937	∑ Coverage: 1.1	SSPVVIDASTAIDAPSNLR (1)	APITGYIIR (1)
Aminoacids: 2477	Spectral counts: 2		
MW [kDa]: 272.3	Score: 90.4		
Calc. pI: 5.76			
Cathepsin L-like proteinase			
Accession: Q67EP7	∑ Coverage: 6.4	SVAGTDKGYVDIAQGDENALK (1)	GYVDIAQGDENALK (1)
Aminoacids: 328	Spectral counts: 2		
MW [kDa]: 36.5	Score: 78.9		
Calc. pI: 6.5			
Ig kappa chain C region, B allele			
Accession: P01835	∑ Coverage: 25.5	DGVLDSVTDQDSK (1)	DGVLDSVTDQDSKDSTYSMSSTLSLTK (1)
Aminoacids: 106	Spectral counts: 2		
MW [kDa]: 11.6	Score: 78.4		
Calc. pI: 5.2			
Cathepsin D1			
Accession: E2D6N9	∑ Coverage: 4.4	VYTVFNVEDR (1)	AEDYILK (1)
Aminoacids: 390	Spectral counts: 2		
MW [kDa]: 43.0	Score: 72.2		
Calc. pI: 5.1			

Proteins originated from *T. infestans* or *R. rattus*. *T. infestans* proteins are underlined. Accession numbers were derived from Uniprot Protein Database (2011). Sequence coverage of the identified peptides is given as Σ Coverage. Significance of the search result is given as score.

Table S8.1.5: Mascot identification data (score 70.1 to 36.3) for a 13 kDa band of small intestines of fifth instars of *T. infestans* at 2 days after feeding surface coat of *T. cruzi* (short-surface group) and after gelelectrophoretic separation.

Protein/Characteristics		Peptide sequences (spectro counts)	
Alpha-1-macroglobulin			
Accession: Q63041	∑ Coverage: 1.2	GYDMKIEVEAK (1)	LLLQEVR (1)
Aminoacids: 1500	Spectral counts: 2		
MW [kDa]: 167.0	Score: 70.1		
Calc. pI: 6.9			
Complement component C9			
Accession: Q62930	∑ Coverage: 3.3	GVELSDVKR (1)	LSSYLSQTK (1)
Aminoacids: 554	Spectral counts: 2		
MW [kDa]: 62.2	Score: 69.8		
Calc. pI: 5.7			
Alpha-1-antiproteinase			
Accession: P17475	∑ Coverage: 4.4	SAILYFPK (1)	MQHLEQTLTK (1)
Aminoacids: 411	Spectral counts: 2		
MW [kDa]: 46.1	Score: 66.1		
Calc. pI: 6.1			
Actin, cytoplasmic 1			
Accession: P60711	∑ Coverage: 7.2	SYELPDGQVITIGNER (1)	AVFPSIVGRPR (1)
Aminoacids: 375	Spectral counts: 2		
MW [kDa]: 41.7	Score: 49.0		
Calc. pI: 5.5			
Serine protease inhibitor A3N			
Accession: P09006	∑ Coverage: 7.4	AVLDVAETGTEAAAATGVK (1)	GNSMEEILEGLK (1)
Aminoacids: 418	Spectral counts: 2		
MW [kDa]: 46.6	Score: 41.2		
Calc. pI: 5.5			
Platelet factor 4			
Accession: P06765	∑ Coverage: 8.6	RITSLEVIK (1)	ITSLEVIK (1)
Aminoacids: 105	Spectral counts: 2		
MW [kDa]: 11.3	Score: 36.3		
Calc. pI: 9.5			

All proteins originated from *R. rattus*. Accession numbers were derived from Uniprot Protein Database (2011). Sequence coverage of the identified peptides is given as Σ Coverage. Significance of the search result is given as score.

Table S8.1.6: Mascot identification data (score 22378.80 to 331.44) for a 13 kDa band of small intestines of fifth instars of *T. infestans* at 2 days after infection with *T. cruzi* (short-trypo group) and after gelelectrophoretic separation.

Protein/Characteristics		Peptide sequences (spectro counts)	
Hemoglobin subunit beta-1			
Accession: P02091	∑ Coverage: 96.6	YFDSFGDLSSASAIMGNPK (238)	VINAFNDGLKHLDNLK (46)
Aminoacids: 147	Spectral counts: 1262	LLGNMIVIVLGHHLGK (216)	LLVVYPWTQR (98)
MW [kDa]: 16.0	Score: 22378.8	VHLTDAEK1AAVNGLWGKVNPDDVGGEALGR (15)	LHVDPENFR (22)
Calc. pI: 8.1		AAVNGLWGKVNPDDVGGEALGR (18)	KVINAFNDGLK (33)
		VVAGVASALAHKYH (145)	VINAFNDGLK (104)
		YFDSFGDLSSASAIMGNPKVK (4)	LHVDPENFR (21)
		LLVVYPWTQRYFDSFGDLSSASAIMGNPK (1)	HLDNLK (2)
		GTFAHLSELHCDKLHVDPENFR (2)	VNPDDVGGEALGR (56)
		KVINAFNDGLKHLDNLK (10)	VVAGVASALAHK (231)
Hemoglobin subunit beta-2			
Accession: P11517	∑ Coverage: 96.3	LLGNMIVIVLGHHLGK (216)	LLVVYPWTQR (98)
Aminoacids: 147	Spectral counts: 1023	FGDLSSASAIMGNPQVK (44)	VINAFNDGLK (104)
MW [kDa]: 16.0	Score: 16812.4	VNADNVGAEALGR (28)	EFTPCAQAAFQK (2)
Calc. pI: 8.8		VHLTDAEKATVSGLWGK (6)	LHVDPENFR (22)
		LHVDPENFRHLDNLK (46)	GTFAHLSELHCDK (3)
		VHLTDAEKATVSGLWGKVNADNVGAEALGR (3)	VHLTDAEK (5)
		GTFAHLSELHCDKLHVDPENFR (2)	KVINAFNDGLK (33)
		FGDLSSASAIMGNPQVKAHGK (2)	ATVSGLWGK (11)
		YFSKFGDLSSASAIMGNPQVK (4)	HLDNLK (2)
		KLHVDPENFRHLDNLK (10)	VVAGVASALAHK (231)
			VVAGVASALAHKYH (146)
Murinoglobulin-1			
Accession: Q03626	∑ Coverage: 9.6	QLSFSLSAEPIQGPYK (10)	FRVVSMDK (1)
Aminoacids: 1487	Spectral counts: 64	NLHPLNELFPLAYIEDPKMNR (12)	TPLVTIQSSGSFSQK (1)
MW [kDa]: 165.2	Score: 1322.6	QSGVKEEHSFTVMEFVLPR (9)	QQPAFALK (1)
Calc. pI: 6.0		VVSMDKNLHPLNELFPLAYIEDPKMNR (5)	QLSFSLSAEPIQGPYK (1)
		ESVVFVQTDKPVYKPGQSVK (4)	FGVDVK (6)
		NKESVVFVQTDKPVYKPGQSVK (3)	IMQWQDIK (3)
		NLHPLNELFPLAYIEDPKMNR (1)	MLSGFIPLKPTVK (3)
		VVSMDKNLHPLNELFPLAYIEDPKMNR (1)	EEHSFTVMEFVLPR (1)
			IMQWQDIKTENGLK (2)
Hemoglobin subunit alpha-1/2			
Accession: P01946	∑ Coverage: 96.5	AADHVEDLPGALSTLSDLHAHK (269)	TYFSHIDVSPGSAQVK (92)
Aminoacids: 142	Spectral counts: 881	IGGHGGEYGEEALQR (67)	FLASVSTVLTSK (155)
MW [kDa]: 15.3	Score: 7867.71	MFAAFPTTKTYFSHIDVSPGSAQVK (226)	FLASVSTVLTSKYR (2)
Calc. pI: 7.97		AADHVEDLPGALSTLSDLHAHKLR (43)	VLSADDKTNIK (22)
Alpha-1-inhibitor 3			
Accession: P14046	∑ Coverage: 10.5	NLHPLNELFPLAYIEDPKMNR (13)	EEHSFTVMEFVLPR (1)
Aminoacids: 1477	Spectral counts: 59	QSGVKEEHSFTVMEFVLPR (9)	IMQWQDVKTENGLK (1)
MW [kDa]: 163.7	Score: 1264.9	VVSMDKNLHPLNELFPLAYIEDPK (3)	IMQWQDVK (2)
Calc. pI: 6.0		QLSFSLSAEPIQGPYK (11)	FGVDVK (6)
		GQNSFQISLEISYMGSRPASNMVIADVK (2)	FRVVSMDK (1)
		ESVVFVQTDKPMYKPGQSVK (2)	QQPAFALK (1)
		NKESVVFVQTDKPMYKPGQSVK (1)	MLSGFIPLKPTVK (3)
		VVSMDKNLHPLNELFPLAYIEDPKMNR (3)	
TiLys1			
Accession: Q7YZS5	∑ Coverage: 20.9	ELVAHGIPRR (1)	ELVAHGIPR (5)
Aminoacids: 139	Spectral counts: 9	GGPNHDGSYDNGLFQINDR (3)	
MW [kDa]: 15.6	Score: 356.1		
Calc. pI: 8.7			
Keratin, type I cytoskeletal 17			
Accession: Q6IFU8	∑ Coverage: 19,2	GQVGGEINVEMDAAPGVDLSR (2)	LASYLDKVR (2)
Aminoacids: 433	Spectral counts: 13	EVATNSELVQSGK (3)	TKFETEQALR (2)
MW [kDa]: 48,1	Score: 331.4	ALEEANTELEVK (2)	LAADDFR (1)
Calc. pI: 5,0		TRLEQEIATYR (1)	

Proteins originated from *T. infestans* or *R. rattus*. *T. infestans* protein is underlined. Accession numbers were derived from Uniprot Protein Database (2011). Sequence coverage of the identified peptides is given as Σ Coverage. Significance of the search result is given as score.

Table S8.1.7: Mascot identification data (score 285.74 to 140.11) for a 13 kDa band of small intestines of fifth instars of *T. infestans* at 2 days after infection with *T. cruzi* (short-trypo group) and after gelelectrophoretic separation.

Protein/Characteristics		Peptide sequences (spectro counts)	
Keratin, type I cytoskeletal 14			
Accession: Q6IFV1	∑ Coverage: 15.9	GQVGGDVNVEMDAAPGVDLSR (3)	TRLEQEIATYR (1)
Aminoacids: 485	Spectral counts: 13	TMQNLEIELQSQLSMK (3)	VTMQNLNDR (2)
MW [kDa]: 52.7	Score: 285.7	EVATNSELVQSGK (3)	LAADDFR (1)
Calc. pI: 5.2			
Keratin, type II cytoskeletal 6A			
Accession: Q4FZU2	∑ Coverage: 13.4	SLDLDSIIAEVK (3)	TAAENEFVTLK (1)
Aminoacids: 552	Spectral counts: 17	TAAENEFVTLKK (2)	LRSEIDHVKK (1)
MW [kDa]: 59.2	Score: 279.8	YEELQITAGR (4)	SRAEAESWYQTK (1)
Calc. pI: 7.9		AEAESWYQTK (1)	FASFIDK (3)
		LALDVEIATYR (1)	
Lysozyme C-1			
Accession: P00697	∑ Coverage: 17.6	NYNPGDQSTDYGIFQINSR (3)	DLSGYIR (1)
Aminoacids: 148	Spectral counts: 4		
MW [kDa]: 16.7	Score: 237.9		
Calc. pI: 9.1			
Keratin, type I cytoskeletal 10			
Accession: Q6IFW6	∑ Coverage: 15.6	ADLEMQIESLTEELAYLK (2)	LENEIQTYR (1)
Aminoacids: 526	Spectral counts: 14	QSVEADINGLR (1)	KDAEAWFNEK (1)
MW [kDa]: 56.5	Score: 223.4	LKYENEVALR (1)	YENEVALR (1)
Calc. pI: 5.2		DAEAWFNEK (3)	SEITELRR (1)
		VTMQNLNDR (2)	LAADDFR (1)
Fibronectin			
Accession: P04937	∑ Coverage: 3.9	TGLDSPTGFDSSDVTANSFTVHWVAPR (3)	FLTTTPNSLLVSWQAPR (4)
Aminoacids: 2477	Spectral counts:14	SSPVVIDASTAIDAPSNLR (1)	ITGYIIK (2)
MW [kDa]: 272.3	Score: 222.3	APITGYIIR (3)	EESPPLIGQQSTVSDVPR (1)
Calc. pI: 5.8			
Keratin, type II cytoskeletal 1			
Accession: Q6IMF3	∑ Coverage: 8.2	FLEQQNQVLQTK (6)	FASFIDK (3)
Aminoacids: 625	Spectral counts: 16	FLEQQNQVLQTKWELLQQVDTSTR (3)	DYQELMNTK (1)
MW [kDa]: 64.8	Score: 177.6	TNAENEFVTIK (3)	
Calc. pI: 7.9			
Serum albumin			
Accession: P02770	∑ Coverage: 6.6	GLVLIAFSQYLQK (2)	FKDLGEQHFK (1)
Aminoacids: 608	Spectral counts: 8	LVQEVTDFAK (3)	ALVAAVR (1)
MW [kDa]: 68.7	Score: 163.8	ALVAAVR (1)	
Calc. pI: 6.5			
Complement component C9			
Accession: Q62930	∑ Coverage: 8.8	AIEDYVNEFSAR (1)	KMFLHVK (1)
Aminoacids: 554	Spectral counts: 6	DSSVDFQFSYFK (1)	LSSYLSQTKK (1)
MW [kDa]: 62.2	Score: 161.2	GVELSDVKR (2)	
Calc. pI: 5.7			
Ribonuclease UK114			
Accession: P52759	∑ Coverage: 19.0	APAAIGAYSQAVLVDR (2)	AAYQVAALPK (1)
Aminoacids: 137	Spectral counts: 3		
MW [kDa]: 14.3	Score: 144.7		
Calc. pI: 8.1			
Ig kappa chain C region, B allele			
Accession: P01835	∑ Coverage: 5.1	DGVLDSVTDQDSKDSTYSMSSTLSLTK (2)	DGVLDSVTDQDSK (2)
Aminoacids: 106	Spectral counts: 5	DSTYSMSSTLSLTK (1)	
MW [kDa]: 11.6	Score: 142.0		
Calc. pI: 11.6			
Keratin, type I cytoskeletal 15			
Accession: Q6IFV3	∑ Coverage: 8.3	ALEEANTELEVK (2)	VTMQNLNDRLASYLDK (1)
Aminoacids: 447	Spectral counts: 8	LASYLDKVR (2)	LAADDFR (1)
MW [kDa]: 48.8	Score: 140.3	VTMQNLNDR (2)	
Calc. pI: 4.9			
Keratin, type I cytoskeletal 42			
Accession: Q6IFU7	∑ Coverage: 10.8	GQVGGDVNVEMDAAPGVDLSR (3)	TKYETELNLR (1)
Aminoacids: 452	Spectral counts: 6	TRLEQEIATYR (1)	LAADDFR (1)
MW [kDa]: 50.2	Score: 140.1		
Calc. pI: 5.2			

All proteins originated from *R. rattus*. Accession numbers were derived from Uniprot Protein Database (2011). Sequence coverage of the identified peptides is given as Σ Coverage. Significance of the search result is given as score.

Table S8.1.8: Mascot identification data (score 128.30 to 68.90) for a 13 kDa band of small intestines of fifth instars of *T. infestans* at 2 days after infection with *T. cruzi* (short-trypo group) and after gelelectrophoretic separation.

Protein/Characteristics		Peptide sequences (spectro counts)	
Keratin, type II cytoskeletal 5			
Accession: Q6P6Q2	∑ Coverage: 12.9	SLDLDSIIAEVK (3)	VDALMDEINFMK (1)
Aminoacids: 576	Spectral counts: 13	LALDVEIATYR (1)	LRSEIDNVKK (2)
MW [kDa]: 61.8	Score: 128.3	TEAESWYQTK (1)	SRTEAESWYQTK (1)
Calc. pI: 7.8		WTLLQEQGTK (1)	FASFIDK (3)
Complement C3			
Accession: P01026	∑ Coverage: 6.5	NYAGVFMDAGLTFK (2)	YYQTIEIPPK (1)
Aminoacids: 1663	Spectral counts: 13	NVDGTAFVIFGVQDEDKK (1)	IGLQEVEVK (1)
MW [kDa]: 186.3	Score: 126.5	VGLVAVDK (1)	EYVLPSFEVLVEPTEK (1)
Calc. pI: 6.5		IFTVDNNLLPVGK (3)	GVFVLNK (1)
		SSVAVPYVIVPLK (2)	
Salivary secreted protein			
Accession: A6YPI9	∑ Coverage: 37.2	RPLITEIDAIDLDSNDKGGYAYVLK (2)	VSEDVTYPVRPIPGR (2)
Aminoacids: 129	Spectral counts: 6	FNLTIFGR (2)	
MW [kDa]: 14.6	Score: 124.7		
Calc. pI: 9.9			
Actin, cytoplasmic 1			
Accession: P60711	∑ Coverage: 15.5	SYELPDGQVITIGNER (3)	AVFPSIVGRPR (2)
Aminoacids: 375	Spectral counts: 7	DLYANTVLSGGTTMYPGIADR (1)	GYSFTTTAER (1)
MW [kDa]: 41.7	Score: 117.9		
Calc. pI: 5.5			
Salivary lipocalin			
Accession: A6YPE8	∑ Coverage: 14.0	FFTGTWFVSHVQK (1)	TGGGQEIPASLK (1)
Aminoacids: 179	Spectral counts: 2		
MW [kDa]: 19.9	Score: 104.9		
Calc. pI: 8.0			
Cathepsin D1			
Accession: E2D6N9	∑ Coverage: 13.9	NQLFGEALQVSDSPFAR (1)	TVSFASLKQ (2)
Aminoacids: 390	Spectral counts: 7	VYTVFNVEDR (2)	LPDITFHINGK (1)
MW [kDa]: 43.0	Score: 104.0	AEDYILK (1)	
Calc. pI: 5.0			
Keratin, type II cytoskeletal 2 epidermal			
Accession: Q6IG02	∑ Coverage: 5.0	GFSSGSAVVSGGSR (2)	VDPEIQNVK (1)
Aminoacids: 685	Spectral counts: 4	LALDVEIATYR (1)	
MW [kDa]: 69.1	Score: 95.7		
Calc. pI: 7.7			
Transthyretin			
Accession: P02767	∑ Coverage: 57.8	TAESGELHGLTTDEKFTEGVYRVELDTK (1)	GSPAVDVAVK (1)
Aminoacids: 147	Spectral counts: 4	ALGISPFHEYAEVVFTANDSGHR (1)	
MW [kDa]: 15.7	Score: 91.8	HYTIAALLSPYSYSTTAVVSNPQN (1)	
Calc. pI: 6.2			
Ig gamma-2C chain C region			
Accession: P20762	∑ Coverage: 7.9	NGELEQDYKNTLPVLDSDESYFLYSK (1)	NTLPVLDSDESYFLYSK (3)
Aminoacids: 329	Spectral counts: 4		
MW [kDa]: 36.5	Score: 87.8		
Calc. pI: 8.2			
Salivary lipocalin			
Accession: A6YPE6	∑ Coverage: 14.0	TSGGQVIPASLK (1)	FFTGTWFVSHVQK (1)
Aminoacids: 179	Spectral counts: 2		
MW [kDa]: 20.0	Score: 77.5		
Calc. pI: 8.0			
Ceruloplasmin			
Accession: P13635	∑ Coverage: 3.9	AEVGDKVSVHVK (2)	GQFPLSIQPMGVR (1)
Aminoacids: 1059	Spectral counts: 4	AGLQAFFQVR (1)	
MW [kDa]: 120.8	Score: 69.9		
Calc. pI: 5.5			
Glutathione peroxidase 3			
Accession: P23764	∑ Coverage: 13.7	QEPGENSEILPSLK (1)	YVRPGGGFVPNFQLFEK (1)
Aminoacids: 226	Spectral counts: 2		
MW [kDa]: 25.4	Score: 68.9		
Calc. pI: 8.1			

Proteins originated from *T. infestans* or *R. rattus*. *T. infestans* proteins are underlined. Accession numbers were derived from Uniprot Protein Database (2011). Sequence coverage of the identified peptides is given as Σ Coverage. Significance of the search result is given as score.

Table S8.1.9: Mascot identification data (score 67.34 to 49.09) for a 13 kDa band of small intestines of fifth instars of *T. infestans* at 2 days after infection with *T. cruzi* (short-trypo group) and after gelelectrophoretic separation.

Protein/Characteristics		Peptide sequences (spectro counts)	
Keratin, type I cytoskeletal 13			
Accession: Q6IFV4	∑ Coverage: 6.6	TRLEQEIATYR (1)	LAADDFR (1)
Aminoacids: 438	Spectral counts: 3	QSVEADINGLR (1)	
MW [kDa]: 47.7	Score: 67.3		
Calc. pI: 4.9			
Salivary lipocalin			
Accession: A6YPE9	∑ Coverage: 14.0	FFTGTWFVSHVQK (1)	TSGGQAIPESLK (1)
Aminoacids: 179	Spectral counts: 2		
MW [kDa]: 20.0	Score: 66.5		
Calc. pI: 8.4			
Alpha-1-antiproteinase			
Accession: P17475	∑ Coverage: 5.6	MQHLEQTLTK (1)	DADFHVDKSTTVK (1)
Aminoacids: 411	Spectral counts: 2		
MW [kDa]: 46.1	Score: 64.9		
Calc. pI: 6.1			
Profilin-1			
Accession: P62963	∑ Coverage: 23.6	STGGAPTFNVTVTMTAK (1)	TFVSITPAEVGVLVGK (1)
Aminoacids: 140	Spectral counts: 2		
MW [kDa]: 14.9	Score: 56.0		
Calc. pI: 8.3			
Serine protease inhibitor A3N			
Accession: P09006	∑ Coverage: 7.4	AVLDVAETGTEAAAATGVK (1)	GNSMEEILEGLK (1)
Aminoacids: 418	Spectral counts: 2		
MW [kDa]: 46.6	Score: 49.1		
Calc. pI: 5.5			

Proteins originated from *T. infestans* or *R. rattus*. *T. infestans* protein is underlined. Accession numbers were derived from Uniprot Protein Database (2011). Sequence coverage of the identified peptides is given as Σ Coverage. Significance of the search result is given as score.

Table S8.1.10: Mascot identification data (score 8839.67 to 2560.82) for a 13 kDa band of small intestines of unfed fifth instars of *T. infestans* (long-control group) after gelelectrophoretic separation.

Protein/Characteristics		Peptide sequences (spectro counts)	
Hemoglobin subunit alpha-D			
Accession: P02001	∑ Coverage: 81.6	AASHQEEFGAEALTR (33)	MLTAEDKK (1)
Aminoacids: 141	Spectral counts: 231	VLGALGNAVK (70)	GHGK (1)
MW [kDa]: 15.7	Score: 8839.7	KVLGALGNAVK (13)	FLSAVSAVLAEK (17)
Calc. pI: 7.6		MFTTYPQTK (42)	NVDNLSQAMAELSNLHAYNLR (17)
		TYFPHFDLSPGSDQVR (25)	DYTPEVHAAFDK (10)
Hemoglobin subunit alpha-A			
Accession: P01994	∑ Coverage: 78.2	VVAALIEAANHIDDIAGTLSK (96)	LRVDPVNFK (29)
Aminoacids: 142	Spectral counts: 407	KVVAALIEAANHIDDIAGTLSK (8)	LSDLHAHK (13)
MW [kDa]: 15.4	Score: 15052.4	TYFPHFDLSHGSAQIK (23)	MFTTYPPTK (85)
Calc. pI: 8.4		IAGHAEEYGAETLER (83)	FLCAVGTVLTAK (2)
		VLSAADKNNVK (68)	
Hemoglobin subunit beta			
Accession: P02112	∑ Coverage: 75.5	FFASFGNLSSPTAILGNPMVR (54)	LLIVYPWTQR (15)
Aminoacids: 147	Spectral counts: 175	VVAHALAR (28)	NLDNIK (3)
MW [kDa]: 16.5	Score: 6668.4	VHWTAEEK (13)	QLITGLWGK (3)
Calc. pI: 8.6		LHVDPENFR (3)	VNVAECGAEALAR (4)
		KVLTSFGDAVK (18)	LLGDILIIVLAAHFSK (1)
		VLTSFGDAVK (33)	
TiLys1			
Accession: Q7YZS5	∑ Coverage: 20.1	GGPNHDGSYDNGLFQINDR (5)	ELVAHGIPR (12)
Aminoacids: 139	Spectral counts: 17		
MW [kDa]: 15.6	Score: 530.4		
Calc. pI: 8.7			
Actin, cytoplasmic 1			
Accession: P60706	∑ Coverage: 9.9	SYELPDGQVITIGNER (1)	AGFAGDDAPR (8)
Aminoacids: 375	Spectral counts: 9		
MW [kDa]: 41.7	Score: 325.1		
Calc. pI: 5.5			
Keratin, type II cytoskeletal cochleal			
Accession: O93532	∑ Coverage: 6.5	NLDLDSIIAEVK (3)	LALDIEIATYR (1)
Aminoacids: 492	Spectral counts: 5	FASFIDKVR (1)	
MW [kDa]: 53.8	Score: 222.0		
Calc. pI: 6.1			
Hemoglobin subunit alpha-A			
Accession: P01994	∑ Coverage: 76.1	VVAALIEAANHIDDIAGTLSK (66)	FLCAVGTVLTAK (2)
Aminoacids: 142	Spectral counts: 307	KVVAALIEAANHIDDIAGTLSK (8)	VLSAADKNNVK (2)
MW [kDa]: 15.4	Score: 13184.8	TYFPHFDLSHGSAQIK (36)	LRVDPVNFK (51)
Calc. pI: 8.4		IAGHAEEYGAETLER (92)	LSDLHAHK (1)
		VLSAADKNNVKGIFTK (33)	NNVKGIFTK (1)
		MVLSAADKNNVK (1)	MFTTYPPTK (9)
		GIFTKIAGHAEEYGAETLER (4)	GIFTK (1)
Hemoglobin subunit beta			
Accession: P02112	∑ Coverage: 82.3	VNVAECGAEALAR (16)	NTFSQLSELHCDK (1)
Aminoacids: 147	Spectral counts: 293	VLTSFGDAVKNLDNIK (3)	VLTSFGDAVKNLDNIK (3)
MW [kDa]: 16.5	Score: 11497.5	FFASFGNLSSPTAILGNPMVR (34)	VLTSFGDAVK (59)
Calc. pI: 8.6		VHWTAEEKQLITGLWGK (2)	LLIVYPWTQR (32)
		NTFSQLSELHCDK (2)	VVAHALAR (9)
		KVLTSFGDAVK (85)	QLITGLWGK (23)
		VHWTAEEK (5)	DFTPECQAAWQK (1)
Hemoglobin subunit alpha-D			
Accession: P02001	∑ Coverage: 74.5	FLSAVSAVLAEK (11)	KVLGALGNAVK (5)
Aminoacids: 141	Spectral counts: 102	NVDNLSQAMAELSNLHAYNLR (16)	MFTTYPQTK (7)
MW [kDa]: 15.7	Score: 3965.8	TYFPHFDLSPGSDQVR (22)	LIQQAWEK (3)
Calc. pI: 7.6		AASHQEEFGAEALTR (9)	KLIQQAWEK (1)
		VLGALGNAVK (27)	DYTPEVHAAFDK (1)
Serum albumin			
Accession: P19121	∑ Coverage: 10.9	LLINLIK (2)	QLIYLSQKYPK (2)
Aminoacids: 615	Spectral counts: 63	MMSNLCSQQDVFSGK (1)	YNDLKEETFKAVAMITFAQYLQR (1)
MW [kDa]: 69.9	Score: 2560.8	AVAMITFAQYLQR (22)	QLIYLSQK (1)
Calc. pI: 5.7		YNDLKEETFK (8)	DVVDLAQK (3)
		LVKDVVDLAQK (22)	
		AVAMITFAQYLQR (1)	

Proteins originated from *T. infestans* or *G. gallus*. *T. infestans* protein is underlined. Accession numbers were derived from Uniprot Protein Database (2011). Sequence coverage of the identified peptides is given as Σ Coverage. Significance of the search result is given as score.

Table S8.1.11: Mascot identification data (score 1111.22 to 240.06) for a 13 kDa band of small intestines of fifth instars of *T. infestans* (long-control group) at 2 days after feeding after gelelectrophoretic separation.

Protein/Characteristics	Peptide sequences (spectro counts)		
Cathepsin D1			
Accession: E2D6N9	∑ Coverage: 8.2	NQLFGEALQVSDSPFAR (18)	QELLDKPVFSVYLNR (3)
Aminoacids: 390	Spectral counts: 21		
MW [kDa]: 43.0	Score: 1111.2		
Calc. pI: 5.1			
Carbonic anhydrase 2			
Accession: P07630	∑ Coverage: 28.5	VVDALNSIQTK (5)	HPDGLAVVGIFMK (3)
Aminoacids: 260	Spectral counts: 24	SVLQGGALDGVYR (5)	AIVNNGHSFNVEFDDSSDK (1)
MW [kDa]: 29.0	Score: 1051.0	YDPALKPLSFSYDAGTAK (10)	
Calc. pI: 7.1			
Ig lambda chain C region			
Accession: P20763	∑ Coverage: 19.4	VAPTITLFPPSKEELNEATK (8)	VAPTITLFPPSK (9)
Aminoacids: 103	Spectral counts: 17		
MW [kDa]: 11.4	Score: 728.1		
Calc. pI: 6.5			
Triosephosphate isomerase			
Accession: P00940	∑ Coverage: 20.6	GAFTGEISPAMIK (4)	SHVSDAVAQSTR (1)
Aminoacids: 248	Spectral counts: 13	AIADNVKDWSK (1)	VVLAYEPVWAIGTGK (7)
MW [kDa]: 26.6	Score: 677.7		
Calc. pI: 7.2			
Apolipoprotein A-I			
Accession: P08250	∑ Coverage: 30.3	LADNLDTLSAAAAK (2)	WTEELEQYR (1)
Aminoacids: 264	Spectral counts: 13	VMEQLSNLR (2)	LREDMAPYYK (1)
MW [kDa]: 30.7	Score: 618.0	ASGKDAIAQFESSAVGK (1)	LTPVAEEAR (1)
Calc. pI: 5.7		VMEQLSNLREK (1)	LISFLDELQK (1)
		DAIAQFESSAVGK (3)	
Actin, cytoplasmic 1			
Accession: P60706	∑ Coverage: 12.8	SYELPDGQVITIGNER (6)	EITALAPSTMK (1)
Aminoacids: 375	Spectral counts: 8	DLYANTVLSGGTTMYPGIADR (1)	
MW [kDa]: 41.7	Score: 403.9		
Calc. pI: 5.5			
Protein MRP-126			
Accession: P28318	∑ Coverage: 20.2	AIDVIIDVFHQYSR (5)	NQVSIDQIFK (7)
Aminoacids: 119	Spectral counts: 12		
MW [kDa]: 14.1	Score: 379.8		
Calc. pI: 7.0			
Proteasome subunit alpha type-7			
Accession: O13268	∑ Coverage: 16.1	NYTDEAIETDDLTIK (4)	GKDIVVLGVEK (1)
Aminoacids: 249	Spectral counts: 8	LTVEDPVTVEYITR (3)	
MW [kDa]: 28.1	Score: 349.6		
Calc. pI: 8.8			
Cathepsin D			
Accession: Q05744	∑ Coverage: 15.1	VTPFFDNVMQQK (1)	FDGILGMAFPR (1)
Aminoacids: 398	Spectral counts: 9	FDGILGMAFPR (1)	DPTAQPGGELLLGGTDPK (1)
MW [kDa]: 43.3	Score: 337.4	NYMDAQYYGEIGIGTPPQK (5)	
Calc. pI: 6.3			
Histone H2B 1/2/3/4/6			
Accession: P0C1H3	∑ Coverage: 19.1	AMGIMNSFVNDIFER (4)	LLLPGELAK (3)
Aminoacids: 126	Spectral counts: 7		
MW [kDa]: 13.9	Score: 300.3		
Calc. pI: 10.3			
Cathepsin B-like proteinase			
Accession: Q67EP8	∑ Coverage: 12.7	DLYYGESAYSLEDEAK (3)	QIQAEILK (4)
Aminoacids: 332	Spectral counts: 8	NGPVEAAFTVYEDLVNYK (1)	
MW [kDa]: 36.3	Score: 263.5		
Calc. pI: 5.5			
Fibronectin			
Accession: P11722	∑ Coverage: 3.2	SSPVVIDASTAIDAPSNLR (3)	ITGYIIR (1)
Aminoacids: 1256	Spectral counts: 5	TYTITGLQPGNDYK (1)	
MW [kDa]: 137.4	Score: 240.1		
Calc. pI: 5.1			

Proteins originated from *T. infestans* or *G. gallus*. *T. infestans* proteins are underlined. Accession numbers were derived from Uniprot Protein Database (2011). Sequence coverage of the identified peptides is given as Σ Coverage. Significance of the search result is given as score.

Table S8.1.12: Mascot identification data (score 153.28 to 70.42) for a 13 kDa band of small intestines of fifth instars of *T. infestans* (long-control group) at 2 days after feeding after gelelectrophoretic separation.

Protein/Characteristics		Peptide sequences (spectro counts)	
Peroxiredoxin-1			
Accession: P0CB50	∑ Coverage: 8.5	IPLVSDTKR (1)	GLFIIDEK (1)
Aminoacids: 199	Spectral counts: 2		
MW [kDa]: 22.3	Score: 153.3		
Calc. pI: 8.1			
14-3-3 protein epsilon			
Accession: Q5ZMT0	∑ Coverage: 7.5	YLAEFATGNDR (1)	NLLSVAYK (2)
Aminoacids: 255	Spectral counts: 3		
MW [kDa]: 29.2	Score: 144.7		
Calc. pI: 4.7			
Histone H3			
Accession: A6YPD4	∑ Coverage: 19.9	STELLIR (2)	EIAQDFKTDLR (1)
Aminoacids: 136	Spectral counts: 4	YRPGTVALR (1)	
MW [kDa]: 15.3	Score: 137.0		
Calc. pI: 11.2			
ATP synthase subunit beta, mitochondrial			
Accession: Q5ZLC5	∑ Coverage: 4.9	VALVYGQMNEPPGAR (1)	IGLFGGAGVGK (1)
Aminoacids: 533	Spectral counts: 2		
MW [kDa]: 56.6	Score: 116.2		
Calc. pI: 5.9			
14-3-3 protein theta			
Accession: Q5ZMD1	∑ Coverage: 9.8	NLLSVAYK (2)	LAEQAERYDDMATCMK (2)
Aminoacids: 245	Spectral counts: 4		
MW [kDa]: 27.8	Score: 91.3		
Calc. pI: 4.8			
14-3-3 protein zeta			
Accession: Q5ZKC9	∑ Coverage: 9.0	SVTEQGAELSNEER (1)	NLLSVAYK (2)
Aminoacids: 245	Spectral counts: 3		
MW [kDa]: 27.8	Score: 90.5		
Calc. pI: 4.8			
F-actin-capping protein subunit beta isoforms 1 and 2			
Accession: P14315	∑ Coverage: 8.3	TGSGTMNLGGSLTR (1)	RLPPQQIEK (1)
Aminoacids: 277	Spectral counts: 2		
MW [kDa]: 31.3	Score: 89.0		
Calc. pI: 5.6			
Lysozyme C			
Accession: P00698	∑ Coverage: 19.1	NTDGSTDYGILQINSR (1)	FESNFNTQATNR (1)
Aminoacids: 147	Spectral counts: 2		
MW [kDa]: 16.2	Score: 88.5		
Calc. pI: 9.1			
Histone H4			
Accession: P62801	∑ Coverage: 21.4	DNIQGITKPAIR (1)	ISGLIYEETR (1)
Aminoacids: 103	Spectral counts: 2		
MW [kDa]: 11.4	Score: 78.6		
Calc. pI: 11.4			
Elongation factor 1-alpha 1			
Accession: Q90835	∑ Coverage: 3.9	STTTGHLIYK (1)	QLIVGVNK (1)
Aminoacids: 462	Spectral counts: 2		
MW [kDa]: 50.1	Score: 71.2		
Calc. pI: 9.0			
Cathepsin B-like cysteine protease			
Accession: A2SZV7	∑ Coverage: 7.5	IQAEILK (1)	NGPIVASFLVYEDLFSYK (1)
Aminoacids: 333	Spectral counts: 2		
MW [kDa]: 36.4	Score: 70.4		
Calc. pI: 6.2			

Proteins originated from *T. infestans* or *G. gallus*. *T. infestans* proteins are underlined. Accession numbers were derived from Uniprot Protein Database (2011). Sequence coverage of the identified peptides is given as Σ Coverage. Significance of the search result is given as score.

Table S8.1.13: Mascot identification data (score 13556.88 to 203.56) for a 13 kDa band of small intestines of fifth instars of *T. infestans* (long-control group) at 3 days after feeding after gelelectrophoretic separation.

Protein/Characteristics		Peptide sequences (spectro counts)	
Hemoglobin subunit alpha-A			
Accession: P01994	∑ Coverage: 75.4	KVVAALIEAANHIDDIAGTLSK (25)	LRVDPVNFK (35)
Aminoacids: 142	Spectral counts: 317	VVAALIEAANHIDDIAGTLSK (59)	LSDLHAHK (1)
MW [kDa]: 15.4	Score: 13556.9	TYFPHFDLSHGSAQIK (37)	MFTTYPPTK (12)
Calc. pI: 8.4		IAGHAEEYGAETLER (129)	FLCAVGTVLTAK (6)
		VLSAADKNNVKGIFTK (6)	VLSAADKNNVK (2)
		IAGHAEEYGAETLERMFTTYPPTK (3)	NNVKGIFTK (2)
Hemoglobin subunit alpha-D			
Accession: P02001	∑ Coverage: 79.4	AASHQEEFGAEALTR (21)	KVLGALGNAVK (15)
Aminoacids: 141	Spectral counts: 328	FLSAVSAVLAEK (49)	KLIQQAWEK (5)
MW [kDa]: 15.7	Score: 12585.8	NVDNLSQAMAELSNLHAYNLR (52)	DYTPEVHAAFDK (4)
Calc. pI: 7.6		TYFPHFDLSPGSDQVR (65)	LIQQAWEK (5)
		NVDNLSQAMAELSNLHAYNLRVDPVNFK (11)	MFTTYPQTK (20)
		VLGALGNAVK (81)	
Hemoglobin subunit beta			
Accession: P02112	∑ Coverage: 73.5	FFASFGNLSSPTAILGNPMVR (48)	QLITGLWGK (12)
Aminoacids: 147	Spectral counts: 207	VNVAECGAEALAR (11)	VLTSFGDAVK (51)
MW [kDa]: 16.5	Score: 7716.1	VLTSFGDAVKNLDNIK (6)	VVAHALAR (8)
Calc. pI: 8.6		NTFSQLSELHCDK (2)	LHVDPENFR (12)
		KVLTSFGDAVK (19)	VHWTAEEK (3)
		LLIVYPWTQR (35)	
Hemoglobin subunit rho			
Accession: P02127	∑ Coverage: 21.8	LLIVYPWTQR (35)	LHVDPENFR (12)
Aminoacids: 147	Spectral counts: 49	VNVEECGAEALAR (2)	
MW [kDa]: 16.6	Score: 1967.5		
Calc. pI: 8.6			
Keratin, type II cytoskeletal cochleal			
Accession: O93532	∑ Coverage: 11.6	DVDAAYmNKVELEAK (2)	NLDLDSIIAEVK (1)
Aminoacids: 492	Spectral counts: 23	NLDLDSIIAEVK (8)	FASFIDKVR (1)
MW [kDa]: 53.8	Score: 1005.8	LALDIEIATYR (9)	FASFIDK (1)
Calc. pI: 6.1		NmQDLVEDFK (1)	
Lysozyme C			
Accession: P00698	∑ Coverage: 35.4	NTDGSTDYGILQINSR (6)	GTDVQAWIR (2)
Aminoacids: 147	Spectral counts: 13	FESNFNTQATNR (4)	IVSDGNGMNAWVAWR (1)
MW [kDa]: 16.2	Score: 657.8		
Calc. pI: 9.1			
Keratin, type I cytoskeletal 19			
Accession: O93256	∑ Coverage: 11.8	VLDELTLAR (2)	MSVEADINGLR (1)
Aminoacids: 423	Spectral counts: 10	TRLEQEIATYR (3)	TKFETEQALR (1)
MW [kDa]: 46.1	Score: 379.0	LASYLDKVR (2)	LASYLDK (1)
Calc. pI: 5.1			
TiLys1			
Accession: Q7YZS5	∑ Coverage: 20.1	GGPNHDGSYDNGLFQINDR (5)	ELVAHGIPR (5)
Aminoacids: 139	Spectral counts: 10		
MW [kDa]: 15.6	Score: 362.7		
Calc. pI: 8.7			
Cathepsin D1			
Accession: E2D6N9	∑ Coverage: 11.0	NQLFGEALQVSDSPFAR (4)	AEDYILK (1)
Aminoacids: 390	Spectral counts: 8	VYTVFNVEDR (2)	TVSFASLKQ (1)
MW [kDa]: 43.0	Score: 305.2		
Calc. pI: 5.1			
Salivary lipocalin			
Accession: A6YPE6	∑ Coverage: 21.8	TSGGQVIPASLK (2)	YIVEYTYQSHTGEQR (1)
Aminoacids: 179	Spectral counts: 6	GYKDDNYLVLSR (2)	DDNYLVLSR (1)
MW [kDa]: 20.0	Score: 238.4		
Calc. pI: 8.0			
Heterochromatin-associated protein MENT			
Accession: O73790	∑ Coverage: 8.1	ELSMFILLPDDIK (3)	LILVNAIYFK (2)
Aminoacids: 140	Spectral counts: 6	DTFPVLIMEK (1)	
MW [kDa]: 47.4	Score: 203.7		
Calc. pI: 9.4			

Proteins originated from *T. infestans* or *G. gallus*. *T. infestans* proteins are underlined. Accession numbers were derived from Uniprot Protein Database (2011). Sequence coverage of the identified peptides is given as Σ Coverage. Significance of the search result is given as score.

Table S8.1.14: Mascot identification data (score 174.90 to 73.64) for a 13 kDa band of small intestines of fifth instars of *T. infestans* (long-control group) at 3 days after feeding after gelelectrophoretic separation.

Protein/Characteristics		Peptide sequences (spectro counts)	
Transthyretin			
Accession: P27731	∑ Coverage: 24.0	AADGTWQDFATGK (3)	KAADGTWQDFATGK (1)
Aminoacids: 150	Spectral counts: 5	TTEFGEIHELTTEEQFVEGVYR (1)	
MW [kDa]: 16.3	Score: 174.9		
Calc. pI: 5.2			
Actin, cytoplasmic 1			
Accession: P60706	∑ Coverage: 9.9	DLYANTVLSGGTTMYPGIADR (1)	SYELPDGQVITIGNER (1)
Aminoacids: 375	Spectral counts: 3		
MW [kDa]: 41.7	Score: 143.8		
Calc. pI: 5.5			
Histone H2B 1/2/3/4/6			
Accession: P0C1H3	∑ Coverage: 19.1	AMGIMNSFVNDIFER (2)	LLLPGELAK (1)
Aminoacids: 126	Spectral counts: 3		
MW [kDa]: 13.9	Score: 133.9		
Calc. pI: 10.3			
Keratin, type I cytoskeletal 14			
Accession: Q6PVZ1	∑ Coverage: 3.6	LAADDFR (1)	TKFETEQALR (1)
Aminoacids: 467	Spectral counts: 2		
MW [kDa]: 51.0	Score: 122.4		
Calc. pI: 5.1			
Protein disulfide-isomerase A3			
Accession: Q8JG64	∑ Coverage: 2.4	LAPEYEAAATR (1)	RLAPEYEAAATR (1)
Aminoacids: 505	Spectral counts: 2		
MW [kDa]: 56.1	Score: 88.4		
Calc. pI: 6.0			
Serum albumin			
Accession: P19121	∑ Coverage: 5.2	LVKDVVDLAQK (1)	YNDLKEETFK (1)
Aminoacids: 615	Spectral counts: 3	QLIYLSQKYPK (1)	
MW [kDa]: 69.9	Score: 83.1		
Calc. pI: 5.7			
Cathepsin D			
Accession: Q05744	∑ Coverage: 9.8	ISSLPVVTLMLGGKPYQLTGEQYVFK (1)	ELQTAIGAKPLIK (1)
Aminoacids: 398	Spectral counts: 2		
MW [kDa]: 43.3	Score: 73.6		
Calc. pI: 6.3			

All proteins originated from *G. gallus*. Accession numbers were derived from Uniprot Protein Database (2011). Sequence coverage of the identified peptides is given as Σ Coverage. Significance of the search result is given as score.

Table S8.1.15: Mascot identification data (score 14891.03 to 185.78) for a 13 kDa band of small intestines of fifth instars of *T. infestans* (long-control group) at 5 days after feeding after gelelectrophoretic separation.

Protein/Characteristics		Peptide sequences (spectro counts)	
Hemoglobin subunit alpha-A			
Accession: P01994	∑ Coverage: 76.1	KVVAALIEAANHIDDIAGTLSK (36)	MVLSAADKNNVK (1)
Aminoacids: 142	Spectral counts: 392	VVAALIEAANHIDDIAGTLSK (83)	LRVDPVNFK (29)
MW [kDa]: 15.4	Score: 14891.0	IAGHAEEYGAETLER (167)	NNVKGIFTK (2)
Calc. pI: 8.4		TYFPHFDLSHGSAQIK (25)	LSDLHAHKLR (7)
		VLSAADKNNVKGIFTK (6)	VLSAADKNNVK (1)
		FLCAVGTVLTAK (2)	MFTTYPPTK (20)
		IAGHAEEYGAETLERMFTTYPPTK (12)	LSDLHAHK (1)
Hemoglobin subunit alpha-D			
Accession: P02001	∑ Coverage: 84.4	FLSAVSAVLAEK (67)	KVLGALGNAVK (15)
Aminoacids: 141	Spectral counts: 385	AASHQEEFGAEALTR (23)	DYTPEVHAAFDK (4)
MW [kDa]: 15.7	Score: 13189.4	NVDNLSQAMAELSNLHAYNLRVDPVNFK (8)	KLIQQAWEK (4)
Calc. pI: 7.6		TYFPHFDLSPGSDQVR (73)	LIQQAWEK (8)
		NVDNLSQAMAELSNLHAYNLR (41)	MFTTYPQTK (31)
		DYTPEVHAAFDKFLSAVSAVLAEK (2)	MLTAEDKK (3)
		VLGALGNAVK (106)	
Hemoglobin subunit beta			
Accession: P02112	∑ Coverage: 92.5	FFASFGNLSSPTAILGNPMVR (54)	LLIVYPWTQR (39)
Aminoacids: 147	Spectral counts: 194	VLTSFGDAVKNLDNIK (7)	VVAHALAR (3)
MW [kDa]: 16.5	Score: 6315.7	LLGDILIIVLAAHFSK (1)	QLITGLWGK (9)
Calc. pI: 8.6		NTFSQLSELHCDK (1)	DFTPECQAAWQK (1)
		VNVAECGAEALAR (4)	LHVDPENFR (10)
		KVLTSFGDAVK (21)	VHWTAEEK (3)
		VLTSFGDAVK (41)	
Hemoglobin subunit rho			
Accession: P02127	∑ Coverage: 21.8	LLIVYPWTQR (39)	LHVDPENFR (10)
Aminoacids: 147	Spectral counts: 50	VNVEECGAEALAR(1)	
MW [kDa]: 26.6	Score: 1768.0		
Calc. pI: 8.6			
Lysozyme C			
Accession: P00698	∑ Coverage: 35.4	NTDGSTDYGILQINSR (6)	IVSDGNGMNAWVAWR (1)
Aminoacids: 147	Spectral counts: 15	FESNFNTQATNR (6)	GTDVQAWIR (2)
MW [kDa]: 16.2	Score: 607.0		
Calc. pI: 9.1			
Keratin, type II cytoskeletal cochleal			
Accession: O93532	∑ Coverage: 6.1	NLDLDSIIAEVK (5)	FASFIDK (1)
Aminoacids: 492	Spectral counts: 8	LALDIEIATYR (2)	
MW [kDa]: 53.8	Score: 313.2		
Calc. pI: 6.1			
Heterochromatin-associated protein MENT			
Accession: O73790	∑ Coverage: 8.1	ELSMFILLPDDIK (2)	DTFPVLIMEK (1)
Aminoacids: 410	Spectral counts: 6	LILVNAIYFK (3)	
MW [kDa]: 47.4	Score: 285.2		
Calc. pI: 9.4			
TiLys1			
Accession: Q7YZS5	∑ Coverage: 20.1	GGPNHDGSYDNGLFQINDR (3)	ELVAHGIPR (5)
Aminoacids: 139	Spectral counts: 8		
MW [kDa]: 15.6	Score: 272.0		
Calc. pI: 8.7			
Ribosomal protein P2			
Accession: A6YPR0	∑ Coverage. 25.4	ILSSVGIEADADKLNK (3)	YVAAYLLAVLGGK (2)
Aminoacids: 114	Spectral counts. 6	ILSSVGIEADADK (1)	
MW [kDa]: 11.7	Score: 232.1		
Calc. pI: 4.9			
Salivary lipocalin			
Accession: A6YPE6	∑ Coverage: 21.8	TSGGQVIPASLK (2)	YIVEYTYQSHTGEQR (1)
Aminoacids: 179	Spectral counts: 5	GYKDDNYLVLSR (2)	
MW [kDa]: 20.0	Score: 185.8		
Calc. pI: 8.0			

Proteins originated from *T. infestans* or *G. gallus*. *T. infestans* proteins are underlined. Accession numbers were derived from Uniprot Protein Database (2011). Sequence coverage of the identified peptides is given as Σ Coverage. Significance of the search result is given as score.

Table S8.1.16: Mascot identification data (score 176.21 to 69.29) for a 13 kDa band of small intestines of fifth instars of *T. infestans* (long-control group) at 5 days after feeding after gelelectrophoretic separation.

Protein/ Characteristics		Peptide sequences (spectro counts)	
Ribosomal protein P1			
Accession: A6YPP2	∑ Coverage: 45.7	ELITNIGSGVGAAPAAGGAPAAAPADAAAAPAGGDKK (1)	
Aminoacids: 116	Spectral counts: 3	ELITNIGSGVGAAPAAGGAPAAAPADAAAAPAGGDK (1)	
MW [kDa]: 11.8	Score: 176.2	AASVDVEPYWPGLFAK (1)	
Calc. pI: 4.5			
Cathepsin D			
Accession: Q05744	∑ Coverage: 17.3	NYMDAQYYGEIGIGTPPQK (1)	ELQTAIGAKPLIK (1)
Aminoacids: 398	Spectral counts: 5	ISSLPVVTLMLGGKPYQLTGEQYVFK (1)	FDGILGMAFPR (2)
MW [kDa]: 43.3	Score: 148.2		
Calc. pI: 6.3			
Keratin, type I cytoskeletal 19			
Accession: O93256	∑ Coverage: 4.3	VLDELTLAR (1)	LASYLDKVR(3)
Aminoacids: 423	Spectral counts: 4		
MW [kDa]: 46.1	Score: 145.6		
Calc. pI: 5.1			
Histone H4			
Accession: P62801	∑ Coverage: 29.1	ISGLIYEETR (1)	VFLENVIR (1)
Aminoacids: 103	Spectral counts: 4	DNIQGITKPAIR (2)	
MW [kDa]: 11.4	Score: 135.3		
Calc. pI: 11.4			
Cathepsin L-like proteinase			
Accession: Q67EP7	∑ Coverage: 6.4	SVAGTDKGYVDIAQGDENALK (2)	GYVDIAQGDENALK (2)
Aminoacids: 328	Spectral counts: 4		
MW [kDa]: 36.5	Score: 126.6		
Calc. pI: 6.5			
Cathepsin D1			
Accession: E2D6N9	∑ Coverage: 8.7	NQLFGEALQVSDSPFAR (1)	AEDYILK (1)
Aminoacids: 390	Spectral counts: 3	VYTVFNVEDR (1)	
MW [kDa]: 43.0	Score: 99.8		
Calc. pI: 5.1			
Actin, cytoplasmic 1			
Accession: P60706	∑ Coverage: 9.3	SYELPDGQVITIGNER (1)	IIAPPERK (1)
Aminoacids: 375	Spectral counts: 3	AVFPSIVGRPR (1)	
MW [kDa]: 41.7	Score: 79.8		
Calc. pI: 5.5			
Histone H2B 1/2/3/4/6			
Accession: P0C1H3	∑ Coverage: 19.1	AMGIMNSFVNDIFER (1)	LLLPGELAK (1)
Aminoacids: 126	Spectral counts: 2		
MW [kDa]: 13.9	Score: 72.5		
Calc. pI: 10.3			
Transthyretin			
Accession: P27731	∑ Coverage: 23.3	TTEFGEIHELTTEEQFVEGVYR (2)	AADGTWQDFATGK (1)
Aminoacids: 150	Spectral counts: 3		
MW [kDa]: 16.3	Score: 71.5		
Calc. pI: 5.2			
Fibronectin			
Accession: P11722	∑ Coverage: 2.1	SSPVVIDASTAIDAPSNLR (1)	ITGYIIR (1)
Aminoacids: 1256	Spectral counts: 2		
MW [kDa]: 137.4	Score: 69.3		
Calc. pI: 5.1			

Proteins originated from *T. infestans* or *G. gallus*. *T. infestans* proteins are underlined. Accession numbers were derived from Uniprot Protein Database (2011). Sequence coverage of the identified peptides is given as Σ Coverage. Significance of the search result is given as score.

Table S8.1.17: RNA quality characteristics for small intestines of fifth instars of *T. infestans* (short-control group) after capillary electrophoresis.

Small intestine				
Feedingstate*	Sample No	RNA$^{\Delta}$	Ratio$^{\#}$	RQI
2	1	144.47	0.68	6.8
2	2	144.77	0.66	6.8
2	3	163.12	0.55	6.9
3	1	181.52	0.54	6.0
3	2	192.28	0.59	6.2
3	3	115.93	0.38	5.6
5	1	268.74	1.85	8.1
5	2	187.56	0.85	6.8
5	3	199.08	0.72	6.6

*uf: unfed, 2-5: 2-5 daf; $^{\Delta}$concentration (ng/µl); $^{\#}$[28S/18S]

Table S8.1.18: RNA quality characteristics for small intestines of unfed fifth instars of *T. infestans* and after infection with *T. cruzi* (short-trypo group) after capillary electrophoresis.

Small intestine				
Feedingstate*	Sample No	RNA$^{\Delta}$	Ratio$^{\#}$	RQI
2	1	138.36	3.41	3.0
2	2	172.75	1.00	8.0
2	3	217.16	1.10	8.8
3	1	179.04	0.57	6.2
3	2	138.44	0.93	8.1
3	3	138.24	0.90	6.9
5	1	165.35	1.02	9.3
5	2	102.43	1.43	9.6
5	3	240.48	0.93	8.7

*uf: unfed, 2-5: 2-5 daf; $^{\Delta}$concentration (ng/µl); $^{\#}$[28S/18S]

Table S8.1.19: RNA quality characteristics for small intestines of fifth instars of *T. infestans* (long-control group) after capillary electrophoresis.

Small intestine				
Feedingstate*	Sample No	RNA$^{\Delta}$	Ratio$^{\#}$	RQI
uf	1	167.02	1.38	9.3
uf	2	95.76	2.28	9.3
uf	3	113.50	1.25	9.2
2	1	135.80	1.26	8.5
2	2	144.54	1.44	8.3
2	3	236.05	1.50	8.3
3	1	421.29	1.66	8.3
3	2	302.83	1.38	8.5
3	3	344.02	1.04	7.7
5	1	343.49	0.57	6.8
5	2	253.60	1.43	8.5
5	3	350.42	1.40	8.3
10	1	266.97	1.23	9.1
10	2	227.65	1.01	8.6
10	3	293.99	1.01	8.5
15	1	212.22	0.54	7.6
15	2	285.28	0.66	8.0
15	3	316.73	0.90	8.7
20	1	175.84	0.38	10.0
20	2	181.98	0.64	7.8
20	3	202.65	0.68	8.0

*uf: unfed, 2-20: 2-20 daf; $^{\Delta}$concentration (ng/µl); $^{\#}$[28S/18S]

8.2 Supplemental data for chapter 4

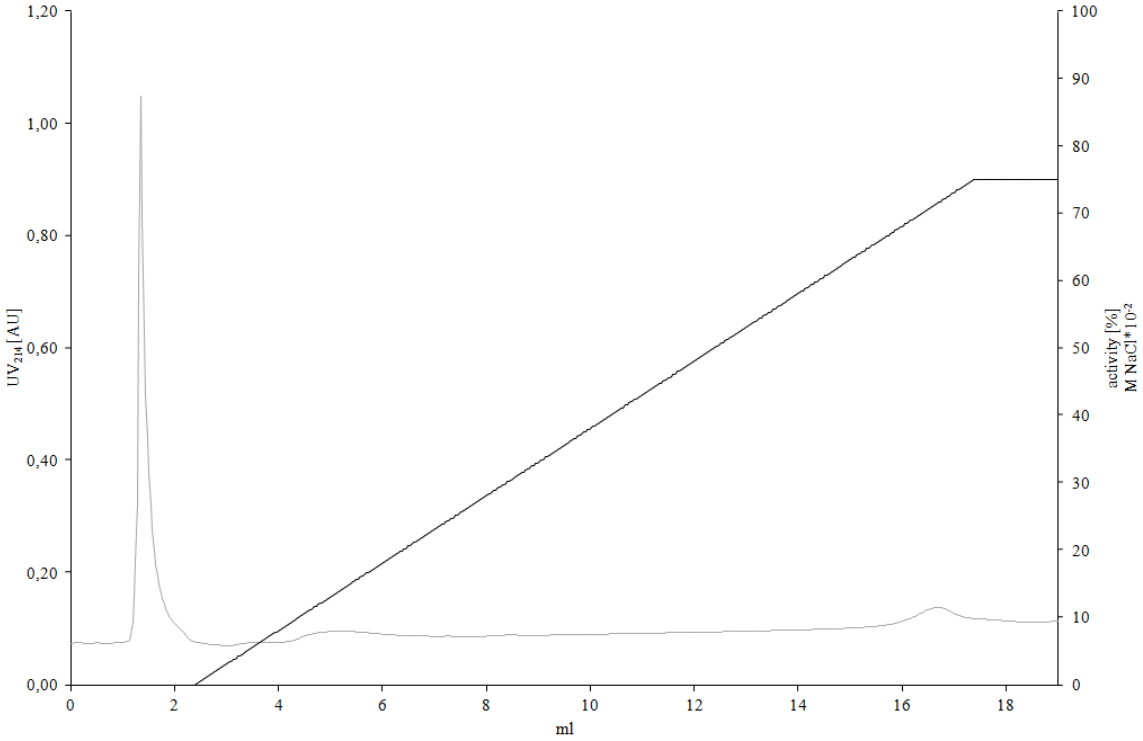

Figure S8.2.1: Second chromatographic separation of bacteriolytic compounds from small intestine homogenates of *T. infestans*.
Anion exchange chromatography: flow-through was separated on a SOURCE Q column equilibrated with 20 mM Tris, pH 7.0. Proteins (grey line) were eluted by a linear gradient of 0-750 mM NaCl and finally 1 M NaCl (dotted line). Lysis of *M. lysodeikticus* by the respective fraction is presented as percentage of the maximal activity (black line).

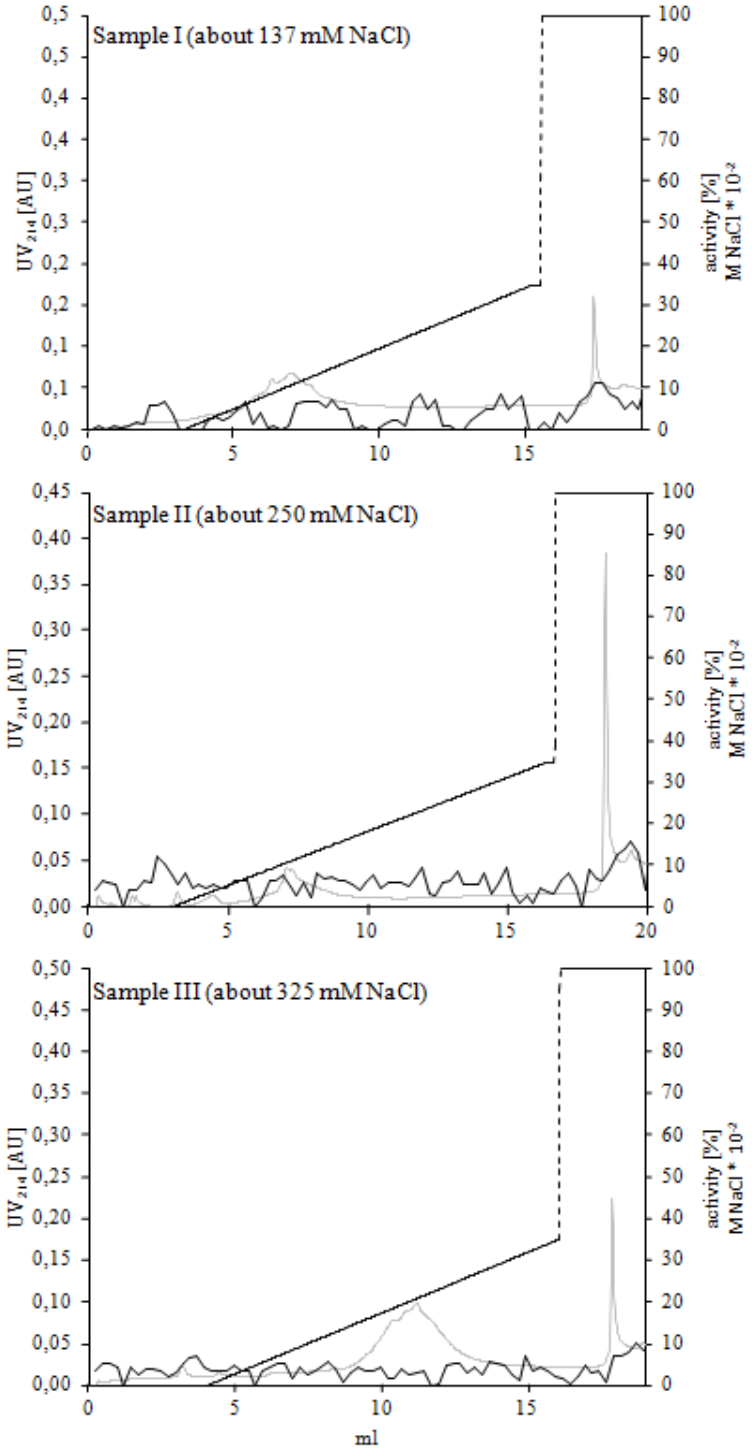

Figure S8.2.2: Third chromatographic separation of bacteriolytic compounds from small intestine homogenates of *T. infestans*.
Anion exchange chromatography: second purification step of fractions containing the majority of bacteriolytic activity on a SOURCE Q column equilibrated with 20 mM Tris, pH 7.0. After pooling of the fractions (I-III) that had eluted in a first chromatographic separation (Figure 4.1) at about 137 mM, 250 mM and 325 mM, respectively, proteins (grey line) were eluted separately within 30 min by linear gradients of 0-350 mM NaCl and finally 1 M NaCl (dotted line). Lysis of *Micrococcus lysodeikticus* (black line) by the respective fraction is presented as percentage of the maximal activity recorded in the previous separation.

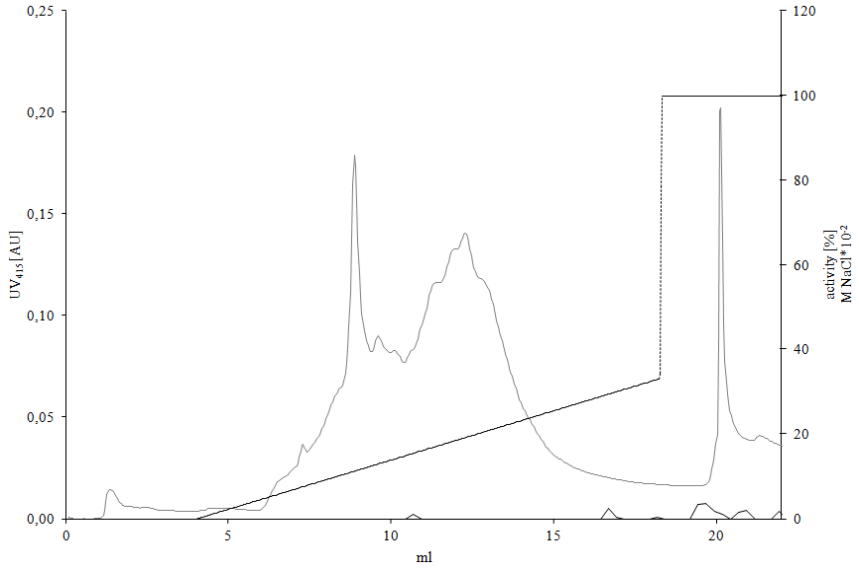

Figure S8.2.3: Fourth chromatographic separation of bacteriolytic compounds from small intestine homogenates of *T. infestans*.

Anion exchange chromatography: purification of pooled samples (I-III) containing the majority of antibacterial activity on a SOURCE Q column equilibrated with 20 mM Tris, pH 7.0. Protein (grey line) was eluted by a linear gradient of 0-350 mM NaCl and finally 1 M NaCl (dotted line) within 30 min. Lysis of *M. lysodeikticus* (black line) is presented as percentage of the maximal activity recorded in the first separation.

Table S8.2.1: Mascot identification data of small intestines of unfed fifth instars of *T. infestans* for flow-through (score 9077.5 to 399.5) after chromatographic separation.

Protein/Characteristics		Peptide sequences	
Hemoglobin subunit alpha-A			
Accession: P01994	∑ Coverage: 58.5	VVAALIEAANHIDDIAGTLSK (23)	MVLSAADKNNVK (1)
Aminoacids: 142	Spectral counts: 148	KVVAALIEAANHIDDIAGTLSK (38)	MFTTYPPTK (5)
MW [kDa]: 15.4	Score: 9077.5	IAGHAEEYGAETLER (64)	LRVDPVNFK (2)
Calc. pI: 8.4		TYFPHFDLSHGSAQIK (12)	VLSAADKNNVK (1)
Hemoglobin subunit alpha-D			
Accession: P02001	∑ Coverage: 74.5	NVDNLSQAMAELSNLHAYNLR (38)	DYTPEVHAAFDK (4)
Aminoacids: 141	Spectral counts: 123	FLSAVSAVLAEK (36)	DYTPEVHAAFDKFLSAVSAVLAEK (1)
MW [kDa]: 15.7	Score: 6637.0	AASHQEEFGAEALTR (15)	KVLGALGNAVK (4)
Calc. pI: 7.56		VLGALGNAVK (11)	MFTTYPQTK (4)
		TYFPHFDLSPGSDQVR (6)	KLIQQAWEK (1)
			LIQQAWEK (2)
Hemoglobin subunit beta			
Accession: P02112	∑ Coverage: 66.0	LLGDILIIVLAAHFSK (13)	QLITGLWGK (2)
Aminoacids: 147	Spectral counts: 100	FFASFGNLSSPTAILGNPMVR (27)	VLTSFGDAVK (12)
MW [kDa]: 16.5	Score: 5302.0	VNVAECGAEALAR (4)	VVAHALAR (1)
Calc. pI: 8.6		KVLTSFGDAVK (9)	LHVDPENFR (1)
		LLIVYPWTQR (31)	
Putative salivary secreted protein			
Accession: A6YPU2	∑ Coverage: 41.7	QVTWNTELVAGTTDQYK (10)	NLFQDYLLAVDK (16)
Aminoacids: 175	Spectral counts: 71	KQVTWNTELVAGTTDQYK (4)	TATPDDSSNIWTLEVYPSHVFLK (8)
MW [kDa]: 19.9	Score: 3308.4	IKNLFQDYLLAVDK (21)	TDAFTANQR (4)
Calc. pI: 6.0		NLFQDYLLAVDK	EASVISR (1)
		NLFQDYLLAVDKTR (2)	IKNLFQDYLLAVDKTR (4)
Glycerol-3-phosphate dehydrogenase			
Accession: B4XU24	∑ Coverage: 43.4	KLTEIINTTHENVK (1)	LIETDYFR (3)
Aminoacids: 355	Spectral counts: 69	LQGPITAEEVNYMLENK (20)	RLAEQFVITGK (3)
MW [kDa]: 39.0	Score: 3113.7	VSIVGSGNWGSAIAK (4)	EGGGIELISSVIK (1)
Calc. pI: 6.2		LAEQFVITGK (4)	KVSIVGSGNWGSAIAK (1)
		SSAVGLSLIK (3)	MYVYEELVDGK (3)
		MYVYEELVDGK (8)	IGLMEMINFIDYFYPK (1)
		IIGANVVNLK (1)	NAELLHK (1)
		LTEIINTTHENVK (4)	MIKPEELITFIK (10)
		FPLFTAVNR (1)	
Salivary lipocalin			
Accession: A6YPE6	∑ Coverage: 29.6	YIVEYTYQSHTGEQR (5)	TSGGQVIPASLK (2)
Aminoacids: 179	Spectral counts: 12	GYKDDNYLVLSR (2)	DDNYLVLSR (1)
MW [kDa]: 20.0	Score: 625.9	FFTGTWFVSHVQK (1)	RFFTGTWFVSHVQK (1)
Calc. pI: 8.0			
Triosephosphate isomerase			
Accession: P00940	∑ Coverage: 11.3	VVLAYEPVWAIGTGK (10)	GAFTGEISPAMIK (1)
Aminoacids: 248	Spectral counts: 11		
MW [kDa]: 26.6	Score: 575.5		
Calc. pI: 7.2			
Elongation factor 1-alpha 1			
Accession: Q90835	∑ Coverage: 7.1	IGGIGTVPVGR (3)	STTTGHLIYK (1)
Aminoacids: 462	Spectral counts: 9	YYVTIIDAPGHR (4)	
MW [kDa]: 50.1	Score: 493.2		
Calc. pI: 9.0			
Salivary lipocalin			
Accession: A6YPP6	∑ Coverage: 32.1	SLNPSVPILFK (2)	LSVIETDYK (2)
Aminoacids: 193	Spectral counts: 11	GISLTYEGQVTVR (3)	TVYHTQGNEFFELR (1)
MW [kDa]: 22.3	Score: 412.2	AYQLEVTQK (2)	IEDFFK (1)
Calc. pI: 9.0			
Platelet inhibitor triplatin-2			
Accession: Q18NS6	∑ Coverage: 28.7	ITVTTSILATDNEK (4)	GWDISTWLSR (2)
Aminoacids: 178	Spectral counts: 8	NGVEQGVQNYFNQK (1)	YFNIPLAYATHSK (1)
MW [kDa]: 19.5	Score: 399.5		
Calc. pI: 7.6			

Protein originated from *T. infestans* or *G. gallus*. *T. infestans* proteins are underlined. Accession numbers were derived from Uniprot Protein Database (2011). Sequence coverage of the identified peptides is given as Σ Coverage. Significance of the search result is given as score.

Table S8.2.2: Mascot identification data of small intestines of unfed fifth instars of *T. infestans* for flow-through (score 381.8 to 104.2) after chromatographic separation.

Protein/Characteristics		Peptide sequences	
Salivary lipocalin			
Accession: A6YPL3	∑ Coverage: 26.6	ITDNYLVLQR (3)	KEDDQISNLDK (1)
Aminoacids: 199	Spectral counts: 8	MTGSTISVTADGYYEIGNK (2)	SQGLVPDNMISR (2)
MW [kDa]: 22.3	Score: 381.8		
Calc. pI: 9.1			
Keratin, type II cytoskeletal cochleal			
Accession: O93532	∑ Coverage: 6.7	NLDLDSIIAEVK (4)	LALDIEIATYR (2)
Aminoacids: 492	Spectral counts: 7	NMQDLVEDFK (1)	
MW [kDa]: 53.8	Score: 364.5		
Calc. pI: 6.1			
Salivary lipocalin			
Accession: A6YPE9	∑ Coverage: 25.1	FFTGTWFVSHVQK (1)	DDNYLVLSR (1)
Aminoacids: 179	Spectral counts: 10	TSGGQAIPESLK (2)	RFFTGTWFVSHVQK (1)
MW [kDa]: 20.0	Score: 359.4	YIVEYSYQSK (5)	
Calc. pI: 8.4			
Lipocalin-like Ti65			
Accession: A6YPR4	∑ Coverage: 17.8	KEDEVISNLDTILK (3)	TDNYLVLQR (1)
Aminoacids: 197	Spectral counts: 7	NTGLVSSQLISR (2)	EDEVISNLDTILK (1)
MW [kDa]: 21.6	Score: 356.7		
Calc. pI: 9.3			
Polyubiquitin-B			
Accession: P0CG62	∑ Coverage: 49.8	IQDKEGIPPDQQR (3)	ESTLHLVLR (1)
Aminoacids: 305	Spectral counts: 6	TITLEVEPSDTIENVK (2)	
MW [kDa]: 34.3	Score: 344.4		
Calc. pI: 7.5			
Salivary lipocalin			
Accession: A6YPH4	∑ Coverage: 17.7	SSILATDNESYAVLQR (3)	RADGKPVTSFTITDR (1)
Aminoacids: 175	Spectral counts: 4		
MW [kDa]: 19.2	Score: 318.4		
Calc. pI: 8.6			
Salivary lipocalin			
Accession: A6YPE8	∑ Coverage: 25.1	FFTGTWFVSHVQK (1)	TGGGQEIPASLK (1)
Aminoacids: 179	Spectral counts: 9	YIVEYSYQSK (5)	RFFTGTWFVSHVQK (1)
MW [kDa]: 19.9	Score: 309.1	DDNYLVLSR (1)	
Calc. pI: 8.0			
Salivary lipocalin			
Accession: A6YPH2	∑ Coverage: 13.4	TGSSLATYITR (3)	SDIETIFK (2)
Aminoacids: 202	Spectral counts: 7	DNVLVLHR (2)	
MW [kDa]: 22.7	Score: 304.4		
Calc. pI: 9.2			
Ig lambda chain C region			
Accession: P20763	∑ Coverage: 28.2	VAPTITLFPPSK (1)	VAPTITLFPPSKEELNEATK (2)
Aminoacids: 103	Spectral counts: 4	SGETTAPQR (1)	
MW [kDa]: 11.4	Score: 251.2		
Calc. pI: 6.5			
Superoxide dismutase [Cu-Zn]			
Accession: A6YPT7	∑ Coverage: 18.2	GTVYFEQESPNAEVK (2)	TLVVHADPDDLGK (1)
Aminoacids: 154	Spectral counts: 3		
MW [kDa]: 15.9	Score: 137.8		
Calc. pI: 6.2			
Salivary lipocalin			
Accession: A6YPG6	∑ Coverage: 13.7	YKDSSNLSGNLLLLQR (1)	DSSNLSGNLLLLQR (1)
Aminoacids: 182	Spectral counts: 3	YFDINEFFR (1)	
MW [kDa]: 20.4	Score: 136.6		
Calc. pI: 8.75			
Keratin, type I cytoskeletal 19			
Accession: O93256	∑ Coverage: 4.3	VLDELTLAR (1)	LEQEIATYR (1)
Aminoacids: 423	Spectral counts: 2		
MW [kDa]: 46.1	Score: 104.2		
Calc. pI: 5.1			

Protein originated from *T. infestans* or *G. gallus*. *T. infestans* proteins are underlined. Accession numbers were derived from Uniprot Protein Database (2011). Sequence coverage of the identified peptides is given as Σ Coverage. Significance of the search result is given as score.

Table S8.2.3: Mascot identification data of small intestines of unfed fifth instars of *T. infestans* for flow-through (score 98.0 to 75.2) after chromatographic separation.

Protein/Characteristics		Peptide sequences	
Salivary lipocalin			
Accession: A6YPN6 Aminoacids: 202 MW [kDa]: 22.4 Calc. pI: 9.1	∑ Coverage: 9.4 Spectral counts: 2 Score: 98.0	IGSSLDTYITR (1)	DNILVLHR (1)
Calponin			
Accession: A6YPG4 Aminoacids: 184 MW [kDa]: 20.3 Calc. pI: 7.8	∑ Coverage: 13.0 Spectral counts: 2 Score: 95.5	AGESIIGLQAGSNK (1)	MMENINSFLK (1)
Ca^{2+}-binding protein			
Accession: A6YPK2 Aminoacids: 178 MW [kDa]: 20.5 Calc. pI: 5.6	∑ Coverage: 14.0 Spectral counts: 2 Score: 85.0	LSTQTIDTIVAK (1)	GTISFQDFGALWK (1)
Salivary lipocalin			
Accession: A6YPH0 Aminoacids: 185 MW [kDa]: 20.5 Calc. pI: 8.9	∑ Coverage: 12.4 Spectral counts: 2 Score: 75.2	YFEINDFFK (1)	DNYDVKLEPEGDSK (1)

All proteins originated from *T. infestans*. Accession numbers were derived from Uniprot Protein Database (2011). Sequence coverage of the identified peptides is given as Σ Coverage. Significance of the search result is given as score.

Table S8.2.4: Mascot identification data of small intestines of unfed fifth instars of *T. infestans* for bacteriolytic active fractions (score 2891.5 to 449.3) after chromatographic separation.

Protein/Characteristics		Peptide sequences (spectro counts)	
Hemoglobin subunit alpha-A			
Accession: P01994	∑ Coverage: 50.0	VVAALIEAANHIDDIAGTLSK (30)	TYFPHFDLSHGSAQIK (3)
Aminoacids: 142	Spectral counts: 55	IAGHAEEYGAETLER (11)	MFTTYPPTK (5)
MW [kDa]: 15.4	Score: 2891.5	LRVDPVNFK (1)	KVVAALIEAANHIDDIAGTLSK (5)
Calc. pI: 8.4			
Heat shock 70 kDa protein			
Accession: P08106	∑ Coverage: 11.2	IINEPTAAAIAYGLDK (13)	STAGDTHLGGEDFDNR (3)
Aminoacids: 634	Spectral counts: 38	TFFPEEISSMVLTK (13)	VEIIANDQGNR (3)
MW [kDa]: 69.7	Score: 1994.4	IINEPTAAAIAYGLDKK (3)	TTPSYVAFTDTER (2)
Calc. pI: 5.7			
Hemoglobin subunit beta			
Accession: P02112	∑ Coverage: 59.9	FFASFGNLSSPTAILGNPMVR (10)	LLIVYPWTQR (12)
Aminoacids: 147	Spectral counts: 34	LLGDILIIVLAAHFSK (5)	VNVAECGAEALAR (1)
MW [kDa]: 16.5	Score: 1908.3	KVLTSFGDAVK (2)	QLITGLWGK (2)
Calc. pI: 8.6		VVAHALAR (2)	
Heat shock cognate 71 kDa protein			
Accession: O73885	∑ Coverage: 12.6	IINEPTAAAIAYGLDK (13)	QTQTFTTYSDNQPGVLIQVYEGER (3)
Aminoacids: 646	Spectral counts: 28	IINEPTAAAIAYGLDKK (3)	VEIIANDQGNR (4)
MW [kDa]: 70.8	Score: 1428.3	STAGDTHLGGEDFDNR (3)	TTPSYVAFTDTER (2)
Calc. pI: 5.6			
78 kDa glucose-regulated protein			
Accession: Q90593	∑ Coverage: 5.8	IINEPTAAAIAYGLDK (13)	VEIIANDQGNR (4)
Aminoacids: 652	Spectral counts: 23	MKETAEAYLGK (6)	
MW [kDa]: 72.0	Score: 1138.4		
Calc. pI: 5.2			
Elongation factor 1-alpha 1			
Accession: Q90835	∑ Coverage: 10.6	IGGIGTVPVGR (5)	STTTGHLIYK (1)
Aminoacids: 462	Spectral counts: 13	YYVTIIDAPGHR (4)	QLIVGVNK (1)
MW [kDa]: 50.1	Score: 804.3	LPLQDVYK (2)	
Calc. pI: 9.0			
Serum albumin			
Accession: P19121	∑ Coverage: 9.3	AVAMITFAQYLQR (6)	SFEAGHDAFMAEFVYEYSR (1)
Aminoacids: 615	Spectral counts: 12	YNDLKEETFK (3)	LLINLIK (1)
MW [kDa]: 69.9	Score: 681.2	QLIYLSQK (1)	
Calc. pI: 5.7			
Serine carboxypeptidase 1			
Accession: Q101N9	∑ Coverage: 14.6	TNDLYITGESYAGK (3)	LWYVDNELAGYAK (1)
Aminoacids: 474	Spectral counts: 15	FTEVLVR (1)	KLWYVDNELAGYAK (1)
MW [kDa]: 53.9	Score: 656.5	NAGHMVPSDQPK (3)	AAMVTLMDGNSVSYSGFLTVNK (5)
Calc. pI: 5.3			
Radixin			
Accession: Q9PU45	∑ Coverage: 4.3	IAQDLEMYGVNYFEIK (10)	IGFPWSEIR (1)
Aminoacids: 583	Spectral counts: 11		
MW [kDa]: 68.5	Score: 614.6		
Calc. pI: 6.5			
Thymosin beta			
Accession: A6YPH1	∑ Coverage: 61.0	VHQNLISGVEGFDK (5)	NILPDPEAIEAEKGQQK (2)
Aminoacids: 169	Spectral counts: 15	ALLEGVEAFDTGK (2)	NPLPDKDAVLQEK (1)
MW [kDa]: 18.6	Score: 586.7	HTETQEKNPLPTK (1)	HTETQEKNPLPDKDAVLQEK (1)
Calc. pI: 5.8		NILPSAEDVATEK (1)	SQLEGFNHDNMKK (1)
		SQLEGFNHDNMK (1)	
DJ-1			
Accession: A6YPG8	∑ Coverage: 33.7	YSEDKVVIDGNLITSR (3)	GGVNVTLAGLK (1)
Aminoacids: 193	Spectral counts: 13	AHGIGLGKR (2)	DVVVVPDKSMEEAIK (2)
MW [kDa]: 20.3	Score: 449.3	GGVNVTLAGLKGNEPTK (2)	RGGVNVTLAGLKGNEPTK (1)
Calc. pI: 6.0		RGGVNVTLAGLK (1)	ELVDSYKYSEDKVVIDGNLITSR (1)

Protein originated from *T. infestans* or *G. gallus*. *T. infestans* proteins are underlined. Accession numbers were derived from Uniprot Protein Database (2011). Sequence coverage of the identified peptides is given as Σ Coverage. Significance of the search result is given as score.

Table S8.2.5: Mascot identification data of small intestines of unfed fifth instars of *T. infestans* for bacteriolytic active fractions (score 421.6 to 213.1) after chromatographic separation.

Protein/Characteristics		Peptide sequences	
Superoxide dismutase [Cu-Zn]			
Accession: A6YPT7	∑ Coverage: 31.1	GTVYFEQESPNAEVK (4)	LSGEVTGLQK (2)
Aminoacids: 154	Spectral counts: 11	TLVVHADPDDLGK (4)	EHGAPTDEIR (1)
MW [kDa]: 15.9	Score: 421.6		
Calc. pI: 6.2			
Cathepsin L-like proteinase			
Accession: Q67EP7	∑ Coverage: 10.7	GYVDIAQGDENALK (3)	NSWGPSWGENGYIK (2)
Aminoacids: 328	Spectral counts: 10	SVAGTDKGYVDIAQGDENALK (5)	
MW [kDa]: 36.5	Score: 421.2		
Calc. pI: 6.5			
Glycerol-3-phosphate dehydrogenase			
Accession: B4XU24	∑ Coverage: 18.3	LQGPITAEEVNYMLENK (4)	LTEIINTTHENVK (1)
Aminoacids: 355	Spectral counts: 10	LAEQFVITGK (1)	RLAEQFVITGK (1)
MW [kDa]: 39.0	Score: 419.7	VSIVGSGNWGSAIAK (2)	FPLFTAVNR (1)
Calc. pI: 6.2			
Stress-70 protein, mitochondrial			
Accession: Q5ZM98	∑ Coverage: 4.6	SQVFSTAADGQTQVEIK (3)	SDIGEVILVGGMTR (2)
Aminoacids: 675	Spectral counts: 5		
MW [kDa]: 73.1	Score: 389.2		
Calc. pI: 6.4			
Actin, cytoplasmic 1			
Accession: P60706	∑ Coverage: 15.2	DLYANTVLSGGTTmYPGIADR (3)	GYSFTTTAER (2)
Aminoacids: 375	Spectral counts: 8	SYELPDGQVITIGNER (2)	AGFAGDDAPR (1)
MW [kDa]: 41.7	Score: 375.2		
Calc. pI: 5.5			
Elongation factor 2			
Accession: Q90705	∑ Coverage: 4.2	AYLPVNESFGFTADLR (3)	SDPVVSYR (1)
Aminoacids: 858	Spectral counts: 5	NMSVIAHVDHGK (1)	
MW [kDa]: 95.3	Score: 370.0		
Calc. pI: 6.8			
Keratin, type II cytoskeletal cochleal			
Accession: O93532	∑ Coverage: 4.7	NLDLDSIIAEVK (4)	LALDIEIATYR (2)
Aminoacids: 492	Spectral counts: 6		
MW [kDa]: 53.8	Score: 319.0		
Calc. pI: 6.1			
Ca^{2+}-binding protein			
Accession: A6YPK2	∑ Coverage: 28.1	GTISFQDFGALWK (3)	LSTQTIDTIVAK (1)
Aminoacids: 178	Spectral counts: 8	LSTQTIDTIVAK (2)	DNSGNIDKGELSTALTTFGYR (1)
MW [kDa]: 20.5	Score: 302.6	GELSTALTTFGYR (1)	
Calc. pI: 5.6		SFDRDNSGNIDKGELSTALTTFGYR (1)	
Calponin			
Accession: A6YPG4	∑ Coverage: 32.6	KDIAQVTTTLFALGR (3)	EFTEEQLR (1)
Aminoacids: 184	Spectral counts: 8	EAQEWIETILGEK (1)	MMENINSFLK (1)
MW [kDa]: 20.3	Score: 279.9	AGESIIGLQAGSNK (2)	
Calc. pI: 7.8			
Salivary secreted protein			
Accession: A6YPI9	∑ Coverage: 45.7	VSEDVTYPVRPIPGR (1)	FNLTIFGR (2)
Aminoacids: 129	Spectral counts: 7	RPLITEIDAIDLDSNDKGGYAYVLK (3)	KGYNDVILFQK (1)
MW [kDa]: 14.6	Score: 276.7		
Calc. pI: 9.9			
Hemoglobin subunit alpha-D			
Accession: P02001	∑ Coverage: 22.0	AASHQEEFGAEALTR (2)	TYFPHFDLSPGSDQVR (1)
Aminoacids: 141	Spectral counts: 3		
MW [kDa]: 15.7	Score: 243.6		
Calc. pI: 7.6			
Polyubiquitin-B			
Accession: P0CG62	∑ Coverage: 49.8	IQDKEGIPPDQQR (2)	ESTLHLVLR (1)
Aminoacids: 305	Spectral counts: 4	TITLEVEPSDTIENVK (1)	
MW [kDa]: 34.3	Score: 213.1		
Calc. pI: 7.5			

Protein originated from *T. infestans* or *G. gallus*. *T. infestans* proteins are underlined. Accession numbers were derived from Uniprot Protein Database (2011). Sequence coverage of the identified peptides is given as Σ Coverage. Significance of the search result is given as score.

Table S8.2.6: Mascot identification data of small intestines of unfed fifth instars of *T. infestans* for bacteriolytic active fractions (score 209.9 to 85.3) after chromatographic separation.

Protein/Characteristics		Peptide sequences	
Actin-related protein 2			
Accession: P53488	∑ Coverage: 8.4	RLDIAGR (1)	ILLTEPPMNPTK (2)
Aminoacids: 394	Spectral counts: 4	GYAFNHSADFETVR (1)	
MW [kDa]: 44.7	Score: 209.9		
Calc. pI: 6.7			
Putative salivary secreted protein			
Accession: A6YPU2	∑ Coverage: 16.6	QVTWNTELVAGTTDQYK (1)	
Aminoacids: 175	Spectral counts: 5	NLFQDYLLAVDK (4)	
MW [kDa]: 19.9	Score: 209.4		
Calc. pI: 6.0			
Putative rab11			
Accession: A6YPR1	∑ Coverage: 15.9	GAVGALLVYDIAK (2)	STIGVEFATR (1)
Aminoacids: 214	Spectral counts: 4	AQIWDTAGQER (1)	
MW [kDa]: 24.3	Score: 166.8		
Calc. pI: 6.0			
Lipocalin-like Ti65			
Accession: A6YPR4	∑ Coverage: 17.8	NTGLVSSQLISR (2)	KEDEVISNLDTILK (1)
Aminoacids: 197	Spectral counts: 4	TDNYLVLQR (1)	
MW [kDa]: 21.6	Score: 152.1		
Calc. pI: 9.3			
Salivary lipocalin			
Accession: A6YPL3	∑ Coverage: 10.6	KEDDQISNLDK (1)	ITDNYLVLQR (1)
Aminoacids: 199	Spectral counts: 2		
MW [kDa]: 22.3	Score: 126.5		
Calc. pI: 9.1			
Actin-related protein Arp2/3 complex subunit ARPC3			
Accession: A6YPU0	∑ Coverage: 28.7	PAYHSSFLDYSQQVGNmAILPLR (1)	QYLQQIR (1)
Aminoacids: 178	Spectral counts: 3	GPAPTTDKDmDIIDEAIYYFK (1)	
MW [kDa]: 20.4	Score: 115.5		
Calc. pI: 8.4			
Trialysin			
Accession: Q8T0Z4	∑ Coverage: 16.1	TNIATYLVVAGEINR (1)	ISPQLFPGATSLDGDIVK (1)
Aminoacids: 205	Spectral counts: 2		
MW [kDa]: 22.2	Score: 113.1		
Calc. pI: 9.5			
Keratin, type I cytoskeletal 19			
Accession: O93256	∑ Coverage: 4.3	VLDELTLAR (1)	LASYLDKVR (1)
Aminoacids: 423	Spectral counts: 2		
MW [kDa]: 46.1	Score: 111.3		
Calc. pI: 5.1			
Ras-related protein Rab-5B			
Accession: Q5ZHW4	∑ Coverage: 11.6	TAMNVNDLFLAIAK (1)	LVLLGESAVGK (1)
Aminoacids: 215	Spectral counts: 2		
MW [kDa]: 23.6	Score: 109.4		
Calc. pI: 8.1			
Cathepsin B-like cysteine protease			
Accession: A2SZV7	∑ Coverage: 12.9	NGPIVASFLVYEDLFSYK (1)	IQAEILK (1)
Aminoacids: 333	Spectral counts: 3	EGVYQHVAGEFLGGHVIK (1)	
MW [kDa]: 36.4	Score: 107.7		
Calc. pI: 6.2			
Cytoplasmic aconitate hydratase			
Accession: Q90875	∑ Coverage: 3.2	AVLAESYER (1)	VILQDFTGVPAVVDFAAMR (1)
Aminoacids: 889	Spectral counts: 2		
MW [kDa]: 98.0	Score: 100.0		
Calc. pI: 7.3			
TiLys1			
Accession: Q7YZS5	∑ Coverage: 12.2	ELVAHGIPR (1)	AWYGWQNK (1)
Aminoacids: 139	Spectral counts: 2		
MW [kDa]: 15.6	Score: 85.3		
Calc. pI: 8.7			

Protein originated from *T. infestans* or *G. gallus*. *T. infestans* proteins are underlined. Accession numbers were derived from Uniprot Protein Database (2011). Sequence coverage of the identified peptides is given as Σ Coverage. Significance of the search result is given as score.

CHAPTER 9

APPENDIX

9. Appendix

9.1 Intestinal aspartate proteases TiCatD and TiCatD2 of the haematophagous bug *Triatoma infestans* (Reduviidae): sequence characterisation, expression pattern and characterisation of proteolytic activity

Carsten Balczun[$*], Janna Siemanowski[$], Jennifer Katharina Pausch[$], Stefan Helling[#], Katrin Marcus[#], Christian Stephan[#], Helmut E. Meyer[#], Tobias Schneider[$], Christian Cizmowski[$], Marina Oldenburg[$], Sandra Höhn[$], Christian Karl Meiser[$], Wolfgang Schuhmann[§] and Günter A. Schaub[$]

[$]Zoology/Parasitology Group, Ruhr-Universität, Bochum, Germany

[#]Medizinisches Proteom-Center, Ruhr-Universität, Bochum, Germany

[§]Analytische Chemie - Elektroanalytik and Sensorik, Ruhr-Universität, Bochum, Germany

Acknowledgements

The authors are grateful to Dr. Florian Leese and Dr. Christoph Mayer for assistance in the bioinformatics analysis and to Sandra Schmidt for excellent technical assistance. We thank Dr. Randy Cassada for correcting the English style. We appreciate the cooperation with Prof. Dr. H. Lübbert and Dr. R. Schulten in using the fluorescence reader. The *Triatoma infestans* photograph in the graphical abstract is courtesy of Dr. R. Pospischil.

9.1.1 Abstract

Two aspartate protease encoding complementary deoxyribonucleic acids (cDNA) were characterised from the small intestine (posterior midgut) of *Triatoma infestans* and the corresponding genes were named *TiCatD* and *TiCatD2*. The deduced 390 and 393 amino acid sequences of both enzymes contain two regions characteristic for cathepsin D proteases and the conserved catalytic aspartate residues forming the catalytic dyad, but only TiCatD2 possesses an entire C-terminal proline loop. The amino acid sequences of TiCatD and TiCatD2 show 51-58% similarity to other insect cathepsin D-like proteases and, respectively, 88 and 58% similarity to the aspartate protease ASP25 from *T. infestans* available in the GenBank database. In phylogenetic analysis, TiCatD and ASP25 clearly separate from cathepsin D-like sequences of other insects, TiCatD2 groups with cathepsin D-like proteases with proline loop. The activity of purified TiCatD and TiCatD2 was highest between pH 2 and 4, respectively, and hence, deviate from the pH values of the lumen of the small intestine, which varied in correlation with the time after feeding between pH 5.2 and 6.7 as determined by means of micro pH electrodes. Both cathepsins, TiCatD and TiCatD2, were purified from the lumen of the small intestine using pepstatin affinity chromatography and identified by nanoLC-ESI-MS/MS analysis as those encoded by the cDNAs. The proteolytic activity of the purified enzymes is highest at pH 3 and the respective genes are expressed in the both regions of the midgut, stomach (anterior midgut) and small intestine, not in the rectum, salivary glands, Malpighian tubules or haemocytes. The temporal expression pattern of both genes in the small intestine after feeding revealed a feeding dependent regulation for *TiCatD* but not for *TiCatD2*.

Key words: aspartate protease, cathepsin D, haematophagous bug, intestinal pH, *Triatoma infestans*

9.1.2 Introduction

All species of the triatomines are obligate haematophagous bugs, their postembryonic stages depending solely on this kind of nutrition. For the development into the next larval instar, a full engorgement of a multiple of the individual's original body weight is required (Schaub, 2008). The distensible stomach (anterior midgut) serves as a blood storing region where only concentration and partial lysis of the erythrocytes takes place (Azambuja et al., 1983). Blood is transferred in small portions to the small intestine (posterior midgut). According to ultrastructural data for *Rhodnius prolixus*, the anterior part of the small intestine is mainly digestive, whereas the posterior region is mainly absorptive (Billingsley and Downe, 1983, 1989; Kollien and Schaub, 2000). The small intestine of *Triatoma infestans* has a morphological subdivision into three regions of similar length with a clearly visible narrow middle region.

Blood sucking hemipteran insects exhibit adaptations of the digestive physiology different from those of other haematophagous insect orders. Unlike in dipterans or lice, the blood digestion in triatomines occurs over the course of several days (Lehane, 1991). In addition, mosquitoes and lice possess serine proteases while triatomines use cysteine and aspartate proteases (Lehane, 1994). The pH value of the midgut lumen of mosquitoes and lice is alkaline; the midgut lumen of triatomines is suggested to be acidic (Schaub, 2009). The acidic proteases cathepsin B and D, lysosomal carboxypeptidase and aminopeptidase have been characterised in the small intestine of *Rhodnius prolixus*, *Triatoma phyllosoma pallidipennis* and *T. infestans* by biochemical approaches using synthetic substrates and specific inhibitors (Garcia and Garcia, 1977; Houseman, 1978; Houseman and Downe, 1980, 1981a, b, 1983a; Kollien et al., 2004). Since the development of intestinal bacterial symbionts and *Trypanosoma cruzi*, the etiological agent of Chagas disease which is transmitted by reduviid bugs, is affected by the nutritional stage and availability of digestion products in the gut lumen (Kollien and Schaub, 2000; Schaub, 2009; Garcia et al., 2010), understanding the digestive mechanisms provides important insights into vector-parasite/microbe interactions.

So far, only a few genes from triatomines encoding acidic proteases have been characterised. A gene encoding a cathepsin L-like protease is exclusively expressed in the intestine of *R. prolixus* (the samples also contained hindgut tissue, but no stomach tissue) (Lopez-Ordoñez et al., 2001). The deduced protein sequence shares characteristic sequence motifs of cathepsin B and L, but the lack of an occluding loop characteristic for cathepsin B-like proteases (Sajid and McKerrow, 2002) clearly classifies this enzyme as a cathepsin L protease. Furthermore, two genes from *T. infestans* encoding a cathepsin B- and a cathepsin L-like

protease have been identified, and for the cathepsin B gene a midgut-specific expression was shown (Kollien et al., 2004). For cathepsin D, only an unpublished sequence from *T. infestans* denoted as aspartyl protease ASP25 is available in the NCBI database (accession number AY495371). Recently, the transcriptome of *R. prolixus* midgut was analysed and compared to a whole body library unrevealing a set of cathepsin B-, L- and D-like proteases-encoding transcripts specifically transcribed in the midgut (Ribeiro *et al*. unpublished).

The present study characterises for the first time the nucleotide sequences of genes encoding cathepsin D-like proteases from *T. infestans*, named *TiCatD* and *TiCatD2*. We have cloned the full-length cDNA sequences from the small intestine and studied the expression pattern of these genes. In addition, analysis of expressed sequences variants of the cathepsin D-like gene was conducted. Since the activities of proteases are suggested to be optimal at acidic pH values, the changes of pH of the stomach and small intestine after feeding were determined using microelectrodes. Furthermore, the enzymes were purified by chromatography, identified by means of mass spectrometry, and their activity profile was characterised.

9.1.3 Experimental procedures

9.1.3.1 Insect origin, maintenance and dissection

T. infestans used for biochemical analysis, pH measurement and quantitative PCR originated from Cachiyuyo, Chile. *T. infestans* used for DNA sequence analysis originated from Rio Caine, Bolivia, and Pampa del Indio, Province of Chaco, Argentina. Bugs were reared at 27±1°C and 60–70% relative humidity, with a 16/8-h light/dark cycle and were fed monthly on hens (Schaub, 1989; Kollien and Schaub, 1998).

For temporal quantitative expression analysis, fifth instars were fed 4 weeks after moulting (40 days after feeding of fourth instar larvae), and the small intestines of unfed insects and of larvae at 2, 3, 5, 10, 15 and 20 days after feeding were dissected. At each time point, three small intestines were pooled and immediately stored in liquid nitrogen until RNA isolation. Stomach and small intestine for comparison of tissue specific transcript levels were dissected out five days after feeding.

For protein isolation, five days after feeding the luminal contents of small intestines of batches of 200 and 140 fifth instars were collected by rinsing out five small intestines in 500 µl sodium citrate/sodium chloride buffer (0.1 M sodium citrate, 0.5 M NaCl, pH 3) on ice. The remaining tissues were collected in pools of 25 small intestines and homogenized in the

same buffer using a pestle. Remnants of tissues were removed by centrifugation for 10 min at 11,000 *g* and 4 °C to remove particles.

For pH measurement, the stomachs and small intestines of fifth instars were dissected at different time points after feeding (unfed, 1, 3, 5, 8, 10, 15 and 20 days after feeding). The tissues were placed on glass slides and the gut wall was penetrated by the electrodes. The pH values in the lumen of the stomach and the three regions of the small intestine were measured separately.

9.1.3.2 Nucleic acid techniques

Total RNA was isolated using the RNeasy Mini Kit (QIAGEN, Hilden, Germany) according to the manufacturer's protocol. RNA samples were incubated with 2 units DNase I (Fermentas, St. Leon-Rot, Germany) at 37°C for 1 h to remove traces of genomic DNA.

Oligonucleotides CathD1for1 (5´-TAGCTGCAGTGGGAATCATT-3´) and CathD1rev1 (5´-CTGTTCTATCTTCTACATTGA-3´) for amplification of partial cDNA of *TiCatD* were derived from the sequence of AY495371. Oligonucleotides 5CathD1TS2 (5´-ACCCTGCATGCAACGCTTGA-3´) and 3CathD1TS1 (5´-TCCTGCGATGATTTGGAT-3´) for 5´ and 3´RACE, respectively, were designed using the nucleotide sequence of the obtained cDNA fragment. An internal fragment of *TiCatD2* was amplified using degenerated oligonucleotides 221 (5`-GCNGCNAARTTYGAYGGNAT-3') and 194 (5'-SWWGTDCCWGTRTCWGCDAT-3'). From this cDNA fragment, oligonucleotide 250 (5´-TCGGAGGCTCAGATCCCGAGAAAT-3´) was derived for 3´RACE. An upstream fragment of *TiCatD2* was amplified with oligonucleotides 326 (5´-AAGGTCTTGCCGTTAACTATC-3´) and 560 (5´-ATGTTAGCACATACGCTG-3´); this was designed using the homologous transcript sequence of Rp-1760 from *Rhodnius prolixus* (Ribeiro *et al*. unpublished). A 5´RACE was conducted with oligonucleotide 563 (5´-ATATTTAAGTGTAAGTTG-3´).

Synthesis of cDNA with ThermoScript reverse transcriptase (Invitrogen, Karlsruhe, Germany) was performed following the manufacturer's recommendations using 2 µg total RNA as starting material. After synthesis of cDNA the RNA was removed by adding 5 units of RNase H (Fermentas) and incubating at 37 °C for 20 min. Synthesis of cDNA and poly(A) tailing of cDNA for RACE experiments were done with the 5´/3´ RACE Kit (Roche, Mannheim, Germany) according to the manufacturer's instructions. PCR with cDNA as template was carried out using 2 µl of cDNA solution as template, 0.6 µM of each oligonucleo-

tide, 2 mM $MgSO_4$, 0.16 mM of each dNTP and 1 unit *Pfu* polymerase (Fermentas) in a final volume of 50 µl. Cycling parameters for PCR with oligonucleotides CathD1for1 and CathD1rev1 were: 94 °C for 2 min for 1 cycle, followed by 35 cycles each at 94 °C for 1 min, 54 °C for 1 min, 72 °C for 1 min and a final extension at 72 °C for 10 min. Annealing temperatures for PCR with oligonucleotides 221 and 194 or 326 and 560 were 50 °C and 53 °C, respectively.

Quality control of cDNA synthesis was conducted by amplification of a fragment of the β-actin gene (Kollien *et al.*, 2004). PCR amplicons were separated on ethidium bromide stained 1% agarose gels and cloned into vector pGEM-T (Promega) for publication quality sequence analysis, i.e. each independent clone was sequenced three times.

Before quantitative PCR all RNA samples were checked for RNA integrity by using the Experion automated electrophoresis system (Biorad, München, Germany) with RNA standard sense chips. RNA samples were not heat denatured before electrophoresis due to the "hidden break" of most insect RNAs (Winnebeck et al., 2010), thus leading to misinterpretation of the RNA profile. Only RNA samples with an RQI value of 8.3 or higher were used for quantitative PCR.

Expression analysis was performed using the MESA GREEN One Step RTqPCR Mastermix for SYBR assay (Eurogentec, Seraing, Belgium) according to the manufacturer's recommendations in a StepOnePlus cycler (Applied Biosystems, Darmstadt, Germany) with oligonucleotides 404 (5´-AAACGGTTGCCCTGGTATTG-3´) and 405 (5´-TCATCGCAG GACACAAATCC-3´) for *TiCatD*, 406 (5´-GAGGCTCAGATCCCGAGAAA-3´) and 407 (5´-TGCAAAAGGTCTTGCCGTTA-3´) for *TiCatD2* or 469 (5´-GTATGTAGC GATCCAAGCTGTTCT-3´) and 470 (5´-CATAACCTTCATAGATGGGGACTG-3´) for β-actin. Each reaction was carried out in triplicates. As a control for successful deoxyribonuclease I treatment, each reverse transcription was carried out twice, with or without reverse transcriptase. Only samples in which the control without reverse transcriptase did not yield a PCR product were used for further quantification analysis. Real time PCR experiments were carried out with three independent samples, and primer efficiency was calculated with LinRegPCR (Ramakers et al., 2003). Amplicon size for each primer pair and sequence accuracy were verified by gel electrophoresis and sequencing. Mean Ct values (threshold cycles) were calculated from the triplicates and used for calculations of expression ratios according to Pfaffl (2001) with primer-specific efficiencies. The Ct values for the amplicons derived from the β-actin messenger RNA were used as reference for normalization. PCR conditions were as

follows: 50 °C for 10 min, 95 °C for 5 min, followed by 40 cycles at 95 °C for 10 s and at 60 °C for 30 s. After melting curve analysis, statistical analysis was carried out using the Relative Expression Software Tool (REST) (Pfaffl et al., 2002).

9.1.3.3 Sequence analysis

Sequence identity analyses of the cathepsin genes were performed using the BLASTX 2.2.17 program (Altschul et al., 1997) and comparing it with the GenBank database. Analysis for putative signal peptide cleavage sites was carried out with SignalP 3.0 (Bendtsen et al., 2004), and calculations of theoretical isoelectric points and molecular masses were conducted with WinPep (Henning, 2001) and ProtParam (Gasteiger et al., 2005). ClustalX 1.83 software (Thompson et al., 1997) was used for multiple sequence alignments, and alignments were displayed with GeneDoc (Nicholas et al., 1997) and refined manually. Phylogenetic reconstruction was conducted using MEGA version 4 (Tamura et al., 2007).

9.1.3.4 pH measurement of the midgut

Glass micropipettes derived from pulled borosilicate capillaries with a tip opening of about 10 to 30 µm were generated as previously described (Reddy et al., 2005; Etienne et al., 2007). The first 0.8 mm of the tips of the reference and measuring electrode were filled with agar and hydrogen ionophore I-cocktail A (Fluka, Buchs, Switzerland), respectively, and both electrodes were filled with internal electrolyte solution (10 mM 2-(N-morpholino)-ethanesulfonic acid (MES), 110 mM potassium chloride, 10 mM sodium chloride, pH 6.22) from the untapered end. Contact was achieved using a AgCl-coated silver wire (Etienne et al., 2007). The resulting pH electrode was calibrated using four different buffer solutions of pH 4.16, 5.14 (100 mM MES, 220 mM potassium chloride, 20 mM sodium chloride), pH 6.22 (10 mM MES, 110 mM potassium chloride, 10 mM sodium chloride) and pH 7.57 (10 mM 4-(2-hydroxyethyl)-1-piperazineethanesulfonic acid (HEPES), 110 mM potassium chloride, 10 mM sodium chloride) leading to a straight calibration line (Etienne et al., 2007).
Three groups with 5 insects per time point were analysed. Following each measurement the calibration of the electrode was verified using the above mentioned buffer solutions in order to exclude damage of the electrodes by penetrating the midgut walls.

9.1.3.5 Pepstatin affinity chromatography

One ml of pepstatin A agarose (Sigma-Aldrich, Steinheim, Germany) in a polypropylene column (Qiagen) was equilibrated to pH 3.0 by washing with 15 ml sodium citrate/sodium chloride buffer (0.1 M sodium citrate, 0.5 M NaCl, pH 3). Samples of small intestine contents were first centrifuged through a filter (0.2 µm pore size) to remove perturbing particles and then loaded on the column. The column was washed with 15 ml sodium citrate/sodium chloride buffer pH 3. Proteins were eluted using 15 ml sodium carbonate/sodium chloride buffer (0.1 M sodium carbonate, 0.5 M NaCl, pH 8.7) and collected in 2 ml fractions, which were concentrated by using spin filters (Inogen, Sprockhövel, Germany) with a 4 kDa molecular cut-off to 20 µl final volume. Samples were stored at -80 °C.

9.1.3.6 Sodium dodecyl sulphate polyacrylamide gel electrophoresis (SDS-PAGE)

Electrophoresis was performed according to Meiser *et al*. (2010). Gels consisted of a 12% acrylamide and bisacrylamide (T) resolving gel and a 4% T stacking gel.

9.1.3.7 Characterisation of proteolytic activity

The pH-optimum of cathepsin D proteases was determined in 100 µl final volume by assaying triplicates of 84 ng or 72 ng of independent protein samples of pooled fractions 1-3 after pepstatin affinity chromatography in Britton-Robinson buffer (Britton and Robinson, 1931) at pH 2, 3, 4, 5, 6 and 7 using 2.5 µM MOCAc-GKPILF~FRLK(Dnp)-D-R-NH2 (Calbiochem, Darmstadt, Germany) as fluorogenic substrate. Controls without enzymes and others with 10 µM Pepstatin A (Sigma) were included. Incubation was carried out in 96 well FLUOTRAC 600 microplates (Greiner Bio-One, Frickenhausen, Germany) for 15 min at 37 C. Reactions were stopped by adding 200 µl 200 mM phosphate-sodium buffer pH 7 and fluorescence was determined immediately in a Mithras LB940 microplate reader (Berthold, Volvoorde, Belgium) with 340 nm excitation and 430 nm emission. The relative activity was determined as percentage of the highest activity over the examined pH range.

9.1.3.8 Enzymatic digestion of protein bands and nanoLC-ESI-MS/MS analysis

In-gel digestion of protein bands was performed according to Meiser *et al.* (2010) using porcine sequencing grade modified trypsin (trypsin NB sequencing grade, Serva Electrophoresis, Heidelberg, Germany). The nano liquid chromatography-electrospray ionization-MS/MS analyses were done using the Famos™, Switchos™, Ultimate™ HPLC-system (all Dionex LC Packings, Idstein, Germany) online coupled to the 4000 QTrap® (Applied Biosystems). Peptides were first separated by reversed phase nanoLC on a 75 µm inner diameter x 250 mm C18 PepMap column (Dionex LC Packings) with pre-concentration for 6 min with 0.1% TFA on a µ-precolumn (300 µm inner diameter x 1 mm, C18 PepMap, Dionex LC Packings). For peptide separation a solvent system consisting of 0.1% (v/v) formic acid (FA) (solvent A) and 0.1% (v/v) FA, 84% (v/v) ACN (solvent B) was used. The gradient was 4% to 48% solvent B in 30 min, 48% to 95% solvent B in 10 min, held at 95% solvent B for 5 min before the column was conditioned for the next run for 18 min with 4% solvent B. The ion trap mass spectrometer was equipped with a nano-electrospray ion source and distal-coated SilicaTips™ (FS360–20-10-N-20; New Objective Inc., Woburn, MA). The peptides were analysed in the positive mode after ionization with 3.3 to 3.8 kV source voltage. MS experiments were combined with subsequent MS/MS experiments in IDA mode (information dependent acquisition) including an "Enhanced MS" scan in the range of 100-1400 m/z and a scan rate of 4000 amu/sec, followed by an "Enhanced Resolution" scan with 250 amu/sec to examine the precursor ion charge state and three "Enhanced Product Ion" scans with 4000 amu/sec in a range of 100-1750 m/z. The three most abundant singly to triply charged precursor ions of a MS scan were selected by the MS control software (Analyst 1.5, Applied Biosystems) for CID-MS/MS (collision induced dissociation-MS/MS) experiments with active exclusion for 2 min after the acquisition of three spectra. Additionally, the experiments included a dynamic fill time for the linear ion trap without prior precursor ion trapping in the first quadrupole (Q0).

9.1.3.9 MS data analysis

All experimental data were stored in the Proteinscape 1.3 database (Bruker Daltonic) (Chamrad et al., 2003; Blüggel et al., 2004). For protein identification the MS output files (mgf-format) were generated with the Analyst 1.5 software. These data sets were compared using the Mascot® V. 2.2 search algorithm and the in-house *Triatoma*-Yeast protein sequence

database, composed of expressed sequence tags of a unidirectionally cloned salivary gland cDNA library from *T. infestans* (Assumpção et al., 2008), combined for statistical reasons to the yeast protein sub-database of the NCBI database (TaxID 4932, 07/05/2007). For checking purposes, additional searches using the whole NCBInr decoy database (2007.11.09; 6340306 sequences) were done. The following search parameters were selected: peptide mass accuracy of 0.6 Da (mono-isotopic), fragment mass accuracy of 1.2 Da (mono-isotopic), variable modification oxidation of methionine, propionamide modification of cysteine, maximally two missed cleavage sites. For positive protein identification a minimum of two unique peptides, adequately explained by additional manual interpretation of the respective fragment ion spectra and by theoretical fragmentation with the MS Product software tool, were required corresponding to at least 5% 315 sequence coverage of the respective protein.

9.1.4 Results

9.1.4.1 Characterisation of the cathepsin D-like protease cDNA*s*

Reverse transcription PCR (RT-PCR) with total RNA isolated from small intestine of *T. infestans* originating from Bolivia as template and subsequent rapid amplification of cDNA ends (RACE) experiments resulted in the identification of a cDNA with 1579 nucleotides. The nucleotide sequence was deposited in the GenBank under accession number GQ871498. The open reading frame consists of 1173 nucleotides flanked by 26 nucleotides untranslated region (UTR) at the 5´end and 380 nucleotides UTR at the 3´end. A putative polyadenylation signal AATAAA is located in the 3´UTR 362 nucleotides downstream of the stop codon. According to the amplification of the entire open reading frame with genomic DNA as template, we conclude no intron is present in this gene. The open reading frame encodes a deduced protein of 390 amino acids with similarities to cathepsin D-like proteases, possessing a predicted molecular mass of 43 kDa and an isoelectric point of 4.87 and named TiCatD. The putative signal peptide is cleaved between C19 and H20 (Fig. 9.1.1). Given similar processing of the activation peptide compared to the bovine cathepsin D at K57, the calculated molecular mass of the mature enzyme is about 36.5 kDa and the theoretical isoelectric point about 4.42.

Using RT-PCR and RACE, a cDNA with 1404 nucleotides encoding an open reading frame of 1182 nucleotides of another cathepsin D-like protease, named *TiCatD2*, was identified (Fig. 9.1.1). The coding sequence is flanked by 17 and 205 nucleotides of 5´UTR and 3´UTR, respectively. The open reading frame encodes a protein of 393 amino acids, resulting

in a predicted molecular mass of 42.5 kDa and an isoelectric point of 5.35. The putative signal peptide is cleaved between G18 and S19 and the putative mature enzyme begins with G59, resulting in a protein with a molecular mass of 36.2 kDa and a deduced isoelectric point of 5.19.

Two conserved regions (V86IFDTGSSNLWIPSA100 and I275ADTGTS281, TiCatD numbering) characteristic for cathepsin D proteases are present in TiCatD and TiCatD2, both containing an aspartate residue including the catalytic active dyad (Fig. 9.1.1). Furthermore, the deduced sequences contain a conserved tyrosine residue involved in substrate interaction as well as six conserved cysteine residues presumably forming disulphide bridges.

The protein sequences of TiCatD and TiCatD2 show, respectively, 51-58% and 58-96% similarity with cathepsin D-like proteases from other insects, and 88% and 58% similarity with ASP25 (AAS72876) from *T. infestans*, respectively (Fig. 9.1.1). A striking difference occurs in the so-called “proline loop” with the consensus sequence DxPxPx(G/A)P. The two proteases ppCAD2 and ppCAD3 from *Musca domestica* are lacking this characteristic motif. TiCatD and ASP25 do not contain the entire proline loop, but two of the three conserved proline residues are present.

Phylogenetic analysis with sequences of cathepsin D-like proteases from different insect orders revealed the formation of three distinct groups, each supported by high bootstrap values (Fig. 9.1.2). Within the cladogram, *T. infestans* sequences ASP25 and TiCatD clearly separate from the group of all other potentially lysosomal cathepsin D-like sequences including TiCatD2 and the coleopteran enzymes suggested being active in the gut lumen, which all possess the proline loop. The third clade contains the cathepsins ppCAD2 and ppCAD3 from *M. domestica* with supposed digestive function which are lacking the proline loop like the *T. infestans* cathepsins ASP25 and TiCatD.

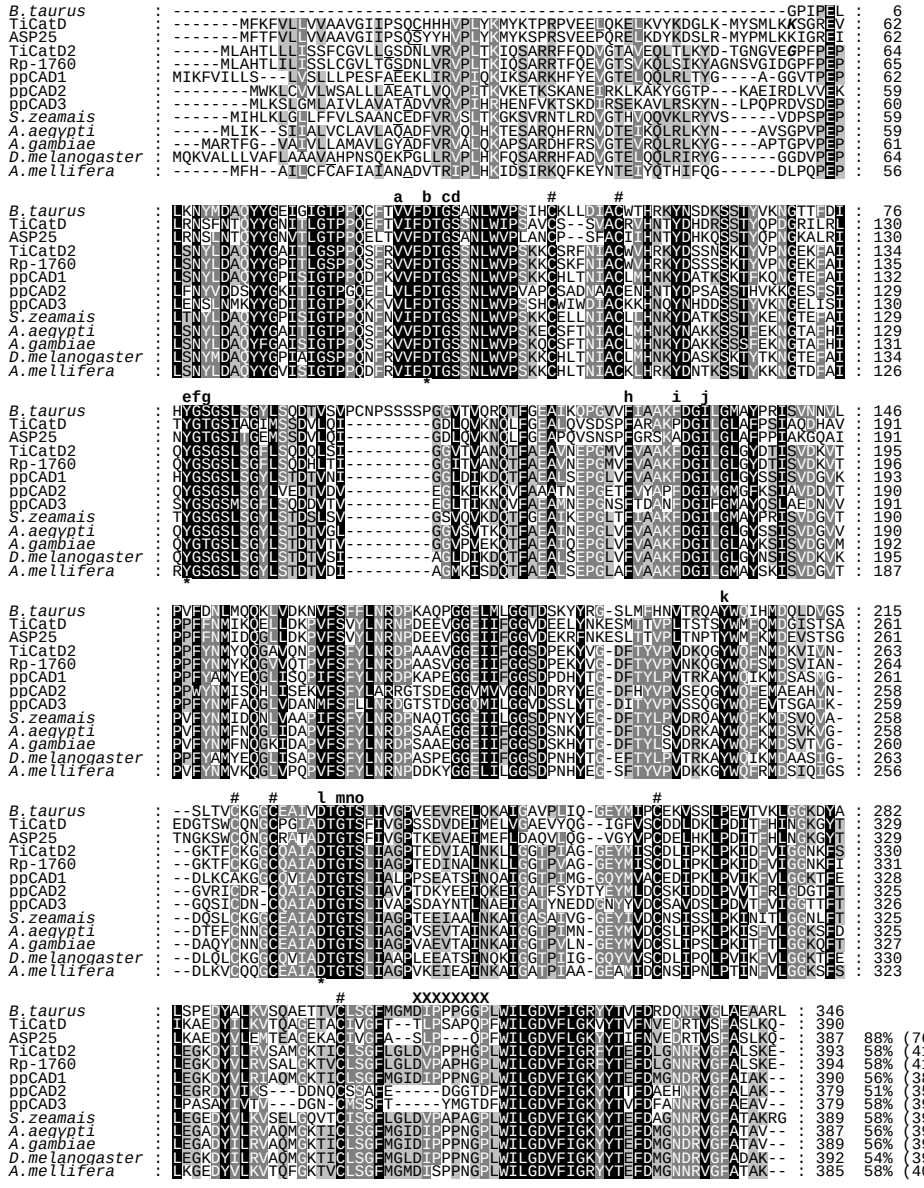

Figure 9.1.1: Multiple sequence alignment of cathepsin D-like proteases of different insects and bovine cathepsin D.

The last amino acid residues of the putative signal peptides as predicted by SignalP 3.0 are underlined and the putative processing sites of the activation peptides in TiCatD and TiCatD2 are in bold and italic. Conserved cysteine residues forming disulfide bonds are marked (#). Conserved residues that form the substrate binding pockets and the catalytic residues are indicated by small letters (a-o) above the sequence. Catalytic aspartate residues and the tyrosine residue which controls substrate specificity are additionally marked with asterisk below the sequence. The proline loop is indicated by "X" above the sequence. Identical amino acid residues are black shaded. Percentages display similarities and identities (in brackets) to TiCatD. The following sequences were used for comparison: *Bos taurus* (**AAB26186.1**); *Aedes aegypti* (**EAT42285**); *Anopheles gambiae* (**EAA03535**); *Drosophila melanogaster* (**AAF23824**); *Apis mellifera* (**XP_392857**); *Triatoma infestans* aspartyl protease (ASP25; **AAS72876**); *Musca domestica* ppCAD1 (**ABM69086**), ppCAD2 (**ABM69085**) and ppCAD3 (**ABL84270**); *Sitophilus zeamais* (**BAH24176**). The nucleotide sequence of TiCatD was deposited in the GenBank under accession number **GQ871498**.

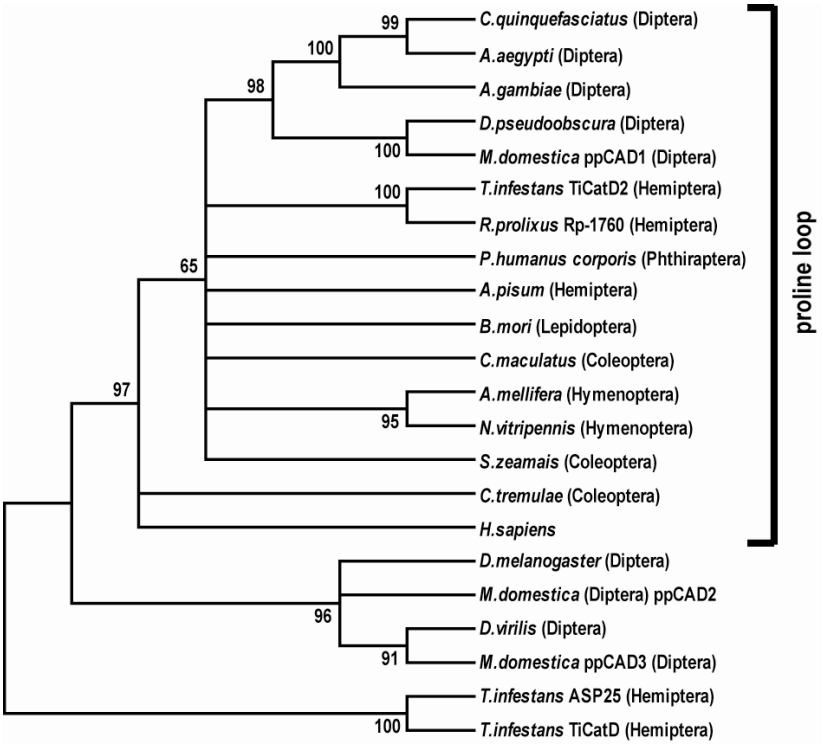

Figure 9.1.2: Neighbor-Joining tree of cathepsin D-like proteases of different insects deposited in GenBank.
The following sequences were used for phylogenetic reconstruction: *T. infestans* ASP25 (**AAS72876**); *Callosobruchus maculatus* (**ACO56332**); *Pediculus humanus corporis* (**XP_002427417**); *Apis mellifera* (**XP_392857**); *Sitophilus zeamais* (**BAH24176**); *Nasonia vitripennis* (**XP_001600543**); *Culex quinquefasciatus* (**XP_001867326**); *Chrysomela tremulae* (**ACP18833**); *Bombyx mori* (**NP_001037351**); *Aedes aegypti* (**EAT42285**); *Anopheles gambiae* (**EAA03535**); *Drosophila melanogaster* (**NP_609458**); *Drosophila pseudoobscura* (**XP_001360320**); *Acyrthosiphon pisum* (**NP_001153867**); *Drosophila virilis* (**XP_002058248**), *Musca domestica* ppCAD1 (**ABM69086**), ppCAD2 (**ABM69085**) and ppCAD3 (**ABL84270**), *Homo sapiens* (**AAP36305**), TiCatD (**GQ871498**), *Rhodnius prolixus* (**Rp-1760**, Ribeiro *et al*., unpublished). Numbers on branches represent bootstrap support (1000 replicates). The scale bar represents numbers of substitutions.

For the identification of putative genomic variation of *TiCatD* within a *T. infestans* population originating from Argentina, total RNA was isolated from the midguts of ten fifth instar larvae (specimens I to X) and used as template for PCR with oligonucleotides CathD1for1 and CathD1rev1. The cDNAs of three independent clones per specimen were sequenced, and deduced amino acid sequences including those from Bolivia (*TiCatD*) were compared (Fig. S1 in the supplement). The sequences of specimens I to X separate from TiCatD from the Bolivian strain and ASP25 by concordant substitutions at seven positions, one of these being located in the conserved region containing the first catalytic aspartate residue (Fig. S1). In contrast, the deduced amino acid sequences of TiCatD from the Bolivian strain and ASP25 possessed a significantly higher divergence, with the highest divergence for

ASP25. None of the conserved catalytic or substrate binding pocket-forming residues of bovine cathepsin D are changed, but some substitutions are in close vicinity to these conserved residues: V88, A238 and S239 (TiCatD numbering Fig. S1).

9.1.4.2 Molecular masses and characteristics of purified TiCatD and TiCatD2

In reducing SDS-PAGE of fractions obtained by pepstatin affinity chromatography, in fraction 1 only faint bands of about 39 and 28 kDa molecular mass were found, both much stronger in fraction 2 (Fig. 9.1.3). In fraction 3 the 28 kDa band was more prominent. The reduced intensity of the bands in this molecular range due to a reduced amount of protein in fraction 3 clearly demonstrated the existence of a double band at 28 and 39 kDa. To verify the luminal origin of the purified proteins, pepstatin affinity chromatography was also applied to samples derived from the homogenized small intestine tissues without the luminal contents. SDS-PAGE of chromatography fractions did not yield visible bands on the Coomassie stained gel (data not shown).

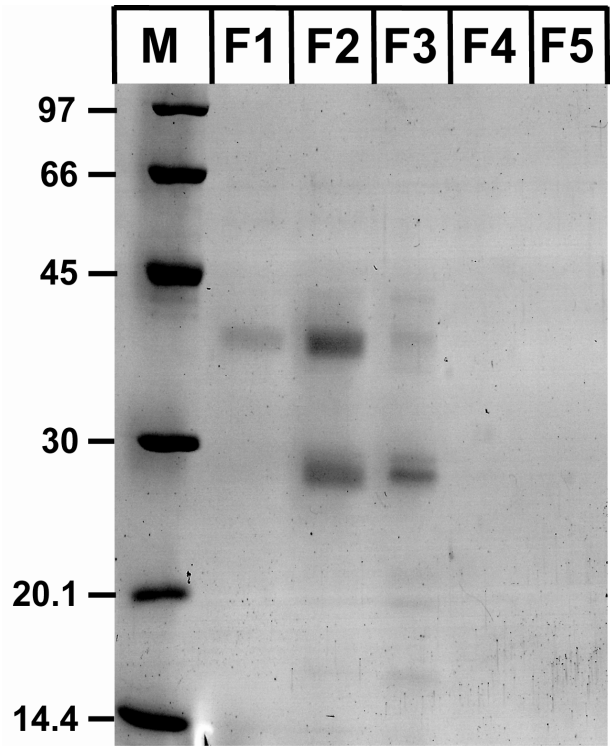

Figure 9.1.3: Reducing SDS-PAGE after Coomassie staining of pepstatin affinity chromatography purified fractions F1 – F5 and marker proteins (M). Molecular masses of marker proteins are indicated in kDa.

Nano liquid chromatography-electrospray ionization-MS/MS analyses of the proteins both from the 39 and 28 kDa bands of one separation and from the upper and lower bands of the respective double bands of about 39 and 28 kDa of another separation in SDS-PAGE resulted in the definite identification of peptides of TiCatD and TiCatD2 from all bands (Fig. 9.1.4 and Fig. S2 in the supplement). Peptides were aligned to sequences of TiCatD and TiCatD2 and covered about 28% and 25% of the deduced mature protein sequences of TiCatD and TiCatD2, respectively (Fig. S2).

The proteolytic activity of purified aspartate proteases TiCatD and TiCatD2 of fractions 1-3 after pepstatin affinity chromatography was highest at acidic pH between pH 2 and 4 with a maximum at pH 3 (Fig. 9.1.5). The activity was strongly decreased at pH 5 and almost disappeared at pH 6.

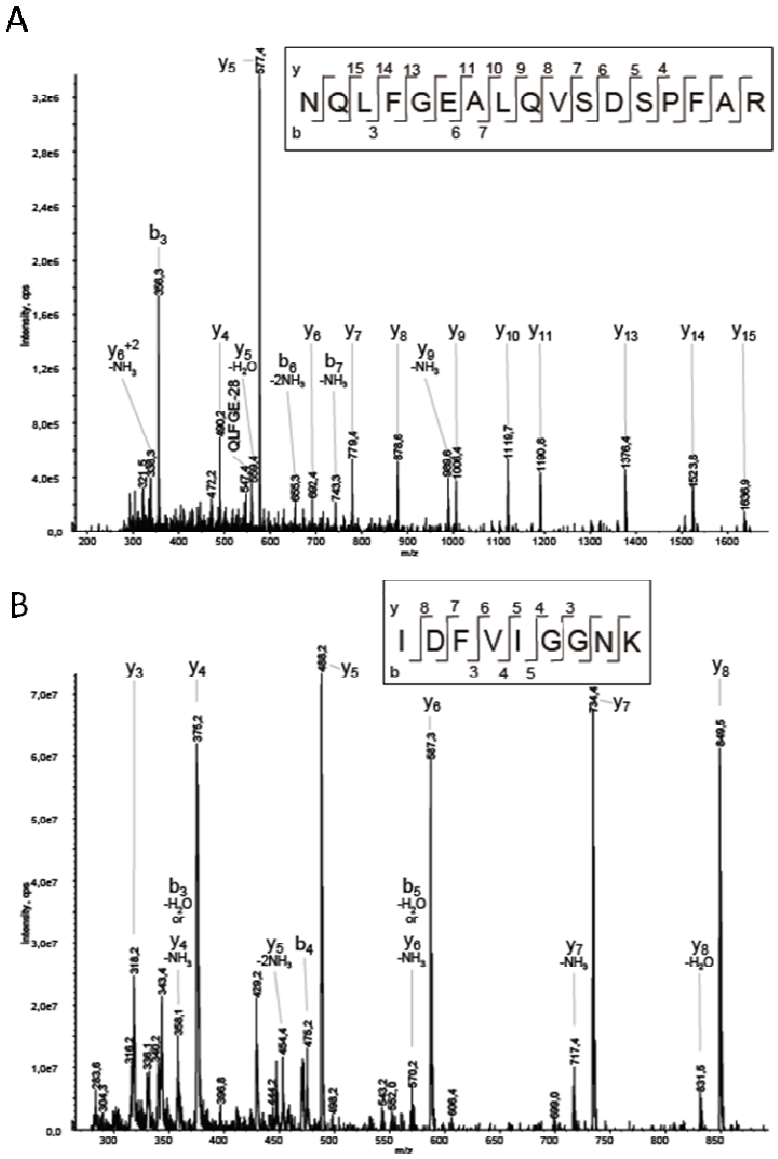

Figure 9.1.4: NanoLC-ESI-MS/MS analysis of pepstatin affinity chromatography purified *T. infestans* proteins. MS/MS spectra are shown for the unique peptides of the identified proteins TiCatD (A): NQLFGEALQVSDSPFAR with the doubly charged precursor ion (m/z 940.02) from the 28 kDa band in Fig. 3 and TiCatD2 (B): IDFVIGGNK with the doubly charged precursor ion (m/z 481.76) from the 39 kDa band in Fig. 3. The peptide sequence explaining C-terminal y-ions and N-terminal b-fragment ions are highlighted in the spectra and at the amino acid sequence.

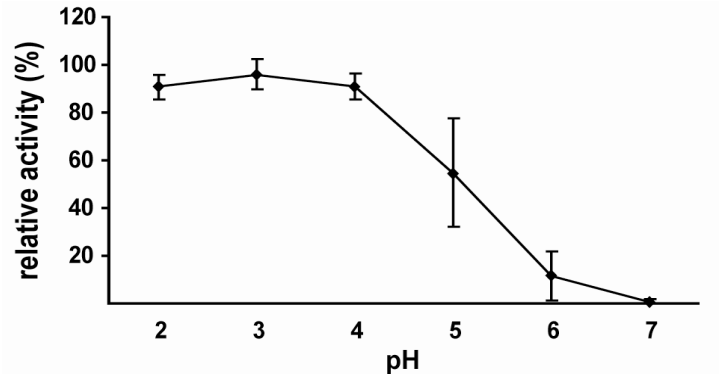

Figure 9.1.5: Proteolytic activity of purified cathepsin D-like proteases.
The relative activity is expressed as percentage of the highest activity over the examined pH range. Data are mean activities ± SD of triplicates of two independent protein samples.

9.1.4.3 pH profile of the midgut

In unfed fifth instar larvae, the pH values of the contents of the stomach and the three regions of the small intestine, which were of similar length, were about 6.3 for the stomach and posterior region of the small intestine and 6.7 and 6.6 for the anterior and middle region of the small intestine, respectively (Fig. 9.1.6). Immediately after feeding the pH value of the stomach contents significantly increased up to 7.4 (Student's t-test $P < 0.001$). The pH of the anterior small intestine contents decreased immediately after feeding ($P < 0.05$) while the contents of the middle and posterior small intestine contents increased ($P < 0.05$). One day after feeding the pH of the stomach contents approached the initial value. The pH of stomach and small intestine contents steadily and significantly decreased to minimum values of about pH 5.2 at eight and ten days after feeding. Following fifteen days after feeding the pH values of stomach and small intestine contents increased, but at 20 days after feeding they were considerably below the values of unfed insects.

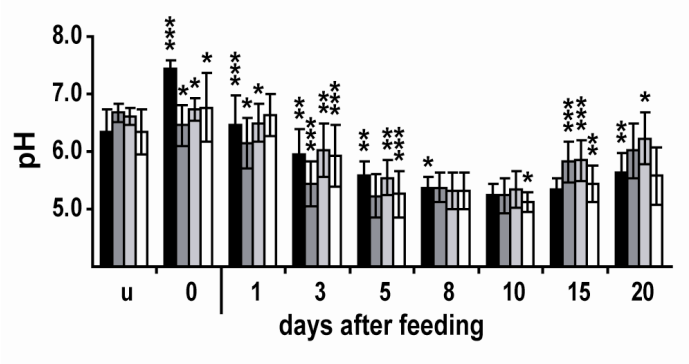

Figure 9.1.6: pH profile of *T. infestans* stomach and midgut regions at different days after feeding.
Data are means ± SD (n = 3 groups of five insects) of pH-values of unfed (u) fifth instar larvae, larvae immediately after feeding (0) and at different days after feeding. Black bars = stomach; dark grey, light grey and white bars = anterior, middle and posterior regions of the small intestine, respectively. Data significantly different with time after feeding are indicated by * ($P \leq 0.05$), ** ($P \leq 0.01$) and *** ($P \leq 0.001$).

9.1.4.4 Tissue-specific expression of the cathepsin D-like protease genes TiCatD and TiCatD2

In order to analyse the tissue specific expression of *TiCatD and TiCatD2*, reverse transcription PCR (RT-PCR) was performed with cDNAs derived from different tissues. Amplification of the open reading frame revealed that *TiCatD* as well as *TiCatD2* were specifically expressed in the small intestine and the stomach of *T. infestans*, and not in the salivary glands, the rectum, haemocytes or Malpighian tubules (Fig. 9.1.7). Negative controls with DNase I treated RNA samples as template verified the absence of genomic DNA in the PCR. In addition, RT-PCR with β-actin specific primers demonstrated successful cDNA synthesis. Sequencing of the amplicons derived from the stomach and small intestine confirmed total nucleotide sequence identity for both genes. Analysis of the expression ratio of *TiCatD* in the small intestine compared to the stomach by quantitative PCR revealed an essentially equal transcript level in both tissues (ratio 0.84±0.33; $P = 0.429$) while expression of *TiCatD2* was about twofold higher in the small intestine (ratio 1.95±0.42; $P \leq 0.001$).

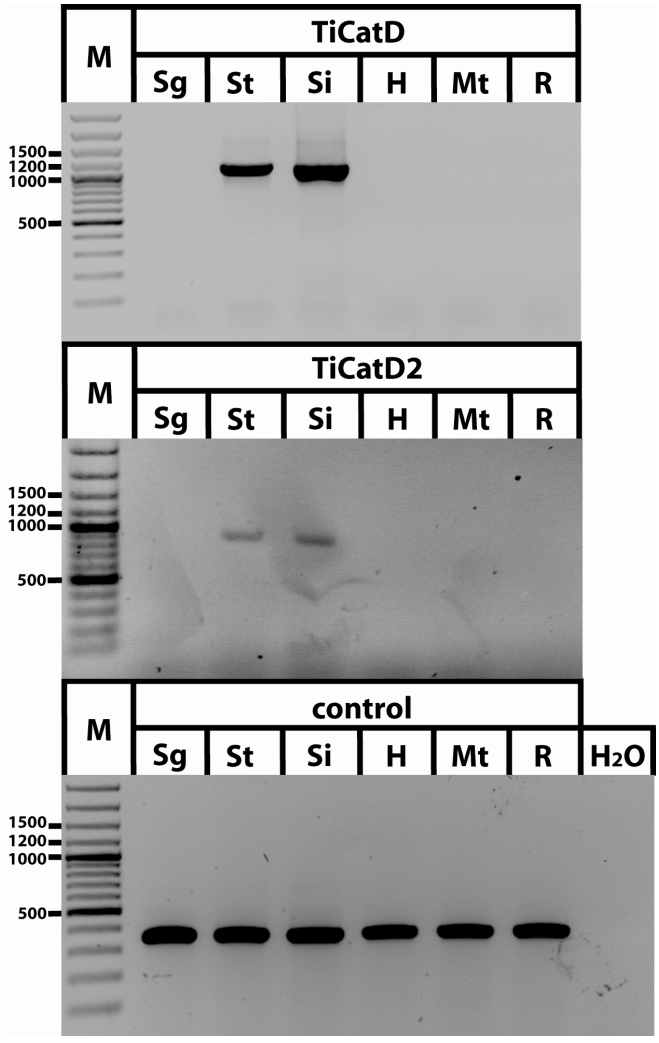

Figure 9.1.7: Tissue specific expression of *TiCatD* and *TiCatD2* in *T. infestans*.
PCR was carried out with cDNA derived from salivary glands (Sg), stomach (St), small intestine (Si), haemocytes (H), Malpighian tubules (Mt) and rectum (R) as template, and water (H_2O) as control using oligonucleotides specific for *TiCatD*, *TiCatD2* or β-actin (control). Fragment sizes of DNA marker molecules (M) in base pairs are given at the left margin.

9.1.4.5 Temporal expression profile of *TiCatD* and *TiCatD2*

For digestive proteases expression of *TiCatD* and *TiCatD2* is expected to depend on feeding. In quantitative PCR with RNA templates derived from small intestine at different time points after feeding the *TiCatD* transcript level was 12 times higher at two days after feeding ($P < 0.002$) compared to unfed insects (Fig. 9.1.8). The induction steadily declined to 2.8 fold more mRNA at 20 days after feeding ($P = 0.006$) with a single increase to 5.8 fold at 15 days after feeding ($P = 0.002$). The transcript level of *TiCatD2* compared to unfed insects was only significantly induced 2 fold and 3.1 fold at 10 days ($P = 0.03$) and 20 days ($P = 0.005$) after feeding, respectively.

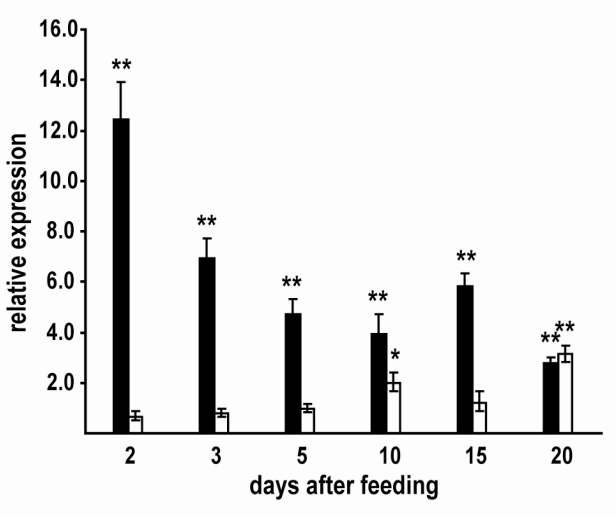

Figure 9.1.8: Temporal expression of *TiCatD* and *TiCatD2* in the small intestine.

Differences in expression levels of *TiCatD* (black bars) and *TiCatD2* (white bars) at different days after feeding are given as mean ratios and standard deviations ($n = 3$) referring to the amount of transcripts of unfed insects. Significance of transcript increase after feeding is indicated above bars by * ($P \leq 0.05$) and ** ($P \leq 0.01$).

9.1.5 Discussion

Insects possess many different proteases; the majority uses serine proteases as primary digestive proteases (Terra, 1990; Waniek et al., 2005), and cysteine and aspartate proteases (cathepsins B, D, H, L) as intracellular lysosomal enzymes (Medina and Vallejo, 1989; Cho et al., 1999). Only in some Coleoptera and cyclorrhaphous Diptera the digestive part of the midgut possesses an acidic pH of 5.4-6.9 and 3.1-6.8, respectively (Terra and Ferreira, 1994). In these insects, cysteine and aspartate proteases are secreted into the lumen of the midgut as major digestive enzymes (Thie and Houseman, 1990; Cristofoletti et al., 2005; Padilha et al., 2009). In the triatomine *Rhodnius prolixus*, according to pH determinations via pH indicators the pH value alternates feeding-dependently between 5.5 and 7.4 (J. M. C. Ribeiro and E. S. Garcia, personal communication). Therefore, also triatomines use those cathepsins as digestive proteases (Terra et al., 1988; 1996).

The cysteine proteases of triatomines possess an activity optimum at pH 5–5.5 according to measurements using artificial substrates and hemoglobin (Houseman, 1978; Terra et al., 1988; Kollien et al., 2004), and are therefore well adapted to the pH value of the small intestine lumen. However, the cathepsin D-like protease in the small intestine of *R. prolixus* has its activity maximum at pH 2.8 (Houseman and Downe, 1982, 1983b) and the purified proteases TiCatD and TiCatD2 at pH 3. A quantitative approach identified cathepsin B as the major midgut protease of *R. prolixus* with 85% of the total protease activity at pH 5.5, whereas cathepsin D possessed 15% of the total protease activity at this pH (Terra et al., 1988).

In the present investigation pH values of the stomach and small intestine of the triatomine *T. infestans* have been precisely determined for the first time using micro electrodes. The pH values of the stomach and small intestine of unfed bugs are about 6.3 or 6.6, respectively, and first decrease to the minimum of pH 5.2 at eight days after feeding. Until 20 days after feeding the pH values increase steadily. For Hemiptera, only few data of the pH of midgut contents are available. Adults of *Lygus disponsi* and *Dysdercus peruvianus* have pH values of 4.8-5.2 and 5.4-6.4 in the different regions of the midgut as determined using pH indicator solutions (Khan and Ford, 1967; Hori, 1971; Silva and Terra, 1994). However, changes of pH values in the course of the digestion of the diet have never been determined.

So far, only cDNA sequences of cathepsin B and L have been characterised from triatomines. The genes of the cysteine proteases cathepsin B and cathepsin L are both expressed in the gut of *T. infestans*, but the cathepsin B gene seemed not to be regulated by

feeding (Kollien et al., 2004). The cathepsin L-like gene from *R. prolixus* is suggested to be expressed exclusively in the intestine of the 1st to 4th larval instars (surprisingly not in the 5th) and showed high transcript levels immediately after feeding until fifteen days after feeding (Lopez-Ordoñez et al., 2001).

In the present investigation, we have characterised for the first time the nucleotide sequences of cathepsin D-like protease genes from a triatomine, *T. infestans*. The deduced amino acid sequences show a high similarity with cathepsin D sequences of other insects and *Ixodus ricinus*, and are with about 43 kDa also congruent with the molecular mass of these enzymes (Terra et al., 1988; Cho et al., 1991; Cho and Raikhel, 1992; Rabossi et al., 2004; Gui et al., 2006; Sojka et al., 2008), except for the cathepsin D from *Tribolium castaneum* in which the molecular mass at 22 kDa is apparently smaller. The cathepsin D-like proteases from *A. aegypti* and *R. prolixus* have first been detected as native enzymes with molecular masses of 80 and 88 kDa, respectively, which seem to be homodimers respectively composed of two 40 and two 44 kDa subunits (Terra et al., 1988; Cho and Raikhel, 1992).

The putative signal peptides of the insect cathepsin D-like proteases which have been predicted by SignalP 3.0 are similar in length to those of the deduced enzymes of *T. infestans*. The GenBank entries of cathepsin D from *A. aegypti*, *Anopheles gambiae* and *Drosophila melanogaster* denote propeptides of 29 to 31 amino acids length predicted by sequence similarity following the signal peptide. Such propeptides are proteolytically cleaved upon arrival at the lysosomes to yield the mature active enzymes (Neurath, 1991; Dunn, 2002). The cathepsin D-like proteases of *T. infestans* possess an activation peptide similar in length compared to the other insect protease sequences. Cysteine residues presumably forming disulphide bridges are present at conserved positions in the alignment with cathepsin D-like proteases. Like other cathepsin D-like proteases the enzymes from *T. infestans* contain two conserved regions, one each in an N- and a C-terminal domain, including the catalytic aspartate residues (Davies, 1990). In addition, cathepsin D belongs to the peptidase family A1 (pepsin family), whose members all have a conserved tyrosine residue which controls substrate specificity (Park et al., 1996; Hong and Tang, 2004; James, 2004); this residue is also present in the *T. infestans* enzymes.

The analysis of 29 individual protein sequences of *T. infestans* from Argentina revealed clustering into two groups presumably representing the different allelic gene loci of *TiCatD*. Exhibiting complete sequence identity, ten sequences belong to allele 1 and fourteen to allele 2. The sequence divergence between the Argentinean and Bolivian population might reflect the different geographical origin of the populations.

TiCatD and *TiCatD2* are exclusively expressed in the stomach and small intestine, *TiCatD* with a comparable transcript level while the expression level of *TiCatD2* is higher in the small intestine. Expression of *TiCatD* is strongly induced after feeding and is still upregulated 20 days after feeding, whereas *TiCatD2* is only upregulated at 10 and 20 days after feeding. In *R. prolixus* no cathepsin D activity was measured in the stomach and rectum (Borges et al., 2006), although analysis of cDNA libraries derived from different tissues of *R. prolixus* have revealed the expression of various aspartate proteases also in the stomach and rectum (Ribeiro, *et al*., unpublished). In *T. infestans*, only a slight cathepsin D activity occurred in the stomach wall after depletion of stomach contents (Gajewski and Schaub, unpublished). It is suggested that only lysis of erythrocytes takes place in the stomach of triatomines (Azambuja et al., 1983). A careful analysis of cathepsin D activity of stomach contents is necessary to elucidate if the blood proteins are not processed in the stomach of triatomines, either by cathepsin D or cathepsins B and L. It is discussed for the gut of the cowpea bruchid *Callosobruchus maculatus* and the tick *Ixodes ricinus* that peptidases with different characteristics form functional networks (Sojka *et al.*, 2008; Ahn & Zhu-Salzman, 2009). In this regard, the aspartate protease from *C. maculatus* is believed to act as a digestive protease as well as triggering the trans-activation of the major digestive cysteine proteases in the gut lumen (Ahn & Zhu-Salzman, 2009). Whether or not such functional networks of proteases also exist in triatomines remains to be elucidated. For *TiCatD*, the feeding dependent induction of gene expression suggests a direct involvement in digestion. In contrast, the expression of *TiCatD2* is only slightly affected by feeding and, thus, this protease might play a role in regulating processes.

The two cathepsin D proteases TiCatD and ASP25 from *T. infestans* evidently split into a separate branch from the sequences of the other insect orders and *H. sapiens* in the cladogram. TiCatD does not contain the entire proline loop but the remaining sequence might result in a similar structure. However, this difference is apparently sufficient to branch TiCatD far from all protein sequences containing this motif in the cladogram. The proline loop was suggested to be a motif found in lysosomal cathepsin D-like enzymes which are not secreted into the lumen of the digestive tract (Padilha *et al*., 2009). Enzymes which are lacking this motif like ppCAD3 from *M. domestica* are therefore luminal digestive enzymes. However, the proteases TiCatD and TiCatD2 were both purified from the luminal content of the small intestine. Therefore, this is the first characterisation of proline loop containing proteases from the lumen of the small intestine of a triatomine. Contamination of the samples with traces of tissue of the small intestine or cell contents due to cell renewal and cell rupture during dissection cannot be

excluded, but processing of the small intestine tissues depleted of the luminal content did not yield visible bands on the Coomassie stained SDS gels after affinity chromatography with pepstatin agarose. Therefore, despite having the proline loop TiCatD2 is a luminal protease in *T. infestans* indicating a unique adaptation of blood sucking triatomines.

Using affinity chromatography with pepstatin agarose, a well established technique to purify cathepsin D and other aspartate proteases in a single-step procedure (Conner, 1989; Geier et al., 1999), distinct forms of TiCatD and TiCatD2 have been identified after reducing SDS-PAGE. By using a strong acidic buffer of pH 3.0 in the purification protocol it is expected to isolate proenzymes as well as mature forms of cathepsin D (Conner, 1989). The discrepancy in molecular masses detected by electrophoresis and the molecular masses of the deduced mature cathepsins might be explained by processing sites in the *T. infestans* proteases different from the predicted sites by homology to known mature enzymes. In addition, a diverse glycosylation pattern of the isoforms potentially contributed to the appearance of double bands in SDS-PAGE since TiCatD is predicted to be N-glycosylated at N74 and O-glycosylated at T240 while TiCatD2 seemed not be glycosylated as predicted by NetNGlyc 1.0 (http://www.cbs.dtu.dk/services/NetNGlyc/) and NetOGlyc 3.1 (http://www.cbs.dtu.dk/services/NetOGlyc/). The appearance of a multiplicity of cathepsin D isoforms is well known after enzyme purification from tissue extracts (Conner, 2002).

Despite its function as protease targeting the ingested blood proteins or for another function, cathepsin D might play a role in triatomine/parasite interactions. An infection of *R. prolixus* with *Trypanosoma cruzi* increased the cathepsin D activity in small intestine contents compared to uninfected insects (Borges et al., 2006). The possibility of another function is supported by the conditions in the small intestine. The activity optimum of pH 3.5 in determinations of the proteolysis of hemoglobin (Terra et al., 1988) or pH 3.0 by using fluorescence substrates (present investigation) is far away from the pH conditions in the gut of triatomines, which range between pH 5.2 and pH 6.7 in *T. infestans* and pH 7.02 and pH 7.16 in *T. brasiliensis* stomach (Barros et al., 2009). In *T. brasiliensis* only the pH value of the stomach in the first 24 hours after blood feeding was measured. The possible involvement in intestinal immune reactions is also supported by the synergistic action of lysozymes and cathepsin D-like proteases in the digestion of bacteria in the region of the gut of the housefly larva with an acidic pH (Espinoza-Fuentes and Terra, 1987; Padilha et al., 2009). In triatomines, investigations on the interaction of digestive proteases in the gut with symbionts or the pathogen *T. cruzi* are of high impact for understanding how microorganisms establish in this harsh environment, and further efforts to elucidate this interplay are indispensable.

9.1.6 References

Altschul, S.F., Madden, T.L., Schäffer, A.A., Zhang, J., Zhang, Z., Miller, W., Lipman, D.J., 1997. Gapped BLAST and PSI-BLAST: a new generation of protein database search programs. Nucl. Acids Res. 25, 3389-3402.

Assumpção, T.C., Francischetti, I.M., Andersen, J.F., Schwarz, A., Santana, J.M., Ribeiro, J.M., 2008. An insight into the sialome of the blood-sucking bug *Triatoma infestans*, a vector of Chagas' disease. Insect Biochem. Mol. Biol. 38, 213-232.

Azambuja, P., Guimaraes, J.A., Garcia, E.S., 1983. Haemolytic factor from the crop of *Rhodnius prolixus*: evidence and partial characterization. J. Insect Physiol. 29, 833-837.

Barros, V.C., Assumpcao, J.G., Cadete, A.M., Santos, V.C., Cavalcante, R.R., Araujo, R.N., Pereira, M.H., Gontijo, N.F., 2009. The role of salivary and intestinal complement system inhibitors in the midgut protection of triatomines and mosquitoes. PLoS One 4, e6047.

Bendtsen, J.D., Nielsen, H., von Heijne, G., Brunak, S., 2004. Improved prediction of signal peptides: SignalP 3.0. J. Mol. Biol. 340, 783-795.

Billingsley, P.F., Downe, A.E.R., 1983. Ultrastructural changes in posterior midgut cells associated with blood feeding in adult female *Rhodnius prolixus* Stal (Hemiptera, Reduviidae). Can. J. Zool. 61, 2574-2586.

Billingsley, P.F., Downe, A.E.R., 1989. Changes in the anterior midgut cells of adult female *Rhodnius prolixus* (Hemiptera, Reduviidae) after feeding. J. Med. Entomol. 26, 104-108.

Blüggel, M., Bailey, S., Korting, G., Stephan, C., Reidegeld, K.A., Thiele, H., Apweiler, R., Hamacher, M., Meyer, H.E., 2004. Towards data management of the HUPO Human Brain Proteome Project pilot phase. Proteomics 4, 2361-2362.

Borges, E.C., Machado, E.M., Garcia, E.S., Azambuja, P., 2006. *Trypanosoma cruzi*: effects of infection on cathepsin D activity in the midgut of *Rhodnius prolixus*. Exp. Parasitol. 112, 130-133.

Britton, H.T.S., Robinson, R.A., 1931. CXCVIII,-Universal buffer solutions and the dissociation constant of veronal. J. Chem. Soc. 198, 1456-1462.

Chamrad, D.C., Koerting, G., Gobom, J., Thiele, H., Klose, J., Meyer, H.E., Blueggel, M., 2003. Interpretation of mass spectrometry data for high-throughput proteomics. Anal. Bioanal. Chem. 376, 1014-1022.

Cho, W.L., Dhadialla, T.S., Raikhel, A.S., 1991. Purification and characterization of a lysosomal aspartic protease with cathepsin D activity from the mosquito. Insect Biochem. 21, 165-176.

Cho, W.L., Raikhel, A.S., 1992. Cloning of cDNA for mosquito lysosomal aspartic protease. Sequence analysis of an insect lysosomal enzyme similar to cathepsins D and E. J. Biol. Chem. 267, 21823-21829.

Cho, W.L., Tsao, S.M., Hays, A.R., Walter, R., Chen, J.S., Snigirevskaya, E.S., Raikhel, A.S., 1999. Mosquito cathepsin B-like protease involved in embryonic degradation of vitellin is produced as a latent extraovarian precursor. J. Biol. Chem. 274, 13311-13321.

Conner, G.E., 1989. Isolation of procathepsin-D from mature cathepsin-D by pepstatin affinity-chromatography - autocatalytic proteolysis of the zymogen form of the enzyme. Biochem. J. 263, 601-604.

Conner, G.E., 2002. Cathepsin D. In *Handbook of proteolytic enzymes* (Barret, A.J., Rawlings, N.D., Wössner, J.F., eds), p 746–751. Academic Press, New York.

Cristofoletti, P.T., Ribeiro, A.F., Terra, W.R., 2005. The cathepsin L-like proteinases from the midgut of *Tenebrio molitor* larvae: sequence, properties, immunocytochemical localization and function. Insect Biochem. Mol. Biol. 35, 883-901.

Davies, D.R., 1990. The structure and function of the aspartic proteinases. Annu. Rev. Biophys. Biophys. Chem. 19, 189-215.

Dunn, B.M., 2002. Structure and mechanism of the pepsin-like family of aspartic peptidases. Chem. Rev. 102, 4431-4458.

Espinoza-Fuentes, F.P., Terra, W.R., 1987. Physiological adaptations for digesting bacteria. Water fluxes and distribution of digestive enzymes in *Musca domestica* larval midgut. Insect Biochem. 17, 809-817.

Etienne, M., Dierkes, P., Erichsen, T., Schuhmann, W., Fritsch, I., 2007. Constant-distance mode scanning potentiometry. High resolution pH measurements in three-dimensions. Electroanal. 19, 318-323.

Garcia, E.S., Garcia, M.L.M., 1977. Control of protease secretion in intestine of fifth instar larvae of *Rhodnius prolixus*. J. Insect Physiol. 23, 247-251.

Garcia, E.S., Genta, F.A., de Azambuja, P., Schaub, G.A., 2010. Interactions between intestinal compounds of triatomines and *Trypanosoma cruzi*. Trends Parasitol. 26, 499-505.

Gasteiger, E., Hoogland, C., Gattiker, A., Duvaud, S., Wilkins, M.R., Appel, R.D., Bairoch, A., 2005. Protein identification and analysis tools on the ExPASy server. In *The proteomics protocols handbook* (Walker, J.M., ed.), pp 571-607. Humana, New York.

Geier, G., Banaj, H.J., Heid, H., Bini, L., Pallini, V., Zwilling, R., 1999. Aspartyl proteases in *Caenorhabditis elegans*. Isolation, identification and characterization by a combined use of affinity chromatography, two-dimensional gel electrophoresis, microsequencing and databank analysis. Eur. J. Biochem. 264, 872-879.

Gui, Z.Z., Lee, K.S., Kim, B.Y., Choi, Y.S., Wei, Y.D., Choo, Y.M., Kang, P.D., Yoon, H.J., Kim, I., Je, Y.H., Seo, S.J., Lee, S.M., Guo, X.J., Sohn, H.D., Jin, B.R., 2006. Functional role of aspartic proteinase cathepsin D in insect metamorphosis. BMC Dev. Biol. 6, 49.

Henning, L., 2001. WinPep 2.11: novel software for PC-based analyses of amino acids sequences. Prep. Biochem. Biotechnol. 31, 201-207.

Hong, L., Tang, J., 2004. Flap position of free memapsin 2 (beta-secretase), a model for flap opening in aspartic protease catalysis. Biochemistry 43, 4689-4695.

Hori, K., 1971. Physiological conditions in midgut in relation to starch digestion and salivary amylase of bug *Lygus disponsi*. J. Insect Physiol. 17, 1153-1167.

Houseman, J., 1978. A thiol-activated digestive proteinase from adults of *Rhodnius prolixus* Stal (Hemiptera-Reduviidae). Can. J. Zool. 56, 1140-1143.

Houseman, J.G., Downe, A.E.R., 1980. Endoproteinase activity in the posterior midgut of *Rhodnius prolixus* Stal (Hemiptera, Reduviidae). Insect Biochem. 10, 363-366.

Houseman, J.G., Downe, A.E.R., 1981a. Exoproteinase activity in the posterior midgut of *Rhodnius prolixus* Stal (Hemiptera, Reduviidae). Insect Biochem. 11, 579-582.

Houseman, J.G., Downe, A.E.R., 1981b. Identification and partial characterization of digestive proteinases from *Triatoma phyllosoma pallidipennis* Stal (Hemiptera, Reduviidae). Comp Biochem Phys B 70, 713-717.

Houseman, J.G., Downe, A.E.R., 1982. Characterization of an acidic proteinase from the posterior midgut of *Rhodnius prolixus* Stal (Hemiptera, Reduviidae). Insect Biochem. 12, 651-655.

Houseman, J.G., Downe, A.E.R., 1983a. Activity cycles and the control of four digestive proteinases in the posterior midgut of *Rhodnius prolixus* Stal (Hemiptera, Reduviidae). J. Insect Physiol. 29, 141-148.

Houseman, J.G., Downe, A.E.R., 1983b. The effects of three metabolic inhibitors on digestive proteinase production in *Rhodnius prolixus* Stal (Hemiptera, Reduviidae). J. Insect Physiol. 29, 317-321.

James, M.N.G., 2004. Catalytic pathway of aspartic peptidases. In *Handbook of proteolytic enzymes* (Barret, A.J., Rawlings, N.D., Wössner, J.F., eds), pp 12-19. Elsevier, London.

Khan, M.R., Ford, J.B., 1967. The distribution and localization of digestive enzymes in the alimentary canal and salivary glands of the cotton stainer, *Dysdercus fasciatus*. J. Insect Physiol. 13, 1619-1628.

Kollien, A.H., Schaub, G.A., 1998. The development of *Trypanosoma cruzi* (Trypanosomatidae) in the reduviid bug *Triatoma infestans* (Insecta): influence of starvation. J. Eukaryot. Microbiol. 45, 59-63.

Kollien, A.H., Schaub, G.A., 2000. The development of *Trypanosoma cruzi* in Triatominae. Parasitol. Today 16, 381-387.

Kollien, A.H., Waniek, P.J., Nisbet, A.J., Billingsley, P.F., Schaub, G.A., 2004. Activity and sequence characterization of two cysteine proteases in the digestive tract of the reduviid bug *Triatoma infestans*. Insect Mol. Biol. 13, 569-579.

Lehane, M.J. (1991) Managing the blood meal. *Biology of Blood-Sucking Insects*.

Lehane, M.J., 1994. Digestive enzymes, hemolysins and symbionts in the search for vaccines against blood sucking insects. Int. J. Parasitol. 24, 27-32.

Lopez-Ordoñez, T., Rodriguez, M.H., Hernandez-Hernandez, F.D., 2001. Characterization of a cDNA encoding a cathepsin L-like protein of *Rhodnius prolixus*. Insect Mol. Biol. 10, 505-511.

Medina, M., Vallejo, C.G., 1989. An aspartic proteinase in *Drosophila*: maternal origin and yolk localization. Int. J. Dev. Biol. 33, 313-315.

Meiser, C.K., Piechura, H., Meyer, H.E., Warscheid, B., Schaub, G.A., Balczun, C., 2010. A salivary serine protease of the haematophagous reduviid *Panstrongylus megistus*: sequence characterization, expression pattern and characterization of proteolytic activity. Insect Mol. Biol. 19, 409-421.

Neurath, H., 1991. Proteolytic processing and regulation. Enzyme 45, 239-243.

Neurath, H., 1994. Proteolytic enzymes past and present: the 2nd golden era. J Cell Biochem, 128-128.

Nicholas, K.B., Nicholas, H.B.J., Deerfield, D.W., 1997. GeneDoc: analysis and visualization of genetic variations. Embnet News 4, 1-4.

Padilha, M.H., Pimentel, A.C., Ribeiro, A.F., Terra, W.R., 2009. Sequence and function of lysosomal and digestive cathepsin D-like proteinases of *Musca domestica* midgut enzymes. Insect Biochem. Mol. Biol. 39, 782-791.

Park, Y.N., Aikawa, J., Nishiyama, M., Horinouchi, S., Beppu, T., 1996. Involvement of a residue at position 75 in the catalytic mechanism of a fungal aspartic proteinase, *Rhizomucor pusillus* pepsin. Replacement of tyrosine 75 on the flap by asparagine enhances catalytic efficiency. Protein Eng. 9, 869-875.

Pfaffl, M.W., 2001. A new mathematical model for relative quantification in real-time RT-PCR. Nucleic Acids Res 29, e45.

Rabossi, A., Stoka, V., Puizdar, V., Turk, V., Quesada-Allue, L.A., 2004. Novel aspartyl proteinase associated to fat body histolysis during *Ceratitis capitata* early metamorphosis. Arch. Insect Biochem. Physiol. 57, 51-67.

Ramakers, C., Ruijter, J.M., Deprez, R.H., Moorman, A.F., 2003. Assumption-free analysis of quantitative real-time polymerase chain reaction (PCR) data. Neurosci. Lett. 339, 62-66.

Reddy, K.R., Turcu, F., Schulte, A., Kayastha, A.M., Schuhmann, W., 2005. Fabrication of a potentiometric/amperometric bifunctional enzyme microbiosensor. Anal. Chem. 77, 5063-5067.

Sajid, M., McKerrow, J.H., 2002. Cysteine proteases of parasitic organisms. Mol. Biochem. Parasitol. 120, 1-21.

Schaub, G.A., 1989. *Trypanosoma cruzi*: quantitative studies of development of two strains in small intestine and rectum of the vector *Triatoma infestans*. Exp. Parasitol. 68, 260-273.

Schaub, G.A., 2008. Kissing bugs. In *Encyclopedia of Parasitology, Vol.1. Biology, Structure, Function* (Mehlhorn, H., ed.), pp 684-686. 3rd edn. Springer-Verlag, Heidelberg.

Schaub, G.A., 2009. Interactions of trypanosomatids and triatomines. Adv. Insect Physiol. 37, 177-242.

Silva, C.P., Terra, W.R., 1994. Digestive and absorptive sites along the midgut of the cotton seed sucker bug *Dysdercus peruvianus* (Hemiptera: Pyrrhocoridae). Insect Biochemical and Molecular Biology 24, 493-505.

Sojka, D., Franta, Z., Horn, M., Hajdusek, O., Caffrey, C.R., Mares, M., Kopacek, P., 2008. Profiling of proteolytic enzymes in the gut of the tick *Ixodes ricinus* reveals an evolutionarily conserved network of aspartic and cysteine peptidases. Parasit Vectors 1, 7.

Tamura, K., Dudley, J., Nei, M., Kumar, S., 2007. MEGA4: Molecular Evolutionary Genetics Analysis (MEGA) software version 4.0. Mol. Biol. Evol. 24, 1596-1599.

Terra, W.R., 1990. Evolution of digestive systems of insects. Annu. Rev. Entomol. 35, 181-200.

Terra, W.R., Ferreira, C., 1994. Insect digestive enzymes - Properties, compartmentalization and function. Comparative Biochemistry and Physiology B-Biochemistry & Molecular Biology 109, 1-62.

Terra, W.R., Ferreira, C., Baker, J.E., 1996. Compartimentalization of digestion. In *Biology of the Insect Midgut* (Lehane, M.J., Billingsley, P.F., eds), pp 206-235. Chapman & Hall, London.

Terra, W.R., Ferreira, C., Garcia, E.S., 1988. Origin, distribution, properties and functions of the major *Rhodnius prolixus* midgut hydrolases. Insect Biochem. 18, 423-434.

Thie, N.M.R., Houseman, J.G., 1990. Identification of cathepsin-B, cathepsin-D and cathepsin-H in the larval midgut of Colorado potato beetle, *Leptinotarsa decemlineata* Say (Coleoptera, Chrysomelidae). Insect Biochem. 20, 313-318.

Thompson, J.D., Gibson, T.J., Plewniak, F., Jeanmougin, F., Higgins, D.G., 1997. The CLUSTAL_X windows interface: flexible strategies for multiple sequence alignment aided by quality analysis tools. Nucleic Acids Res 25, 4876-4882.

Waniek, P.J., Hendgen-Cotta, U.B., Stock, P., Mayer, C., Kollien, A.H., Schaub, G.A., 2005. Serine proteinases of the human body louse (*Pediculus humanus*): sequence characterization and expression patterns. Parasitol. Res. 97, 486-500.

Winnebeck, E.C., Millar, C.D., Warman, G.R., 2010. Why does insect RNA look degraded? J. Insect Sci. 10, 159.

9.1.7 Supplemental

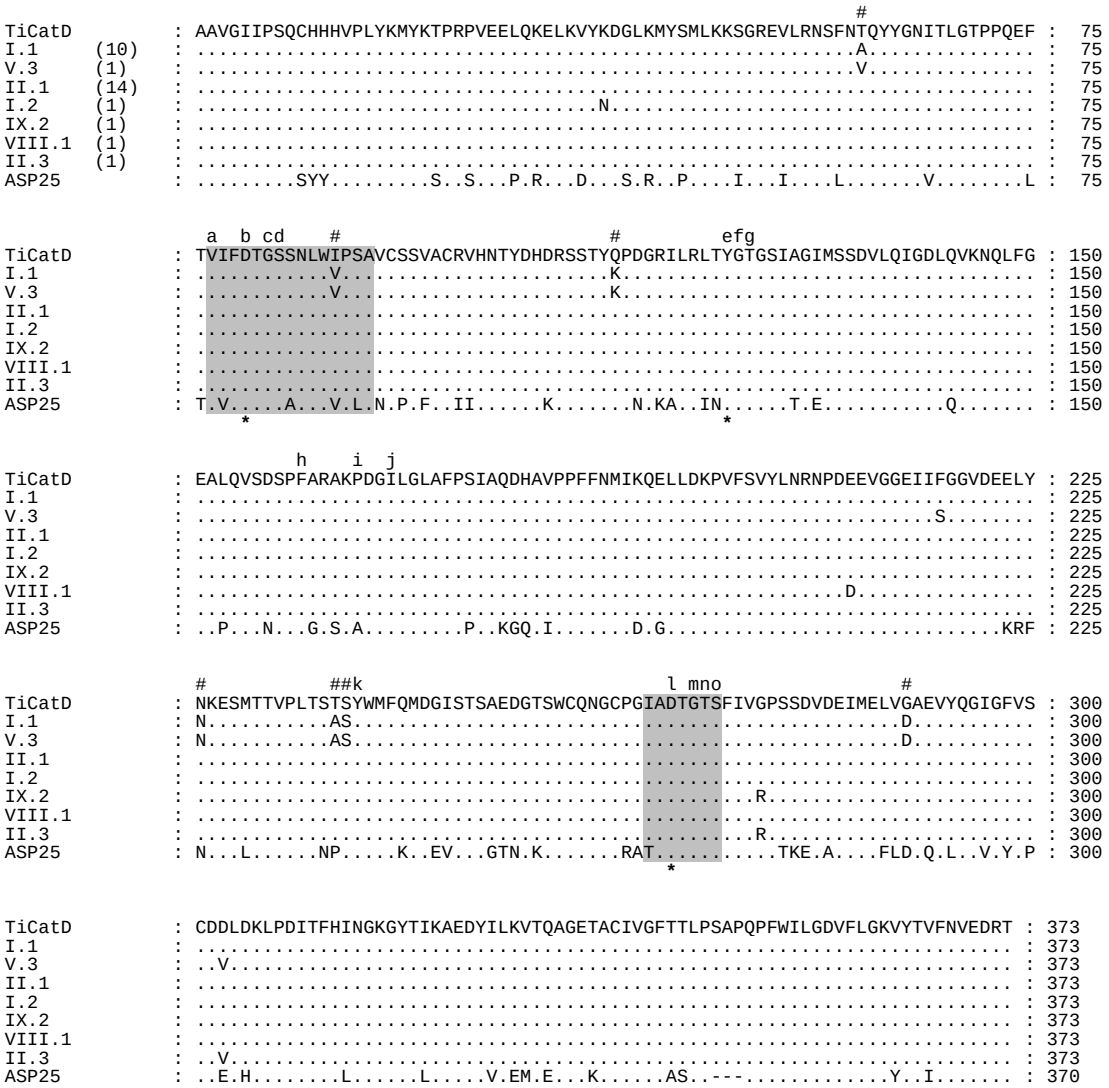

Figure S1: Multiple sequence alignment of TiCatD from different *T. infestans* specimens.

Roman numerals indicate the different individuals from the Argentinean strain, the following Arabic numerals different sequences from one specific individual. TiCatD (ADK47877.1) denotes the sequence from the Bolivian strain and ASP25 (AAS72876.1) is from the database. Numbers in brackets indicate the number of clones with identical sequence. The ten identical sequences are from: I.1, I.3, II.2, III.1, III.2, III.3, V.1, VIII.2, X.1, X.2 and the fourteen from II.1, IV.1, IV.2, IV.3, V.2, VI.1, VI.2, VII.1, VII.2, VII.3, VIII.3, IX.1, IX.3, X.3. Only differences in amino acid sequences are displayed. For comparison, full sequence of TiCatD is shown. Positions important for sequence grouping are marked (#). Conserved residues that form the substrate binding pockets and the catalytic residues are indicated by small letters (a-o) above the sequence. Catalytic aspartate residues and the tyrosine residue which controls substrate specificity are additionally marked with asterisk below the sequence. Two conserved regions of aspartic proteases are grey shaded.

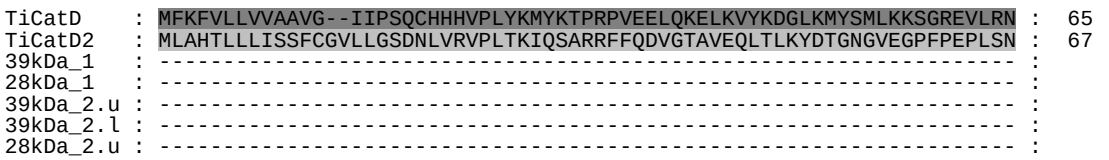

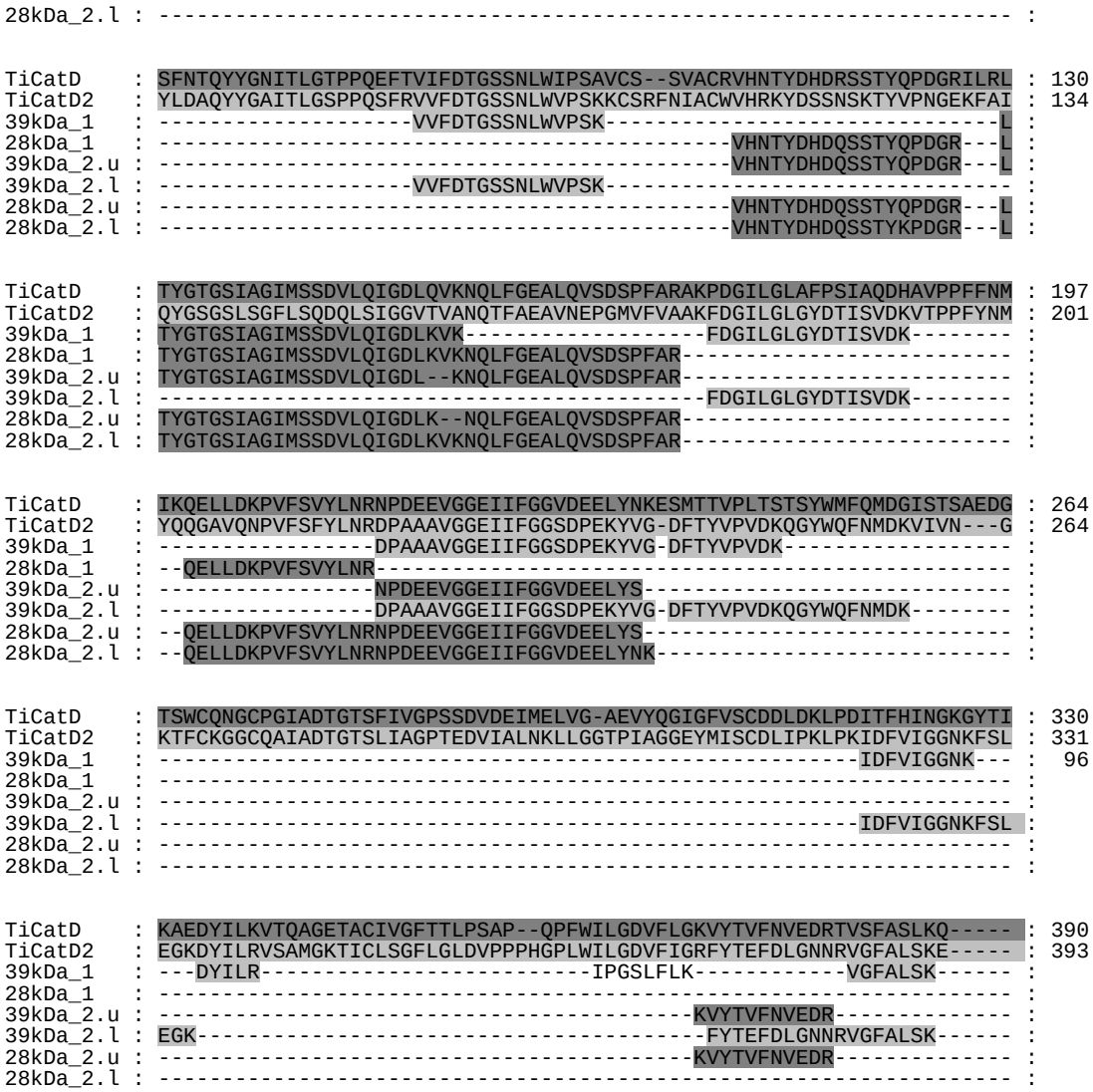

Figure S2: Multiple sequence alignment of *T. infestans* aspartate proteases TiCatD and TiCatD2 and peptide sequences identified by nano liquid chromatography-electrospray ionization-MS/MS analyses.
Sequences of TiCatD and TiCatD2 and the corresponding peptides are differentially grey shaded. The peptides were derived from samples of the 39kDa and 28kDa protein double bands after pepstatin affinity chromatography. Numbers denote samples from independent experiments. Samples derived from upper (u) and lower (l) bands of double protein bands are indicated, e.g. 39kDa_2.u indicates the upper protein band of the 39kDa double band of the second experiment.

CURRICULUM VITAE

Jennifer Katharina Pausch

An der Kommende 2L
46238 Bottrop
Jennifer_Pausch@gmx.de

Date of birth:	01.11.1983
Place of birth:	Bottrop
Nationality:	German
Marital status:	unmarried

School

2002	University entrance diploma (Abitur) at Janusz-Korczak-Gesamtschule, Bottrop
1993-2002	Janusz-Korczak-Gesamtschule, Bottrop
1989-1993	Grundschule Welheim, Bottrop

Academic education

since 2008	PhD candidate at Ruhr-Universität Bochum, Research Group Zoology/Parasitology
2008	Diploma thesis: "Heterologe Expression der für Lysozym 1 und Lysozym 2 kodierenden Gene aus *Triatoma infestans* (Reduviidae, Insecta)"
2002-2008	Biological studies (Diplom) at Ruhr-Universität Bochum

Further education

2008-2009	Courses on Laboratory Animal Sciences, which contents are in accordance with the recommendations of the Federation of European Laboratory Animal Science Associations (FELASA) on the education and training of persons carrying out animal experiments (FELASA, category B).

Foreign investigations

2008	DAAD founded project PROBRAL "Immunology of triatomines: biochemistry and molecular biology of involved factors", Instituto Oswaldo Cruz, Rio de Janeiro, Brazil (1 month)
2009	DAAD founded project PROBRAL "Immunology of triatomines: biochemistry and molecular biology of involved factors", Instituto Oswaldo Cruz, Rio de Janeiro, Brazil (4 months)

A: Publications

Balczun, C.; Siemanowski, J.; **Pausch, J.K.**; Helling, S.; Marcus, K.; Stephan, C.; Meyer, H.E.; Schneider, T.; Cizmowski, M.; Oldenburg, M.; Meiser, C.K.; Schuhmann, W.; Schmidt, S.; Schaub, G.A. (2012):
Intestinal aspartate proteases of the haematophagous bug *Triatoma infestans* (Reduviidae): sequence characterization, expression pattern and characterization of proteolytic activity. *Insect biochemistry and molecular biology*: http://dx.doi.org/10.1016/j.ibmb.2011.12.006

Pausch, J.K.; Balczun, C.; Schaub, G.A.:
Interactions of *Trypanosoma cruzi*, the etiological agent of Chagas disease, and triatomines (Reduviidae). *Mitteilungen der Deutschen Gesellschaft für allgemeine und angewandte Entomologie* Band 18 (in press)

Balczun, C.; **Pausch, J.K.**; Schaub, G.A.:
Blood digestion in triatomines – a review. *Mitteilungen der Deutschen Gesellschaft für allgemeine und angewandte Entomologie* Band 18 (in press)

Pausch, J.K.; Meiser, C.K.; Loroch, S.; Kuhlmann, K.; Meyer, H.E.; Schaub, G.A.:
Feeding induced changes of bacteriolytic activity and of the pattern of bacteriolytic compounds in small intestine of the haematophagous bug *Triatoma infestans* (Hemiptera). (in preparation)

Pausch, J.K.; Meiser, C.K.; Soukou, C.; Loroch, S.; Kuhlmann, K.; Meyer, H.E.; Schaub, G.A.; Balczun, C.:
Influence of *Trypanosoma cruzi* on the intestinal bacteriolytic activity and expression pattern of lysozymes of *Triatoma infestans*. (in preparation)

B: Abstracts

Pausch, J.K.: Balczun, C.; Schaub, G.A.:
Heterologous expression of the lysozyme1 gene and lysozyme2 gene from *Triatoma infestans*. Deutsche Gesellschaft für Parasitologie (DGP), 23rd Annual meeting, Hamburg. *In:* Abstracts, 110, 2008. (Poster presentation)

Meiser, C.; **Pausch, J.K.**; Oldenburg, M.; Knorr, E.; Kollien, A.H.; Balczun, C.; Schmidt, S.; Schuhmann, W.; Schaub, G.A.:
Intestinal antibacterial factors and symbionts of *Triatoma infestans.*
Annual meeting Deutsche Gesellschaft für allgemeine und angewandte Entomologie, Göttingen. *In:* Abstracts, 155, 2009. (Presenting author)

Meiser, C.; **Pausch, J.K.**; Oldenburg, M.; Knorr, E.; Kollien, A.H.; Balczun, C.; Schmidt, S.; Schuhmann, W.; Schaub, G.A.:
Intestinal antibacterial factors and their interaction with symbionts in *Triatoma infestans.*
Annual meeting Deutsche Gesellschaft für Medizinische Entomologie und Acarologie, Frankfurt. *In:* Abstracts, 18, 2009. (Presenting author)

Meiser, C.; **Pausch, J.K.**; Oldenburg, M.; Knorr, E.; Kollien, A.H.; Balczun, C.; Schmidt, S.; Schuhmann, W.; Schaub, G.A.:
Intestinal antibacterial factors and their interaction with symbionts in the reduviid bug *Triatoma infestans* (Insecta).
Joint Meeting of the German Societies of Parasitology and Protozoology, Düsseldorf.
In: Abstracts, 153, 2010. (Presenting author)

Characterization of intestinal antibacterial factors of *Triatoma infestans* (Reduviidae, Insecta) and their interaction with *Trypanosoma cruzi* (Trypanosomatidae, Kinetoplastida)

Dissertation, Jennifer K. Pausch, Research Group Zoology/Parasitology

1st referee: Prof. Dr. Günter A. Schaub

2nd referee: Prof. Dr. Klemens Störtkuhl

Bochum, February 2012

1. **Pausch, J.K.***; Balczun, C.*; Schaub, G.A.:
   Interactions of *Trypanosoma cruzi*, the etiological agent of Chagas disease, and triatomines (Reduviidae). *Mitteilungen der Deutschen Gesellschaft für allgemeine und angewandte Entomologie*, Band 18 (in press)

   **authors contributed equally*

   40 % planning and 40 % writing the manuscript

2. Balczun, C.; **Pausch, J.K.**; Schaub, G.A.:
   Blood digestion in triatomines – a review. *Mitteilungen der Deutschen Gesellschaft für allgemeine und angewandte Entomologie* Band 18 (in press)

   30 % planning and 30 % writing the manuscript

3. **Pausch, J.K.**; Meiser, C.K.; Soukou, C.; Loroch, S.; Kuhlmann, K.; Meyer, H.E.; Schaub, G.A.; Balczun, C.:
   Influence of *Trypanosoma cruzi* on the intestinal bacteriolytic activity and expression pattern of lysozymes of *Triatoma infestans*. (in preparation)

   80 % planning, 90 % performance, 75 % evaluation of the experiments and 80 % writing the manuscript

4. **Pausch, J.K.**; Meiser, C.K.; Loroch, S.; Kuhlmann, K.; Meyer, H.E.; Schaub, G.A.:
   Feeding induced changes of bacteriolytic activity and of the pattern of bacteriolytic compounds in small intestine of the haematophagous bug *Triatoma infestans* (Hemiptera). (in preparation)

   80 % planning, 75 % performance, 70 % evaluation of the experiments and 80 % writing the manuscript

5. Balczun, C.; Siemanowski, J.; **Pausch, J.K.**; Helling, S.; Marcus, K.; Stephan, C.; Meyer, H.E.; Schneider, T.; Cizmowski, M.; Oldenburg, M.; Meiser, C.K.; Schuhmann, W.; Schmidt, S.; Schaub, G.A. (2012):
   Intestinal aspartate proteases of the haematophagous bug *Triatoma infestans* (Reduviidae): sequence characterization, expression pattern and characterization of proteolytic activity. *Insect biochemistry and molecular biology*: http://dx.doi.org/10.1016/j.ibmb.2011.12.006

   15 % planning, 10 % performance, 10 % evaluation of the experiments and 10 % writing the manuscript

ERKLÄRUNG

Hiermit erkläre ich, dass ich die vorliegende Arbeit selber verfasst und bei keiner anderen Fakultät eingereicht und dass ich keine anderen als die angegebenen Hilfsmittel verwendet habe. Es handelt sich bei der heute von mir eingereichten Dissertation um sechs in Wort und Bild völlig übereinstimmende Exemplare.
Weiterhin erkläre ich, dass digitale Abbildungen nur die originalen Daten enthalten und in keinem Fall inhaltsverändernde Bildbearbeitung vorgenommen wurde.

Bochum, den 13.02.2012

_____

Jennifer Katharina Pausch